

Distribution Agreement

In presenting this dissertation as a partial fulfillment of the requirements for an advanced degree from Emory University, I agree that the library of the University shall make it available for inspection and circulation in accordance with its regulations, governing materials of this type. I agree that permissions to copy from, or to publish, this dissertation may be granted by the professor under whose direction it was written, or in his absence, by the Dean of the Graduate School when such copying or publication is solely for scholarly purpose and does not involve potential gain. It is understood that any copying from, or publication of this dissertation which involves potential gain will not be allowed without written permission.

Signature:

Jessica Hurtak

Date

Exo-mode oxacyclization strategies for synthesis of *trans*-fused polycyclic ethers:
the ABC ring sector of brevenal

By

Jessica Hurtak
Doctor of Philosophy

Chemistry

Dr. Frank E. McDonald
Advisor

Dr. Simon B. Blakey
Committee Member

Dr. Nathan T. Jui
Committee Member

Accepted:

Lisa A. Tedesco, Ph. D.
Dean of the James T. Laney School of Graduate School

Date

Exo-mode oxacyclization strategies for synthesis of *trans*-fused polycyclic ethers:
the ABC ring sector of brevenal

By

Jessica Hurtak

B. S., University of Tampa, 2011

Advisor: Frank E. McDonald

An abstract of

A dissertation submitted to the Faculty of the Graduate
James T. Laney School of Graduate Studies of Emory University
in partial fulfillment of the requirements for the degree of
Doctor of Philosophy
in Chemistry

2017

Abstract:

Chapter 1. Fused polycyclic ether natural products

Brevenal is a non-toxic metabolite of the dinoflagellate *Karenia brevis*, and acts as a competitive inhibitor of red tide toxins including brevetoxin. Both brevenal and brevetoxin B2 share a *trans*-fused polycyclic ether core. Our research explores *exo*-mode sequential cyclization pathways for the synthesis of polycyclic ether natural products from both alkyne and alkene substrates. This work culminates with synthesis of the ABC domain of the core structure of brevenal.

Chapter 2. Mercury-promoted reductive oxacyclization reactions of alkynyl alcohols

Mercury-promoted reductive oxacyclization reactions provide opportunity to construct polycyclic ether structures rapidly from alkynol substrates. Alkynyldiols undergo oxacyclization with substoichiometric $\text{Hg}(\text{OTf})_2$, and the resulting oxocarbenium ion either undergoes hydration, resulting in formation of hemiketals, or diastereoselective reduction with Et_3SiH , furnishing *trans*-fused tetrahydropyrans. Beta-oxygen substituents are incompatible with this methodology as they are prone to elimination, and 8-*endo* cyclization predominates over 7-*exo* cyclization. Thus, this methodology is limited to cascade synthesis of 6,8-fused ethers.

Chapter 3. Alkenol oxacyclizations: Synthesis of the ABC ring substructure of brevenal

Our research explores regio- and stereoselective *exo*-mode cyclization pathways to the *trans, syn, trans*- fused polycyclic ether structure of brevenal. Sequential oxacyclizations of linear triene or diene precursors form the ABC ring substructure of brevenal. Our strategy constructs each cyclic ether with various hydroxy-alkene cyclizations, with stereoiduction from allylic oxygen substituents in the C-O bond forming/ ring-closing steps.

Exo-mode oxacyclization strategies for synthesis of *trans*-fused polycyclic ethers:
the ABC ring sector of brevenal

By

Jessica Hurtak

B. S., University of Tampa, 2011

Advisor: Frank E. McDonald

A dissertation submitted to the Faculty of the Graduate
James T. Laney School of Graduate Studies of Emory University
in partial fulfillment of the requirements for the degree of
Doctor of Philosophy
in Chemistry
2017

Table of Contents

Chapter 1. Fused polycyclic ether natural products

1.1 Background	2
1.1.1 Red Tide Events and the Brevetoxins	2
1.1.2 Biogenesis of fused polycyclic ether marine natural products.....	5
1.1.3 Biomimetic synthesis: <i>endo</i> -mode polyepoxide cascades	6
1.1.4 Brevenal	14
1.1.5 Synthesis of brevenal	15
1.2 Introduction.....	19
1.2.1 <i>Exo</i> -mode oxacyclization	19

Chapter 2. Mercury-promoted reductive oxacyclization reactions of alkynyl alcohols

2.1. Introduction and Background	22
2.1.1 Motivation for catalytic mercury-promoted oxacyclization.....	22
2.1.2 Mercury(II) triflate promoted oxacyclization	24
2.1.3. Catalytic mercury: demercuration.....	27
2.2. Results and Discussion	31
2.2.1. Synthesis of alkynyldiol 30	31
2.2.2. Reductive cyclization of alkynyldiol 30	32
2.2.3. Synthesis of 1,4- diyne 39	37

2.2.4. Alternative synthesis of 1,4- diyne 39	40
2.2.5 Cyclization of 1,4- diyne 39	42
2.2.6 Synthesis of 1,5- diyne 64	45
2.2.7 Cyclization of 1,5- diyne 64	47
2.2.8 Synthesis of tetrahydropyran- templated alkynol 76	49
2.2.9 Cyclization of tetrahydropyran– templated alkynol 76	52
2.3 Conclusion	56
2.4 Experimental Details.....	57
2.5 NMR spectra of selected compounds	104

Chapter 3. Alkenol oxacyclization: Synthesis of the ABC ring substructure of brevenal

3.1. Background and Introduction	126
3.1.1 Background	126
3.1.2 Individual ring precedents: A and B rings	127
3.1.2.1 Individual ring precedent: A ring	127
3.1.2.2 Individual ring precedent: B ring.....	128
3.1.3 <i>Exo</i> -mode oxacyclization strategy for brevenal	130
3.1.3 C ring.....	134
3.2. Results and Discussion	135
3.2.1 Electrophile-promoted oxacyclization of alkenyl alcohols.....	135

3.2.1.1	Synthesis of acetonide-protected diol 37	135
3.2.1.2	Synthesis of benzylidene protected diol 49	137
3.2.1.3	Synthesis of vicinal diol 60	139
3.2.1.4	Cyclization of acetonide protected diol 37	140
3.2.1.5	Cyclization benzylidene protected diol 49	142
3.2.1.6	Cyclization of vicinal diol 60	143
3.2.2	AB ring model.....	145
3.2.2.1	Synthesis of <i>bis</i> -acetate-diene 74	145
3.2.2.2	Cyclization of <i>bis</i> -acetate-diene 74	148
3.2.2.3	Synthesis of diene 22	150
3.2.2.4	Cyclization of diene 22	151
3.2.3	BC ring model.....	155
3.2.3.1	Synthesis of dienyl ketone 96	157
3.2.3.2	Cyclization of saturated dienyl ketone 96	159
3.2.3.3	Synthesis of unsaturated dienyl ketones 113 and 114	160
3.2.3.4	Cyclization of unsaturated dienyl ketones 113 and 114	162
3.2.4	ABC linear precursor.....	166
3.2.4.1	Synthesis of triene 126	167
3.2.4.2	Cyclization of triene 124	169
3.2.5	ABC model.....	170

3.2.5.1 Synthesis of C-ring precursor 130	171
3.2.5.2 Cyclizations of C-ring precursor 130	173
3.2.5.3 Demercuration and deiodination of tricyclic compound 132	174
3.3 Conclusion	178
3.4 Experimental Details.....	180
3.5 X-RAY data of compounds 78 and 84	268
3.6 NMR spectra of selected compounds	296
References.....	329

List of Figures

Chapter 1. Fused polycyclic ether natural products

Figure 1. Brevetoxin B.....	2
Figure 2. Representative members from the polycyclic ether natural product family.....	4
Figure 3. Sasaki's retrosynthetic analysis of brevenal.....	16
Figure 4. Yamamoto's and Kadota's retrosynthetic analysis of brevenal	17
Figure 5. Rainier's retrosynthetic analysis of brevenal	18

Chapter 2. Mercury-promoted reductive oxacyclization reactions of alkynyl alcohols

Figure 6. MTPA-ester data for compound (<i>S</i>)- 66	81
Figure 7. MTPA-ester data for compound 72	85
Figure 8. MTPA-ester data for compound (<i>R</i>)- 33	89

Chapter 3. Alkenol oxacyclization: Synthesis of the ABC ring substructure of brevenal

Figure 9. Pentacyclic marine natural product brevenal and ABC substructure 27	127
Figure 10. Conformational model for A-ring cyclization.....	128
Figure 11. Conformational model for B-ring cyclization	130
Figure 12. NOE correlations of tetrahydropyran 62	144
Figure 13. X-ray crystal structure of cis, trans- fused bicyclic compound 78	150
Figure 14. NOESY correlations of cyclic compounds 83 and 86	153

Figure 15. X-ray crystal structure of AB bicyclic compound 84	154
Figure 16. Model for 1,3-stereocontrol in ketone reduction of β -cyclic ether 125	172
Figure 17. Key spectral data of tricyclic compound 133	175
Figure 18. MTPA-ester data for 58a	203
Figure 19. MTPA-ester data for compound 70	221
Figure 20. MTPA-ester data for compound (<i>S</i>)- 141	261
Figure 21. Key NOE correlations of compound 133	265

List of Schemes

Chapter 1. Fused polycyclic ether natural products

Scheme 1. Nakanishi's proposed biosynthesis of brevetoxin B 1	6
Scheme 2. Regiochemical pathways for epoxide-opening oxacyclization.....	8
Scheme 3. Nicolaou's 6- <i>exo</i> and 6- <i>endo</i> cyclization in the synthesis of brevetoxin B 1 ...	9
Scheme 4. McDonald's <i>endo</i> -mode polyepoxide cascades via epoxonium ion to access <i>trans</i> -fused trisoxepanes 16 and 18	10
Scheme 5. McDonald's <i>endo</i> -mode polyepoxide cascade to synthesize <i>trans</i> -fused pyrans	11
Scheme 6. Jamison's water-promoted <i>endo</i> -epoxide cascade to access <i>trans</i> -fused pyrans	12
Scheme 7. Nicolaou's unsuccessful extension of templated approach.....	13
Scheme 8. Jamison's Rh(I)-catalyzed <i>endo</i> -epoxide cascade to access 6- and 7- membered cyclic ethers.....	13
Scheme 9. Holton's biomimetic synthesis of hemibrevetoxin B	20

Chapter 2. Mercury-promoted reductive oxacyclization reactions of alkynyl alcohols

Scheme 10. Mercury (II) promoted cyclization of 1,2-disubstituted alkene 1	23
Scheme 11. Iodine promoted cyclization of 1,1-disubstituted alkene 4	23
Scheme 12. Selenium promoted cyclization of trisubstituted alkene 5	23
Scheme 13. Hg(OTf) ₂ -promoted oxacyclization to form the tetrahydropyran in gelsemine	27

Scheme 14. Hg(OTf) ₂ -catalyzed oxacyclization and protiodemercuration of alkyne 12 ...	28
Scheme 15. Hg(OTf) ₂ -catalyzed oxacyclization and protiodemercuration of alkene 17 .	29
Scheme 16. Schreiber's intramolecular mercury-catalyzed transesterification cyclization	30
Scheme 17. Schwartz's mercury-promoted oxacyclization of alkynyl alcohol 26	30
Scheme 18. Proposed oxacyclization of alkynol 30 to synthesize tetrahydropyran 3	31
Scheme 19. Synthesis of monocyclization substrate 30	32
Scheme 20. Cyclization of alkynol 30 with mercuric triflate and ligated base	33
Scheme 21. Cyclization of alkynol 30 resulting in hemiketal 34	34
Scheme 22. Proposed mechanism of formation of hemiketal 34	35
Scheme 23. Model of diastereoselectivity for hydride addition to tetrahydropyran 21	35
Scheme 24. Reductive oxacyclization to yield <i>trans</i> -tetrahydropyran 3	36
Scheme 25. AB rings of adriatoxin 41	37
Scheme 26. Proposed tandem cyclization of diyne 39 to synthesize bispyran 40	38
Scheme 27. Synthesis of diyne 39	38
Scheme 28. Synthesis of propargylic aldehyde 49	39
Scheme 29. Alternative synthesis of diyne 39	41
Scheme 30. Attempted tandem cyclization of diyne 39 resulting in enyne 53	42
Scheme 31. Proposed mechanism of formation of enyne 53	43
Scheme 32. Yokoyama's elimination of beta-oxygen to synthesize tetrahydropyran 60 . 44	44
Scheme 33. Synthesis of model system 62	44
Scheme 34. DE rings of adriatoxin 41	46
Scheme 35. Proposed bicyclization of diyne 64 to synthesize 6,7-bicyclic product 63 ...	46

Scheme 36. Synthesis of diyne 64	47
Scheme 37. Tandem cyclization of diyne 41 resulting in bispyran 73	48
Scheme 38. Proposed mechanism of formation of bispyran 73	49
Scheme 39. Retrosynthesis of cyclization substrate 76	50
Scheme 40. Synthesis of substituted tetrahydropyran templated alkynol 76	51
Scheme 41. Synthesis of substituted tetrahydropyran templated alkynol R-76	52
Scheme 42. Initial attempts at templated cyclization of alkynol R-76	53
Scheme 43. Model system 84 for dehydrative cyclization and oxacyclization	54
Scheme 44. 8-endo cyclization from tetrahydropyran template R-76	56
Scheme 45. Mercuric ion-promoted oxacyclization and attempts at tandem cyclization.	57

Chapter 3. Alkenol oxacyclization: Synthesis of the ABC ring

substructure of brevenal

Scheme 46. Iodine-promoted oxacyclization of 1,1-disubstituted alkenyldiol 2	127
Scheme 47. 8- <i>Endo</i> iodocyclization cyclizations of hydroxy-alkenes 6	128
Scheme 48. Intramolecular oxa-Michael addition on unsaturated ester 8	129
Scheme 49. Proposed <i>exo</i> -mode oxacyclizations of polyene 10 to synthesize pentacyclic core 11	131
Scheme 50. Individual ring models: <i>exo</i> -oxacyclization	132
Scheme 51. Proposed cyclizations of triene 26 to synthesize ABC compound 27	133
Scheme 52. Proposed bicyclization sequence of diene 22 to synthesize AB compound 23	133
Scheme 53. Proposed cyclizations of triene 24 to synthesize BC compound 25	133
Scheme 54. C-ring retrosynthetic analysis.....	134

Scheme 55. Mootoo's iodocyclization of acetal alkene 30 to form <i>trans</i> - 31	134
Scheme 56. Iodocyclization of acetal 32 to furnish C-ring model 36	135
Scheme 57. Synthesis of acetonide-protected C-ring cyclization substrates 37a and 37b	137
Scheme 58. Synthesis of benzylidene acetal C-ring cyclization substrate 49a	139
Scheme 59. Synthesis of vicinal diol C-ring cyclization substrate 60	140
Scheme 60. Cyclization of acetonide-protected nucleophile.....	141
Scheme 61. Cyclization of benzylidene acetal C-ring cyclization substrate 49a	143
Scheme 62. Cyclization of vicinal diol C-ring cyclization substrate 60	144
Scheme 63. Proposed synthesis of AB bicyclic compound 23 through tandem cyclization of diene 22	145
Scheme 64. Synthesis of bis-acetate dienes 74 and 75	147
Scheme 65. Cyclization of diene 74 to afford cis-fused bicyclic product 78	149
Scheme 66. Synthesis of AB tandem cyclization substrate, diene 22	151
Scheme 67. Tandem cyclization of diene 22	152
Scheme 68. Iodocyclization of <i>E</i> -alkenol 117 and attempted intramolecular conjugate addition	154
Scheme 69. Proposed cyclizations of diene 88 to synthesize BC compound 91	155
Scheme 70. Saturated (92) and unsaturated (6) tether in B ring model system.....	157
Scheme 71. Synthesis of BC cyclization substrate 96	158
Scheme 72. Attempted conjugate addition and deprotection of saturated tether 96	159
Scheme 73. Synthesis of BC ring models with unsaturated tether 81 and 89	162

Scheme 74. Attempted conjugate addition and deprotection of unsaturated tethers 113 and 114	163
Scheme 75. Deprotection of 112 to afford bis-allylic alcohol substrate 118	163
Scheme 76. Attempts to cyclize bis-allylic alcohol triene 118	164
Scheme 77. 8- <i>Endo</i> selectivity observed on substrate 8	165
Scheme 78. Unsuccessful BC-model conjugate addition of dienylketone 113	166
Scheme 79. Proposed ABC-model conjugate addition of dienylketone 124	166
Scheme 80. Proposed ABC-model for conjugate addition of dienylketone 124	167
Scheme 81. Synthesis of ABC cyclization substrate, triene 126	168
Scheme 82. Cyclization of triene 126 to form AB bicyclic compound 125	169
Scheme 83. Proposal for alternative synthesis of AB enone 125 to investigate synthesis of tricyclic core substructure 27	171
Scheme 84. Synthesis of allylic alcohol 130	172
Scheme 85. Setting stereochemistry at C ₁₈ in compound 130	172
Scheme 86. Electrophile-promoted cyclizations of 130a and 130b	173
Scheme 87. Reduction of iodo-organomercury compound 132 to furnish ABC core substructure 27	175
Scheme 88. Relative rates of reduction of thiocarbonyl esters 137-140	177
Scheme 89. Attempts at deiodination of cyclic compounds.....	178
Scheme 90. C-ring and BC-ring cyclization results.....	179
Scheme 91. AB and ABC cyclization results	180

List of Tables

Chapter 2. Mercury-promoted reductive oxacyclization reactions of alkynyl alcohols

Table 1. MTPA-ester data for compound (<i>S</i>)- 66	80
Table 2. MTPA-ester data for compound 72	85
Table 3. MTPA-ester data for compound (<i>R</i>)- 33	89

Chapter 3. Alkenol oxacyclization: Synthesis of the ABC ring substructure of brevenal

Table 4. MTPA-ester data for compound 58a	203
Table 5. MTPA-ester data for compound 70	221
Table 6. MTPA-ester data for compound (<i>S</i>)- 141	260
Table 7. Crystal data and structure	270
Table 8. Fractional Atomic Coordinates ($\times 10^4$) and Equivalent Isotropic Displacement Parameters ($\text{\AA}^2 \times 10^3$) for compound 78 . U_{eq} is defined as 1/3 of the trace of the orthogonalized U_{ij}	271
Table 9. Anisotropic Displacement Parameters ($\times 10^4$) for compound 78 . The anisotropic displacement factor exponent takes the form: $-2\pi^2[a^{*2} \times U_{11} + \dots 2hka^* \times b^* \times U_{12}]$	274
Table 10. Bond Lengths in \AA for compound 78	276
Table 11. Bond Angles in $^\circ$ for compound 78	278

Table 12. Hydrogen Fractional Atomic Coordinates ($\times 10^4$) and Equivalent Isotropic Displacement Parameters ($\text{\AA}^2 \times 10^3$) for compound 78 . U_{eq} is defined as 1/3 of the trace of the orthogonalised U_{ij}	282
Table 13. Hydrogen Bond information for compound 78	285
Table 14. Crystal data and structure refinement for compound 84 (JAH-11-102).	285
Table 15. Atomic coordinates ($\times 10^4$) and equivalent isotropic displacement parameters ($\text{\AA}^2 \times 10^3$) for compound 84 . $U(eq)$ is defined as one third of the trace of the orthogonalized U^{ij} tensor.	287
Table 16. Bond lengths [\AA] and angles [$^\circ$] for compound 84	288
Table 17. Anisotropic displacement parameters ($\text{\AA}^2 \times 10^3$) for compound 84 . The anisotropic displacement factor exponent takes the form: $-2\pi^2 [h^2 a^{*2} U^{11} + \dots + 2 h k a^* b^* U^{12}]$	293
Table 18. Hydrogen coordinates ($\times 10^4$) and isotropic displacement parameters ($\text{\AA}^2 \times 10^3$) for compound 84	294
Table 19. Hydrogen bonds for compound 84 [\AA and $^\circ$].	294

Abbreviations

Ac	Acetyl
AIBN	2,2'-azobisisobutyronitrile
Aq	aqueous
Ar	aryl
<i>t</i> -BuOOH	<i>tert</i> -butylhydroperoxide
<i>n</i> -BuLi	<i>n</i> -butyllithium
<i>t</i> -BuLi	<i>tert</i> -butyllithium
Bz	benzoyl
Cat	catalytic
CBS	Corey-Bakshi-Shibata
d	doublet
dppp	1, 3-bis(diphenylphosphino)propane
DIBAL-H	diisobutylaluminum hydride
DMAP	<i>N, N</i> -dimethylaminopyridine
DMF	<i>N, N</i> -dimethylformamide
DMSO	dimethylsulfoxide
Equiv	equivalent
EtOAc	ethyl acetate
Hg(OTf) ₂	mercuric trifluoromethanesulfonate
HRMS	high-resolution mass spectroscopy
IDCP	iodonium <i>sym</i> -collidine perchlorate
KHMDS	potassium bis(trimethylsilyl)amide

LA	Lewis acid
LAH	lithium aluminum hydride
LDA	lithium diisopropylamide
LiHMDS	lithium bis(trimethylsilyl)amide
m	multiplet
mL	milliliter
mmol	millimole
MS	molecular sieves
Ms	methanesulfonyl
NBS	<i>N</i> -bromosuccinimide
NHK	Nozaki-Hiyama-Kishi
NIS	<i>N</i> -iodosuccinimide
NMR	nuclear magnetic resonance
Ph	phenyl
PhNTf ₂	<i>N</i> -phenyltrifluoromethanesulfonimide
Pyr	pyridine
q	quartet
Red-Al	sodium bis(2-methoxyethoxy)aluminum hydride
rt	room temperature
s	singlet
Sat	saturated
t	triplet
TBAF	tetrabutylammonium fluoride

TBAI	tetrabutylammonium iodide
TBS	<i>tert</i> -butyldimethylsilyl
TEA	triethylamine
TFA	trifluoroacetic acid
THF	tetrahydrofuran
THP	tetrahydropyran
TIPS	triisopropylsilyl
TLC	thin layer chromatography
TMEDA	<i>N,N,N',N'</i> -tetramethylethylenediamine
TMS	trimethylsilyl
Tol	toluene

Chapter 1. Fused polycyclic ether natural products

Chapter 1. Fused polycyclic ether natural products

1.1 Background

1.1.1 Red Tide Events and the Brevetoxins

Near the coasts of the Gulf of Mexico, large algal blooms result in devastating effects on the ecosystem. Dense aggregations of these dinoflagellate blooms cause the water to take on a red color, giving the phenomenon the name “red tide event”. These blooms also produce toxic compounds that are responsible for the mortalities of marine and coastal varieties of fish, birds, mammals, and other organisms, causing devastating effects on the ecosystem. A public health risk is posed by the toxins as aerosolized droplets are transmitted through the air, causing respiratory and eye irritation. Ingestion of contaminated shellfish can lead to neurotoxic shellfish poisoning (NSP)¹.

In 1981, Nakanshi reported the structure of brevetoxin B (BTX-B, **1**)², a toxic metabolite of *Gymnodinium breve* (in the Pacific Ocean) and *Karenia brevis* (in Atlantic waters) found to be responsible for the neurotoxic effects red tide (Figure 1).³ With this discovery, the scientific community was introduced to the ladder-shaped marine polycyclic ether natural product family.

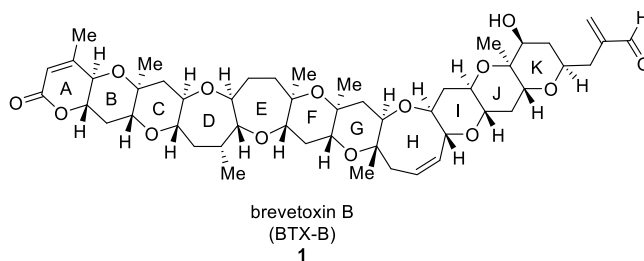


Figure 1. Brevetoxin B

Marine polycyclic ether natural products have attracted significant attention from biochemists and chemists due to potent biological activity and structural novelty, regularity, and complexity. Members of this class are characterized by their ladder shape, originating from polycyclic ether (five- to nine- membered) ring backbones. Whereas the smallest structure has four contiguous ring (hemibrevetoxin B, **2**), gymnocin A (**8**) has 14 rings. Maitotoxin (not shown), the largest and most complex nonbiopolymeric structure from nature characterized to date, has 32 rings in four separate ladder segments.⁴ All ladder ethers share a fused ring system with repeating stereodefined oxygen-carbon-carbon (O-C-C) units, having *trans-syn-trans*-fusions across the rings. Functionality on the ether ring is limited to occasional unsaturations, and hydroxyl and/or methyl substituents. Representative members of this class include: hemibrevetoxin B (**2**)⁵, brevetoxin A (**3**)⁶, ciguatoxin (**4**)⁷⁻⁹, gambieric acid (**5**)¹⁰⁻¹², brevenal (**6**)³, and adriatoxin (**7**)¹³, and gymnocin A (**8**)¹⁴ (Figure 2).

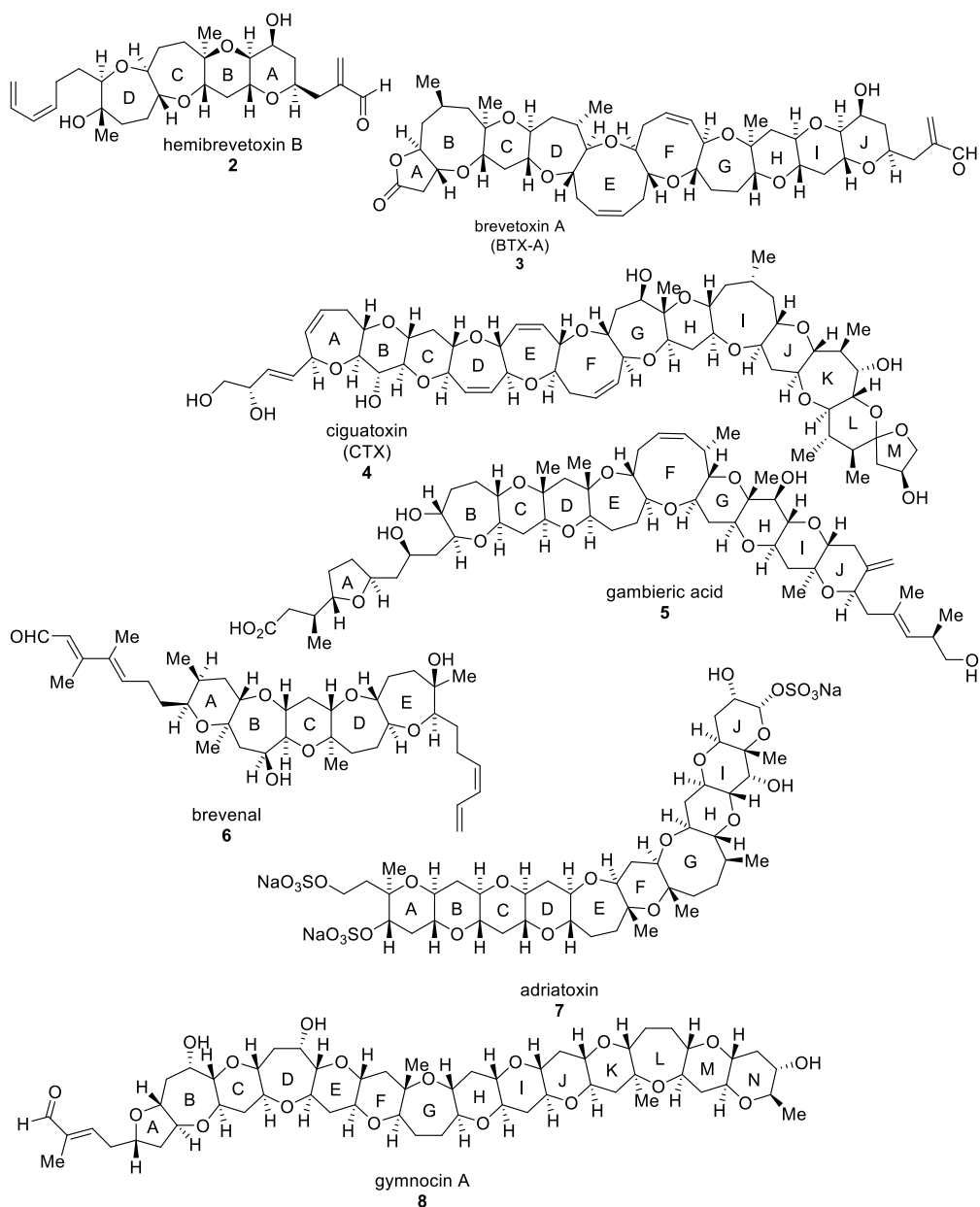


Figure 2. Representative members from the polycyclic ether natural product family

Despite the shared motifs, members of this class display diverse biological activities including neurotoxicity, cytotoxicity, and antifungal activity.^{1,15} The target receptor protein has been identified in the brevetoxins,^{16–19} ciguatoxins,^{20–22} and gambierol.^{23–25} The origin of neurotoxicity in the brevetoxins and ciguatoxins results from

their high affinity to bind site 5 of voltage-gated sodium channels, while gambierol is a potent voltage-gated potassium channel inhibitor.^{24,25}

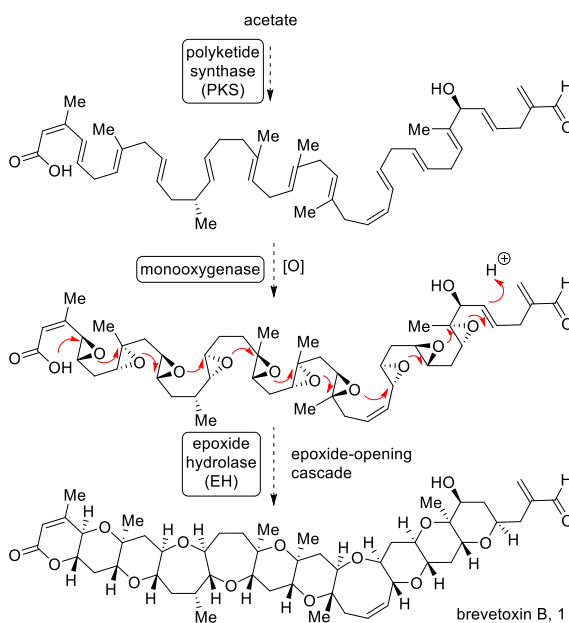
Limited availability of pure compounds available from natural sources has slowed biological evaluation. Chemical synthesis plays an important role in producing viable quantities of pure compound for detailed biological studies²⁶. In addition to providing useful information for the study of ion channels in biological systems, the study of their structure-activity relationships (SAR) of analogues of these compounds may provide valuable insight into the structural motifs responsible for their biological activities.

1.1.2 Biogenesis of fused polycyclic ether marine natural products

Shimizu²⁷ and Nakanshi²⁸⁻³⁰ have independently conducted isotopic enrichment studies using ¹³C-labeled acetate elucidating the polyketide origin of the BTX-B (**1**). Rather than direct metabolism of acetate, the citric acid cycle seems to play a role in the condensation reactions that form the carbon backbone, which may account for observed anomalies in skeleton formation. From this point, the remaining biosynthetic pathway is undetermined, but the prevailing hypothesis was posed by Nakanishi 30 years ago.²⁹ His laboratory proposed acetate condensation with a polyketide synthase (PKS) to form an acyclic polyene precursor, which would undergo epoxidation with a monooxygenase enzyme before undergoing cascade oxacyclization of the polyepoxide backbone, perhaps catalyzed by enzyme hydroxylases (EH) (Scheme 1). This postulate rationalized the structural and stereochemical regularity of the ladder ethers. Moreover, this hypothesis has been supported by identification of molecular oxygen (O₂) as the source of the ether oxygen

atoms in yessotoxin, determined through ^{18}O -labeling experiments.³¹ When nature conducts these reactions, *endo*-cyclizations are likely directed under enzymatic control rather than with the use of directing groups. As of 2016, two classes of epoxide hydrolases have been identified in the transcriptome libraries of *Karenia brevis*, but evaluation of their potential role in polycyclic ether synthesis has not yet been determined.³² To date, no monooxygenase enzymes have been identified for this family of natural products, nor have polyene precursors to polyepoxides been isolated.

Scheme 1. Nakanishi's proposed biosynthesis of brevetoxin B 1



1.1.3 Biomimetic synthesis: *endo*-mode polyepoxide cascades

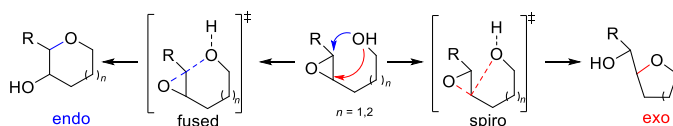
The tremendous size and complexity of the ladder ethers has been an inspiration to the synthetic community since their discovery. A measure of the synthetic challenge is notably Nicolaou's total synthesis of brevetoxin B, a Herculean effort involving more than 100 synthetic manipulations.³³ Many new synthetic methodologies have been developed

through attempts to make these molecules.³⁴ Due to their complexity and size, most efforts have focused on convergent assembly of preformed rings, usually involving cyclization to form one or two rings followed by linking them together two to five rings at a time. Some of these approaches will be highlighted in the context of the natural product brevenal in the following section, but biomimetic approaches using the Nakanishi hypothesis as inspiration will first be discussed.

The Nakanishi hypothesis for the biogenesis of polycyclic ether natural products has inspired biomimetic synthesis *via* polyepoxide cascades. Numerous labs have undertaken the task of searching for chemical evidence for this hypothesis through development of *endo*-regioselective polyepoxide cascade reactions, which are potentially step economical and atom-efficient ways to rapidly build complexity.³⁵⁻³⁹ In 1996, the Shi laboratory reported a chiral ketone catalyst for highly enantioselective epoxidations of *trans*-dialkyl and alkyl trisubstituted alkenes.⁴⁰ Their discovery enabled stereoselective synthesis of the requisite stereodefined polyepoxide acyclic precursors corresponding to the *trans*, *syn*, *trans*-fused polycyclic ether natural products.^{41,42} Synthetic access to the polyepoxide precursors opened the door to exploration of the anti-specific, *endo*-selective epoxide-opening cascades required for required to access the natural product cores. Several research laboratories, notably Floreancig (Pittsburgh)^{43,44}, McDonald (Emory)³⁶, Murai (Hokkaido)⁴⁵, and Jamison (MIT)³⁵ have contributed to this area, resulting in development of cascades which result in fused polypyran and polyoxepane structures.

From the biogenetic polyepoxide, an entirely *endo*-regioselective, anti-stereospecific oxacyclization cascade must occur to provide fused polycyclic ether cores. Intramolecular epoxide opening reactions can proceed by two regiochemical pathways, involving *endo*- or *exo*- mode ring closure (Scheme 2)⁴⁶. Simple epoxy alcohols preferentially undergo *exo*-cyclization through a kinetically-favored spiro transition state⁴⁷, whereas the fused transition state to access the *endo*-products is less-favored. In this manner, 5-*exo* cyclization is preferred to 6-*endo* cyclization, and 6-*exo* cyclization is preferred to 7-*endo* cyclization.⁴⁸ To overcome this limitation, synthetic chemists have developed a number of strategies to overcome the preference for *exo*-cyclization.

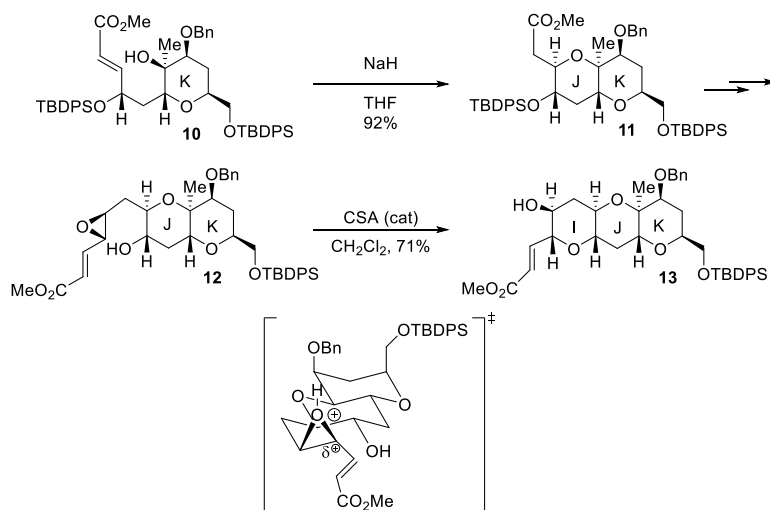
Scheme 2. Regiochemical pathways for epoxide-opening oxacyclization



In Nicolaou's synthesis of the IJK ring sector of brevetoxin B, regioselective and stereospecific oxacyclization reactions were used to form the tetrahydropyran rings (Scheme 3).³³ Intramolecular conjugate addition (*oxa*-Michael addition) of substrate **10** afforded the J-ring tetrahydropyran **11** through 6-*exo* cyclization. Epoxide cyclization of substrate **12** afforded the I-ring tetrahydropyran **13** through 6-*endo* cyclization. The allyl fragment stabilizes the fused transition state due to stabilization of the developing positive charge at the *endo*-carbon from the pi-orbitals of the alkene, resulting in *endo*-cyclization. Although Nicolaou's approach is iterative, using a directing group to influence the cyclization is a powerful way to access the complex core polycyclic ether core structures.

Although Nicolaou executes a single ring-closing reaction at a time, the same principles can be seen in the development of polyepoxide cascade reactions. By either stabilizing positive charge at the *endo* carbon, favoring the fused transition state, or destabilizing positive charge at the *exo* carbon, disfavoring the spiro transition state, there have been great advancements in biomimetic epoxide cascades.^{34,39}

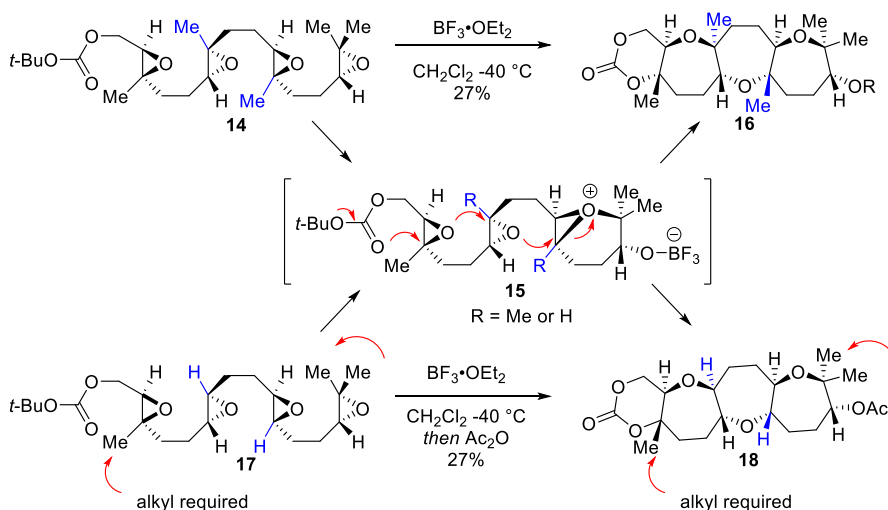
Scheme 3. Nicolaou's 6-exo and 6-endo cyclization in the synthesis of brevetoxin B **1**



Among the first to describe *endo*-mode polyepoxide cyclization cascade reactions, the McDonald lab reported the cascade cyclization of tetraepoxide **14** (derived from geranylgeraniol) to provide the trisoxepane **16** (Scheme 4).⁴¹ Lewis acid activation of the terminal epoxide promoted formation of the proposed bicyclic epoxonium ion **15**, which underwent ring-opening addition by the nearest epoxide oxygen, generating a new epoxonium ion which participated in the same cycle. The cascade was terminated by the carbonate nucleophile, which was a crucial element to the regioselectivity observed in these reactions. Similarly, cyclization of triepoxide **17** afforded trisoxepane **18** through

epoxonium intermediate **16** (Scheme 4)⁴⁹. Although the requirement of alkyl substituents on each epoxide was reduced, a standing limitation of this methodology is the requirement for an alkyl substituent at the end of the chain and on the epoxide adjacent to the terminating nucleophile, elements critical in achieving the all *endo*-selectivity.

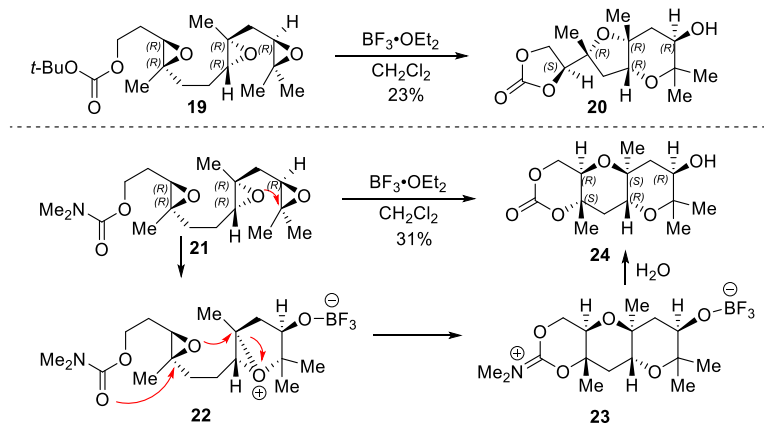
Scheme 4. McDonald's *endo*-mode polyepoxide cascades via epoxonium ion to access *trans*-fused trisoxepanes **16** and **18**



The McDonald laboratory's extension of this work to synthesize polypyrans was informative about the role of the terminating nucleophile and highlighted a limitation of this methodology for accessing six-membered rings (Scheme 5).⁴⁹ Oxacyclization of triepoxide **19** with a *tert*-butyl carbonate nucleophile resulted in *cis*-fused bicyclic product **20** resulting from 5-*exo* cyclization. *Cis*-fused product **20** was suggestive of a carbocationic intermediate, resulting from ion-pair separation of the proposed epoxonium, yielding undesired retention of configuration at the site of carbonyl oxygen addition rather than desired inversion. By increasing the rate of nucleophilic addition relative to the rate

of ion pair separation with a more nucleophilic carbamate **21**, the desired *trans*-fused bicyclic product **24** outcompeted formation of *cis*-fused **18**.

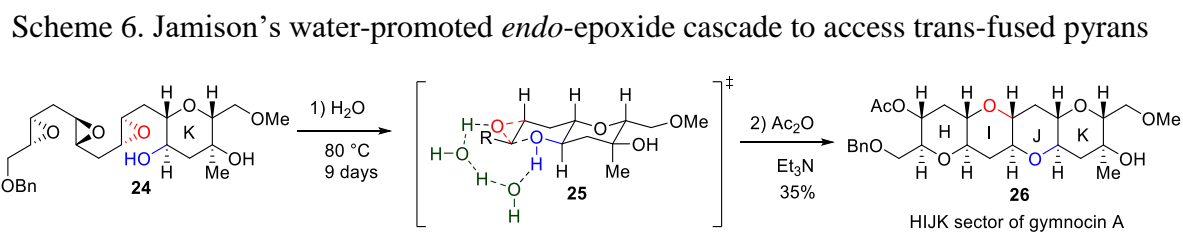
Scheme 5. McDonald's *endo*-mode polyepoxide cascade to synthesize *trans*-fused pyrans



Although McDonald's polyepoxide cascade reactions were robust for the formation of fused oxepane systems, forming the corresponding fused pyran systems was much more challenging and substrate-specific. An additional limitation of this methodology, the requirement of methyl group adjacent to the terminating nucleophile, was a restriction for both oxepane and pyran formation, and did not correspond to several of the polycyclic ether natural product structures.

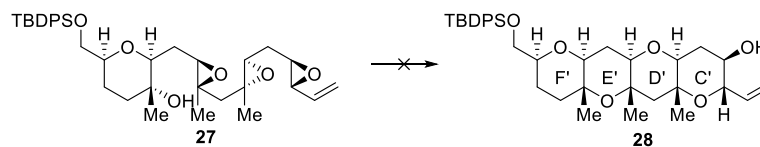
In searching for the chemical evidence for the biogenesis of these remarkable compounds, the Jamison lab has developed a templated approach that circumvents the use of directing groups to access *endo*-regioselectivity. In this templated approach, an *endo*-selective polyepoxide cascade was performed in water at neutral pH, yielding *trans*-fused tetrahydropyrans.⁵⁰ This methodology was showcased in the synthesis of the HIJK sector

of gymnocin A (**26**) in one step from triepoxide **24** (Scheme 6).⁵¹ The THP template served to pre-organize the substrate in a conformation (**25**) which biased the fused transition state in the *endo*-mode pathway, leading to the fused polycyclic ether product. Scheme 6 shows a proposed rationale for this observation in which two water molecules work cooperatively to activate and orient both the hydroxyl nucleophile and the epoxide electrophile for *endo*-cyclization.⁵⁰



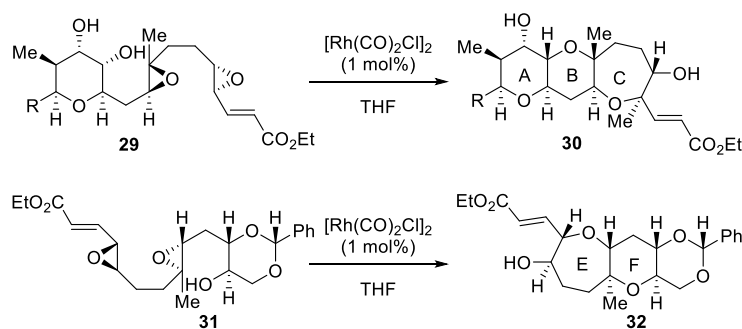
While Jamison's laboratory has successfully applied this methodology to the partial synthesis of a natural product, the methodology is limited by an inability to access oxepanes, and is not compatible with some of the alkyl substituents in many polycyclic ether natural products. Nicolaou unsuccessfully attempted to extend Jamison's templated approach to the C'D'E'F sector of maitotoxin, which has alkyl substituents at each ring fusion⁵². Despite several attempts to cyclize triepoxide **27** under various reaction conditions, fused-product **28** was not obtained from this approach. Likely the desired cyclization pathway was prohibited by unfavorable 1,3-diaxial interactions between the methyl groups on the D' and E' rings in the transition states leading to product.

Scheme 7. Nicolaou's unsuccessful extension of templated approach



Jamison recently reported the Rh(I)-catalyzed *endo*-selective epoxide-opening cascades in the formal synthesis of brevesin (Scheme 8)⁵³. Reaction of diepoxide **29** resulted in the ABC ring subsector of brevesin, **30**, through 7-*endo*, 6-*endo* tandem cyclization. Reaction of diepoxide resulted in the EF ring subsector of brevesin, **32**, through 7-*endo*, 6-*endo* tandem cyclization. Through site-specific Rh(I)-coordination of the alkenyl epoxide, both oxepane and tetrahydropyran rings have been formed in diepoxide cascades through this methodology.

Scheme 8. Jamison's Rh(I)-catalyzed *endo*-epoxide cascade to access 6- and 7-membered cyclic ethers



The major synthetic advances in biomimetic cascade oxacyclization provided primarily by the Jamison and McDonald laboratories have yet to produce satisfactory chemical evidence to confirm the Nakanishi hypothesis. The existing methodology has limitations in ring size and substitution patterns which fail to accommodate all the

complexities of the natural products. The Jamison laboratory's templated polyepoxide methodology allows access to unsubstituted polypyran core structures, while the McDonald laboratory's complementary approach is successful in synthesizing polyoxepanes with specific alkyl substitution patterns. While the feasibility of *endo*-mode polyepoxide cyclization as a method to prepare natural products has been successfully demonstrated, entirely *endo*-selective approaches are limited in substrate scope. On-going work in this area offers exciting developments which refine the necessary parameters for successful chemical synthesis of fused polycyclic ether natural products.

1.1.4 Brevenal

The marine dinoflagellate *Karenia brevis*, responsible for red tide events, produces several polyether natural products in addition to the neurotoxic brevetoxin B (**1**, Figure 1) and brevetoxin A (**2**, Figure 2). Although the brevetoxins are responsible for red tide poisoning events, in 2004 a pentacyclic member of this family capable of counteracting the neurotoxic effects of the brevetoxins was discovered and characterized as brevenal (**6**, Figure 2)³. Brevenal competitively displaces brevetoxin in a synaptosome receptor binding assay that evaluates sodium channel receptor site binding for natural brevetoxins⁵⁴. Brevenal has also been shown to exhibit improved biological activity over amiloride, a sodium channel blocking therapeutic for treatment of cystic fibrosis.⁵⁵ Brevenal is non-toxic and has a pentacyclic polyether core consisting of *trans*-fused six- and seven-membered rings. Due to its relatively small size and interesting biological activity, structural analogs may find use as a potential therapeutic agent.

1.1.5 Synthesis of brevenal

Brevenal (**6**, Figure 2) has been synthesized by three separate laboratories in five reported syntheses. The first chemical synthesis was reported by Sasaki in 2006,⁵⁶ correcting the stereochemical assignment of the tertiary alcohol on the E ring on two years after the isolation and structural elucidation were reported⁵⁷. Refined over three generations, as of 2011, gram-scale quantities of the pentacyclic core are now accessible^{58,59}. Total syntheses of brevenal have also been reported by Kadota and Yamamoto in 2009⁶⁰, and Rainier in 2011⁶¹.

Sasaki's retrosynthetic analysis of the brevenal core from the third generation of synthesis is shown in Figure 3⁵⁹. As with all synthesis discussed, the two side chains were installed late stage after completing the polycyclic ether core **33** using Wittig olefination and Stille coupling⁵⁹. The pentacyclic core was constructed from Suzuki-Miyaura coupling between AB ring borane **34** and DE ring enol phosphate **35** followed by A-ring closure *via* mixed-thioacetalization and methylation. AB fragment **36** was synthesized through Suzuki-Miyaura coupling of borate **38** with B-ring enol phosphate **39**, which was synthesized from oxidative lactonization of diol **37**. The B ring oxepane was formed through oxidative lactonization of diol **42**. DE fragment **35** was synthesized through oxidative lactonization of diol **37** followed by enol phosphate formation. Diol **37** arose from Suzuki-Miyaura coupling of E ring enol phosphate **41** with borane **42**. Oxidative lactonization of diol **43** formed the E ring, which was converted to enol phosphate **41**. Overall, the Sasaki laboratory prepared pentacyclic core **33** in gram-scale quantities with a longest linear sequence of 34 steps.

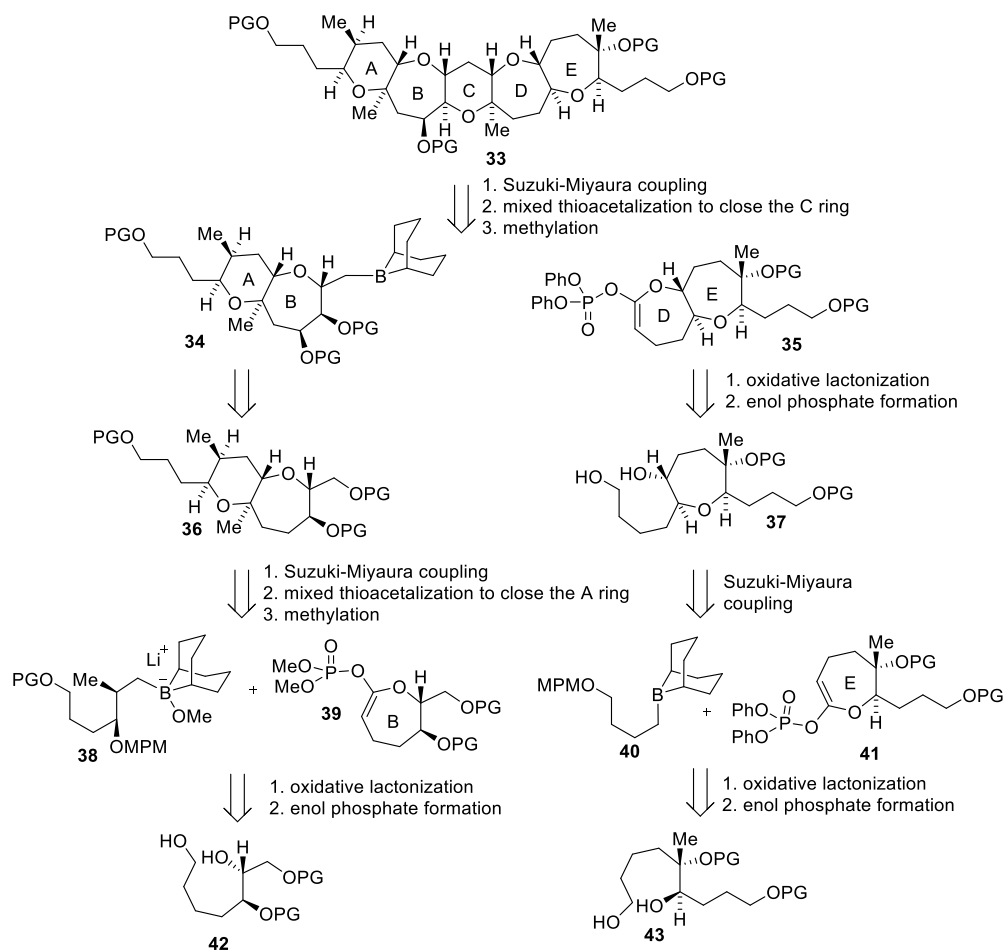


Figure 3. Sasaki's retrosynthetic analysis of brevenal

In 2009, Kadota and Yamamoto reported the total synthesis of brevenal^{60,62}. Their retrosynthetic analysis of the brevenal core is shown in Figure 4. As in Sasaki's synthesis, they also proposed a late stage installation of the two side chains, but with a shorter strategy using a Wittig reaction and a Horner-Wadsworth Emmons reaction respectively. In their synthesis, the pentacyclic core of brevenal **33** was completed using an intramolecular allylation of stannyl α -acetoxy ether **43** and ring-closing metathesis reaction sequence. The α -acetoxy ether **43** was synthesized from Yamaguchi esterification of alcohol **44** and acid **45**. Tricyclic compound **44** was synthesized through Suzuki-Miyaura coupling of enol

phosphate **47** with borate **46** followed by A-ring closure by mixed thioacetalization. Overall, they accessed pentacyclic core **33** in a longest linear sequence of 40 steps.

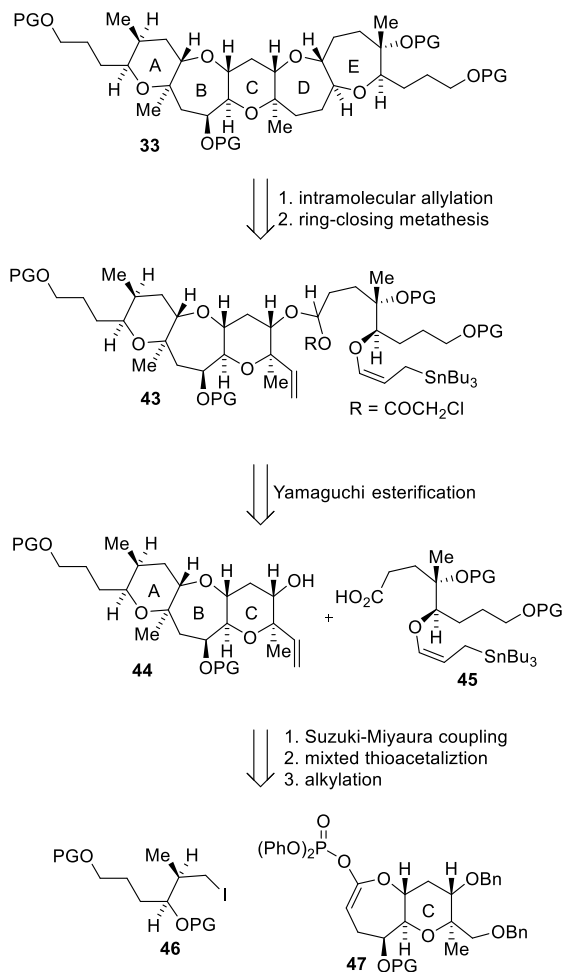


Figure 4. Yamamoto's and Kadota's retrosynthetic analysis of brevenal

In 2011, Rainier's laboratory reported the total synthesis of brevenal⁶¹. Their retrosynthetic analysis of brevenal core **33** is shown in Figure 5. They modified Kadota's and Yamamoto's procedure for late-stage installation of the side-chains onto the pentacyclic core. Brevenal core **33** is completed through reductive cyclization of compound **48** to close the D ring. The C ring was closed through an olefinic ester

cyclization of ester **49**, which was synthesized from esterification of AB ring alcohol **50** and E ring alcohol **51**. Titanium-promoted iterative cyclic enol ether/C-glycoside formation reactions were used to synthesize the A, C, and E rings. Overall, the pentacyclic core **30** was accessed in a longest linear sequence of 26 steps.

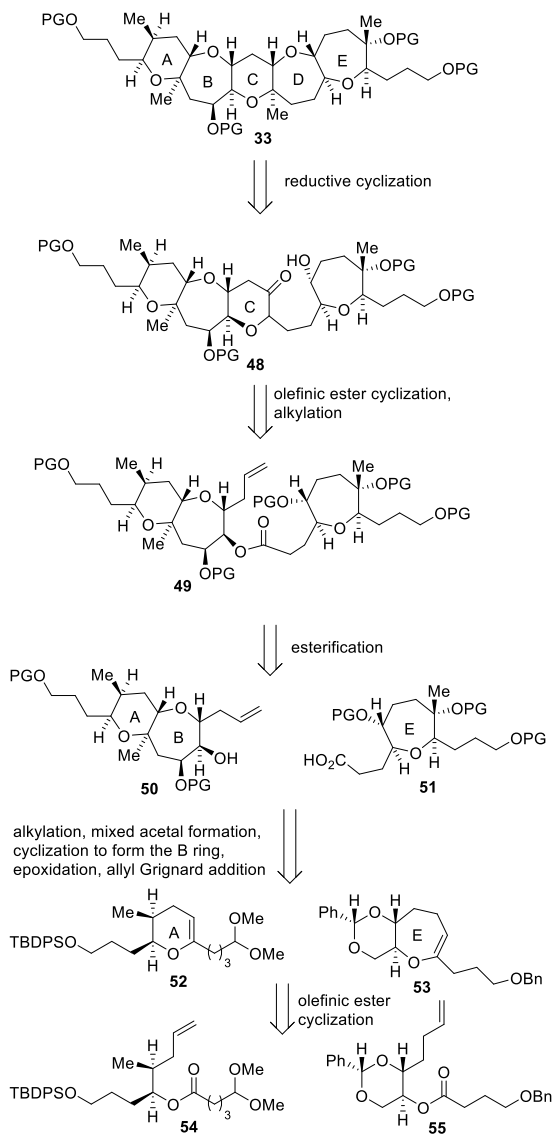


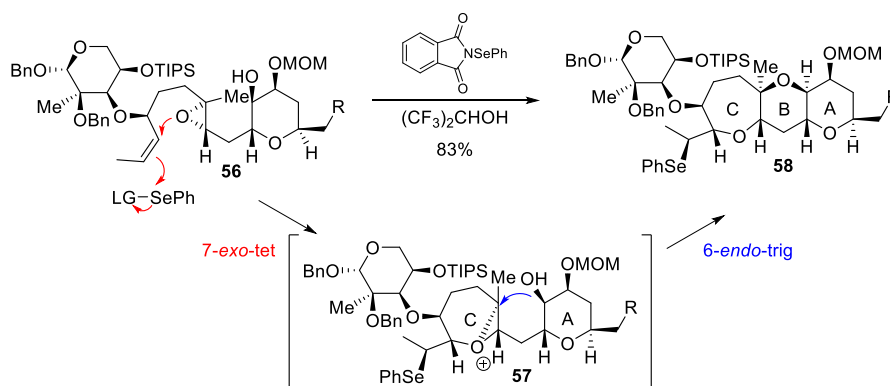
Figure 5. Rainier's retrosynthetic analysis of brevenal

1.2 Introduction

1.2.1 Exo-mode oxacyclization

In Holton's convergent synthesis of hemibrevetoxin B, a biomimetic *endo*-selective epoxy alcohol cyclization was successfully implemented (Scheme 9).⁶³ This was the first example of a total synthesis accomplished using *endo*-selective biomimetic cascade oxacyclization of an epoxide. In the key step of the synthesis, treatment of compound **56** with *N*-(phenylseleno)phthalimide induced cascade cyclization to give tricyclic compound **58** as a single diastereomer through 7-*exo*-addition of the epoxide to the selenonium, resulting in intermediate **57**. The resulting epoxonium ion then underwent 6-*endo*-addition by the alcohol nucleophile, resulting in tricyclic compound **58**. The epoxide served not only as a nucleophile to open the selenonium ion, but also as a site of electrophilic addition by the pendant hydroxyl group. While this synthesis demonstrates the efficacy of biomimetic synthesis, truly biomimetic synthesis remains far from mainstream due to the unique demands of each molecule. As it stands, entirely *endo*-selective biomimetic polyepoxide cascades have many limitations hindering their versatility, but by pairing the methodology with alternative complementary oxacyclization reactions, a broader range of natural products can be accessed.

Scheme 9. Holton's biomimetic synthesis of hemibrevetoxin B



Our goal is to develop a toolbox of diastereoselective *exo*-mode oxacyclization reactions to enable rapid and flexible synthesis of fused polycyclic ether natural products. Complementary to *endo*-mode polyepoxide cascades, we would then like to extend the various oxacyclization reactions to tandem and sequential ring-forming reactions, creating multiple cyclic ethers in a sequence of cyclization reactions from an acyclic carbon chain bearing allylic oxygen substituents for stereoinduction. Our laboratory's efforts in this area began in 2010 with postdoctoral fellow Dr. Kento Ishida's systematic study on the diastereoselectivity of electrophile promoted oxacyclizations of 1,4-dihydroxy-5-alkenes, resulting in 3-hydroxytetrahydropyran rings.⁶⁴ In the following chapters, two different approaches to access fused polycyclic ether rings inspired by Dr. Ishida's work will be described. Chapter 2 will discuss catalytic reductive oxacyclization of alkyne substrates. Chapter 3 will discuss oxacyclization of alkene substrates as applied to the synthesis of the ABC tricyclic subsector of the brevetal core.

Chapter 2. Mercury-promoted reductive oxacyclization reactions of alkynyl alcohols

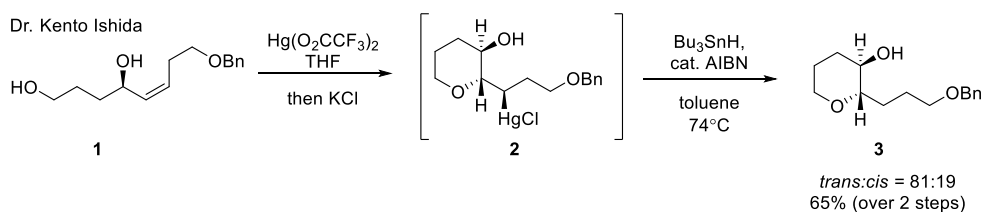
Chapter 2. Mercury-promoted reductive oxacyclization reactions of alkynyl alcohols

2.1. Introduction and Background

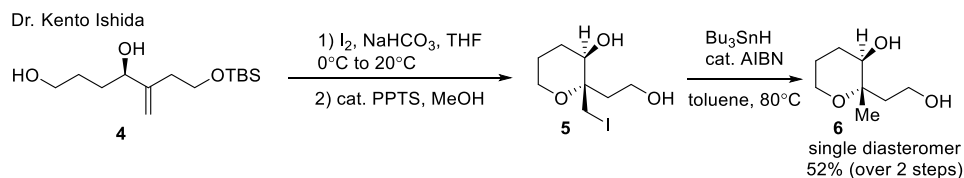
2.1.1 Motivation for catalytic mercury-promoted oxacyclization

The McDonald laboratory began investigating a novel *exo*-mode approach for synthesizing *trans*-fused cyclic ethers in 2010 with postdoctoral fellow Dr. Kento Ishida. The *trans*-terminology refers to the adduct resulting from *anti*-addition, with substituents in thermodynamically favorable equatorial positions. He examined the regio- and diastereoselectivity of various electrophile-promoted oxacyclization reactions of 1,4-dihydroxy-5-alkene substrates, furnishing 3-hydroxytetrahydropyrans.⁶⁴ Iodine, mercury, and selenium were used to promote cyclization of alkenes with various substitution patterns that shared a common allylic oxygen substituent, which was found to influence the diastereoselectivity of the cyclization reactions. Mercury (II) (Scheme 10), iodine (Scheme 11), and selenium (Scheme 12) were found to promote 6-*exo*-trig cyclization, forming tetrahydropyrans from 1,2-disubstituted alkenes (**1**), 1,1-disubstituted alkenes (**4**), and trisubstituted alkenes (**7**) with varying diastereoselectivities.

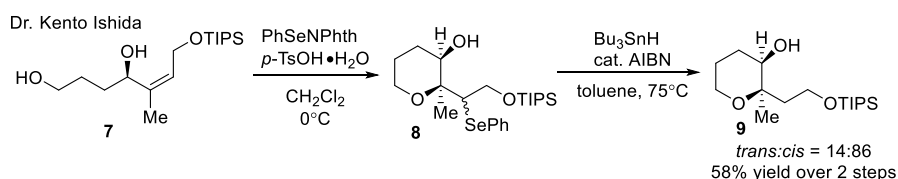
Scheme 10. Mercury (II) promoted cyclization of 1,2-disubstituted alkene **1**



Scheme 11. Iodine promoted cyclization of 1,1-disubstituted alkene **4**



Scheme 12. Selenium promoted cyclization of trisubstituted alkene **5**



Particularly notable was the superior *trans*-selectivity observed from oxacyclization of 1,2 -cis disubstituted alkene **1** with stoichiometric mercury (II), resulting in tetrahydropyran **3**. While the results were promising, the requirement of stoichiometric toxic mercuric trifluoroacetate and tributyltin hydride required for this methodology was a limitation, especially in the context of polycyclization sequences. Therefore, we became interested in extending this methodology to oxacyclization promoted by substoichiometric mercury. Not only would such a method decrease the requisite amount of mercury, turnover of the metal would obviate the need for a separate reduction of the organomercury

intermediate using trialkyltin reagents. With the development of such methodology, polycyclization would become more feasible.

2.1.2 Mercury(II) triflate promoted oxacyclization

Soft Lewis acids such as mercury(II), copper(I), gold (I), gold(III), and platinum(II) exhibit powerful π -electrophilicity, which can enable remarkable transformations under mild reaction conditions.^{65,66} These soft Lewis acids, also referred to as π -Lewis acids, form activated complexes with unsaturated carbon groups. In contrast, hard Lewis acids, sometimes referred to as σ -Lewis acids, form activated complexes with carbonyl and imine groups. Many transition metal salts exhibit both types of reactivity, with Pt(II) and Au(I) being particularly notable in this regard.⁶⁷⁻⁶⁹ Our laboratory's previous work on *endo*-mode polyepoxide cascades utilized oxophilic Lewis acids (BF₃, La(OTf)₃) to activate the oxygen of an epoxide for *endo*-mode nucleophilic addition (this is discussed in Chapter 1.1.3).⁷⁰⁻⁷² In our complementary *exo*-mode approach to synthesize fused polycyclic ethers, we planned to use a π -carbophilic Lewis acid to activate a site of unsaturation for *exo*-mode nucleophilic addition, with the goal of synthesizing multiple *trans*-fused polycyclic ether rings.

Oxacyclization reactions are intramolecular electrophilic alkene hydration reactions which result in Markovnikov addition of X-OH across the unsaturation. Brønsted acid hydration of an alkene or alkyne results in the 1,2-addition of the elements of H₂O across the unsaturation. Requiring harsh acidic conditions which are incompatible with

many functional groups, the reaction proceeds through a carbocation intermediate which is susceptible to rearrangements. Oxymercuration-demercuration provides a milder way to conduct the same overall transformation. Replacement of the proton of the acid by isolobal Hg^{II} results in *trans*-addition of Hg-OH across the unsaturation, forming reaction products with the same selectivity as Brønsted-acid promoted reactions, but under much milder reaction conditions.⁷³ The “soft” mercury(II) ion has a d^{10} electronic configuration, and although its coordination numbers can range from two to eight, it does not exhibit a strong geometry preference.⁷⁴ Switching from Brønsted acid to Lewis acid catalysis, the same reactions occur under milder conditions. The “soft” character of the polarizable π -Lewis acid exhibits a greater affinity for the substrate than a “harder” proton, enabling selective activation. The product of oxymercuration is a stoichiometric organomercury adduct, which then must undergo reduction to the corresponding alkyl group in a separate demercuration step. The polycyclic ether rings we are interested in synthesizing are not accessible by Brønsted acid catalysis alone, due to the prevalence of acid-promoted side-reactions. Through electrophilic activation of the unsaturation with mercuric reagents, we may synthesize the desired fused polycyclic ether rings under relatively mild reaction conditions.

Oxymercuration-demercuration reaction sequences are synthetically useful as a regio- and diastereoselective method of forming 5- and 6- membered cyclic ethers.^{75–82} While oxymercuration allows for more general application of alkene hydration reactions on acid-sensitive substrates, such as the fused polycyclic ether we are investigating, a limitation of this method is the requirement for stoichiometric mercury, and oftentimes, the

need for stoichiometric tin to reduce the organomercurial intermediate. The vast majority of oxymercuration reactions of alkenes require stoichiometric mercury due to the kinetic stability of the Csp^3 -Hg bond of the organomercurial intermediate, which prohibits protodemercuration.^{83,84}

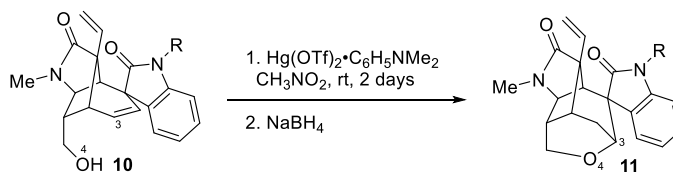
Traditionally, mercuric acetate and mercuric trifluoroacetate have been employed in intramolecular oxymercuration-demercuration reactions.⁷⁵⁻⁸² Mercury (II) trifluoromethanesulfonate ($Hg(OTf)_2$) was developed as an olefin cyclization reagent^{85,86} by Nishizawa in 1983⁸⁷ and has since found use as an oxymercuration catalyst.⁸⁷⁻⁸⁹ $Hg(OTf)_2$ has seen broader applications than classical acetoxy and trifluoroacetoxy $Hg(II)$ reagents. Mercuric triflate is often complexed with a bulky, non-nucleophilic base to attenuate reactivity and shift the equilibrium of the reaction towards cyclized products.^{85,87} Complexation with a base decreases the electrophilicity of the metal, often allowing for greater selectivity. Selective ligation with a base is especially important with cyclizations of internal acetylenes, which are sterically larger and less reactive toward cyclization. Consequentially, more electrophilic metal centers are necessary to effect these reactions.⁹⁰

Mercuric triflate exhibits increased reactivity (which can be attenuated by complexation to a base) compared to mercuric acetate and mercuric trifluoroacetate, likely due to the weakly-coordinating triflate counterion. The conjugate acid of the triflate counterion, triflic acid, has a pK_a of -14 in H_2O . Triflic acid is a much stronger acid than acetic acid ($pK_a = 4.76$ in H_2O) or trifluoroacetic acid ($pK_a = +05$ in H_2O). During a typical

cycloetherification reaction, the counterion becomes protonated, forming catalytic acid. In suitable substrates, catalytic triflic acid is competent to affect protodemercuration, which has rarely been observed with mercuric acetate⁸⁴ and mercuric trifluoroacetate. Through controlled generation of catalytic amounts of triflic acid, acid-promoted side reactions are minimized.

A notable use of mercuric triflate in complex molecule synthesis is in the synthesis of the natural product gelsemine (**11**), shown in Scheme 13. Oxymercuration of intermediate **10** with $\text{Hg}(\text{OTf})_2 \cdot N,N\text{-dimethylaniline}$ proved to be the only option for forging the C₃-O₄ bond in construction of the complex ether system.⁹¹⁻⁹⁴ The organomercury intermediate was reduced to the alkane using sodium borohydride.⁹¹⁻⁹⁴ Speckamp, Fukuyama, and Danishefsky all relied on this transformation in their syntheses.

Scheme 13. $\text{Hg}(\text{OTf})_2$ -promoted oxacyclization to form the tetrahydropyran in gelsemine

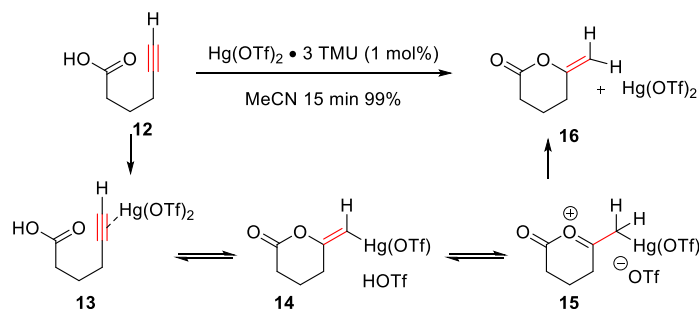


2.1.3. Catalytic mercury: demercuration

Mercuric triflate is unique in its ability to effect protodemercuration on several suitable substrates. A representative example of catalytic oxacyclization-protodemercuration using mercuric triflate on an alkyne substrate is described in Scheme

14.⁹⁵ The reaction of $\text{Hg}(\text{OTf})_2$ with alkyne **12** formed π -complex **13**. Oxacyclization resulted in vinylmercuric intermediate **14**. Protonation of enol ether **14** with *in-situ* generated triflic acid allowed formation of oxocarbenium ion **15**, which was able to donate electrons, facilitating smooth demercuration to furnish 6-*exo* product **16**, along with regenerating the catalyst, thereby establishing a catalytic cycle.

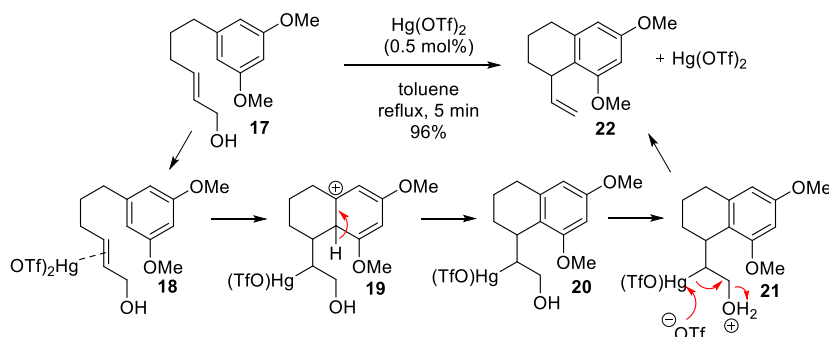
Scheme 14. $\text{Hg}(\text{OTf})_2$ -catalyzed oxacyclization and protodemercuration of alkyne **12**



While vinyl mercury intermediates such as enol ether **14** are able to undergo protodemercuration^{96–98}, the corresponding reaction on an olefin substrate rather than an alkyne substrate requires stoichiometric mercury because of the stable $\text{sp}^3\text{C-Hg}$ bond in the product, which would not undergo facile protodemercuration. A strategy developed to achieve catalytic cyclization on alkene substrates (through protodemercuration of $\text{sp}^3\text{C-Hg}$ bonds) involves introduction of an oxygen-based functional group at the allylic position for the protonation site. This strategy has been effective in facilitating smooth demercuration.^{99–101} In the $\text{Hg}(\text{OTf})_2$ catalyzed arylenene cyclization of substrate **17** (Scheme 15)⁹⁹, Friedel-Crafts type cyclization of π -complex **18** resulted in carbocation **19**, which rapidly rearomatized to form compound **20**. Protonation of the hydroxyl of

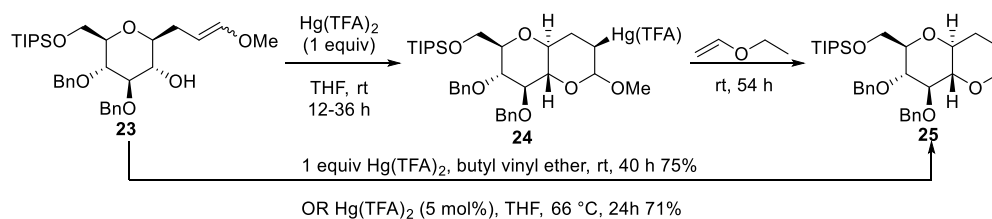
organomercuric intermediate **20** by *in-situ* generated triflic acid formed oxonium ion **21**, which underwent demercuration to afford product **22**, while regenerating the Hg(OTf)₂ catalyst.

Scheme 15. Hg(OTf)₂-catalyzed oxacyclization and protodemercuration of alkene **17**



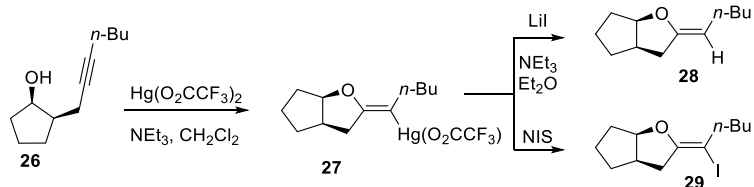
In a related transformation, Tan and Schreiber utilized substoichiometric mercury(II)-promoted cyclization as a means of forming bicyclic dihydropyrans (Scheme 16).¹⁰² Initial oxymercuration of substrate **23** resulted in isolation of organomercurial intermediate **24**, which underwent intermolecular mercury-catalyzed transesterification with the butyl vinyl ether solvent, resulting in *trans*-fused adduct **25**. Remarkably, they found that simply by refluxing the reaction in THF without the butyl vinyl ether, using catalytic amounts of mercury, the oxacyclization reaction proceeded catalytically, furnishing 71% yield of dihydropyran **25**. Presumably, elimination of the methoxy group through a transient oxocarbenium ion intermediate was sufficient to aid in demercuration.

Scheme 16. Schreiber's intramolecular mercury-catalyzed transesterification cyclization



In a reaction closely related to our desired transformation, Schwartz reported synthesis of endocyclic enol-ethers from acetylenic alcohols (Scheme 17)⁹⁰. Treatment of alkynol **26** with stoichiometric mercuric trifluoroacetate and base resulted in organomercurial intermediate **27** through 5-*exo* cyclization. Demercuration, likely aided by an oxocarbenium ion intermediate, resulted in enol ether **28**, or iodo-substituted halo-ether **29** when quenched with an electrophilic source of iodine. In this example, an exocyclic enol ether is isolated from *in-situ* demercuration.

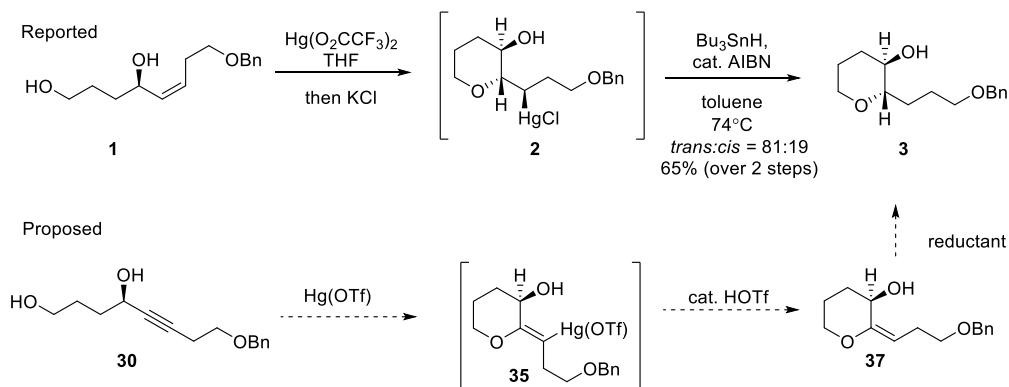
Scheme 17. Schwartz's mercury-promoted oxacyclization of alkynyl alcohol **26**



From reviewing the literature, we hypothesized that by using alkyne **30** with mercuric triflate, rather than 1,2-cis disubstituted alkene **1** with mercuric trifluoroacetate⁶⁴, we could affect protodemercuration of organomercurial intermediate **36**, resulting in

turnover of mercury and formation of exocyclic enol ether **37** (Scheme 18). We could then reduce the enol ether to form desired *trans*-fused tetrahydropyran **3**. As alkynyldiol **30** was an intermediate in the synthesis of *cis*-alkenol **1** (Dr. Ishida subjected **30** to P2-Ni reduction¹⁰³ to synthesize **1**), oxacyclization of alkynyldiol **30** would be a more efficient method to synthesize tetrahydropyran **3**. Alkynyldiol **30** was prepared as a test substrate to investigate the feasibility of mercury-promoted oxacyclization and protiodemercuration.

Scheme 18. Proposed oxacyclization of alkynol **30** to synthesize tetrahydropyran **3**

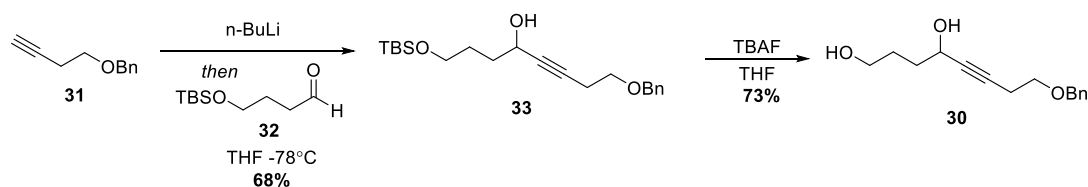


2.2. Results and Discussion

2.2.1. Synthesis of alkynyldiol **30**

Alkynyldiol **30** was synthesized through coupling of the lithium acetylide of terminal alkyne **31** with aldehyde **32**, forming racemic propargylic alcohol **33**, which underwent desilylation to afford alkynyldiol **30**, our cyclization substrate (Scheme 19).

Scheme 19. Synthesis of monocyclization substrate **30**



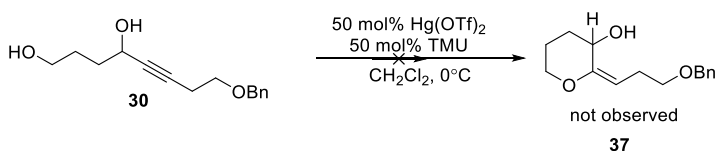
2.2.2. Reductive cyclization of alkyndiol **30**

Both mercuric triflate ($\text{Hg}(\text{OTf})_2$) and mercuric trifluoroacetate ($\text{Hg}(\text{TFA})_2$) were explored as reagents for the oxacyclization of alkyndiol **30**. Initially, we used 50 mol % mercury loading to evaluate the potential for *in-situ* protodemercuration, regenerating the active mercury species. Mercuric trifluoroacetate exhibited sluggish reactivity and with extended time (2 days) produced complex mixtures by proton NMR. Initial experiments with mercuric triflate were used in complexation with a bulky, non-nucleophilic base, as described in the literature.^{85,87,89} We knew that the allylic alcohols in Dr. Ishida's alkene substrates were sensitive to trace acid, as he observed dehydrative cyclizations in iodocyclization reactions, which were suppressed with excess base. Thus, we expected that propargyl alcohol substrate would also be susceptible to acid-promoted dehydrative cyclization. By including tetramethylurea (TMU) to neutralize triflic acid generated *in-situ*, we hoped to achieve Lewis-acid promoted cyclization through mercuric ion coordination to the alkyne.

Further cyclization attempts were carried out with $\text{Hg}(\text{OTf})_2$ and tetramethyl urea at 0°C . Initial cyclizations with 50 mol% $\text{Hg}(\text{OTf})_2$ and 150 mol% tetramethylurea in acetonitrile resulted in several spots by TLC and a very messy proton NMR (Scheme 20).

Upon switching the solvent to CH₂Cl₂, conversion to several unspecified products was seen by NMR after 20 hours, although the reaction was sluggish. Subsequently decreasing the tetramethyl urea to 50 mol% reflected the same observed reactivity as 150 mol %.

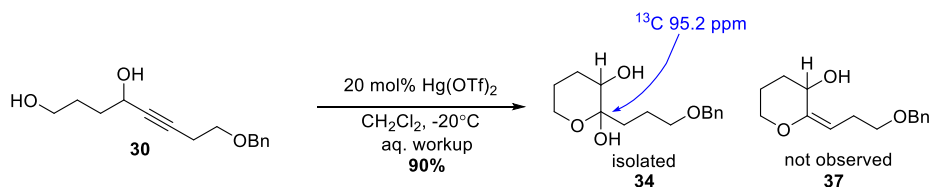
Scheme 20. Cyclization of alkynol **30** with mercuric triflate and ligated base



Exclusion of the base led to full conversion to a single less polar spot by TLC within 5 minutes (0.77 R_f in 1:1 hexanes: ethyl acetate) (Scheme 21). This was consistent with the observations of Schwartz⁹⁰, who reported that internal alkynes were less reactive towards cyclization due to the increased steric bulk over a terminal alkyne, necessitating more strongly electrophilic metal centers to effect such transformations. After aqueous workup, hemiketal **34** was isolated rather than the expected enol ether **37**. A key spectral feature was the acetal signal in the carbon at 95.2 ppm. Although HRMS did not identify the desired product (formula of C₁₅H₂₄O₄), a signal was identified associated with the formula of C₁₅H₂₂O₃, corresponding to dehydration of hemiketal **34**, which would not be unusual under ionizing conditions. Optimization of this reaction included: using degassed CH₂Cl₂, decreasing the temperature to -20 °C, and quenching with water. These changes resulted in a 90% yield of hemiketal **18** on 1 mmol scale (Scheme 21). The ligating base,

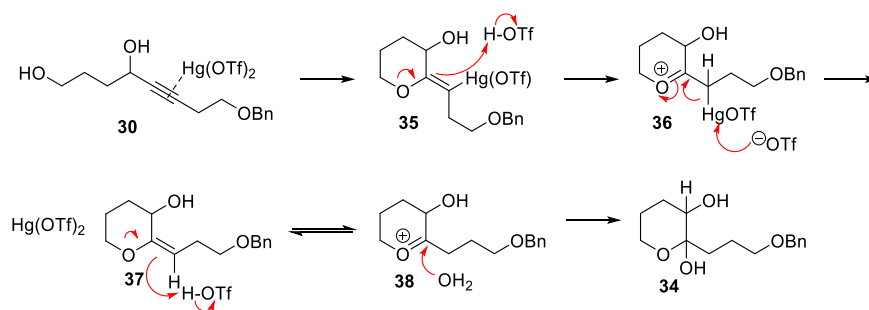
TMU, had decreased the reactivity of the mercury sufficiently to deactivate cyclization pathways entirely, including acid-promoted background dehydrative cyclization, but in the absence of TMU we could effect 6-*exo* oxacyclization with protiodemercuration of substrate **30**.

Scheme 21. Cyclization of alkynol **30** resulting in hemiketal **34**



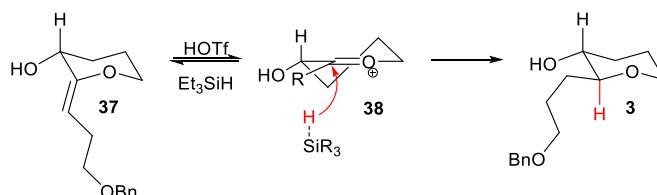
Although we did not isolate the expected exocyclic enol ether **37**, isolation of hemiketal **34** suggested intermediacy of oxocarbenium ion **38**, as desired when we designed this system. Our proposed mechanism, supported by Nishizawa⁹⁵, is shown in Scheme 22. Addition of the tethered hydroxyl nucleophile to π -complex **30**, resulted in 6-*exo* cyclization to form vinyl organomercurial intermediate **35**. Protonation of intermediate **35** with triflic acid, which was generated *in-situ*, resulted in oxocarbenium **36**. Protiodemercuration of **36** resulted in exocyclic enol ether **37**, which would be in equilibrium with oxocarbenium **38** under acidic conditions. Addition of water to oxocarbenium **38** would account for the observed product, hemiketal **34**.

Scheme 22. Proposed mechanism of formation of hemiketal **34**



Recognizing that the desired tetrahydropyran **3** could be obtained through hydride addition to oxocarbenium ion **38** instead of addition of water, we decided to add hydride to the reaction mixture. Nucleophiles are well-known to undergo axial addition to oxocarbenium ions in six-membered rings,¹⁰⁴ which yields the desired *trans*- diastereomer **3** with the hydrogens in a *trans*-diaxial configuration (Scheme 23).

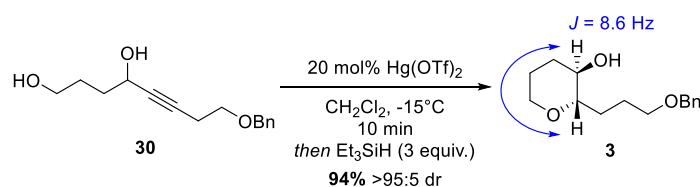
Scheme 23. Model of diastereoselectivity for hydride addition to tetrahydropyran **21**



We conducted additional oxacyclization reactions with triethylsilane as a reductant in attempts to effect a one-pot reductive cyclization to synthesize tetrahydropyran **3** from alkyne **30** (Scheme 24). Triethylsilane was added to the reaction at the same time as the mercury catalyst, causing fine grey particles to become finely dispersed in the reaction

mixture, which ultimately settled at the bottom of the flask. We suspected that the silane addition could be causing reduction of the mercury(II) salt to insoluble, inactive mercury (0). Knowing that the cyclization reaction is rapid, even at low temperature, we decided to add the silane quench a few minutes after the onset of the reaction in case the mercury was being reduced. We suspected that the starting material would exhibit undesired reactivity (dehydrative cyclization, alkyne hydration¹⁰⁵) under acidic conditions, although we required acid for reduction of the oxocarbenium ion **38**. Therefore, rapid mercuric-promoted cycloisomerization was advantageous because the acid-sensitive starting material would be consumed before acid-promoted processes could predominate, and sufficient acid would be *in-situ* to reduce oxocarbenium ion **38**. In later reactions, triethylsilane was added to the reaction after disappearance of starting material by TLC, usually after about 10 minutes. Use of 1.2 equivalents of triethylsilane resulted in a 49% yield of reduced product **3** (81:19 dr *trans*: *cis*, **22:23**) and a 35% yield of hydrated product **34** after 6 hours. Ultimately, use of 3 equivalents of silane resulted in a 94% yield of *trans*-diastereomer of reduced product **3** (>95:5 dr) after 15 hours (Scheme 24).

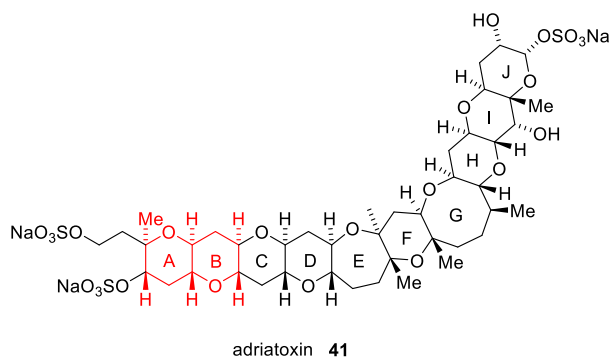
Scheme 24. Reductive oxacyclization to yield *trans*-tetrahydropyran **3**



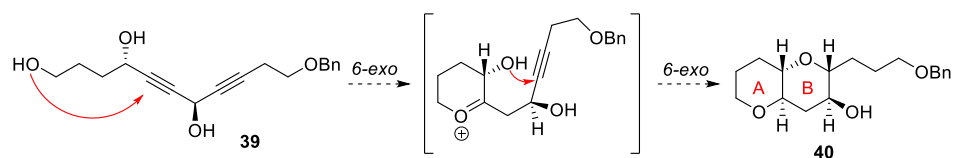
2.2.3. Synthesis of 1,4- diyne 39

With successful method for forming *trans*-fused tetrahydropyran **3**, our next goal was to extend this methodology for formation of multiple cyclic ether rings from an acyclic carbon chain. We proposed to first investigate tandem cyclization to access 6,6-fused bispyran compound **40** through tandem *exo*-mode cyclization. This motif shows up several times in the marine natural product adriatoxin (**41**). Through retrosynthetic analysis, we proposed diyne **39** as a test substrate for the tandem cyclization (Scheme 25). We hoped to synthesize *trans*-fused bispyran **40** through sequential 6-*exo* reductive oxacyclization of diyne **39** (Scheme 26).

Scheme 25. AB rings of adriatoxin **41**

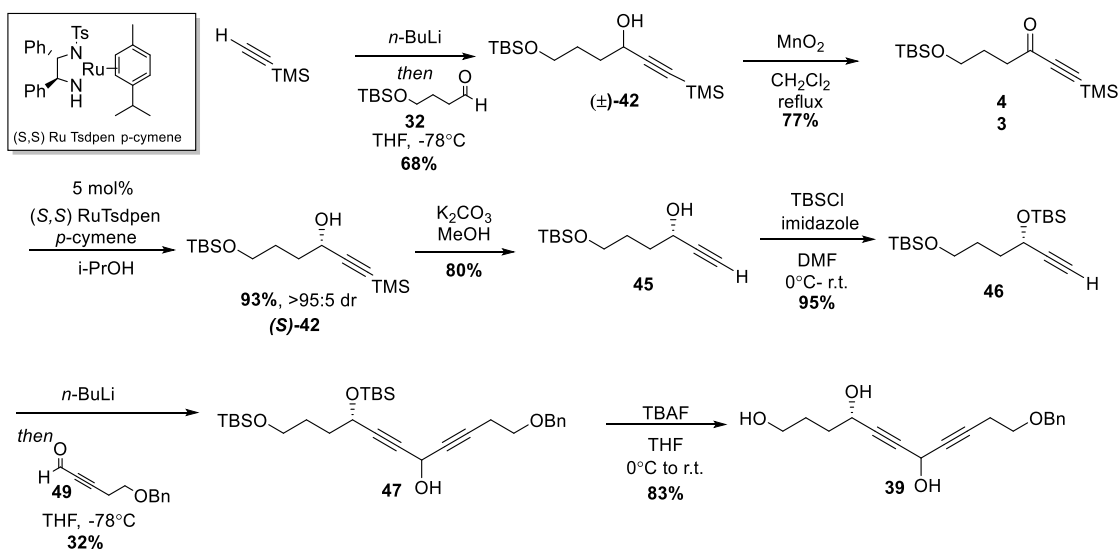


Scheme 26. Proposed tandem cyclization of diyne **39** to synthesize bispyran **40**



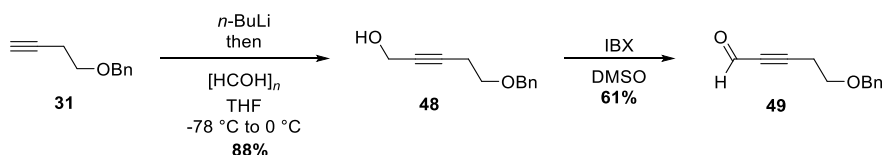
For the synthesis of diyne **39** (Scheme 27) the lithium acetylide of trimethylsilyl-protected acetylene was added to aldehyde **32**. Newly formed propargylic alcohol **42** was oxidized with MnO_2 , yielding propargylic ketone **43**. Ketone **43** underwent Noyori asymmetric reduction¹⁰⁶ to furnish the *S*-enantiomer of propargylic alcohol (*S*)-**42** in good yield and >95:5 er by Mosher ester analysis.¹⁰⁷ Deprotection of silylated alkyne (*S*)-**42** with K_2CO_3 in methanol yielded terminal alkyne **45**, which was O-silylated to form bis-silyl ether **46**.

Scheme 27. Synthesis of diyne **39**



Forming the carbon-carbon bond and setting the stereochemistry at the propargylic center was problematic. We envisioned setting this stereocenter through asymmetric alkylation. We suspected that an oxidation-reduction protocol to set the stereocenter would be ineffective due to the similarly low steric demand of both alkynes. The most promising option would be to set the bis-propargylic stereocenter and effect the carbon-carbon bond formation through Carreira's enantioselective zinc-acetylide coupling methodology using *N*-methylephedrine as the chiral ligand¹⁰⁸. Unfortunately, we were not able to access any coupled adduct from attempted Carreira alkylation of alkyne **46** with aldehyde **49** (Scheme 28). As we were working on another route at the same time in which the bispropargylic stereocenter was set at an earlier stage (Section 2.2.4), we decided to perform a *n*-BuLi coupling and move forward to cyclization reactions with the mixture of diastereomers.

Scheme 28. Synthesis of propargylic aldehyde **49**



Although coupled material was accessible through coupling of the lithium acetylide of compound **46** with propargylic aldehyde **49**, furnishing bis-propargylic alcohol **47**, it was consistently a low-yielding reaction, even after attempts at optimization. Bis-propargylic alcohol **47** was deprotected with TBAF to form triol **39**. Although the diastereomers of triol **39** were not visible by ¹H-NMR, they were visible in the ¹³C-NMR. The presence of eight carbon signals corresponding to the alkyne carbons, at δ 84.72, 84.68,

82.79, 82.75, 81.81, 78.85, 77.54, 76.91, is in accordance with the expected pair of diastereomers. Diyne **39** was used in cyclization reactions.

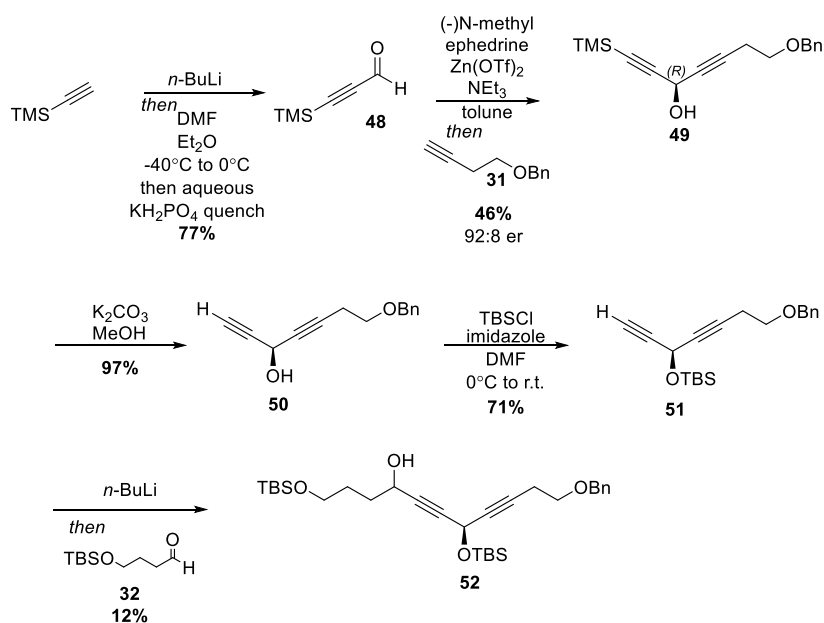
2.2.4. Alternative synthesis of 1,4- diyne 39

In the previous route (Scheme 28), we could not set the stereochemistry of the bispropargylic center due to an inability to execute late-stage enantioselective addition of alkyne **46** with propargylic aldehyde **49**. Since both sides of the bispropargylic alcohol have similar steric demands, oxidation to the acetylenic ketone and subsequent enantioselective reduction would be not effective. We decided instead to set the stereocenter earlier in the synthesis, at the stage of the first carbon-carbon bond formation, rather than later in the synthesis.

We embarked on an alternative route to see if we could set the stereocenter earlier through enantioselective addition to aldehyde **48** (Scheme 29). Formylation of trimethylsilyl acetylene formed propargylic aldehyde **48**. To our delight, Carreira coupling of terminal alkyne **31** with aldehyde **48** resulted in bis-propargylic alcohol **49** in 47% yield (92:8 er determined by Mosher ester analysis¹⁰⁷). Desilylation of alkyne **49** and silylation of the alcohol **50** furnished alkyne **51**. We attempted a second Carreira coupling of alkyne **51** with aldehyde **32** to construct the final carbon-carbon bond, but unfortunately these efforts resulted only in recovery of alkyne **51**. In the literature, Carreira coupling is limited to α -branched aldehydes, so enolizable aldehyde **32** is reasonably beyond the scope of this methodology.¹⁰⁸ (We later found a way to overcome this problem with use of a different

chiral ligand and addition of the aldehyde *via* syringe pump, discussed in Section 2.2.8.) Although we could synthesize adduct **52** through lithium acetylide addition to aldehyde **32**, the reaction was very messy and proceeded in poor yield. The risk of epimerization at the bis-propargylic position is even greater than the risk of epimerization at the singly propargylic position, a disadvantage to this route. Although we could set the bis-propargylic stereocenter in this route, we did not control the previously obtained mono-propargylic stereocenter. The final stereocenter would likely be accessible through Noyori hydrogenation, but with knowledge of the reactivity of diyne **39** (Section 2.2.5), we did not further pursue synthesis of this substrate as a single diastereomer.

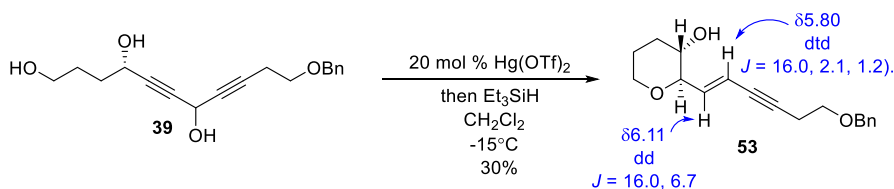
Scheme 29. Alternative synthesis of diyne **39**



2.2.5 Cyclization of 1,4- diyne **39**

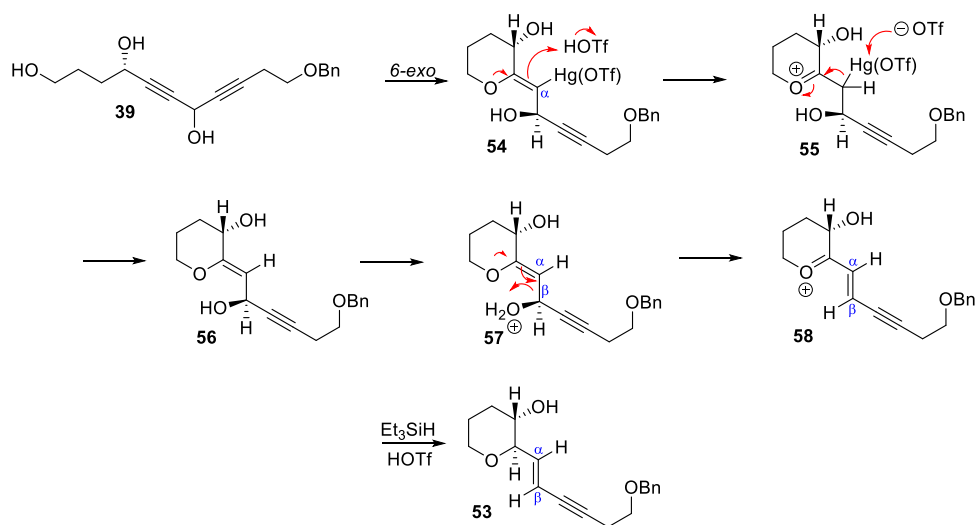
Using the same conditions as the successful reductive cyclization of **30**, we attempted tandem cyclization on diyne **39** (Scheme 30). Upon addition of the silane (6 equivalents, 15 minutes after addition of the mercuric salts), the reaction mixture turned black. Upon quenching with triethylamine, 7 hours later, the color reverted to the pale brownish yellow observed in the monocyclization reactions. The reaction proceeded several minor spots and one major spot TLC (major spot $R_f=0.81$, starting material $R_f=0.42$ in ethyl acetate). After purification, the major spot was tentatively assigned the structure of enyne **53** from $^1\text{H-NMR}$ and HRMS data. A diagnostic feature of the spectra was the *trans*-alkene of the enyne, which exhibited 16 Hz coupling.

Scheme 30. Attempted tandem cyclization of diyne **39** resulting in enyne **53**



To account for the formation of *trans*-enyne **53**, we proposed the mechanism outlined in Scheme 31. Following successful 6-*exo* cyclization of the first alkyne of diyne **39** to form intermediate **54**, protonation resulted in **55**, which underwent demercuration to afford enol ether **56**. In the presence of acid, the alcohol would become protonated, resulting in **57**, which underwent a Grob-type fragmentation¹⁰⁹ with loss of water to form oxocarbenium **58**, which was reduced to form enyne **53**.

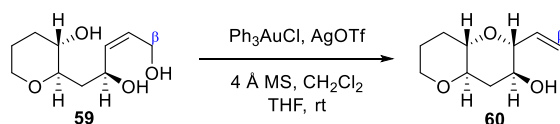
Scheme 31. Proposed mechanism of formation of enyne **53**



As discussed in Section 2.1, introduction of an oxygen-based functional group at the allylic position for the protonation site has been employed as a strategy to aide demetallation. Tan and Schreiber¹⁰² observed elimination of stable α -mercurial acetals without the need for transesterification, suggesting an equilibrium between the α -mercurial acetal, possibly passing through an oxocarbenium ion, and the saturated product. Although our system is different, the concept of such an equilibrium controlling the product distribution, leading to an unsaturation, is relevant. Additionally, in 2016, Yokoyama reported synthesis of trans-fused bispyran **60** from pyran **59** (Scheme 32)¹¹⁰. Bispyran **60** resulted from elimination of the beta-oxygen substituent, which aided in demetallation with *anti*-elimination (Scheme 32). At the time, we did not expect elimination of the beta-hydroxyl to form enyne **53**; however, after thorough examination of the literature it was not an unexpected outcome for this reaction. The beta-oxygen substituent, which would be the nucleophile for the second cyclization reaction, is incompatible with the described

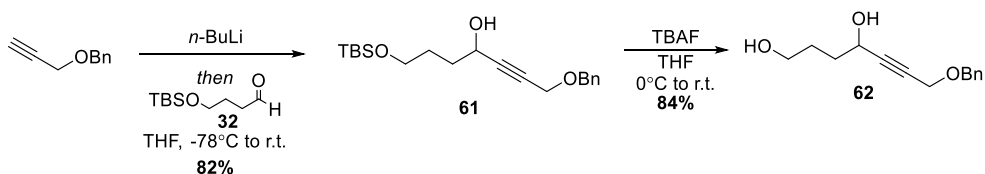
methodology. The presence of a beta-oxygen substituent is a limitation of the reductive oxacyclization methodology. Tandem 6-*exo* cyclization to form fused bispyrans from bis-alkyne substrates such as alkynol **39** is not feasible through this methodology.

Scheme 32. Yokoyama's elimination of beta-oxygen to synthesize tetrahydropyran **60**



We were curious if through use of different Lewis acids, we could prevent the elimination of the beta-oxygen substituent. Due to the complexity of diyne **39**, we synthesized alkyne **62** as a model system to study the elimination of the beta-oxygen in the bicyclization (Scheme 33). Moving the oxygen substituent over by one methylene unit, shifts the oxygen substituent to the beta-position, resulting in a suitable system to explore the elimination. Commercially available benzyl-protected propargyl alcohol was deprotonated to form the lithium acetylide before addition to aldehyde **32**. Coupling adduct **61** was desilylated to yield substrate **62**.

Scheme 33. Synthesis of model system **62**

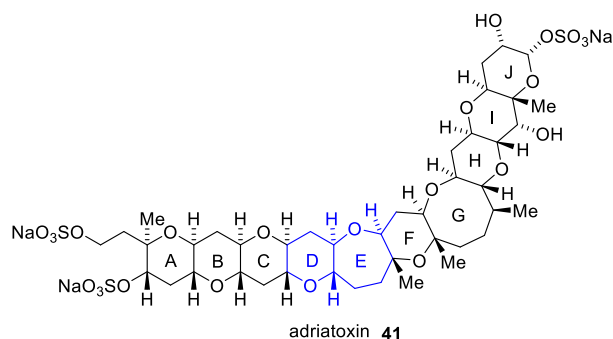


Though only differing from alkyne **30** by a single methylene group, alkyne **62** exhibited significantly different reactivity. Reaction with Hg(OTf)₂ was a messy reaction with obvious terminal alkene signals in the proton NMR, corresponding to elimination of the benzyloxy group. Several mercury, gold, and silver catalysts were explored in presence and absence of a base, but no clean reactions were obtained. Numerous products were formed in all cases, with terminal alkene visible in all crude NMR spectra. The difficulties encountered in attempted cyclizations of this substrate highlighted a limitation of the previous methodology.

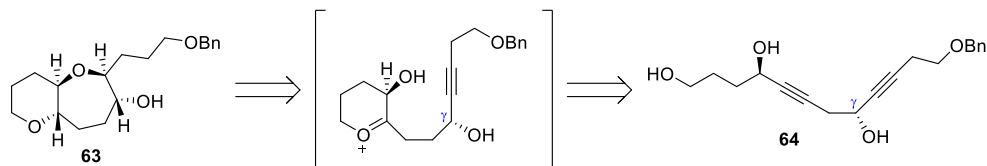
2.2.6 Synthesis of 1,5-diyne 64

As the beta-oxygen substituents in substrate **39**, which are required for synthesis of 6,6-fused bicyclic product **34**, presented a limitation of the mercury-promoted oxacyclization methodology due to their susceptibility to elimination, we decided to attempt to extend this methodology to 6,7-bicyclic systems in order to evaluate the systems' potential for sequentail cyclization. The 6,7-*trans* fused motif also shows up in the DE ring system of the marine natural product adriatoxin (**41**) (Scheme 34). We hypothesized that by moving the oxygen substituent to the γ -position, the elimination pathway would be deactivated, resulting in cyclization with protiodemercuration. Through retrosynthetic analysis, we proposed diyne **64** as a test substrate for the tandem cyclization (Scheme 35). We aimed to form *trans*-fused 6-*exo*,7-*exo* adduct **63** through sequential reductive oxacyclization of diyne **64**.

Scheme 34. DE rings of adriatoxin **41**



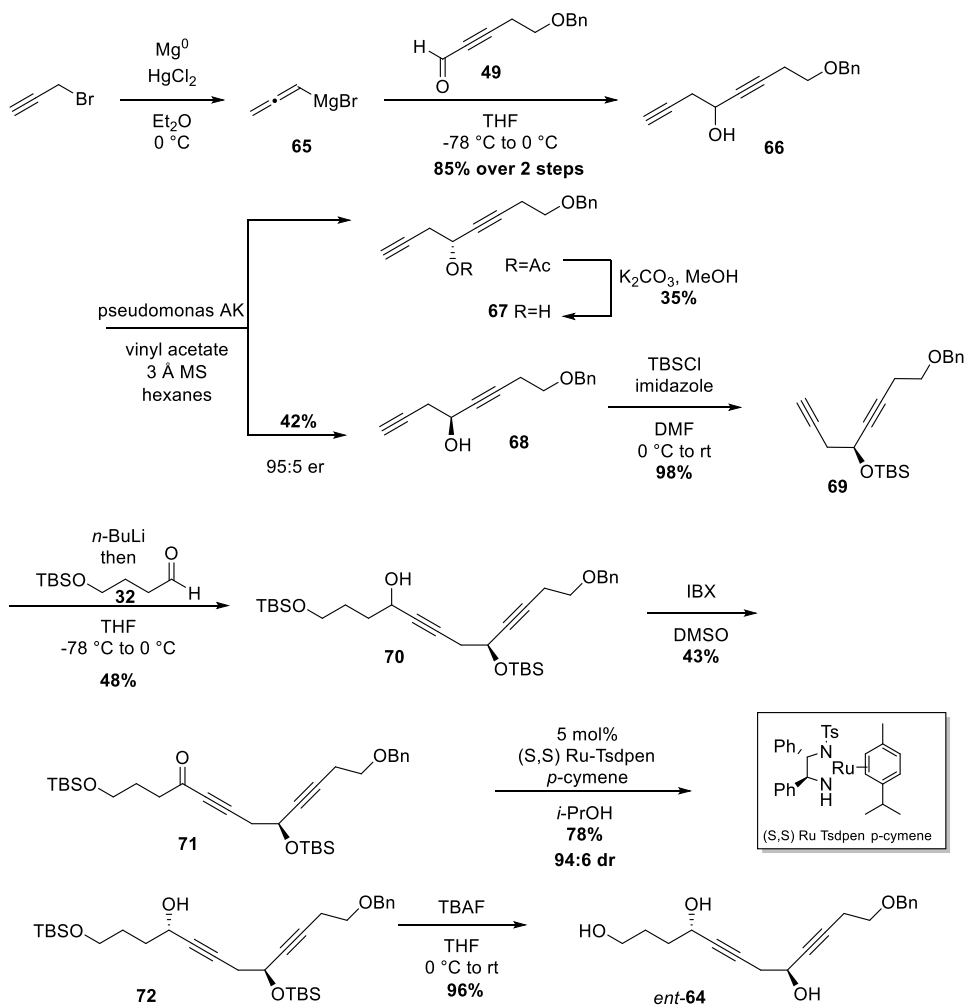
Scheme 35. Proposed bicyclization of diyne **64** to synthesize 6,7-bicyclic product **63**



Synthesis of diyne **64** began with addition of propargyl Grignard reagent **65**¹¹¹ to alkyne aldehyde **49** furnishing diyne **66** (Scheme 36). Enzymatic resolution¹¹² of diastereomeric alcohol **66** allowed access to both stereoisomers separately. Both **67** and **68** were carried forward separately through the sequence described in Scheme 36 to afford **64** and *ent*-**64**, respectively. The route to *ent*-**64** from **68** is described due to superior documentation, although the cyclization of diyne **64** is depicted, as the product matches the enantiomer described later in this document. Both *ent*-**64** and **64** underwent cyclization with similar results, affording bispyran *ent*-**73** and **73**, respectively. Silylation of (*S*)-alcohol **68** furnished alkyne **69**. The lithium acetylide of **69** was added to aldehyde **32**, yielding alcohol **70**, which had the entire carbon skeleton of diyne *ent*-**64**. Oxidation of the alcohol to ynone **71** and subsequent Noyori reduction¹⁰⁶ of the ketone set the second

stereocenter, resulting in compound **72** (to afford diyne **64**, (*R,R*)Tsdpen was used). Desilylation furnished cyclization substrate *ent*-**64** as a single diastereomer. This was the first diyne test substrate with stereocontrolled synthesis of both chiral centers.

Scheme 36. Synthesis of diyne *ent*-**64**

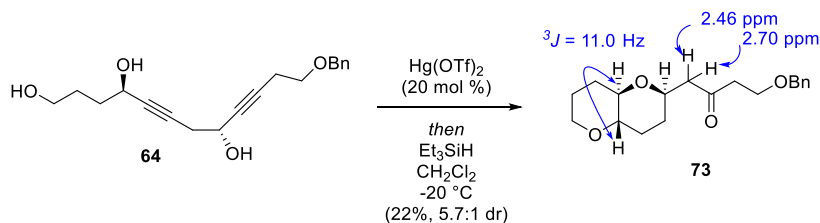


2.2.7 Cyclization of 1,5- diyne **64**

Tandem cyclization was attempted on diyne *ent*-**64** and diyne **64** using the same conditions as successful reductive cyclization of **30** (Scheme 37). The reaction proceeded

to numerous products by TLC and ^1H NMR. Although the reaction was messy, bispyran **73** was isolated as the major product in 22% yield as 5.7:1 mixture of diastereomers. At this point, the structure of product **73** was tentatively assigned by proton NMR. Notably, the protons across the ring fusion displayed a large coupling constant of 11.0 Hz, as consistent with a *trans*-orientation. The proton at the newly-formed stereocenter (identified by COSY) is hidden underneath the equatorial pyran proton, obfuscating the coupling constants. As this was an undesired product, we did not conduct further spectral analysis on product **73** at this point, although this product was fully characterized when it resulted from cyclization of alkynol **64** (Section 2.2.9). Compound **73** does not undergo acylation, supporting the proposed structure.

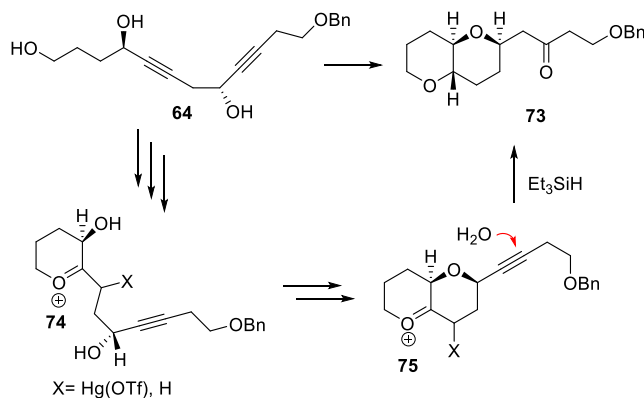
Scheme 37. Tandem cyclization of diyne **64** resulting in bispyran **73**



Our proposed mechanism for formation of bispyran **73** is shown in Scheme 38. First, desired 6-*exo* cyclization of the primary alcohol nucleophile occurred, resulting in oxocarbenium **74** (Scheme 38). At this point, Brønsted acid promoted dehydrative cyclization outcompeted the desired 7-*exo* cyclization, resulting in intermediate **75** before undergoing a regioselective alkyne hydration (likely guided by sterics) and oxocarbenium ion reduction upon addition of triethylsilane to furnish product **73**. In this proposed mechanism, it is difficult to rationalize at what step protodemercuration most likely

occurred, but if it were after the formation of intermediate **74**, the covalently bound mercury would have been unavailable to activate the second alkyne for nucleophilic addition. We speculated that slow protodemercuration compared to the acid-promoted dehydrative cyclization could account for the observation of **73**.

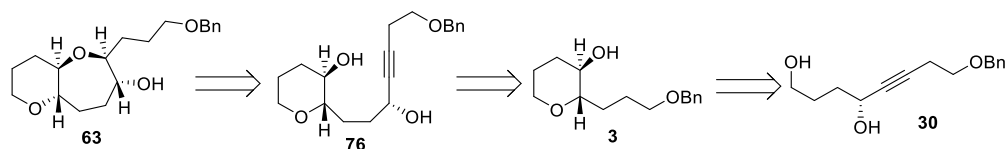
Scheme 38. Proposed mechanism of formation of bispyran **73**



2.2.8 Synthesis of tetrahydropyran- templated alkynol **76**

To investigate the second cyclization *en-route* to synthesize 6,7-bicyclic compound **63**, we prepared intermediate **76** (corresponding to hydride reduction of oxocarbenium **74**) to probe the cyclization without the complications introduced in attempted bicyclization of diynes (Scheme 39). We hoped to suppress dehydrative cyclization and determine if 7-*exo* or 8-*endo* cyclization was preferred. We prepared tetrahydropyran-templated substrate **76** from tetrahydropyran **3**, which we planned to synthesize from reductive oxacyclization of a single enantiomer of alkynol **30**.

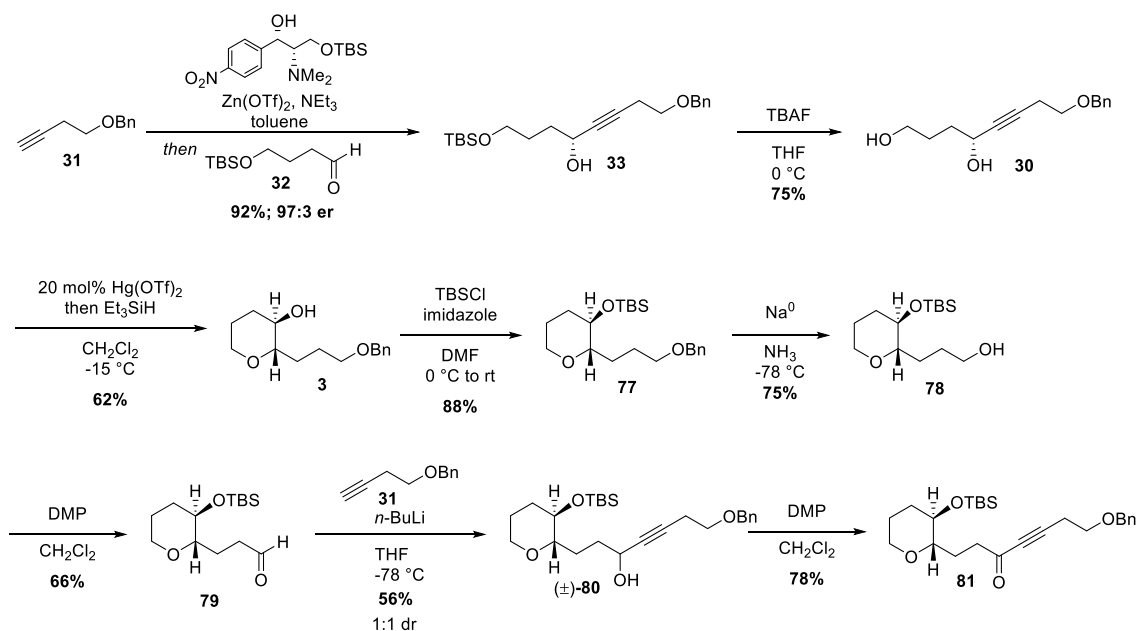
Scheme 39. Retrosynthesis of cyclization substrate **76**



We previously synthesized **30** as a mixture of enantiomers through *n*-BuLi coupling of aldehyde **32** with alkyne **31**. Instead of going through a three-step protocol involving coupling followed by oxidation to the ketone and Noyori reduction (as in substrates **42**, **52**, and **70**) we attempted enantioselective Carreira alkyne addition to alkyl aldehyde **32** to access a single diastereomer of coupling adduct in one step, but we failed to isolate any product. Likely contributing to the lack of success in these attempts is enolizable aldehyde **32**, which is outside the reported substrate scope for this methodology.¹⁰⁸ The enolizable aldehyde was rarely recovered, leading us to believe it readily participated in self-condensation reactions competitive with acetylide-addition. In the synthesis of **30**, we overcame this limitation by using an alternative chiral amino alcohol-based ligand developed by Jiang¹¹³, instead of the (+)-*N*-methylephedrine ligand employed in Carreira's work. Through use of Jiang's ligand and slow addition of the aldehyde by syringe pump, we prepared compound **33** in 92% yield with 97:3 er on a 24.8 mmol scale. Desilylation afforded alkyndiol **30**, which underwent reductive oxacyclization with mercuric triflate and triethylsilane to afford *trans*-fused tetrahydropyran **3** as a single stereoisomer (Scheme 40). Protection of the alcohol as the silyl ether (**77**) followed by lithium-ammonia hydrogenolysis of the benzyloxy protecting group afforded primary alcohol **78**, which was oxidized to aldehyde **79**. Coupling of aldehyde **79** to the lithium acetylide of **31** resulted

in propargylic alcohol (\pm)-**80** as a mixture of diastereomers. At this point, we had constructed the entire carbon-framework of the cyclization substrate. We only needed to set the stereochemistry of the propargylic alcohol to complete the synthesis of substrate for cyclization.

Scheme 40. Synthesis of substituted tetrahydropyran templated alkynol **76**

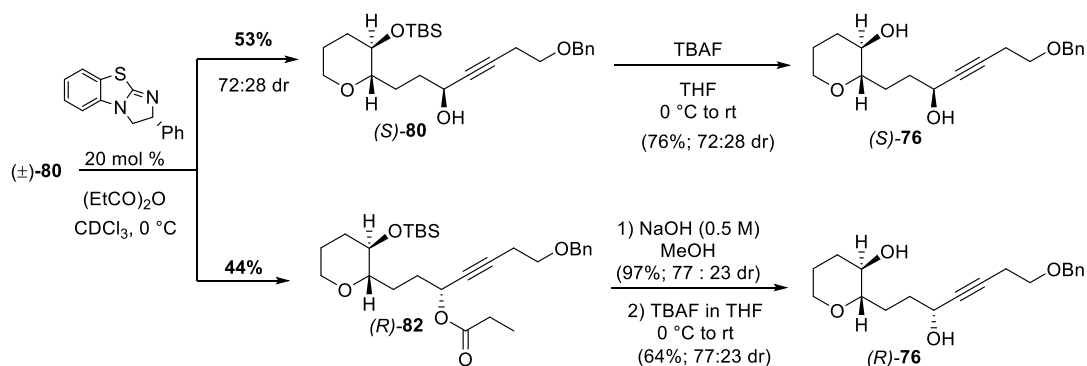


Setting the stereochemistry of propargylic alcohol (\pm)-**80** was challenging (Scheme 41). Throughout synthesis of several acyclic carbon chains, we could control stereochemistry of propargylic alcohols through an oxidation-reduction sequence using Noyori hydrogenation. This approach was unsuccessful for imparting enantioselectivity in reduction of acyclic ketone **81**. Corey-Bakshi-Shibata (CBS) reduction^{114,115}, Midland Alpine-Borane reduction¹¹⁶ were also unsuccessful in controlling the stereocenter. As we had also had recent success with enantioselective alkylation using the Jiang ligand, next

we tried the reaction with the alkyne **31** and aldehyde **79**, resulting only in recovery of alkyne **31**.

As we had not yet found satisfactory reaction conditions to access the stereodefined propargylic alcohol **80** through ynone reduction, we tried enzymatic resolution (Scheme 41). *Pseudomonas* AK, was successful in acylating acyclic ynone **66**, was not competent for acylation of cyclic compound (\pm)-**80**. Ultimately, we wound up using Birman's organocatalytic resolution using (+)-benzotetramisole¹¹⁷ facilitated acylation to access both diastereomeric alcohols with roughly 3 : 1 dr (Scheme 41). Hydrolysis of the ester and desilylation furnished the desired (*R*)-**76** (77 : 23 dr) and (*S*)-**76** (72 : 28 dr). Although the diastereoselectivity was modest, we decided to move forward with this unoptimized result to probe reactivity of substrate **76**.

Scheme 41. Synthesis of substituted tetrahydropyran templated alkynol (*R*)-**76**

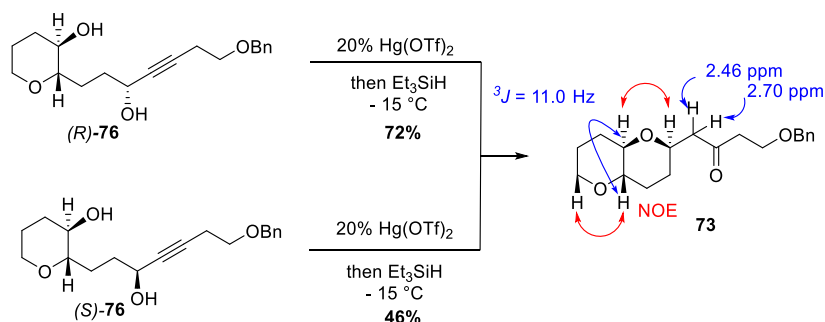


2.2.9 Cyclization of tetrahydropyran– templated alkynol **76**

We were very excited to try reductive cyclization of alkynol (*R*)-**76**. Cyclization of diyne **64** had ambiguous results. We imagined that the tetrahydropyran template of alkynol

76 would result in a cleaner, less-ambiguous reaction resulting from installation of the first tetrahydropyran ring. Initial attempts at mercury-promoted reductive oxacyclization of (*R*)-**76** resulted in 6,6-fused bispyran **73**, proposed to originate from dehydrative cyclization accompanied by alkyne hydration (Scheme 42). The same product was isolated from cyclization of the fully acyclic diyne **64**. Both diastereomers of **76** furnished the same bispyran product **73** as a single diastereomer.

Scheme 42. Initial attempts at templated cyclization of alkyne **R-76**

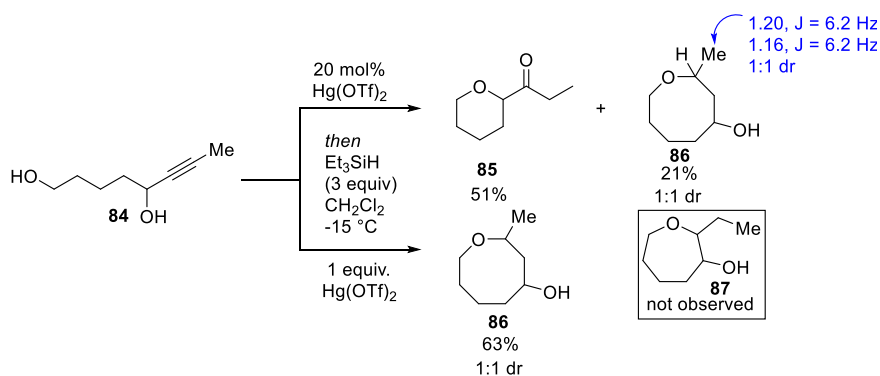


With dehydrative cyclization as the major reaction pathway for both acyclic diyne **64** and tetrahydropyran-templated alkynes (*R*)-**76** and (*S*)-**76**, we needed to suppress the dehydrative cyclization to allow other reaction pathways. As (*R*)-**76** was limited in supply due to the complexity of the molecule, we constructed a simple model system, alkyne **84** (2 steps from propyne) to allow us to investigate suppression of the dehydrative cyclization (Scheme 43).

Initial reductive cyclization reaction of substrate **84** resulted in 3 distinct spots by TLC (Scheme 43). After column chromatography, the top spot was isolated in 76% yield,

and the bottom two spots were isolated in 21% combined yield. By proton NMR, the top spot, product **85**, was consistent with the expected product of dehydrative cyclization accompanied by alkyne hydration. By proton NMR, the bottom spots were consistent with the expected spectra from 8-*endo* cyclization, oxocane **86**. The key diagnostic NMR features are methyl doublets (δ 1.20, $J = 6.2$ Hz and δ 1.16, $J = 6.2$ Hz) in a 1:1 ratio. The chemical shifts and coupling constants of these doublets and other signals are consistent with methyl substituted oxocane rings from the literature¹¹⁸ and our laboratory.¹¹⁹

Scheme 43. Model system **84** for dehydrative cyclization and oxacyclization



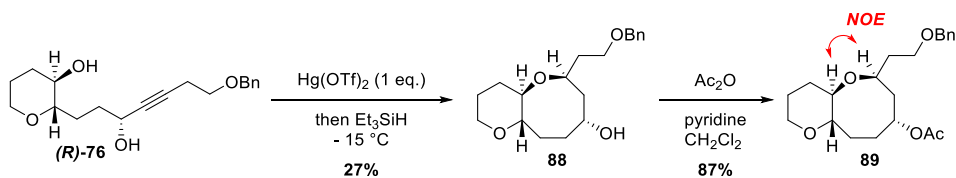
From these results, we noted that the yield of oxocane **86** reflected the catalytic loading of mercury. This led us to believe that in this system, the mercury was acting as a stoichiometric Lewis acid, furnishing oxocane **86**, but was not turning over at a rate competitive with dehydrative cyclization. We proposed protodemercuration was slower than the competitive Brønsted acid promoted dehydrative cyclization-alkyne hydration reaction. We hypothesized that by increasing the loading of the mercury, we could outcompete the undesired Brønsted acid promoted reaction pathway, allowing protodemercuration to occur after all the substrate was consumed in the Lewis acid

promoted oxacyclization. To our delight, increasing the loading of mercuric triflate to 100 mol % resulted in oxocane **86** in 63% yield, with no observation of pyran **85** by TLC or proton NMR. The reaction first went one major spot by TLC within 20 minutes (0.50 R_f in 1:1 ethyl acetate: hexanes, pink by anisaldehyde) before converting to the spots corresponding to oxocane **86** after 6 hours. Unfortunately, oxocane **86** was obtained as a mixture of diastereomers, and we did not observe any sign of desired oxepane **87**, resulting from the desired 7-*exo* cyclization, in the crude reaction mixture. Although substrate **86** demonstrated a preference for 8-*endo* selectivity over 7-*exo* selectivity under the reaction conditions described, we were curious if the same *endo*-mode selectivity would be preferred with the conformational restriction of the tetrahydropyran template in (*R*)-**76**.

Using what we learned about suppressing the dehydrative cyclization from model system **84**, we subjected substrate (*R*)-**76** to oxacyclization using a stoichiometric loading (1 equiv.) of mercuric triflate and excess silane, tentatively assigning 6,8-*trans*-fused bicyclic product **88** to the principle products (Scheme 44). The reaction went to one major spot by TLC within 15 minutes (0.69 R_f in 1:1 ethyl acetate: hexanes, light blue by anisaldehyde). After 7 hours, that spot decreased in intensity along with the appearance of additional more polar spots by TLC (R_f=0.50, pink by anisaldehyde; R_f=0.37, blue by anisaldehyde, 1:1 ethyl acetate: hexanes) after 7 hours. We separated the top spot and the bottom two spots by column chromatography. The top spot was not assignable by proton NMR, and the bottom spots appeared to be diastereomers of oxocane **88**. The two spots converged to a single spot by TLC after acetylation (**89**). The 6,8-bicyclic structural assignment was supported through a combination of COSY, HMBC, and HMQC

spectroscopy, which enabled determination of stereochemistry across the C-O-C portion of the oxocane through an apparent correlation by NOESY. The tetrahydropyran template allowed us to study the regioselectivity of the second ring closure. In summary, the undesired 8-*endo* regioselectivity predominated over 7-*exo* regioselectivity on substrate (*R*)-**76**.

Scheme 44. 8-*endo* cyclization from tetrahydropyran template (*R*)-**76**



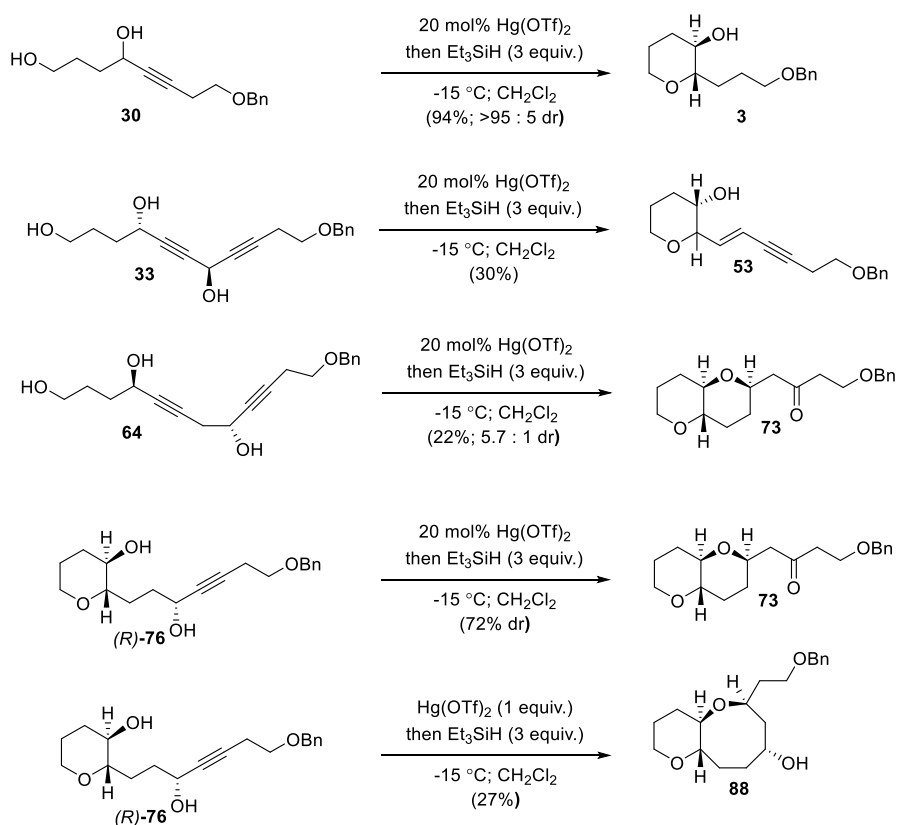
2.3 Conclusion

Although mercury-promoted reductive oxacyclization reactions provide opportunity to construct fused polycyclic ether ring systems from alkynol substrates, there are several substrate limitations which limit their synthetic utility. The mercuric ion's π -electrophilicity promotes nucleophilic attack of a tethered hydroxyl group, forming cyclic ethers, which can then be reduced diastereoselectively in tetrahydropyran systems. Alkynyldiol **30** underwent oxacyclization with substoichiometric $\text{Hg}(\text{OTf})_2$ and the resulting oxocarbenium ion was reduced diastereoselectively with Et_3SiH , furnishing *trans*-fused tetrahydropyran **3** (Scheme 45).

We attempted to apply the reductive cyclization to tandem cyclizations to form both 6,6-bicyclic ring systems and 6,7-bicyclic ring systems (Scheme 45). In investigation of

6,6-bicyclic systems, we encountered a limitation of the methodology involving incompatibility of a β -oxygen substituent with the reaction conditions due to elimination. In investigation of 6,7-bicyclic systems, we encountered a limitation of the methodology due to the preference for 8-*endo* cyclization over 7-*exo* cyclization.

Scheme 45. Mercuric ion-promoted oxacyclization and attempts at tandem cyclization



2.4 Experimental Details

^1H and ^{13}C NMR spectra were recorded on Varian INOVA 600, INOVA 400, and Bruker AVANCE 600 spectrometers. NMR spectra were generally measured from solutions of deuterated chloroform (CDCl_3), with the residual chloroform (7.27 ppm for ^1H NMR and

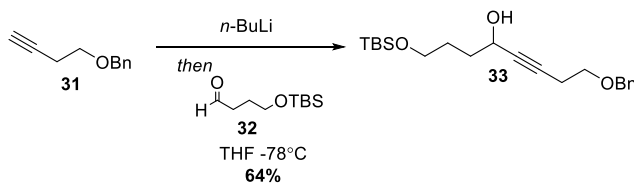
77.23 ppm for ^{13}C NMR) taken as the internal standard, and are reported in parts per million (ppm). Abbreviations for signal coupling are as follows: s, singlet; d, doublet; t, triplet; q, quartet; dd, doublet of doublet; ddd, doublet of doublet of doublet; dt, doublet of triplet; m, multiplet.

IR spectra were collected on a Thermo Scientific Nicolet iS10 FT-IR spectrometer as neat films on sodium chloride discs. Mass spectra (high resolution ESI and APCI) were recorded on a Thermo LTQ FTMS Mass spectrometer. Optical rotations were measured using a Perkin-Elmer 341 polarimeter (concentration in g/100mL). Thin Layer Chromatography (TLC) was performed on a precoated glass backed plates purchased from Silacyle (silica gel 60F₂₅₄; 0.25mm thickness). Flash column chromatography was carried out with silica gel 60 (230-400 mesh ASTM) from Silacyle.

All reactions were carried out with anhydrous solvents in oven dried and argon-charged glassware. All anhydrous solvents were dried with 4Å molecular sieves purchased from Sigma Aldrich and tested for trace water content with Coulometric KF titrator from Denver Instruments. All solvents used in extraction procedures and chromatography were used as received from commercial suppliers without prior purification.

General procedure for preparing MTPA (Mosher) ester in NMR tube: The secondary alcohol (about 0.02 mmol) was added to a dried NMR tube. (+)- or (-)- MTPACl (1 drop), pyridine-*d*₅ (3 drops), and chloroform-*d* (0.5 mL) were added in that order. The

NMR tube was shaken and left overnight. Enantiomeric ratios were determined by integration of $^1\text{H-NMR}$ of the MTPA ester.



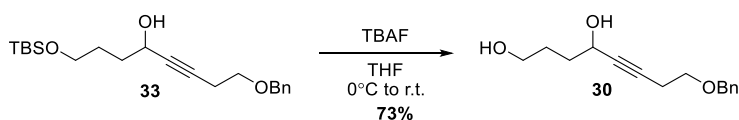
Silyl-alkynylalcohol 33: Terminal alkyne **31**¹²⁰ (5.76 g, 36.0 mmol) was dissolved in THF (90 mL) and cooled to -78°C and *n*-butyllithium (1.55 M, 21.3 mL, 33.0 mmol) was added dropwise over 10 minutes. The reaction mixture was stirred at -78°C for 10 minutes before being warmed to -40°C for 30 minutes and cooled back down to -78°C before dropwise addition of a solution of aldehyde **32**¹²¹ (6.06 g, 30.0 mmol) in THF (30 mL). The reaction was warmed to 0°C and stirred for 3 hours and then quenched with saturated aqueous ammonium chloride (10 mL). The reaction was diluted with ethyl acetate (10 mL) and the layers were separated. The aqueous layer was extracted with ethyl acetate (3 x 10 mL), and the combined organic extracts were washed with brine, dried over MgSO_4 , filtered, and concentrated under reduced pressure. The resulting oil was purified by flash column chromatography (10% EtOAc in hexanes to 20% EtOAc in hexanes) to give the propargylic alcohol **33** as a pale-yellow oil (6.94g, 19.2 mmol) in 64% yield.

ν_{max} (liquid film) 3427, 3031, 2953, 2928, 2858, 2238, 1740, 1471, 1389, 1362, 1254, 1101, 1028, 836, 777, 737 cm^{-1}

HRMS (APCI) calc'd for $\text{C}_{21}\text{H}_{35}\text{O}_3\text{Si}$ $[\text{M}+\text{H}]^+$ 363.23500, found 363.23523.

¹H NMR (400 MHz, CDCl₃) δ 7.37 – 7.28 (m, 5H), 4.55 (s, 2H), 4.41 (m, 1H), 3.67 (m, 2H), 3.59 (t, *J* = 7.2 Hz, 2H), 3.10 (d, *J* = 5.9, -OH), 2.54 (td, *J* = 7.1, 2.0 Hz, 2H), 1.87 – 1.60 (m, 4H), 0.91 (s, 9H), 0.08 (s, 6H).

¹³C NMR (101 MHz, CDCl₃) δ 138.2, 128.6, 127.9, 127.1, 82.5, 81.8, 73.1, 68.6, 63.4, 62.4, 35.7, 28.7, 26.1, 20.3, 18.5, -5.2 (2C).



Alkyndiol 30: A solution of silylated alcohol **33** (6.76 g, 17.8 mmol) in THF (180 mL) was cooled to 0°C. and tetrabutylammonium fluoride (1 M in THF, 26.8 mL, 26.8 mmol) was added dropwise. The resulting solution was warmed to room temperature and stirred for two hours. The solvent was removed under reduced pressure and the crude oil was diluted with ethyl acetate (30 mL) and saturated aqueous ammonium chloride (15 mL). The layers were separated and the aqueous later was extracted with ethyl acetate (5 x 10 mL). The combined organic extracts were washed with brine and dried over Na₂SO₄, filtered, concentrated under reduced pressure. The resulting oil was purified by flash column chromatography (70% ethyl acetate in hexanes) to give alkyndiol **30** as a viscous pale yellow oil (3.21 g, 13.0 mmol) in 73% yield.

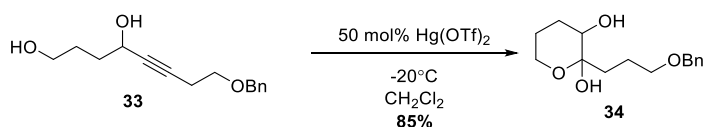
ν_{\max} (liquid film) 3345, 2930, 2865, 1453, 1363, 1093, 1027, 735, 697 cm⁻¹

HRMS (ESI) calc'd for C₁₅H₂₀O₃Na [M+Na]⁺ 271.13047, found 271.13043.

¹H NMR (600 MHz, CDCl₃) δ 7.38 – 7.29 (m, 5H), 4.56 (s, 2H), 4.45 (m, 1H), 3.68 (broad, -OH), 3.67 (m, 2H), 3.60 (t, *J* = 6.9, 2H), 2.50 (m, 2H), 1.89 (broad, (OH)), 1.72 (m, 4H).

¹³C NMR (101 MHz, CDCl₃) δ 138.1, 128.7, 128.0 (2C), 82.5, 82.2, 73.1, 68.6, 62.6, 62.3, 35.2, 28.6, 20.3.

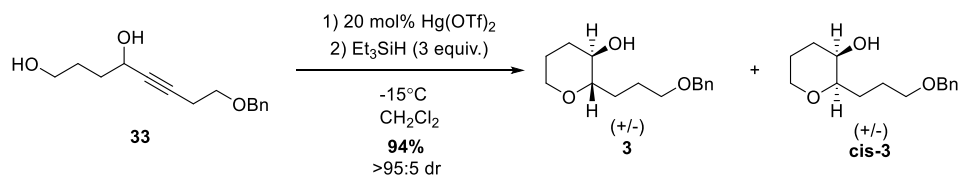
2.4.2. Reductive cyclization of alkynyldiol 33



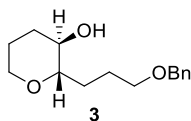
Hemiketal 34: Mercuric triflate (508 mg, 1.01 mmol) was added to CH₂Cl₂ (8 mL) and cooled to -20°C. The starting material (505 mg; 2.0 mmol) was dissolved in CH₂Cl₂ (2 mL) and added to the catalyst solution dropwise. After 15 minutes, the reaction was quenched with triethylamine (100 μL) and filtered through a pad of silica gel before being concentrated under reduced pressure. The crude off-white powder was purified by flash column chromatography (10% EtOAc in hexanes) to afford hemiketal **34** as a white powder (452 mg, 1.69 mmol) in 85% yield.

¹H NMR (600 MHz, CDCl₃) δ 7.47 – 7.08 (m, 5H), 4.52 (s, 2H), 3.94 – 3.91 (m, 1H), 3.86 (dd, *J* = 11.6, 5.0 Hz, 1H), 3.63 (td, *J* = 12.5, 2.5 Hz, 1H), 3.53 (t, *J* = 6.3 Hz, 2H), 2.00 – 1.64 (m, 5H), 1.24 – 1.16 (m, 1H).

¹³C NMR (151 MHz, CDCl₃) δ 138.6, 128.3, 127.6, 127.5, 95.2, 72.7, 70.6, 64.6, 64.0, 29.4, 26.3, 22.2, 19.2.



Hg(OTf)₂ (19 mg, 0.038 mmol) was added to CH₂Cl₂ (2 mL) and cooled to -15°C. The starting material (54.1 mg; 0.21 mmol) was dissolved in CH₂Cl₂ (1 mL) and added to the catalyst solution dropwise. After 15 minutes, the reaction was quenched with triethylsilane (130 μL). After 16 hours at -15°C, the reaction was quenched with triethylamine and filtered through a pad of silica gel before being concentrated under reduced pressure. The crude oil was purified by flash column chromatography (10% EtOAc in hexanes to 20% EtOAc) to afford the product **3** as a pale-yellow oil (50.7 mg) in 94% yield. Earlier runs of this reaction using 1.2 equivalents of triethylsilane resulted in a 49% yield of reduced product (81:19 dr, **3** : *cis*-**3**).



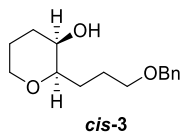
Tetrahydropyran **3**:

ν_{\max} (liquid film) 3433, 2935, 2853, 1720, 1454, 1361, 1270, 1205, 1095, 940, 737 cm⁻¹

HRMS (ESI): m/z calcd. for C₁₅H₂₃O₃ (M+H⁺) calc'd 251.16418 found 251.16417.

¹H NMR (600 MHz, CDCl₃) δ 7.31 – 7.15 (m, 5H), 4.44 (s, 2H), 3.80 (m, 1H), 3.44 (t, J = 6.3 Hz, 2H), 3.27 – 3.17 (m, 2H), 2.93 (td, J = 8.6, 2.9 Hz, 1H), 2.16 (broad, -OH), 2.02 – 1.97 (m, 1H), 1.90 – 1.84 (m, 1H), 1.79 (m, 1H), 1.67 – 1.55 (m, 3H), 1.44 (m, 1H), 1.36 – 1.25 (m, 1H).

^{13}C NMR (151 MHz, CDCl_3) δ 138.4, 128.3, 127.6, 127.4, 82.1, 72.8, 70.3, 70.1, 67.5, 32.7, 28.6, 25.6, 25.2.



Tetrahydropyran cis-3:

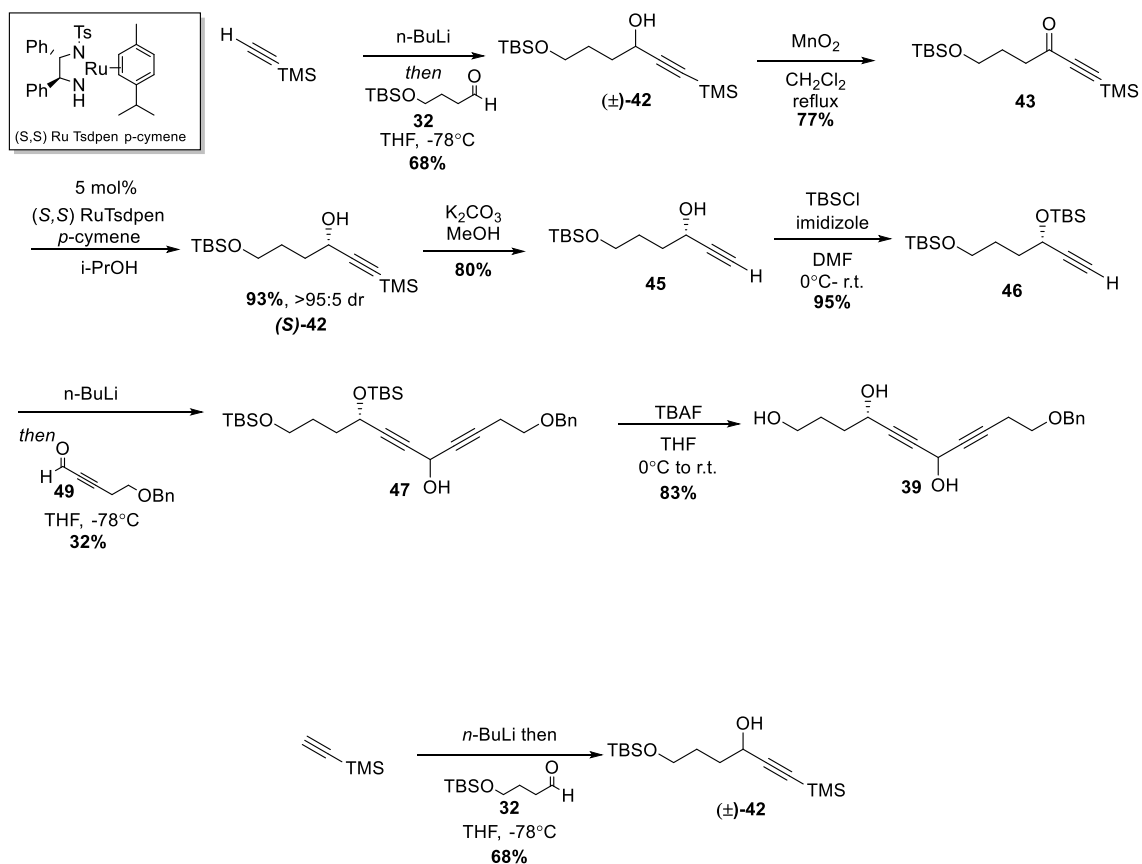
ν_{max} (liquid film) 3452, 2942, 2852, 1718, 1496, 1454, 1362, 1275, 1206, 1095, 992, 907, 738 cm^{-1}

HRMS (ESI): m/z calcd. for $\text{C}_{15}\text{H}_{23}\text{O}_3$ ($\text{M}+\text{H}^+$): calc'd 251.16417, found 251.16425.

^1H NMR (600 MHz, CDCl_3) δ 7.39 – 7.27 (m, 5H), 4.52 (s, 2H), 4.03 – 3.84 (m, 1H), 3.60 (d, $J = 4.1$ Hz, 1H), 3.53 – 3.37 (m, 3H), 3.26 (t, $J=6.2$ Hz, 1H), 2.08 – 1.79 (m, 3H), 1.77 – 1.52 (m, 6H), 1.43 – 1.31 (m, 1H).

^{13}C NMR (151 MHz, CDCl_3) δ 138.5, 128.3, 127.6, 127.5, 79.8, 72.8, 70.1, 68.5, 66.6, 30.6, 28.5, 25.7, 20.2.

Note: Much of this exploratory work was not fully optimized as the ultimate goals were not achieved. However, some of these unexpected results provide valuable insights and are archived herein.

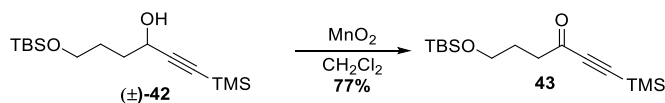


Alkynyl alcohol (±)-42: A solution of TMS acetylene (8.48 mL, 60 mmol) in THF (160 mL) was cooled to -78°C . After cooling, *n*-BuLi (21.4 mL, 2.21 M) was added dropwise. The resulting mixture was stirred for one hour before addition of aldehyde **32** (8.09 g, 40 mmol) in THF (50 mL) via cannula. The resulting mixture was stirred for 3 hours before being quenched with saturated aqueous ammonium chloride. It was then extracted with Et₂O (3x25 mL). The combined organic extracts were washed with brine and dried over MgSO₄, filtered, concentrated under reduced pressure. The crude oil was purified by flash column chromatography (6% ethyl acetate in hexanes). Adduct **42** was obtained as a clear, colorless oil (8.10 g, 27.0. mmol) in 68 % yield.

HRMS (ESI): *m/z* calcd. for C₁₅H₃₂O₂Si₂Na (M+Na⁺): 323.18331 found 322.18344.

¹H NMR (600 MHz, CDCl₃) δ 4.48 – 4.39 (m, 1H), 3.75 – 3.64 (m, 2H), 3.28 (d, *J* = 6.2 Hz, -OH), 2.06 (s, 1H), 1.88 – 1.78 (m, 4H), 1.76 – 1.64 (m, 2H), 0.92 (s, 9H), 0.17 (s, 9H), 0.09 (d, *J* = 3.1 Hz, 6H).

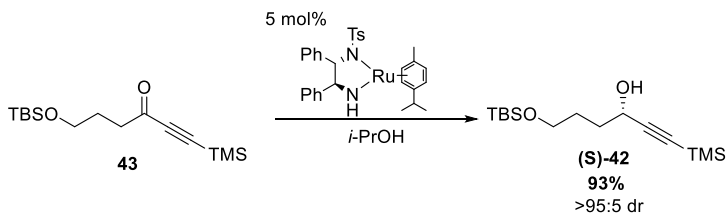
¹³C NMR (101 MHz, CDCl₃) δ 107.1, 88.9, 68.1, 63.0, 30.4, 29.7, 26.1, 21.6, 0.1, -5.2.



Ynone 43: A suspension of propargyl alcohol **42** (4.18 g, 13.97 mmol) and manganese dioxide (36.43 g, 419.1 mmol) in CH₂Cl₂ (200 mL) was gently refluxed for 16 hours. The mixture was filtered through Celite[®], washed exhaustively, and the solvent was removed under reduced pressure. The crude oil was purified by flash column chromatography (2% Et₂O in pentane). Ynone **43** was obtained as a light-yellow oil (3.20 g, 9.6 mmol) in 77 % yield.

HRMS (ESI): *m/z* calcd. for C₁₅H₃₀O₂Si₂Na (M+Na⁺): 321.16766 found 321.16776.

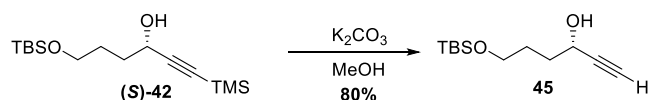
¹H NMR (400 MHz, CDCl₃) δ 3.63 (t, *J* = 6.1 Hz, 2H), 2.65 (t, *J* = 7.2 Hz, 2H), 1.97 – 1.78 (m, 1H), 0.89 (s, 9H), 0.24 (s, 9H), 0.05 (s, 6H).



Alkynyl alcohol (S)-42: The catalyst was prepared prior to reaction.^{106,122} Potassium hydroxide (31 mg, 0.54 mmol) was added to a solution of RuCl[(S, S)-NTsCHPhCHPhNH₂](η^6 -cymene) complex (384 mg, 0.54 mmol) in CH₂Cl₂ (8 mL). The reaction became dark violet in color. After the mixture was stirred at room temperature for 5 minutes, water (6 mL) was added. The layers were separated and the organic layer was washed with additional water (6 mL), and dried over CaH₂. After filtration, the solvent was removed under reduced pressure to give the Ru[(S, S)-NTsCHPhCHPhNH₂](η^6 -cymene) complex as a dark violet powder, which was used as a hydrogen transfer catalyst. The reduction was performed with freshly-made catalyst. A solution of (S, S)-Noyori catalyst (384 mg, 0.54 mmol) in CH₂Cl₂ (8 mL) was added to a solution of acetylenic ketone # (1.05 g, 10.78 mmol) in isopropyl alcohol (120 mL, degassed by sparging with argon, dried over 3Å molecular sieves). After stirring at room temperature for 20 h, the solvent was removed under reduced pressure, and the residue was purified by flash column chromatography (5% Et₂O in pentane) to afford the (S)-propargyl alcohol (3.00 g, 9.98 mmol) in 93% yield with >95:5 dr.

HRMS (APCI): *m/z* calcd. for C₁₅H₃₃O₂Si₂ (M+H⁺): 301.20136 found 301.20140.

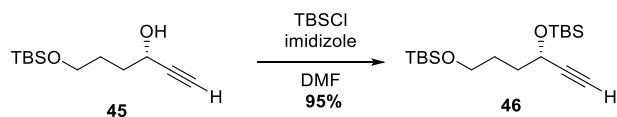
¹H NMR (400 MHz, CDCl₃) δ 4.43 (dd, *J* = 11.2 Hz, 5.5 Hz, 1H), 3.69 (m, 2 H), 3.30 (d, *J* = 6.3 Hz, -OH), 1.82 (m, 3H), 1.69 (m, 1H), 0.91 (s, 9H), 0.17 (s, 9H), 0.08 (s, 6H).



Terminal alkyne 45: Silyl-protected alkyne # (3.00g, 9.98 mmol) was dissolved in methanol (100 mL) and K_2CO_3 (1.79g, 12.07 mmol) was added. The mixture was stirred at room temperature for 3 hours. The reaction mixture was concentrated under reduced pressure before dilution of the reaction mixture with water and extraction with EtOAc (x3). The combined organic layers were washed with brine, dried over $MgSO_4$, filtered, and concentrated under reduced pressure. The residue was purified by flash column chromatography (5% EtOAc in hexanes) to yield alkyne **45** as a clear oil (1.82 g, 7.88 mmol) in 80% yield.

HRMS (APCI): m/z calcd. for $C_{12}H_{25}O_2Si$ ($M+H^+$): 229.16184 found 229.16178.

1H NMR (400 MHz, $CDCl_3$) δ 4.56 – 4.30 (m, 1H), 3.81 – 3.60 (m, 2H), 3.44 (d, $J = 6.3$ Hz, -OH), 2.44 (d, $J = 2.1$ Hz, 1H), 1.86 (m, 2H), 1.70 (m, 2H), 0.91 (s, 9H), 0.09 (d, $J = 1.5$ Hz, 6H).

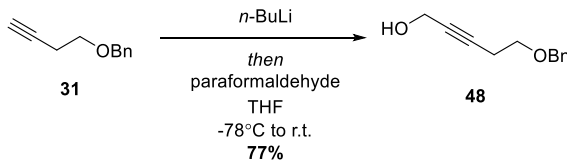


Bis-silyl ether 46: To a solution alcohol (1.80 g, 6.24 mmol) and TBSCl (1.41 g, 9.36 mmol) in DMF (20 mL) at $0^\circ C$ was added imidazole (855 mg, 12.48 mmol) in one portion. The solution was slowly warmed to room temperature and after 6 hours was quenched with water. The aqueous and organic layers were separated and the aqueous layer was extracted with Et_2O (x7). The combined organic extracts were washed with H_2O and brine before being dried over $MgSO_4$, filtered, and concentrated under reduced pressure. The residue

was purified by flash column chromatography (5% Et₂O in pentane) to yield bis-silyl ether **46** as a clear oil (2.03g, 5.92 mmol) in 95% yield.

HRMS (APCI): m/z calcd. for C₁₈H₃₉O₂Si₂ (M+H⁺): 343.24831 found 343.24861.

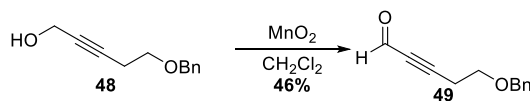
¹H NMR (400 MHz, CDCl₃) δ 4.39 (td, $J = 6.2, 2.0$ Hz, 1H), 3.65 (t, $J = 6.1$ Hz, 2H), 2.39 (d, $J = 2.0$ Hz, 1H), 1.82 – 1.59 (m, 4H), 0.91 (s, 9H), 0.90 (s, 9H), 0.14 (s, 3H), 0.12 (s, 3H), 0.06 (s, 6H).



Alcohol 48: A solution of terminal alkyne (1.70g, 10.61 mmol) in 30 mL THF was cooled to -78°C before addition of *n*-BuLi (5.30 mL, 11.67 mmol) was added dropwise. The mixture stirred at low temperature for 30 minutes before allowing the mixture to warm to 0°C and solid paraformaldehyde (642 mg, 21.22 mmol) was added. After stirring at room temperature for 5 hours the reaction was quenched with saturated aqueous ammonium chloride. The layers were separated and the organic layer was extracted with Et₂O (x3). The combined organic layers were washed with water and brine, dried over Na₂SO₄, decanted, and concentrated under reduced pressure. The crude oil was purified by flash column chromatography (30% Et₂O in pentane) to furnish the product as a pale-yellow oil (1.54 g, 8.16 mmol) in 77% yield.

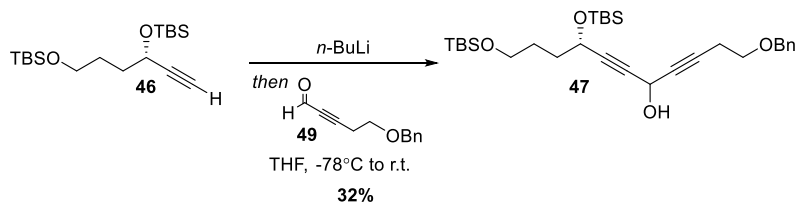
HRMS (ESI): m/z calcd. for C₁₂H₁₄O₂Na (M+Na⁺): 213.08860 found 213.08845.

¹H NMR (400 MHz, CDCl₃) δ 7.39 – 7.28 (m, 5H), 4.56 (s, 2H), 4.25 (t, *J* = 2.2 Hz, 2H), 3.59 (t, *J* = 6.9 Hz, 2H), 2.55 (tt, *J* = 6.9, 2.2 Hz, 2H), 1.72 (broad, -OH).



Propargylic aldehyde 49: The substrate (1.535 g, 8.06 mmol) and manganese dioxide (3.55 g, 40.78 mmol) were added to CH₂Cl₂ (20 mL) and allowed stirred for 22 hours. The mixture was filtered through Celite[®] and solvent removed under reduced pressure. The crude oil was purified by flash column chromatography (2% Et₂O in pentane). Product **49** was obtained as a light-yellow oil (690 mg, 3.67 mmol) in 46 % yield.

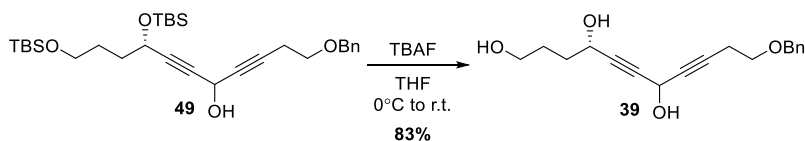
¹H NMR (400 MHz, CDCl₃) δ 9.10 (s, 1H), 7.54 – 6.96 (m, 5H), 4.49 (s, 2H), 3.58 (t, *J* = 6.6 Hz, 2H), 2.64 (t, *J* = 6.6 Hz, 2H).



Propargylic alcohol 49: Alkyne **46** (1.17 g, 3.41 mmol) was diluted with THF (7 ml) and cooled to -78 °C before dropwise addition of *n*-BuLi (1.50 mL, 2.11 M). After stirring at -78°C for 30 minutes, the reaction was warmed to -40°C where it was stirred for one hour. The reaction was cooled back down to -78°C before dropwise addition of aldehyde **49** (540 mg, 2.84 mmol) in THF (10 mL). The reaction was maintained at -78°C for 6.5 hours

before allowing warming to room temperature where it was quenched with saturated aqueous ammonium chloride. The layers were separated and the organic layer was extracted with Et₂O (x3), washed with brine, dried over MgSO₄, filtered, and concentrated under reduced pressure. The residue was purified by flash column chromatography (1% MeOH in CH₂Cl₂) to furnish propargylic alcohol **49** (570 mg, 0.98 mmol) as a yellow oil in 32% yield.

¹H NMR (400 MHz, CDCl₃) δ 7.37 – 7.28 (m, 5H), 5.11 (m, 1H), 4.56 (s, 2H), 4.42 (m, 1H), 3.63 (m, 2H), 3.60 (t, *J* = 7.0 Hz, 2H), 2.55 (td, *J* = 7.1, 2.1 Hz, 2H), 1.68 (m, 4H), 0.90 (s, 9H), 0.89 (s, 9H), 0.14 (s, 3H), 0.11 (s, 3H), 0.05 (s, 6H).

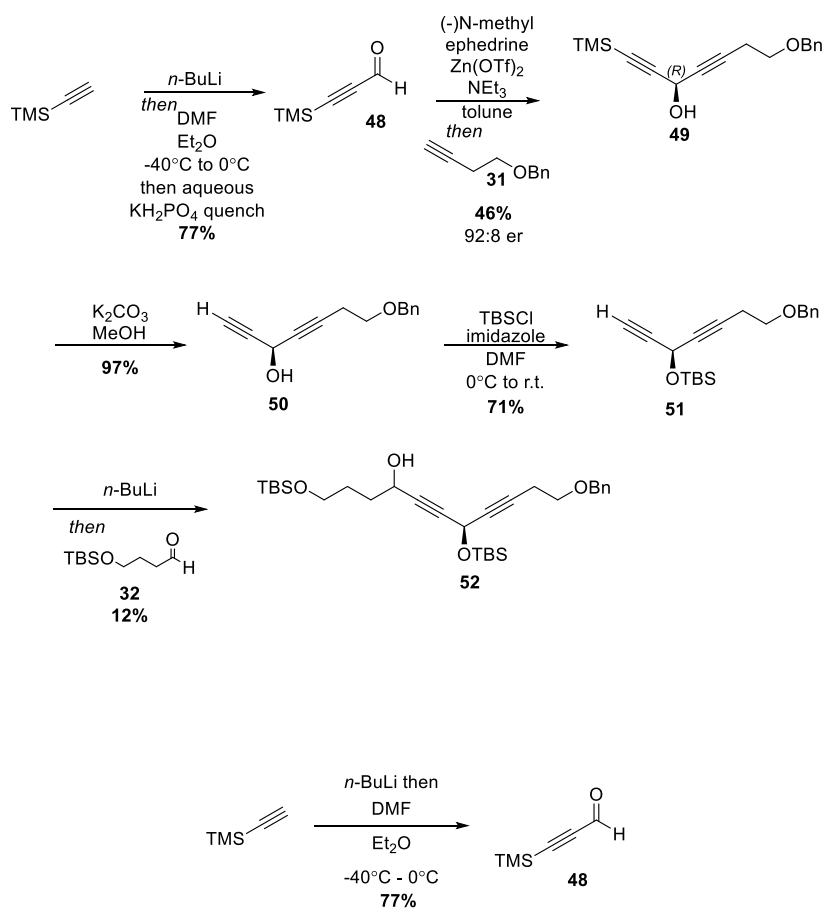


Diyne 39: A solution of starting material (570 mg, 1.08 mmol) in THF (10 mL) was cooled to 0°C. TBAF in THF (1.0 M, 3.23 mL) was added dropwise and the resulting solution was warmed to room temperature. After two hours, the reaction mixture was quenched with saturated aqueous ammonium chloride before being extracted with ethyl acetate five times. The combined organic extracts were washed with brine and dried over MgSO₄, filtered, concentrated under reduced pressure. The resulting oil was purified by flash column chromatography (50% EtOAc in hexanes to 80% EtOAc in hexanes). The resulting diyne **39** was obtained as a yellow oil (492 mg, 1.63 mmol in 83% yield).

HRMS (ESI): *m/z* calcd. for C₁₈H₂₂O₄Na (M+Na⁺): 325.14103 found 325.14069.

^1H NMR (600 MHz, CDCl_3) δ 7.40 – 7.29 (m, 5H), 5.14 (br s, 1H), 4.57 (s, 2H), 4.51 (t, J = 5.6 Hz, 1H), 3.74 (m, 1H), 3.71 – 3.66 (m, 1H), 3.61 (t, J = 6.8 Hz, 2H), 2.56 (td, J = 6.9, 1.6 Hz, 2H), 1.86 (t, J = 5.6 Hz, 4H), 1.75 (m, 2H), 1.60 (broad, -OH).

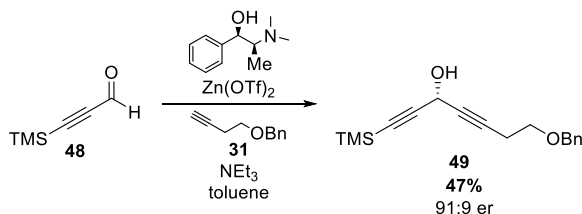
^{13}C NMR (101 MHz, CDCl_3) δ 137.82, 128.62, 127.97, 84.72, 84.68, 82.79, 82.75, 81.81, 78.85, 77.54, 77.23, 76.91, 73.02, 68.06, 62.25, 61.78, 51.85, 34.44, 28.18, 20.17.



Propargylic aldehyde 48: The substrate (4.24 mL, 30 mmol) was dissolved in THF (30 mL) and cooled to -40°C before addition of $n\text{-BuLi}$ (2.21 M, 13.5 mL) dropwise. After stirring for one hour, DMF (4.65 mL, 60 mmol) was added in one portion before removal of the cooling bath. After warming to room temperature, the mixture was stirred for 30

minutes. The reaction mixture was then poured into a rapidly stirred suspension of KH_2PO_4 in H_2O (16.69 g, 162 mL) and Et_2O (150 mL) cooled to 0°C and allowed to stir for 20 minutes. The organic layer was separated and the aqueous layer was extracted with Et_2O (5 x 25 mL). The combined organic extracts were dried over MgSO_4 , filtered, and concentrated under vacuum. The crude oil was filtered through a silica plug (20% Et_2O in pentane) and concentrated under vacuum. Propargylic aldehyde **48** was obtained as a pale-yellow oil (2.89g, 22.92 mmol) in 77% yield.

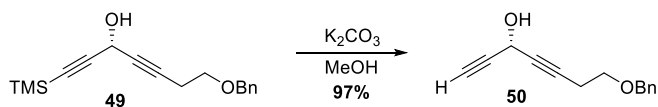
$^1\text{H NMR}$ (300 MHz, CDCl_3) δ 9.16 (s, 1H), 0.26 (s, 9H).



Bis-propargylic alcohol 49: A flask was charged with Zn(OTf)_2 (2.02 g, 5.5 mmol) and (-)-N-methylephedrine (1.10g, 6.0 mmol) and purged with argon for 20 minutes. Toluene (13 mL) and triethylamine (0.84 mL, 6 mmol) were added and the suspension was stirred for 2 hours at room temperature before addition of alkyne **31** (845 mg, 5 mmol) in one portion. After stirring for 15 minutes, aldehyde **48** (638 mg, 5 mmol) was added in one portion. After 2 hours of stirring at room temperature the reaction was quenched with saturated aqueous ammonium chloride. The layers were separated and the organic layer was extracted with Et_2O (x3). The organic layers were combined and washed with brine and dried over MgSO_4 before concentration under reduced pressure. The residue was purified by flash column chromatography (10% to 20% EtOAc in hexanes) to yield bis-

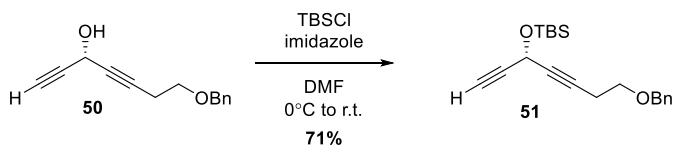
propargylic alcohol **49** as a bright yellow oil (665 mg, 2.32 mmol) in 46% yield as a 91:9 mixture of enantiomers as determined by Mosher ester analysis.

$^1\text{H NMR}$ (600 MHz, CDCl_3) δ 7.47 – 7.26 (m, 5H), 5.11 (m, 2H), 4.57 (s, 2H), 3.61 (t, J = 7.0 Hz, 2H), 2.57 (td, J = 7.1, 2.1 Hz, 2H), 0.20 (s, 9H).



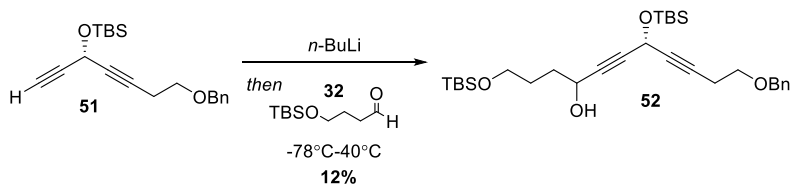
Terminal alkyne 50: Silylated alkyne **49** (2.20 g, 7.68 mmol) was dissolved in methanol (145 mL) and K_2CO_3 (2.97 g, 21.5 mmol) was added. The mixture was stirred at room temperature for 8 hours. The reaction mixture was concentrated under reduced pressure before dilution of the reaction mixture with water and extraction with EtOAc (x3). The combined organic layers were washed with brine, dried over MgSO_4 , filtered, and concentrated under reduced pressure. The residue was purified by flash column chromatography (10% EtOAc in hexanes) to afford terminal alkyne **50** as a clear oil (1.60 g, 7.47 mmol) in 97% yield.

$^1\text{H NMR}$ (400 MHz, CDCl_3) δ 7.40 – 7.28 (m, 5H), 5.11 (broad d, J = 2.3 Hz, 1H), 4.57 (s, 2H), 3.61 (t, J = 6.9 Hz, 2H), 2.62 – 2.50 (m, 3H), 2.37 (broad s, -OH).



Silyl ether 51: To a solution of alcohol **50** (1.630 g, 7.60 mmol) and TBSCl (2.412 g, 16.0 mmol) in DMF (25 mL) at 0°C was added imidazole (2.90 g, 42.6 mmol) in one portion. The solution was slowly warmed to room temperature and after 6 hours was quenched with water. The aqueous and organic layers were separated and the aqueous layer was extracted with Et₂O (x7). The combined organic extracts were washed with H₂O and brine before being dried over MgSO₄, filtered, and concentrated under reduced pressure. The residue was purified by flash column chromatography (7% Et₂O in pentane) to afford silyl ether **51** as a clear oil (1.77g, 5.39 mmol) in 71% yield.

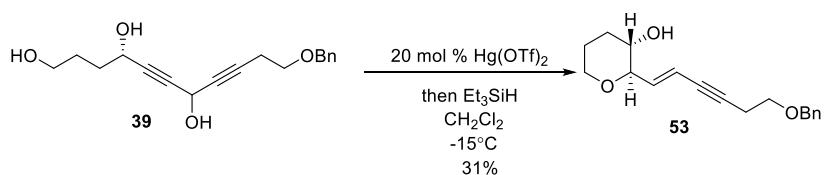
¹H NMR (400 MHz, CDCl₃) δ 7.36 (m, 5H), 5.20 (q, *J* = 2.0 Hz, 1H), 4.56 (s, 2H), 3.61 (t, *J* = 7.1 Hz, 2H), 2.56 (td, *J* = 7.1, 2.1 Hz, 3H), 2.49 (d, *J* = 2.3 Hz, 1H), 0.92 (s, 9H), 0.18 (d, *J* = 1.4 Hz, 6H).



Propargylic alcohol 52: Alkyne **51** (493 mg, 1.50 mmol) was diluted with THF (1.5 ml) and cooled to -78 °C before dropwise addition of *n*-BuLi (0.62 mL, 2.20 M). After stirring at -78°C for 30 minutes, aldehyde **32** in THF (260 mg, 1.25 mmol; 5 mL) was added dropwise. The reaction was maintained at -78°C for 5 hours before allowing warming to -40°C where it was quenched with saturated aqueous ammonium chloride. The layers were separated and the organic later was extracted with Et₂O (x3), washed with brine, dried over MgSO₄, filtered, and concentrated under reduced pressure. The residue was purified by

flash column chromatography (10% EtOAc in hexanes) to afford propargylic alcohol **52** (78.2 mg, 0.147 mmol) as a yellow oil in 12% yield.

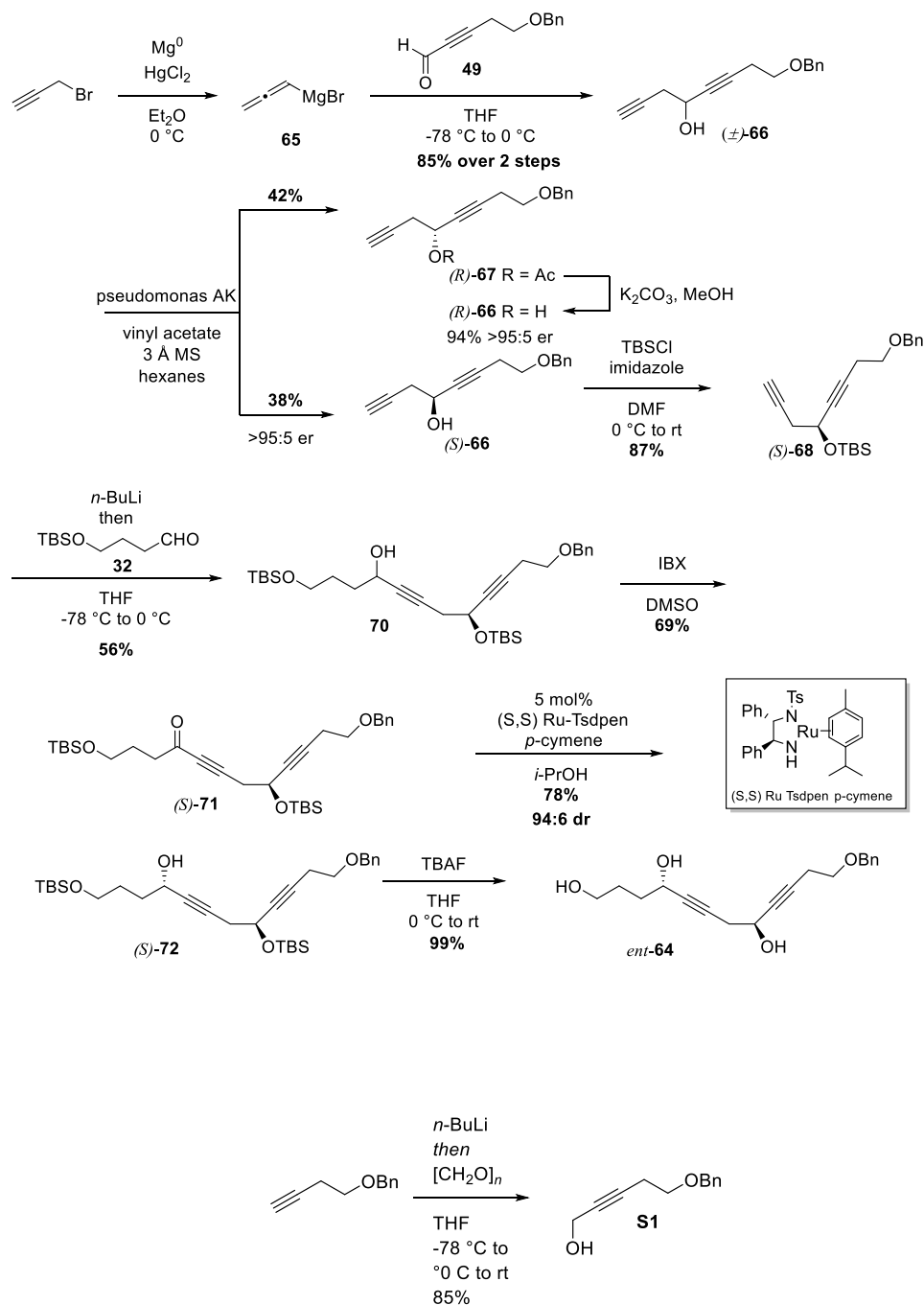
¹H NMR (400 MHz, CDCl₃) δ 7.32 – 7.20 (m, 5H), 5.35 – 4.97 (m, 1H), 4.47 (s, 2H), 4.38 (m, 1H), 3.70 – 3.45 (m, 4H), 2.46 (td, *J* = 7.1, 2.1 Hz, 2H), 1.86 – 1.47 (m, 4H), 0.84 (s, 9H), 0.82 (s, 9H), 0.08 (s, 3H), 0.02 (s, 3H), -0.01 (s, 6H).



Enyne 53: Hg(OTf)₂ (16.2 mg, 0.033 mmol) was added to CH₂Cl₂ (1 mL) and cooled to -15°C. The starting material (50.7 mg; 0.165 mmol) was dissolved in CH₂Cl₂ (2 mL) and added to the catalyst solution dropwise. After 15 minutes, Et₃SiH (160 μL, 1 mmol) was added to the reaction. After 7 hours, the reaction was quenched with triethylamine and filtered through a pad of silica gel before being concentrated under reduced pressure. The crude oil was purified via flash column chromatography (5% EtOAc in hexanes) to afford diyne **53** (14.5 mg, 0.506 mmol) a yellow oil in 31% yield. The structure is tentatively assigned by proton NMR.

HRMS (APCI): *m/z* calcd. for C₁₈H₂₃O₃ (M+H⁺): 287.16417 found 287.16376.

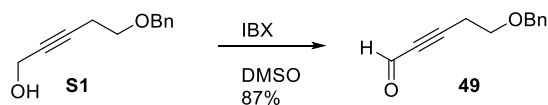
¹H NMR (600 MHz, CDCl₃) δ 7.39 – 7.28 (m, 5H), 6.11 (dd, *J* = 16.0, 6.7 Hz, 1H), 5.80 (dtd, *J* = 16.0, 2.1, 1.2 Hz, 1H), δ 4.57 (s, 2H), 3.93 (m, 1H), 3.61 (t, *J* = 7.0 Hz, 1H), 3.52 (dd, *J* = 8.8, 6.9 Hz, 1H), 3.43 – 3.28 (m, 3H), 2.63 (td, *J* = 7.0, 2.2 Hz, 1H), 1.61 (m, 4H).



Alkyne alcohol S1: The terminal alkyne (2.25 g; 14.0 mmol) was dissolved in THF and cooled to -78°C before dropwise addition of *n*-BuLi (2.12 M; 7.28 mL; 15.5 mmol). After 5 minutes, the reaction was warmed to 0°C , at which time solid paraformaldehyde (847 mg; 29.1 mmol) was added. The reaction was gradually warmed to room temperature and stirred for 3.5

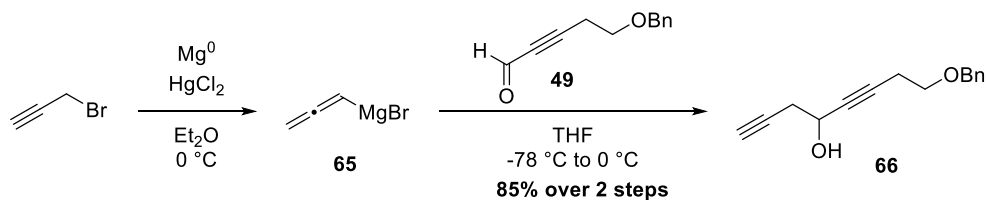
hours. The reaction was quenched by addition of saturated aqueous ammonium chloride (12 mL). The organic layer was separated and the aqueous layer was extracted with diethyl ether (3 x 10 mL). The combined organic extracts were washed with brine, dried over Na₂SO₄, filtered, and concentrated under reduced pressure to afford the crude product as a yellow oil, which was purified by silica gel flash column chromatography (20% ethyl acetate in hexanes) to afford alkynyl alcohol **S1** (2.25g; 11.8 mmol) as a clear oil in 85% yield.

¹H NMR (400 MHz, CDCl₃) δ 7.44 – 7.29 (m, 5H), 4.56 (s, 2H), 4.25 (dt, J = 6.0, 2.2 Hz, 2H), 3.59 (t, J = 6.9 Hz, 2H), 2.55 (tt, J = 6.9, 2.2 Hz, 2H).



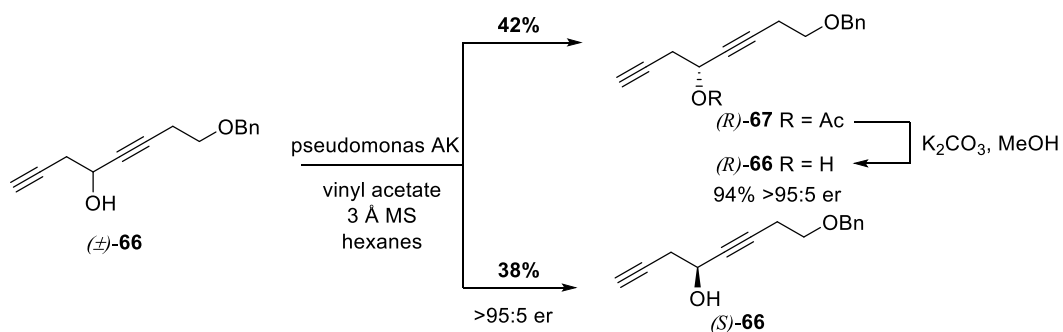
Alkynyl aldehyde 49: Alkynyl alcohol (2.25 g; 14.0 mmol) was dissolved in THF and cooled to -78 °C before dropwise addition of *n*-BuLi (2.12 M; 7.28 mL; 15.5 mmol). After 5 minutes the reaction was warmed to 0 °C, at which time solid paraformaldehyde (847 mg; 29.1 mmol) was added. The reaction was gradually warmed to room temperature and stirred for 3.5 hours. The reaction was quenched by addition of saturated aqueous ammonium chloride (12 mL). The organic layer was separated and the aqueous layer was extracted with diethyl ether (3 x 10 mL). The combined organic extracts were washed with brine, dried over Na₂SO₄, filtered, and concentrated under reduced pressure to afford the crude product as a yellow oil, which was purified by silica gel flash column chromatography (20% ethyl acetate in hexanes) to afford alkynyl aldehyde **49** (2.25g; 11.8 mmol) as a clear oil.

¹H NMR (400 MHz, CDCl₃) δ 9.19 (t, J = 0.9 Hz, 1H), 7.40 – 7.29 (m, 5H), 4.58 (s, 2H), 3.67 (t, J = 6.7 Hz, 2H), 2.73 (td, J = 6.6, 0.9 Hz, 2H).

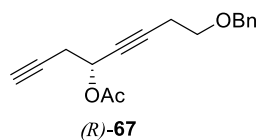


Diynyl alcohol (\pm)-66: HgCl₂ (90 mg; 0.33 mmol) and Mg⁰ (3.65 g; 150 mmol) were added to a two-neck oven-dried 250 mL round bottom flask equipped with reflux condenser. A solution of propargyl bromide (0.4 mL) in Et₂O (16 mL) was added. The resulting suspension was heated gently with a heating gun to initiate the reaction, resulting in bubbling which persisted after heating ceased. The flask was then cooled to 0 °C, before dropwise addition of the remaining propargyl bromide (5.2 mL; 50 mmol total) in Et₂O (30 mL) over 20 min. The reaction continued to bubble upon and after addition of propargyl bromide. After stirring at 0 °C for 15 min, the grey Grignard solution was transferred via cannula to a flask containing propargyl aldehyde **49**¹²³ (2.38 g; 12.6 mmol) in THF (62 mL) at -78 °C. The reaction was stirred at -78 °C for 3 h, after which time it was quenched by addition of sat'd aq. NH₄Cl (20 mL) and allowed to warm to room temperature. The organic layer was separated and the aqueous layer was extracted with Et₂O (3 x 20 mL). The combined organic extracts were washed with brine, dried over Na₂SO₄, filtered, and concentrated under reduced pressure to afford the crude product as a yellow oil, which was purified by silica gel flash column chromatography (20% EtOAc in hexanes) to afford racemic diynyl alcohol **8** as a clear, colorless oil (2.44 g; 10.7 mmol; 85% yield).

¹H NMR (600 MHz, CDCl₃) δ 7.38 – 7.28 (m, 5H), 4.56 (s, 2H), 4.52 (dtd, J = 8.1, 6.0, 2.0 Hz, 1H), 3.60 (t, J = 7.0 Hz, 2H), 2.67 – 2.56 (m, 2H), 2.56 (td, J = 7.0, 1.9 Hz, 2H), 2.20 (d, J = 6.3 Hz, 1H), 2.11 (t, J = 2.6 Hz, 1H).

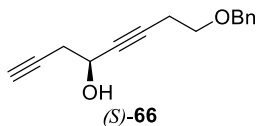


Resolution of (\pm) -**66** to prepare diynyl ester (R) -**67** and diynyl alcohol (S) -**66**: Powdered 3Å molecular sieves (1.5 g) and Pseudomonas AK (1.12 g) were added to a solution of racemic diynyl alcohol (\pm) -**66** (2.24 g; 9.80 mmol) in hexanes (100 mL). Vinyl acetate (4.0 mL) was then added. The suspension was stirred and monitored for conversion by 1H NMR spectroscopy. After 4 h, the reaction had reached 50% conversion by 1H NMR. The reaction mixture was filtered through Celite, rinsed with CH_2Cl_2 , and concentrated under reduced pressure to afford a pale-yellow oil. The crude reaction mixture was purified by silica gel flash column chromatography (18% EtOAc in hexanes) to afford diynyl ester (R) -**67** (1.10 g; 4.07 mmol; 42% yield) and diynyl alcohol (S) -**66** (854 mg; 3.74 mmol; 38% recovery; 80% combined yield of (R) -**67** and (S) -**66**). MTPA-esters confirmed the stereochemical assignment and purity of (S) -**66** (er > 95:5; the other stereoisomer was not visible).



Data for diynyl ester (R) -**9**: $[\alpha]_D^{25} +48.8$ (c=1.0, $CHCl_3$)

¹H NMR (600 MHz, CDCl₃) δ 7.39 – 7.30 (m, 5H), 5.50 (app. tt, *J* = 6.3, 2.0 Hz, 1H), 4.56 (s, 2H), 3.60 (t, *J* = 7.1 Hz, 2H), 2.67 (dd, *J* = 6.2, 2.6 Hz, 2H), 2.56 (td, *J* = 7.1, 2.0 Hz, 2H), 2.11 (s, 3H), 2.05 (t, *J* = 2.7 Hz, 1H).



¹H NMR (600 MHz, CDCl₃) δ 7.38 – 7.28 (m, 5H), 4.56 (s, 2H), 4.52 (dtd, *J* = 8.1, 6.0, 2.0 Hz, 1H), 3.60 (t, *J* = 7.0 Hz, 2H), 2.67 – 2.56 (m, 2H), 2.56 (td, *J* = 7.0, 1.9 Hz, 2H), 2.20 (d, *J* = 6.3 Hz, 1H), 2.11 (t, *J* = 2.6 Hz, 1H).

(*R*)-MTPA-ester from (*S*)-**66**: **¹H NMR** (600 MHz, CDCl₃) δ 7.38 – 7.30 (m, 5H), 5.63 (dtd, *J* = 7.6, 5.8, 1.9 Hz, 1H), 4.49 (s, 2H), 3.51 (td, *J* = 7.0, 1.7 Hz, 2H), 2.71 (m, 2H), 2.47 (td, *J* = 7.0, 2.0 Hz, 2H), 2.04 (t, *J* = 2.6 Hz, 1H).

(*S*)-MTPA-ester from (*S*)-**66**: **¹H NMR** (600 MHz, CDCl₃) δ 7.34 – 7.30 (m, 5H), 5.66 (tt, *J* = 6.9, 2.0 Hz, 1H), 4.50 (s, 2H), 3.54 (m, 2H), 2.66 (m, 2H), 2.52 (td, *J* = 6.9, 2.0 Hz, 3H), 1.95 (t, *J* = 2.6 Hz, 1H).

Table 1. MTPA-ester data for compound (*S*)-**66**

MTPA-ester resonance	δ <i>S</i> -ester (ppm)	δ <i>R</i> -ester (ppm)	Δ(δ _{<i>S</i>} -δ _{<i>R</i>}) (ppm)	Δ(δ _{<i>S</i>} -δ _{<i>R</i>}) (Hz)
e	2.52	2.47	0.05	30
c	3.54	3.51	0.03	18
b	4.50	4.49	0.01	6
a	5.66	5.63	n/a	n/a
d	2.66	2.71	-0.05	-30
f	1.95	2.04	-0.09	-54

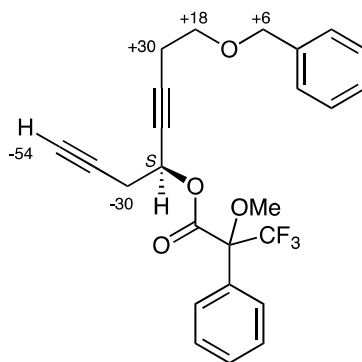
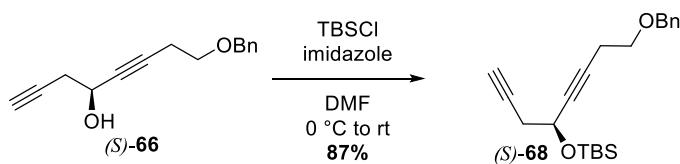
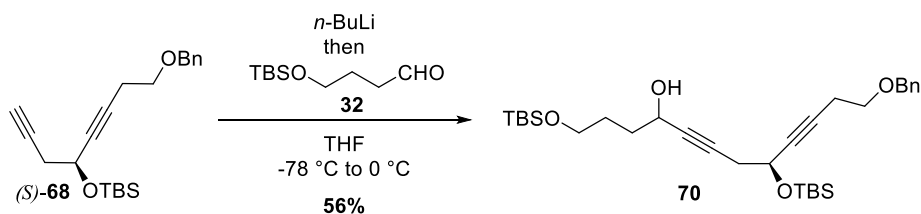


Figure 6. MTPA-ester data for compound (*S*)-**66**



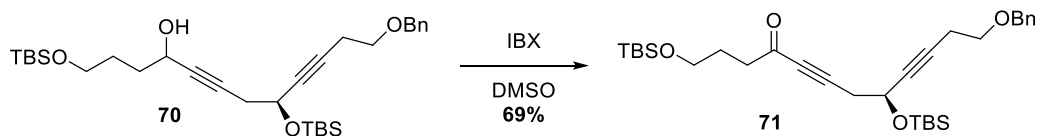
Preparation of silyl ether (*S*)-**68**: A solution of diynyl alcohol (*S*)-**66** (854 mg; 3.74 mmol) in DMF (12 mL) was cooled to 0 °C, prior to addition of imidazole (1.42 g; 20.9 mmol) and TBSCl (1.18 g; 7.86 mmol). The reaction was stirred at room temperature for 5 h, then diluted with Et₂O (15 mL), followed by addition of sat'd aq. NH₄Cl (10 mL). The organic layer was separated, and the aqueous layer was extracted with Et₂O (3 x 10 mL). The combined organic extracts were washed with water (4 x 40 mL) and brine, dried over MgSO₄, filtered and concentrated under reduced pressure to afford a clear oil. The crude oil was purified by silica gel column chromatography (2% EtOAc in hexanes to 5% EtOAc in hexanes) to afford silyl ether (*S*)-**66** as a clear colorless oil (1.12 g; 3.42 mmol; 87% yield).

¹H NMR (400 MHz, CDCl₃) δ 7.36 – 7.28 (m, 5H), 4.55 (s, 2H), 4.50 (tt, *J* = 6.7, 2.0 Hz, 1H), 3.60 (t, *J* = 7.1 Hz, 2H), 2.58 – 2.49 (m, 4H), 2.02 (t, *J* = 2.7 Hz, 1H), 0.91 (s, 9H), 0.14 (s, 3H), 0.13 (s, 3H).



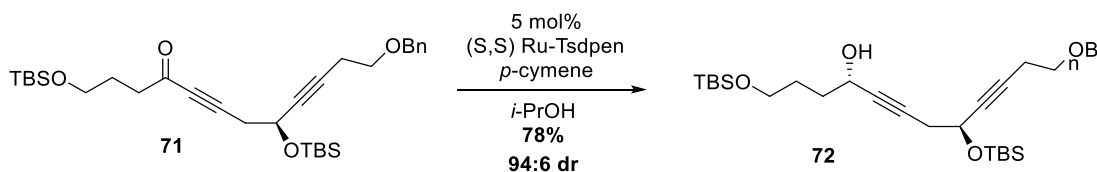
Diynyl alcohol **70**: A solution of terminal alkyne (*S*)-**68** (1.12 g; 3.42 mmol) was dissolved in THF (9 mL), and cooled to $-78\text{ }^\circ\text{C}$. *n*-BuLi (1.95 M; 1.75 mL; 3.42 mmol) was added dropwise. The reaction mixture was stirred at low temperature for 10 min, before warming to $0\text{ }^\circ\text{C}$ for 10 min, and then cooling back down to $-78\text{ }^\circ\text{C}$. A solution of aldehyde **32** (910 mg; 4.44 mmol) in THF (4.5 mL) was added dropwise, and the reaction mixture was gradually warmed to room temperature. After 3 h, the reaction mixture was quenched by addition of sat'd aq. NH_4Cl (22 mL), and allowed to warm to room temperature. The organic layer was separated, and the aqueous layer was extracted with Et_2O (3 x 15 mL). The combined organic extracts were washed with brine, dried over Na_2SO_4 , filtered, and concentrated under reduced pressure to afford the crude product as a yellow oil, which was purified by silica gel flash column chromatography (10% EtOAc in hexanes) to afford diynyl alcohol **70** as a clear, colorless oil (1.04 g; 1.92 mmol; 56% yield; 1:1 mixture of diastereomers).

$^1\text{H NMR}$ (4600 MHz, CDCl_3) δ 7.38 – 7.28 (m, 5H), 4.55 (d, $J = 1.1\text{ Hz}$, 2H), 4.46 (app. tq, $J = 7.1, 1.7\text{ Hz}$, 1H), 4.38 (m, 1H), 3.66 (m, 2H), 3.59 (t, $J = 7.1\text{ Hz}$, 2H), 2.97 (dd, $J = 5.9, 1.1\text{ Hz}$, -OH, 0.5H), 2.93 (dd, $J = 5.7, 1.1\text{ Hz}$, -OH, 0.5H), 2.56 (dd, $J = 6.8, 1.7\text{ Hz}$, 2H), 2.52 (tt, $J = 7.1, 1.5\text{ Hz}$, 2H), 1.82 – 1.74 (m, 3H), 1.73 – 1.60 (m, 1H), 0.91 (dd, $J = 2.1, 1.2\text{ Hz}$, 18H), 0.14 (d, $J = 1.1\text{ Hz}$, 3H), 0.13 (d, $J = 1.2\text{ Hz}$, 3H), 0.07 (d, $J = 1.3\text{ Hz}$, 6H).



Enone 71: Diynyl alcohol **70** (1.04 g; 1.92 mmol) was dissolved in DMSO (3.5 mL), prior to adding a solution of IBX (1.07 g; 3.82 mmol) in DMSO (6.5 mL). The reaction was stirred at room temperature for 20 h. The reaction mixture was diluted with Et₂O (20 mL) and water (50 mL), and filtered. The organic layer was separated, and the aqueous layer was extracted with Et₂O (3 x 15 mL). The combined organic extracts were washed with brine, dried over Na₂SO₄, filtered, and concentrated under reduced pressure to afford the crude product as a yellow oil, which was purified by silica gel flash column chromatography (3.5% EtOAc in hexanes to 5% EtOAc in hexanes) to afford diynyl ketone (*S*)-**71** as a clear, pale yellow oil (713 mg; 1.31 mmol; 69% yield). The aldehyde resulting from loss of the primary silyl ether and alcohol oxidation was also isolated as a yellow oil (87 mg; 0.20 mmol; 11% yield).

¹H NMR (400 MHz, CDCl₃) δ 7.41 – 7.28 (m, 4H), 4.55 (s, 3H), 3.69 – 3.48 (m, 4H), 2.72 (dd, J = 6.5, 1.6 Hz, 2H), 2.62 (t, J = 7.3 Hz, 2H), 2.53 (td, J = 7.1, 1.9 Hz, 2H), 1.86 (m, 2H), 0.91 (s, 9H), 0.89 (s, 9H), 0.15 (s, 3H), 0.14 (s, 3H), 0.04 (s, 6H).



Preparation of Noyori hydrogen transfer catalyst: RuCl[(*S,S*)-NTsCHPhCHPhNH₂](η⁶-cymene) complex (47 mg, 0.065 mmol) was dissolved in CH₂Cl₂ (2 mL), and KOH (4 mg, 0.065 mmol) was added. After the mixture was stirred at room temperature for 5 min, water (2 mL) was added. The organic layer was washed with additional water (2 mL) and dried over CaH₂. The violet organic layer was filtered and the solvent was removed under reduced pressure to afford the purple Ru[(*S,S*)-NTsCHPhCHPhNH₂](η⁶-cymene) complex, which was used as the hydrogen transfer catalyst.

Diyndl triol (*S,S*)-6: Ru(*S,S*)-(Tsdpen)(η⁶-cymene) (47 mg; 0.065 mmol) was added to a solution of diyndl ketone (*S*)-**71** (713 mg; 1.31 mmol) in isopropyl alcohol (18 mL, degassed by sparging with argon, dried over 3Å molecular sieves). The reaction mixture was stirred at room temperature for 22 h. The solvent was removed under reduced pressure, and the residue was purified by flash column chromatography (10% EtOAc in hexanes) to afford the diyndl alcohol **72** as the (*S,S*)-diastereomer (555 mg; 1.03 mmol; 78% yield; 94:6 dr; confirmed by MTPA-ester analysis).

¹H NMR (400 MHz, CDCl₃) δ 7.30 – 7.21 (m, 4H), 4.47 (s, 2H), 4.41 – 4.33 (m, 1H), 4.30 (m, 1H), 3.66 (m, 2H), 3.59 (t, J = 7.1 Hz, 2H), 2.96 (d, J = 5.6 Hz, OH), 2.48 (dd, J = 6.7, 2.0 Hz, 2H), 2.44 (td, J = 7.1, 2.0 Hz, 2H), 1.77 – 1.63 (m, 3H), 1.59 (m, 1H), 0.91 (s, 9H), 0.91 (s, 9H), 0.14 (s, 3H), 0.13 (s, 3H), 0.07 (s, 6H).

(*R*)-MTPA-ester **72** (key signals): **¹H NMR** (600 MHz, CDCl₃) δ 5.55 (dd, J = 7.7, 5.7 Hz, 1H), 4.38 (tt, J = 6.7, 2.0 Hz, 1H), 3.59 (t, J = 6.1 Hz, 2H), 2.51 (dd, J = 6.7, 1.9 Hz, 2H), 2.46 (td, J = 7.1, 1.9 Hz, 2H), 1.86 (dtd, J = 9.3, 6.4, 3.3 Hz, 2H), 1.67 – 1.57 (m, 2H).

(*S*)-MTPA-ester **72** (key signals): $^1\text{H NMR}$ (600 MHz, CDCl_3) δ 5.59 (ddt, $J = 6.6, 3.8, 2.0$ Hz, 1H), 4.43 (tt, $J = 6.7, 2.0$ Hz, 1H), 3.54 – 3.51 (m, 5H), 2.54 (dd, $J = 6.6, 1.9$ Hz, 2H), 2.46 (td, $J = 7.1, 1.9$ Hz, 2H), 1.86 – 1.73 (m, 2H), 1.64 – 1.46 (m, 2H).

Table 2. MTPA-ester data for compound **72**

MTPA-ester resonance	δ <i>S</i> -ester (ppm)	δ <i>R</i> -ester (ppm)	$\Delta(\delta_S - \delta_R)$ (ppm)	$\Delta(\delta_S - \delta_R)$ (Hz)
b	4.43	4.38	0.05	30
d	2.54	2.51	0.03	18
e	2.46	2.46	0.00	0
a	5.59	5.55	n/a	n/a
c	3.53	3.59	-0.06	-36

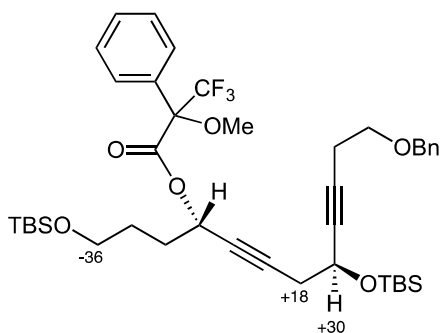
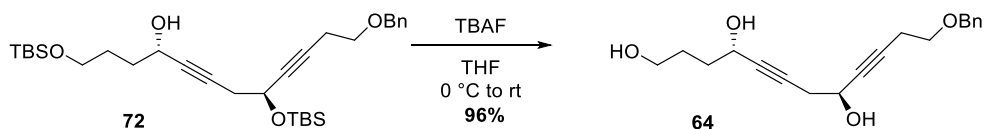


Figure 7. MTPA-ester data for compound **72**



Diynyl triol 64: Bis-silyl ether **72** (554 mg; 1.02 mmol) was dissolved in THF (10 mL) and cooled to 0 °C. TBAF (1.0 M in THF; 1.50 mL; 1.50 mmol) was added, and the reaction mixture was gradually warmed to room temperature. After 3.5 h, the solvent was removed under reduced pressure, and the resulting oil was purified by silica gel flash column

chromatography (75% EtOAc in hexanes) to afford diynyl triol (*S,S*)-**64** as a viscous light yellow clear oil (320 mg; 1.01 mmol; 99% yield).

$[\alpha]_D^{25}$: -20.5 (c=1.00, CHCl₃)

HRMS (NSI) m/z calcd. for C₁₉H₂₄O₄Na (M+Na⁺): 339.15708 found 339.15708.

IR (thin film): 3354 (br), 3088 (w), 2922, 2857, 2360 (w), 2231 (w), 1718, 1453, 1267, 1028 cm⁻¹.

¹H NMR (600 MHz, CDCl₃) δ 7.39 – 7.29 (m, 5H), 4.56 (s, 2H), 4.49 (m, 1H), 4.45 (m, 1H), 3.76 – 3.68 (m, 1H), 3.65 (ddd, J = 11.0, 7.1, 4.8 Hz, 1H), 3.60 (t, J = 6.8 Hz, 2H), 3.04 (br s, OH), 2.69 – 2.58 (m, 2H), 2.56 – 2.52 (m, 2H), 2.17 (br s, OH), 1.90 – 1.78 (m, 3H), 1.78 – 1.69 (m, 1H).

¹H NMR (600 MHz, acetone-*d*₆) δ 7.38 – 7.25 (m, 5H), 4.54 (s, 2H), 4.40 (dtd, J = 8.1, 6.2, 5.3, 3.0 Hz, 1H), 4.36 – 4.28 (m, 1H), 3.57 (m, 4H), 2.55 – 2.44 (m, 4H), 1.75 – 1.58 (m, 3H), 1.30 (m, 1H).

¹³C NMR (151 MHz, acetone-*d*₆) δ 138.1, 127.5, 126.8, 126.7, 83.5, 81.3, 80.6, 79.2, 71.6, 67.7, 60.8, 60.8, 60.2, 34.3, 28.2, 28.0, 19.0.

stirred for 15 min. A solution of the aldehyde **32** (5.02 g; 24.8 mmol) dissolved in toluene (25 mL) was added via syringe pump over a period of 8 h, and stirred for an additional 8 h. The reaction mixture was quenched with sat'd aq. NH_4Cl (25 mL), and extracted with Et_2O (5 x 30 mL). The combined organic layers were washed with brine (20 mL), and dried over MgSO_4 . The solution was filtered and concentrated under reduced pressure to give a brown-orange oil. The crude product was purified by silica gel flash column chromatography (10% EtOAc in hexanes) to afford the alkynyl alcohol (*R*)-**33** as an orange-yellow clear oil as the *R*-enantiomer (8.24 g; 22.7 mmol; 92% yield; 97:3 *er* by MTPA ester analysis).

^1H NMR (600 MHz, CDCl_3) δ 7.37 – 7.28 (m, 5H), 4.55 (s, 2H), 4.41 (m, 1H), 3.67 (m, 2H), 3.59 (t, $J = 7.2$ Hz, 2H), 3.10 (d, $J = 5.9$, -OH), 2.54 (td, $J = 7.1, 2.0$ Hz, 2H), 1.87 – 1.60 (m, 4H), 0.91 (s, 9H), 0.08 (s, 6H).

^{13}C NMR (101 MHz, CDCl_3) δ 138.20, 128.64, 127.86, 127.13, 82.54, 81.77, 73.09, 68.58, 63.38, 62.40, 35.66, 28.74, 26.09, 20.30, 18.48, -5.20.

(*R*)-MTPA ester (*R*)-**33** (selected signals): **^1H NMR** (600 MHz, CDCl_3) δ 5.58 (tt, $J = 6.6, 2.1$ Hz, 1H), 4.51 (s, 2H), 3.54 (m, 2H), 2.52 (td, $J = 7.0, 2.0$ Hz, 2H), 1.82 (q, $J = 7.5$ Hz, 2H), 1.54 (ddq, $J = 19.4, 15.4, 6.8$ Hz, 2H), 0.85 (s, 9H), -0.00 (s, 6H).

(*S*)-MTPA ester (*R*)-**33** (selected signals): **^1H NMR** (600 MHz, CDCl_3) δ 5.55 (ddd, $J = 6.6, 4.6, 2.0$ Hz, 1H), 4.50 (s, 2H), 3.60 (t, $J = 6.2$ Hz, 2H), 2.49 (td, $J = 7.1, 1.9$ Hz, 2H), 1.87 (dtd, $J = 8.6, 6.5, 2.2$ Hz, 2H), 1.64 (ddt, $J = 12.6, 8.4, 6.8$ Hz, 2H), 0.86 (d, $J = 0.6$ Hz, 9H), 0.01 (s, 6H).

Table 3. MTPA-ester data for compound (*R*)-**33**

MTPA-ester resonance	δ <i>S</i> -ester (ppm)	δ <i>R</i> -ester (ppm)	$\Delta(\delta_S-\delta_R)$ (ppm)	$\Delta(\delta_S-\delta_R)$ (Hz)
f	1.64	1.54	0.10	60
c	3.60	3.54	0.06	36
e	1.87	1.82	0.05	30
g	0.86	0.85	0.01	6
h	0.01	0.00	0.01	6
a	5.55	5.58	n/a	n/a
b	4.50	4.51	-0.01	-6
d	2.49	2.52	-0.03	-18

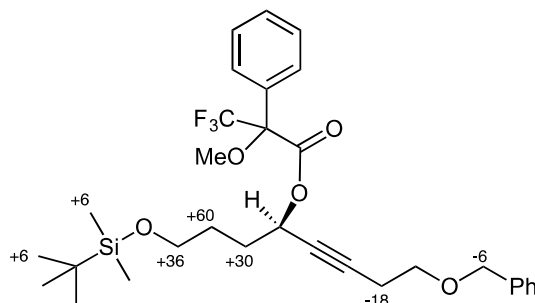
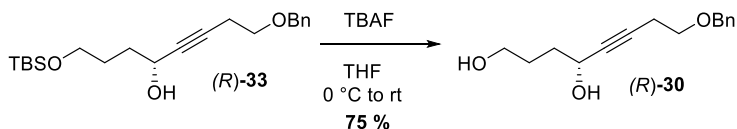


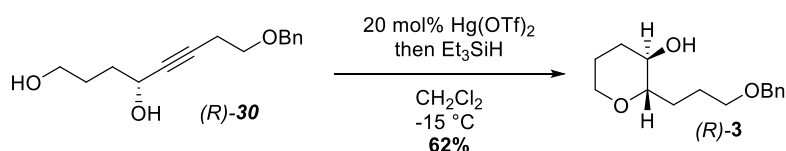
Figure 8. MTPA-ester data for compound (*R*)-**33**



Alkynol (*R*)-30: Silylated alcohol (*R*)-**33** (4.10 g; 11.3 mmol) was dissolved in THF (110 mL) and cooled to 0 °C before addition of TBAF in THF (1.0 M; 17.0 mL; 17 mmol). The resulting solution was gradually warmed to room temperature and stirred for 3 hours before removal of solvent under reduced pressure. The resulting oil was purified by silica gel flash column chromatography (65% ethyl acetate in hexanes to 75% ethyl acetate in hexanes) to afford alkynyl diol (*R*)-**30** as a viscous yellow oil (2.12 g; 8.5 mmol) in 75% yield.

¹H NMR (600 MHz, CDCl₃) δ 7.38 – 7.29 (m, 5H), 4.56 (s, 2H), 4.48 – 4.41 (m, 1H), 3.68 (broad, -OH), 3.67 (m, 2H), 3.60 (t, *J* = 6.9, 2H), 2.60 – 2.45 (m, 2H), 1.89 (broad, (OH)), 1.72 (m, 4H).

¹³C NMR (101 MHz, CDCl₃) δ 138.1, 128.7, 128.0 (2 C), 82.5, 82.2, 73.14, 68.6, 62.6, 62.3, 35.2, 28.6, 20.3.

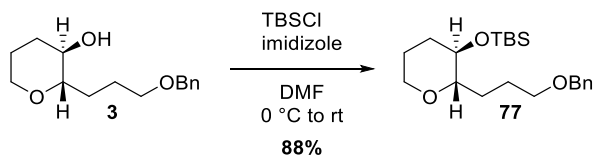


Tetrahydropyran (*R*)-3**:** Hg(OTf)₂ (268 mg; 0.53 mmol) was added to CH₂Cl₂ (27 mL) and cooled to -15 °C. Alkyne diol (*R*)-**30** (665 mg; 2.68 mmol) was dissolved in CH₂Cl₂ (13 mL) and added dropwise to the Hg(OTf)₂ solution. After 15 min, triethylsilane was added (1.71 mL; 10.7 mmol), and the reaction mixture was stirred for 18 h. The reaction mixture was quenched with triethylamine, and filtered through a plug of silica gel, before being concentrated under reduced pressure. The crude oil was purified by flash column chromatography (25-30% EtOAc in hexanes) to afford tetrahydropyran alcohol (*R*)-**3** as a pale-yellow oil (415 mg; 1.66 mmol; 62% yield).

HRMS (ESI) *m/z* calcd. for C₁₅H₂₃O₃ (M+H⁺): 251.16417 found 251.16418.

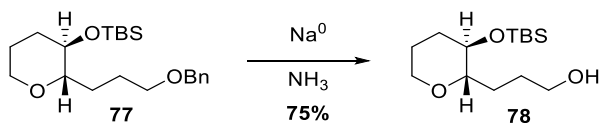
¹H NMR (600 MHz, CDCl₃) δ 7.31 – 7.15 (m, 5H), 4.44 (s, 2H), 3.85 – 3.75 (m, 1H), 3.44 (t, *J* = 6.3 Hz, 2H), 3.27 – 3.17 (m, 2H), 2.93 (td, *J* = 8.6, 2.9 Hz, 1H), 2.16 (broad, -OH), 2.02 – 1.97 (m, 1H), 1.90 – 1.84 (m, 1H), 1.79 (m, 1H), 1.67 – 1.55 (m, 3H), 1.44 (m, 1H), 1.36 – 1.25 (m, 1H).

^{13}C NMR (151 MHz, CDCl_3) δ 138.41, 128.29, 127.61, 127.44, 82.05, 72.76, 70.32, 70.06, 67.47, 32.68, 28.57, 25.61, 25.23.



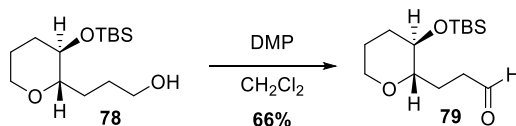
Silyl ether 77: Tetrahydropyranyl alcohol (*R*)-**3** (414 mg, 1.65 mmol) and TBSCl (527 mg, 3.47 mmol) were dissolved in DMF (6 mL). The mixture was cooled to 0° C, and imidazole (633 mg, 9.24 mmol) was added in one portion. The solution was slowly warmed to room temperature, and after 15 h was quenched with water. The aqueous and organic layers were separated, and the aqueous layer was extracted with Et_2O (5 mL x 7). The combined organic extracts were washed with H_2O (5 mL x 5) and brine, before being dried over MgSO_4 , filtered, and concentrated under reduced pressure. The residue was purified by flash column chromatography (5% EtOAc in hexanes) to yield the silyl ether **IV** as a clear oil (600 mg, 1.65 mmol; 88% yield).

^1H NMR (400 MHz, CDCl_3) δ 7.39 – 7.23 (m, 5H), 4.51 (s, 2H), 3.94 – 3.80 (m, 1H), 3.58 – 3.42 (m, 2H), 3.35 – 3.24 (m, 2H), 3.00 (td, J = 9.0, 2.5 Hz, 1H), 2.06 – 1.94 (m, 2H), 1.89 – 1.77 (m, 1H), 1.75 – 1.59 (m, 3H), 1.47 – 1.26 (m, 2H), 0.91 – 0.84 (s, 9H), 0.07 (s, 6H).



Alcohol 78: Ammonia (25 mL) was condensed via cold finger into a 100 mL round bottom flask in a dry-ice acetone bath. Freshly cut and hexanes-rinsed sodium metal (200 mg; 8.69 mmol) was added slowly in small portions, and the Na / NH₃ suspension was stirred at -78 °C for 15 min. Compound **77** (600 mg; 1.65 mmol) in THF (2 mL) was added to the deep blue solution, which was stirred at -78 °C for 75 min. Solid NH₄Cl (250 mg) was added to the reaction mixture, which was warmed slowly to room temperature. The resulting material was dissolved in EtOAc and washed with water. The aqueous and organic layers were separated, and the aqueous layer was extracted with EtOAc (5 mL x 3). The combined organic extracts were washed with H₂O (5 mL) and brine, before being dried over MgSO₄, filtered, and concentrated under reduced pressure. The residue was purified by flash column chromatography (25% to 30% EtOAc in hexanes) to afford alcohol **78** as a clear oil (339 mg; 1.24 mmol; 75% yield). Benzyl ether **77** was also recovered (68 mg; 0.19 mmol; 11% yield).

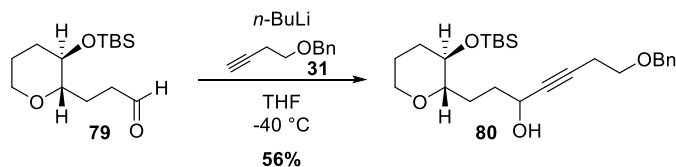
¹H NMR (400 MHz, CDCl₃) δ 3.98 – 3.84 (m, 1H), 3.64 (m, 2H), 3.40 – 3.21 (m, 2H), 3.05 (td, *J* = 8.8, 2.3 Hz, 1H), 2.65 (-OH, t, *J* = 5.9 Hz, 1H), 2.01 (m, 2H), 1.90 – 1.62 (m, 4H), 1.43 (m, 2H), 0.89 (s, 9H), 0.07 (s, 6H).



Aldehyde 79: The alcohol **78** (330 mg; 1.20 mmol) was dissolved in CH₂Cl₂ (25 mL), and DMP (515 mg; 1.20 mmol) was added. After stirring for 1.5 h, additional DMP (510 mg; 1.19 mmol) was added. After another 1.5 h, more DMP (180 mg; 0.42 mmol) was added.

After 30 min, the reaction mixture was poured into a rapidly stirred solution of Na₂S₂O₃ (25 g dissolved in 100 mL sat'd aq. NaHCO₃). The suspension was stirred for 30 min until the layers turned clear. The layers were separated, and the organic layer was washed with water (15 mL x 3), dried over MgSO₄, filtered, and concentrated under reduced pressure. The resulting crude aldehyde **79** was obtained as a clear oil and was used without further purification (216 mg; 0.79 mmol; 66% yield).

¹H NMR (600 MHz, CDCl₃) δ 9.76 (t, *J* = 1.9 Hz, 1H), 3.85 (ddt, *J* = 11.4, 4.2, 2.2 Hz, 1H), 3.33 – 3.24 (m, 2H), 3.00 (td, *J* = 9.1, 2.7 Hz, 1H), 2.65 – 2.43 (m, 2H), 2.28 – 2.15 (m, 1H), 2.06 – 1.91 (m, 2H), 1.72 – 1.60 (m, 3H), 1.49 – 1.39 (m, 2H), 0.89 (s, 9H), 0.08 (s, 6H).

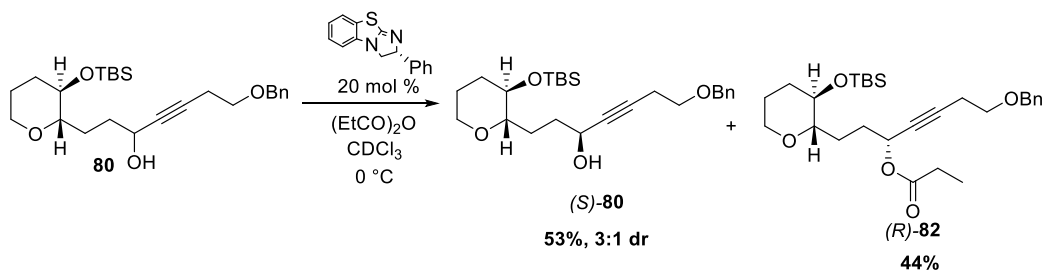


Alkynyl alcohol 80: A solution of terminal alkyne **31** (155 mg, 0.95 mmol) in 2.8 mL THF was cooled to -40 °C. *n*-BuLi (1.83 M; 0.48 mL; 0.87 mmol) was then added dropwise. The reaction mixture was stirred at -40 °C for 30 min, then cooled to -78 °C. The aldehyde **79** (216 mg, 0.79 mmol) dissolved in THF (1.2 mL) was slowly added to the lithium acetylide solution. The reaction mixture was stirred at -78 °C for 4.5 h, before warming to 0 °C, and quenching with sat'd aq. NH₄Cl (1 mL). The layers were separated and the organic layer was extracted with EtOAc (5 mL x 3). The combined organic layers were washed with water and brine, dried over Na₂SO₄, decanted, and concentrated under reduced

pressure. The crude oil was purified by flash column chromatography (10% to 15% EtOAc in hexanes) to yield alkynyl alcohol **80** as a pale-yellow oil (190 mg; 0.44 mmol; 56% yield; 1:1 dr). The diastereomers were not fully resolvable; the only distinct signals in the ^1H NMR spectrum were the carbinol protons of the newly formed stereocenter.

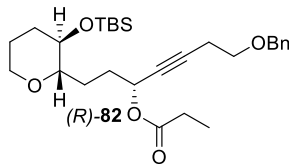
HRMS (ESI): m/z calcd. for $\text{C}_{25}\text{H}_{39}\text{O}_4\text{Si}$ ($\text{M}+\text{H}^+$): 431.26130 found 431.26121.

^1H NMR (600 MHz, CDCl_3) δ 7.35 (m, 5H), 4.55 (d, $J = 1.6$ Hz, 2H), 4.43 (t, 0.5 H), 4.36 (t, 0.5 H), 3.90 (m, 1H), 3.59 (td, $J = 7.3, 1.1$ Hz, 2H), 3.39 – 3.26 (m, 2H), 3.02 (m, 1H), 2.54 (tt, $J = 7.6, 2.3$ Hz, 2H), 2.16 – 1.94 (m, 2H), 1.84 (m, 1H), 1.64 (m, 3H), 1.53 – 1.39 (m, 3H), 0.89 (s, 9H), 0.07 (d, $J = 1.5$ Hz, 6H).

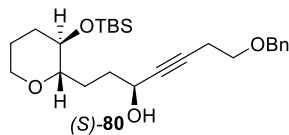


Resolution of **80** to prepare propargylic ester (R) -**82** and propargylic alcohol (S) -**80**: The propargylic alcohol **19** (326 mg; 0.75 mmol) was dissolved in CDCl_3 (3 mL) and cooled to $0\text{ }^\circ\text{C}$. The (+) benzotetramisole catalyst **20** (38 mg; 0.15 mmol) and $(\text{EtCO})_2\text{O}$ (75 μL ; 0.56 mmol) were added. The reaction mixture was stirred at $0\text{ }^\circ\text{C}$ for 3 h, before being quenched with MeOH (0.2 mL) and concentrated under reduced pressure. The resulting material was purified by silica gel flash column chromatography (10% to 20% EtOAc) to obtain (R) -ester **82** (164 mg; 0.34 mmol; 44% yield; diastereomeric ratio could not be

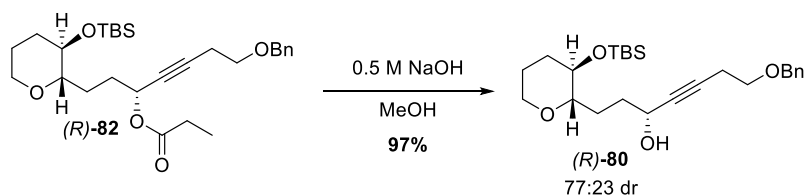
determined at this stage) with recovery of the (*S*)-alcohol, **80** (147 mg; 0.36 mmol; 53% yield; 72:28 dr).



¹H NMR (600 MHz, CDCl₃) δ 7.38 – 7.28 (m, 5H), 5.39 (t, *J* = 6.0 Hz, 1H), 4.54 (s, 2H), 3.92 – 3.81 (m, 1H), 3.57 (t, *J* = 7.3 Hz, 2H), 3.35 – 3.18 (m, 2H), 2.99 (td, *J* = 9.0, 2.1 Hz, 1H), 2.52 (td, *J* = 7.3, 1.9 Hz, 2H), 2.33 (m, 2H), 2.04 – 1.93 (m, 3H), 1.86 – 1.72 (m, 1H), 1.74 – 1.58 (m, 2H), 1.49 – 1.36 (m, 2H), 1.14 (t, *J* = 7.5 Hz, 3H), 0.88 (s, 9H), 0.06 (d, *J* = 3.6 Hz, 6H).



¹H NMR (600 MHz, CDCl₃) δ 7.38 – 7.28 (m, 5H), 4.55 (s, 2H), 4.43 (t, *J* = 6.0 Hz, 0.3H), 4.36 (t, *J* = 6.4 Hz, 0.7H), 3.90 (m, 1H), 3.59 (m, 2H), 3.38 – 3.26 (m, 2H), 3.06 (td, *J* = 8.9, 2.7 Hz, 0.7H), 3.01 (td, *J* = 9.2, 2.2 Hz, 0.3H), 2.56 – 2.50 (m, 2H), 2.11 (m, 1H), 2.07 – 1.96 (m, 1H), 1.89 – 1.83 (m, 2H), 1.65 (m, 3H), 1.51 – 1.39 (m, 2H), 0.89 (s, 9H), 0.07 (d, *J* = 2.3 Hz, 6H).



Alkynol (*R*)-64: A solution of silyl ether (*R*)-80 (134 mg; 0.36 mmol) in THF (4.8 mL) was cooled to 0 °C. TBAF in THF (1.0 M, 0.7 mL) was added dropwise, and the resulting solution was warmed to room temperature. After 1 h, the reaction mixture was concentrated under reduced pressure. The resulting oil was purified by flash column chromatography (75% to 100% Et₂O in pentane). Alkynyl diol (*R*)-64 was obtained as a pale yellow clear oil (73 mg; 0.23 mmol; 64% yield; 77:23 dr as predominantly the (*R*) propargylic alcohol).

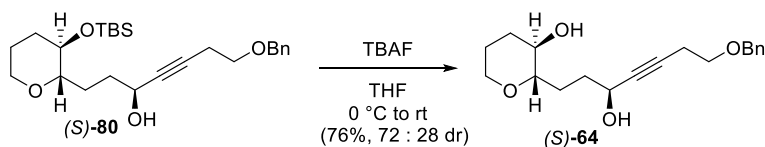
$[\alpha]_D^{25}$ -13.1 (c=1.0, CHCl₃)

IR (thin film): 3374 (br), 2930, 2857, 1454, 1332, 1142, 734 cm⁻¹.

HRMS (NSI): *m/z* calcd. for C₁₉H₂₇O₄ [M+H⁺]: 319.19039, found 319.18986.

¹H NMR (600 MHz, CDCl₃) δ 7.42 – 7.28 (m, 5H), 4.56 (s, 2H), 4.45 (tt, *J* = 5.7, 1.9 Hz, 0.7H), 4.41 (t, *J* = 5.3 Hz, 0.3H), 3.97 – 3.85 (m, 1H), 3.60 (t, *J* = 7.0 Hz, 2H), 3.33 (m, 2H), 3.07 (td, *J* = 8.7, 2.7 Hz, 0.3H), 3.03 (td, *J* = 8.9, 2.5 Hz, 0.7H), 2.97 (br –OH), 2.54 (td, *J* = 7.0, 2.0 Hz, 2H), 2.16 – 2.02 (m, 2H), 1.87 (m, 2H), 1.76 – 1.65 (m, 5H).

¹³C NMR (151 MHz, CDCl₃) δ 138.26, 128.63, 127.91, 82.72, 82.52, 82.38, 82.10, 73.11, 70.29, 68.64, 67.85, 62.70, 62.49, 34.27, 33.04, 27.86, 27.43, 25.72, 20.35.



Alkynol (*S*)-64: A solution of silyl ether (*S*)-80 (147 mg; 0.36 mmol) in THF (4.8 mL) was cooled to 0°C. TBAF in THF (1.0 M, 0.7 mL) was added dropwise, and the resulting solution warmed to room temperature. After 1 h, the reaction mixture was concentrated under reduced pressure. The resulting oil was purified by flash column chromatography (75% to 100% Et₂O in pentane). Alkynyl diol (*S*)-64 was obtained as a pale yellow clear oil (87 mg, 0.27 mmol; 76% yield; 72:28 dr as predominantly the (*S*) propargylic alcohol).

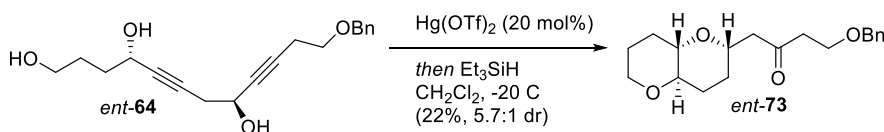
$[\alpha]_D^{25}$: -10.0 (c=1.03, CHCl₃)

IR (thin film): 3398 (br), 2927, 2856, 2360 (w), 1721, 1464, 1270, 1095 cm⁻¹.

HRMS (NSI): *m/z* calcd. for C₁₉H₂₇O₄ [M+H⁺]: 319.19039, found 319.19018.

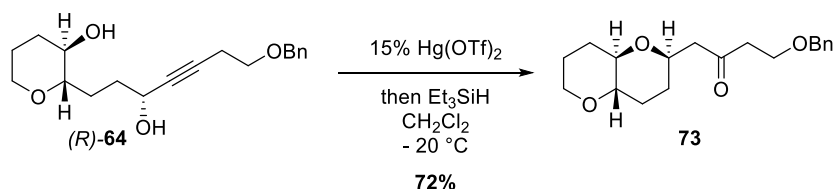
¹H NMR (600 MHz, CDCl₃) δ 7.48 – 7.27 (m, 5H), 4.56 (s, 2H), 4.44 (t, *J* = 7.0 Hz, 0.3H), 4.40 (t, *J* = 6.2 Hz, 0.7H), 3.91 (m, 1H), 3.60 (t, *J* = 7.0 Hz, 2H), 3.34 (m, 2H), 3.07 (td, *J* = 8.6, 2.7 Hz, 0.7H), 3.03 (td, *J* = 8.9, 2.5 Hz, 0.3H), 2.94 (br s, -OH) 2.54 (td, *J* = 7.0, 2.0 Hz, 2H), 2.15 – 2.05 (m, 2H), 1.94 – 1.83 (m, 2H), 1.75 – 1.65 (m, 5H).

¹³C NMR (151 MHz, CDCl₃) δ 138.23, 128.69, 127.92, 82.71, 82.61, 82.36, 81.92, 73.10, 70.16, 68.60, 67.85, 62.68, 34.18, 33.02, 27.84, 25.75, 25.70, 20.32.



Bispyran *ent*-73, from diyne triol substrate *ent*-64: Hg(OTf)₂ (11 mg, 0.023 mmol) was added to CH₂Cl₂ (2.4 mL) and cooled to -20 °C. Diynyl triol (*S,S*)-64 (63 mg; 0.20 mmol)

was dissolved in CH₂Cl₂ (3.0 mL) and added to the solution slowly and the reaction mixture turned bright yellow. After 15 min, the reaction was quenched with triethylsilane (195 μL; 1.20 mmol). After 15 h, the reaction was quenched with triethylamine and filtered through a plug of silica gel before being concentrated under reduced pressure. The crude oil was purified by flash column chromatography (10-30% EtOAc in hexanes) to afford bispyran *ent*-**73** as a clear yellow oil (14 mg; 0.044 mmol; 22% yield). Spectral data match that of the enantiomer, **73**, resulting from cyclization of (*R*)-**64** and (*S*)-**64**.



Bispyran 73, from alkynyl diol substrate (*R*)-64**:** Hg(OTf)₂ (9 mg, 0.017 mmol) was added to CH₂Cl₂ (2.4 mL) and cooled to -20 °C. Alkynyl diol (*R*)-**64** (36 mg; 0.13 mmol; 77:23 dr) was dissolved in CH₂Cl₂ (1.2 mL), and was slowly added to the Hg(OTf)₂ solution. After 20 min, triethylsilane was added (75 μL; 0.45 mmol), and the mixture was stirred for 14 h. The reaction mixture was quenched with triethylamine, and filtered through a plug of silica gel before being concentrated under reduced pressure. The crude oil was purified by flash column chromatography (15-30% EtOAc in hexanes) to afford product *ent*-**73** as clear yellow oil (26 mg; 0.012 mmol; 72% yield). ¹H, ¹³C, COSY, APT, HMQC, HMBC, and NOESY NMR spectral data are consistent with the structure proposed for compound *ent*-**73** and **73**.

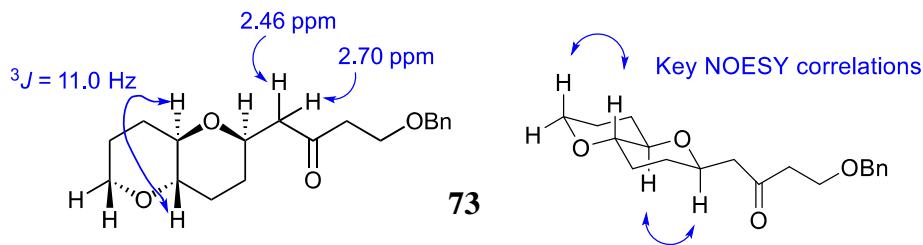
Data for **73**: [α]_D²⁵ -1.6 (c=1.12, CHCl₃)

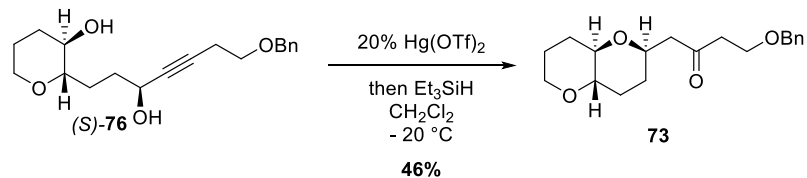
HRMS (NSI): m/z calcd. for $C_{19}H_{27}O_4$ $[M+H^+]$: 319.19039, found 319.18997.

1H NMR (600 MHz, $CDCl_3$) δ 7.36 – 7.25 (m, 5H), 4.49 (s, 2H), 3.92 – 3.80 (m, 2H), 3.73 (m, 2H), 3.37 (td, $J = 11.7, 3.0$ Hz, 1H), 3.04 (ddd, $J = 11.1, 8.8, 4.3$ Hz, 1H), 2.92 (ddd, $J = 11.0, 8.8, 4.4$ Hz, 1H), 2.74 (t, $J = 6.2$ Hz, 2H), 2.70 (dd, $J = 15.9, 7.3$ Hz, 1H), 2.46 (dd, $J = 16.0, 5.3$ Hz, 1H), 1.95 (m, 2H), 1.84 – 1.75 (m, 1H), 1.75 – 1.62 (m, 2H), 1.50 (qd, $J = 12.6, 12.2, 4.0$ Hz, 1H), 1.45 – 1.34 (m, 2H).

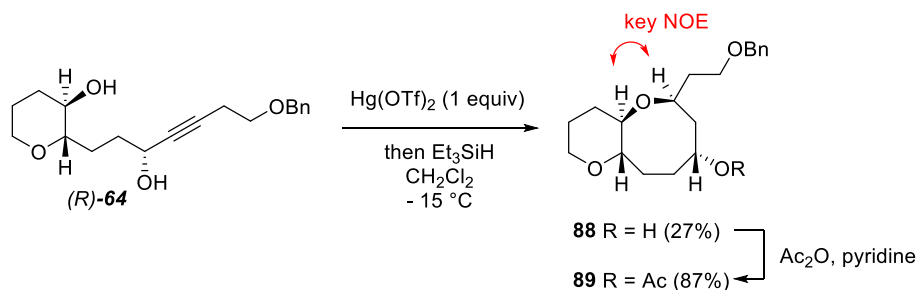
1H NMR (600 MHz, C_6D_6) δ 7.40 – 7.18 (m, 3H), 7.14 – 7.01 (m, 2H), 4.28 (s, 2H), 3.76 (dddd, $J = 12.8, 7.3, 4.9, 2.2$ Hz, 1H), 3.68 (ddt, $J = 11.3, 4.7, 1.6$ Hz, 1H), 3.61 (dt, $J = 9.4, 6.3$ Hz, 1H), 3.56 (dt, $J = 9.4, 6.2$ Hz, 1H), 3.07 (td, $J = 12.4, 2.4$ Hz, 1H), 2.91 (ddd, $J = 11.0, 8.7, 4.3$ Hz, 1H), 2.80 (ddd, $J = 11.1, 8.8, 4.4$ Hz, 1H), 2.47 (dd, $J = 15.8, 7.5$ Hz, 1H), 2.42 (td, $J = 6.3, 1.8$ Hz, 2H), 2.07 (dd, $J = 15.8, 4.9$ Hz, 1H), 1.91 – 1.86 (m, 1H), 1.82 (m, 1H), 1.51 – 1.24 (m, 3H), 1.22 – 1.06 (m, 2H), 1.06 – 0.84 (m, 1H).

^{13}C NMR (151 MHz, C_6D_6) δ 205.58, 139.07, 128.56, 128.14, 127.98, 78.68, 78.52, 73.78, 73.25, 67.80, 65.58, 49.43, 43.87, 30.23, 30.17, 30.05, 26.09.



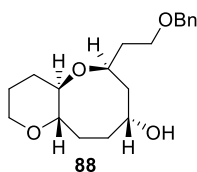


Bispyran 73, from alkynyl diol substrate (S)-64: Hg(OTf)_2 (11 mg, 0.023 mmol) was added to CH_2Cl_2 (2.4 mL) and cooled to -20°C . Alkynyl diol (S)-64 (35 mg; 0.13 mmol; 72:28 *S*:*R* dr) was dissolved in CH_2Cl_2 (1.2 mL), and was slowly added to the Hg(OTf)_2 solution. After 20 min, triethylsilane was added (75 μL ; 0.45 mmol), and the mixture was stirred for 14 h. The reaction mixture was quenched with triethylamine, and filtered through a plug of silica gel before being concentrated under reduced pressure. The crude oil was purified by flash column chromatography (15-30% EtOAc in hexanes) to afford product *ent*-73 as clear yellow oil (16 mg; 0.060 mmol; 46% yield). ^1H , ^{13}C , COSY, APT, HMQC, HMBC, and NOESY NMR spectral data are consistent with the structure proposed for compound *ent*-73.



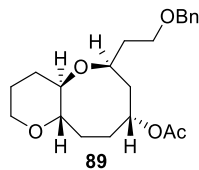
Bicyclic product 88, from cyclization of alkynyl diol substrate (R)-64: Hg(OTf)_2 (122 mg, 0.24 mmol) was added to CH_2Cl_2 (5 mL) and cooled to -15°C . Alkynyl diol (R)-64 (77 mg; 0.24 mmol; 73:27 *R*:*S* dr) was dissolved in CH_2Cl_2 (2.5 mL) and was slowly added

to the Hg(OTf)₂ solution. Within 20 seconds of the last addition of alkynyl diol, triethylsilane (160 μ L; 0.97 mmol) was added, and the reaction mixture was stirred for 16 h. The reaction mixture was quenched with triethylamine, filtered through a plug of silica gel, and concentrated under reduced pressure. The crude oil was purified by flash column chromatography (25-50% EtOAc in hexanes) to afford the product **88** as a yellow oil (17 mg; 27% yield).



¹H NMR (600 MHz, CDCl₃) δ 7.40 – 7.28 (m, 5H), 4.52 (dd, $J = 11.9, 11.6$ Hz, 2H), 4.06 – 3.99 (m, 1H), 3.93 – 3.86 (m, 2H), 3.70 – 3.58 (m, 3H), 3.40 (td, $J = 11.7, 3.0$ Hz, 1H), 3.10 (ddd, $J = 11.2, 8.8, 4.3$ Hz, 1H), 2.97 (ddd, $J = 10.4, 8.7, 4.4$ Hz, 1H), 1.99 (m, 2H), 1.82 – 1.62 (m, 5H), 1.62 – 1.55 (m, 1H), 1.54 – 1.41 (m, 2H).

Compound **88** was dissolved in CH₂Cl₂ (1 mL), and Ac₂O (0.1 mL) and pyridine (0.1 mL) were added. The reaction mixture was stirred overnight. The crude product was concentrated under reduced pressure and purified by silica gel flash column chromatography to afford the acetate ester **89** as a yellow oil (16 mg; 0.46 mmol; 87% yield). COSY, HMBC, HMQC, and NOESY of compound **89** support the structural and stereochemical assignment.



[α]_D²⁵: -5.2 (c=0.90, CHCl₃)

IR (thin film): 2926, 2853, 1734, 1243, 1097, 734 cm⁻¹.

HRMS (NSI): *m/z* calcd. for C₂₁H₃₁O₅ [M+H⁺]: 363.21660, found 363.21617.

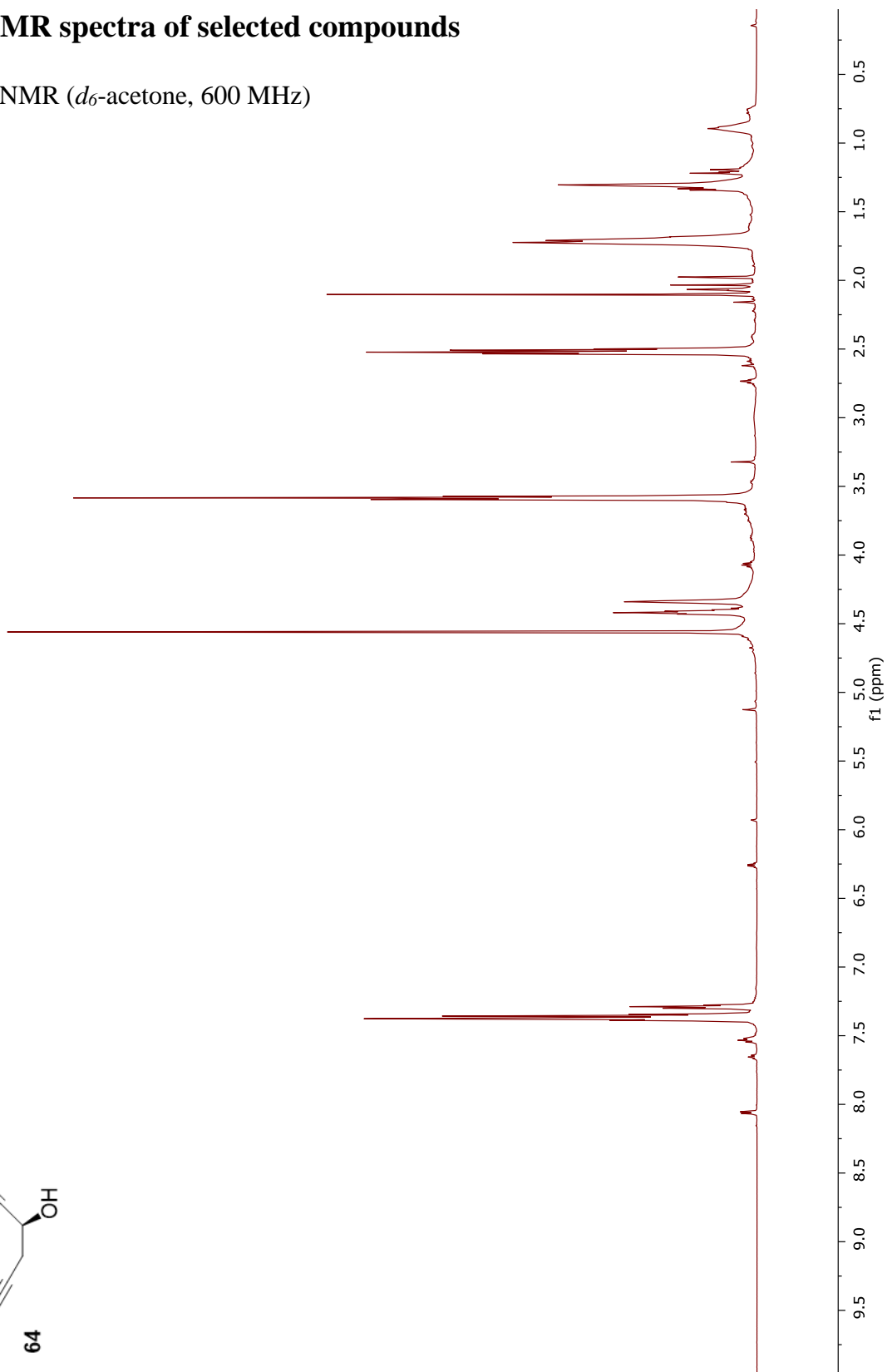
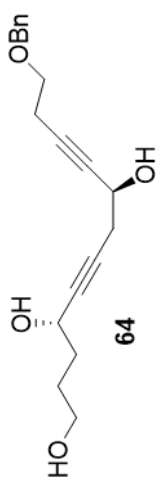
¹H NMR (600 MHz, CDCl₃) δ 7.39 – 7.27 (m, 5H), 5.21 (dddd, *J* = 8.3, 6.9, 5.7, 4.4 Hz, 1H), 4.55 – 4.40 (dd, *J* = 11.9, 3.2 Hz, 2H), 3.89 (m, 1H), 3.55 – 3.42 (m, 3H), 3.38 (td, *J* = 11.6, 3.0 Hz, 1H), 2.96 (m, 2H), 2.18 (s, 3H), 1.99 – 1.92 (m, 1H), 1.93 – 1.81 (m, 4H), 1.77 (m, 1H), 1.75 – 1.65 (m, 2H), 1.62 (m, 1H), 1.51 – 1.34 (m, 3H).

¹H NMR (600 MHz, C₆D₆) δ 7.32 – 7.29 (m, 2H), 7.20 – 7.17 (m, 2H), 7.09 (ddt, *J* = 8.8, 6.9, 1.4 Hz, 1H), 5.45 (tt, *J* = 7.4, 5.4 Hz, 1H), 4.30 (m, 2H), 3.70 (ddt, *J* = 11.3, 4.8, 1.6 Hz, 1H), 3.39 (t, *J* = 6.3 Hz, 2H), 3.37 (app dt, *J* = 7.3, 2.5, 1H), 3.09 (ddd, *J* = 12.5, 11.3, 2.4 Hz, 1H), 2.93 (ddd, *J* = 11.0, 10.8, 4.3, 1H), 2.84 (ddd, *J* = 10.7, 8.7, 4.4 Hz, 1H), 1.92 (dddd, *J* = 10.7, 8.4, 3.8, 2.6 Hz, 1H), 1.88 (m, 1H), 1.87 – 1.82 (m, 2H), 1.73 (s, 3H), 1.52 – 1.42 (m, 4H), 1.35 – 1.29 (m, 2H), 1.23 – 1.17 (m, 2H).

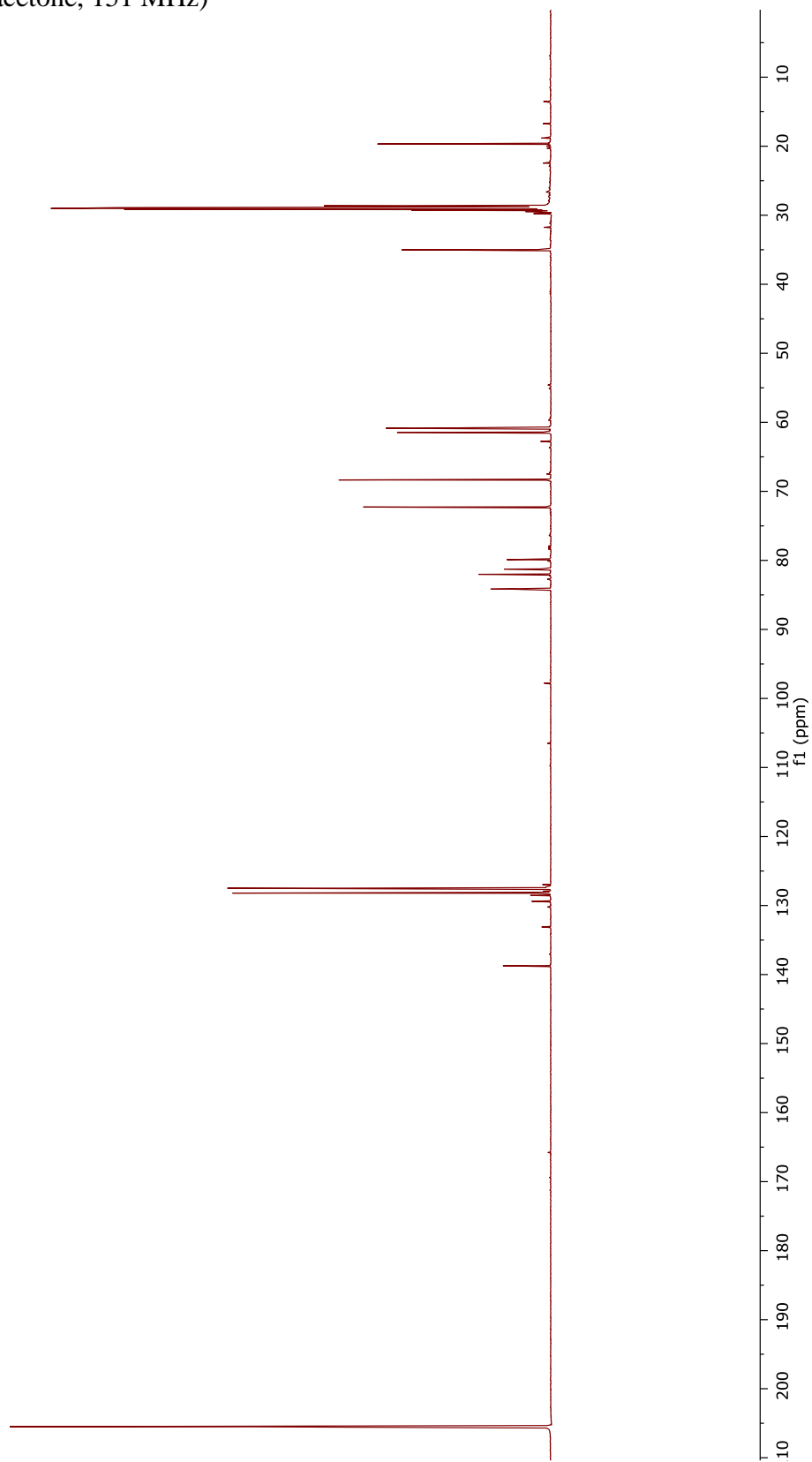
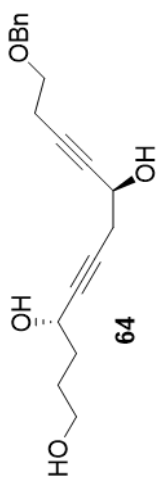
¹³C NMR (151 MHz, C₆D₆) δ 170.10, 139.52, 128.89, 128.66, 128.01, 79.13, 78.83, 75.42, 73.51, 69.87, 68.12, 67.22, 41.33, 35.44, 32.15, 30.56, 30.51, 26.48, 21.33.

2.5 NMR spectra of selected compounds

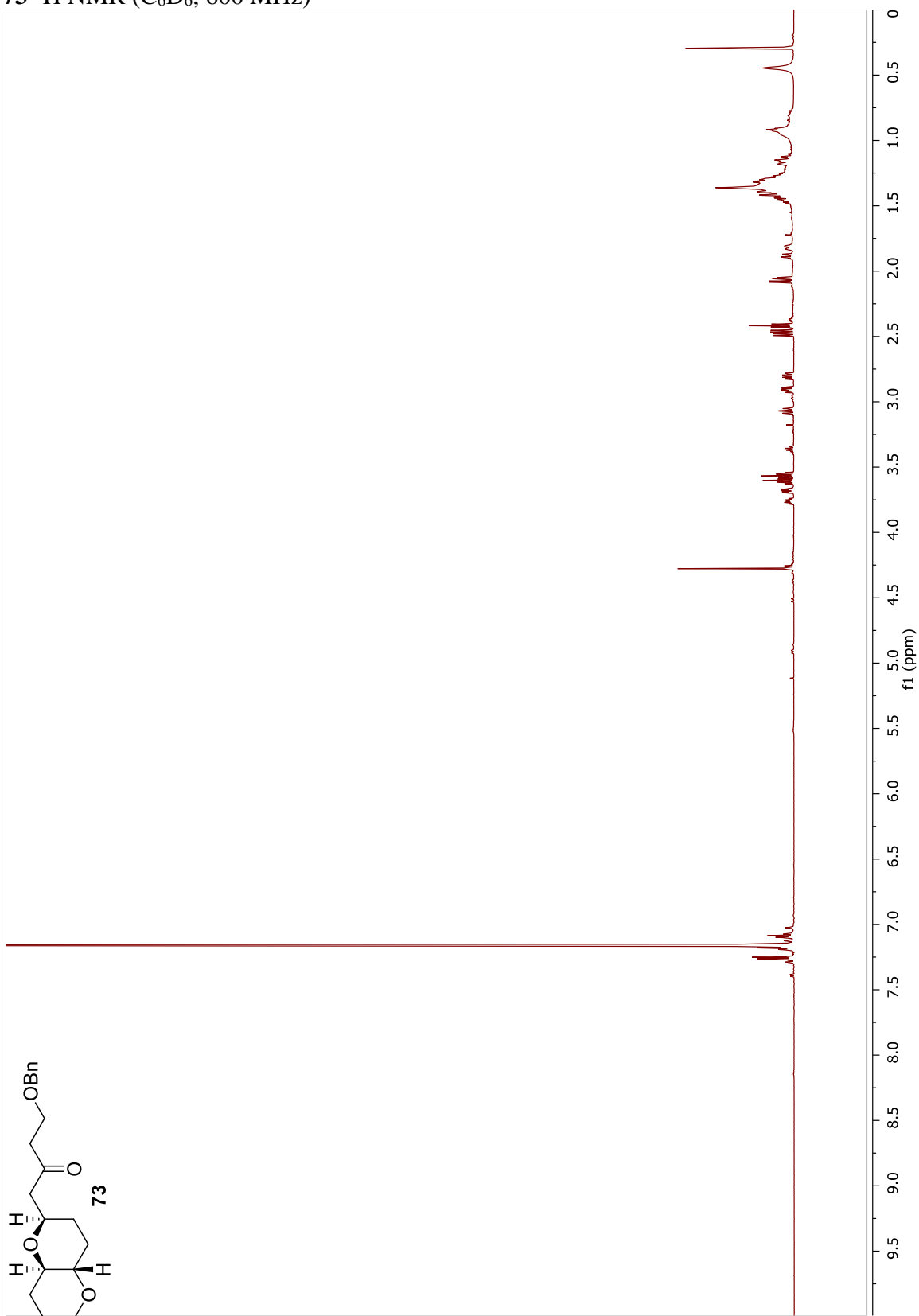
64 ^1H NMR (d_6 -acetone, 600 MHz)



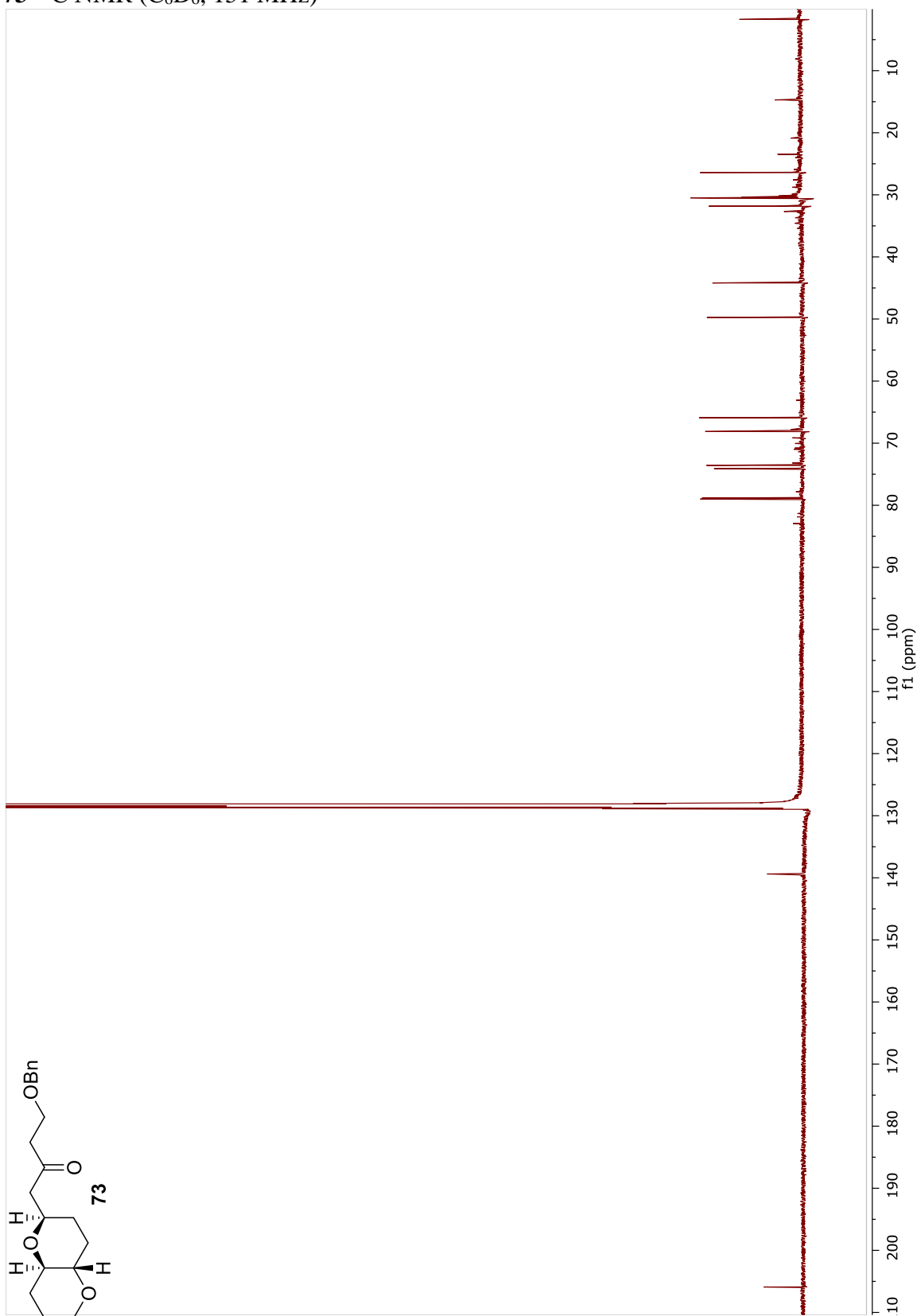
64 ^{13}C NMR (d_6 -acetone, 151 MHz)

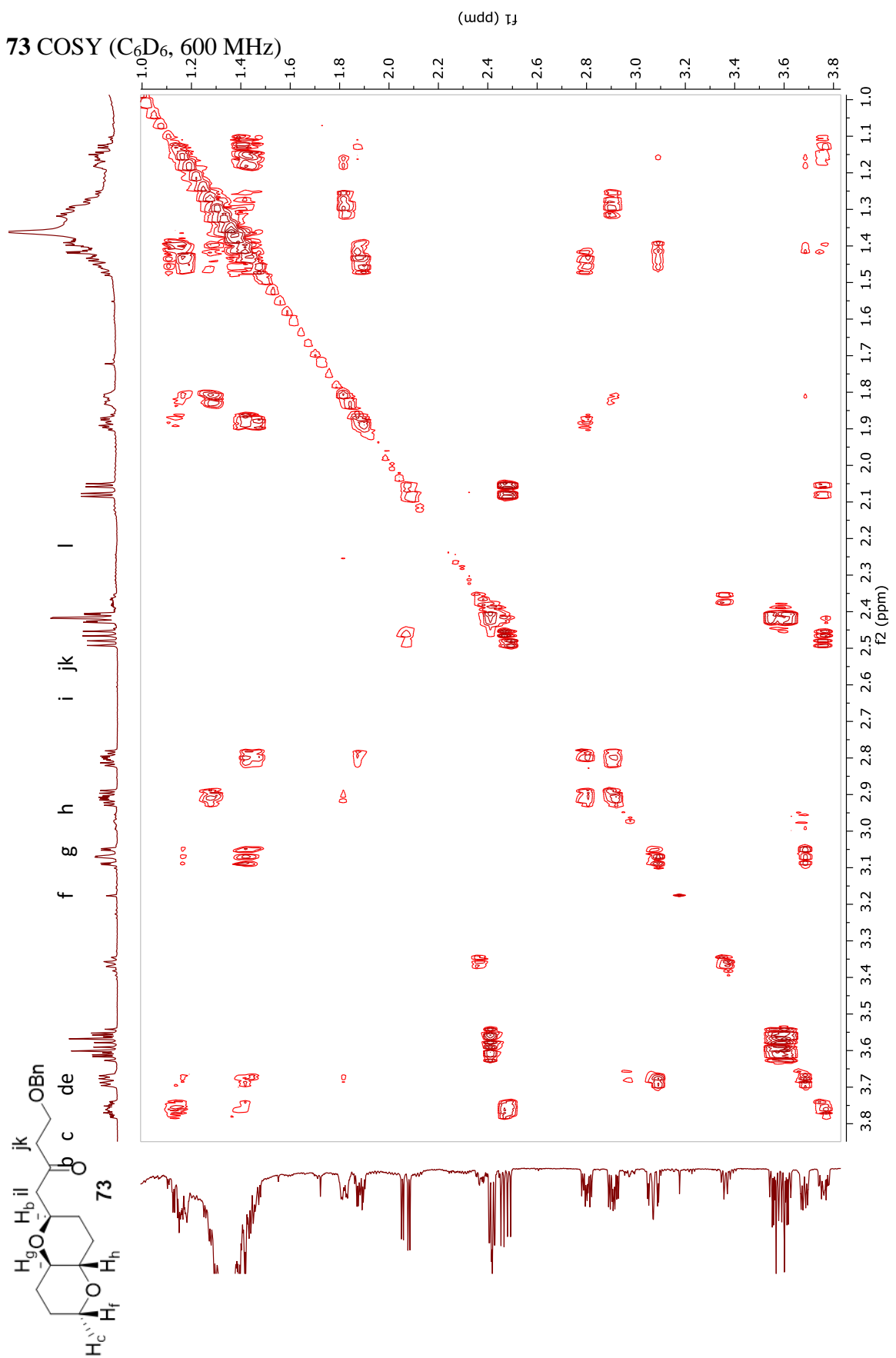


73 ^1H NMR (C_6D_6 , 600 MHz)

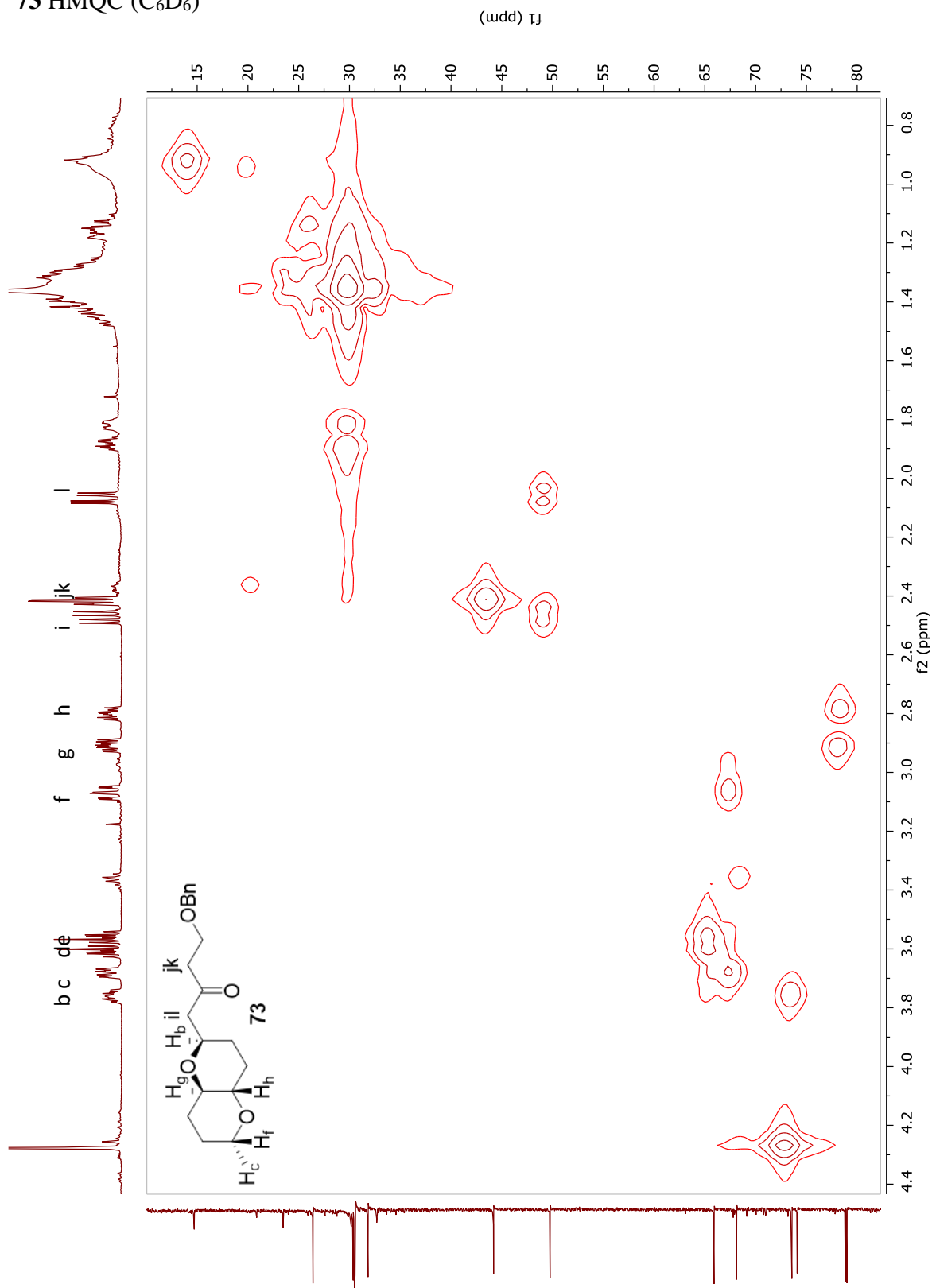


73 ^{13}C NMR (C_6D_6 , 151 MHz)

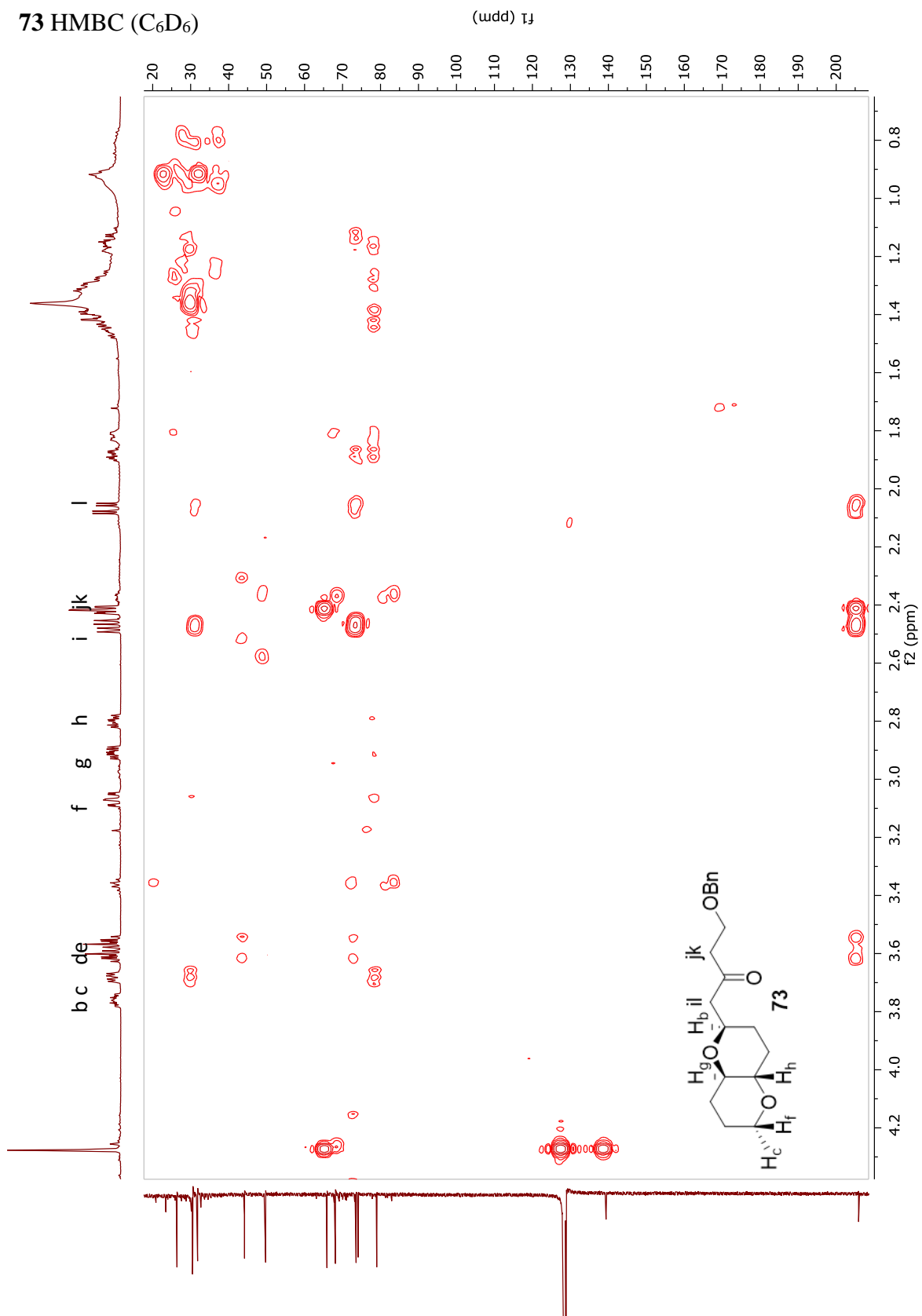




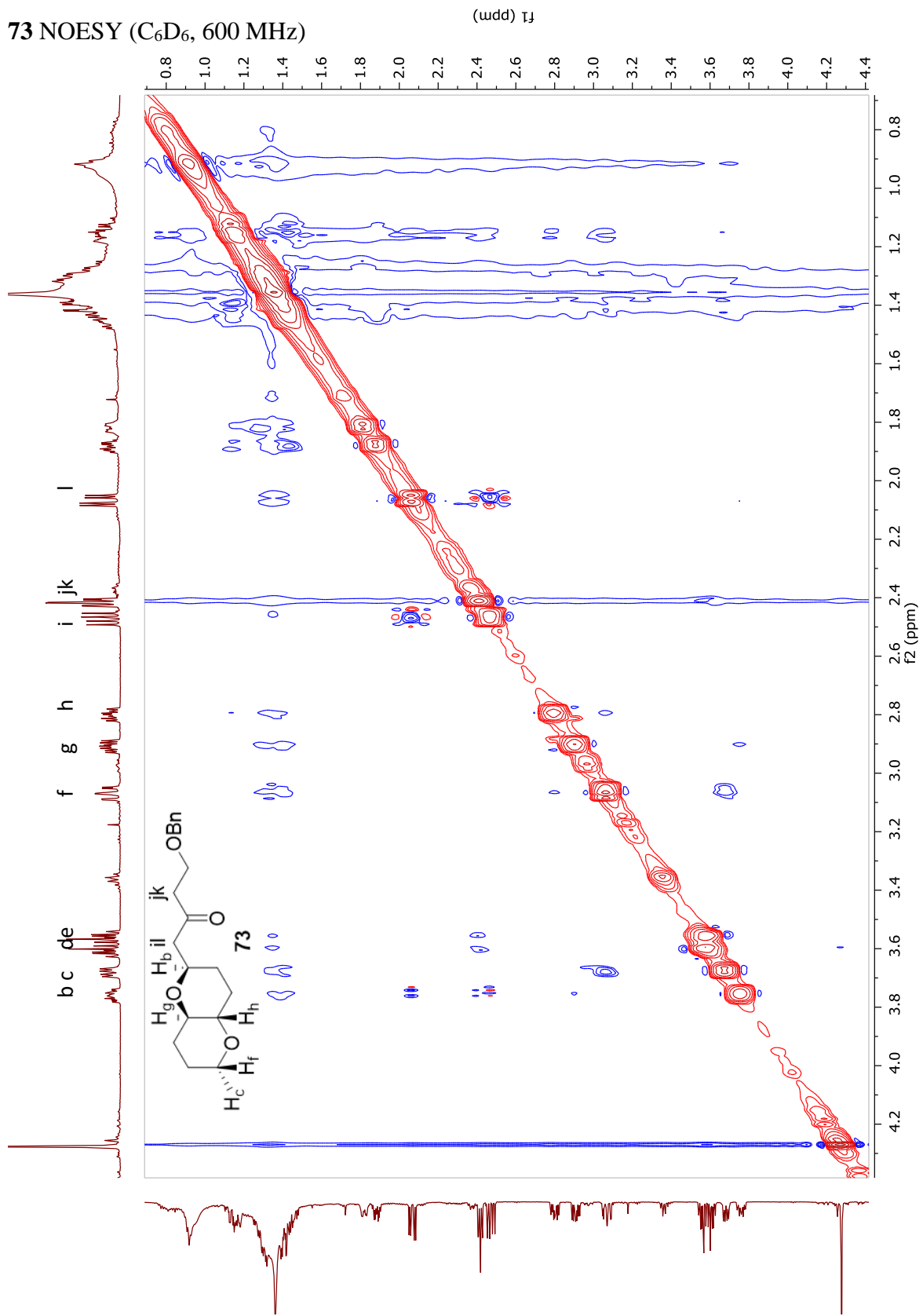
73 HMQC (C₆D₆)



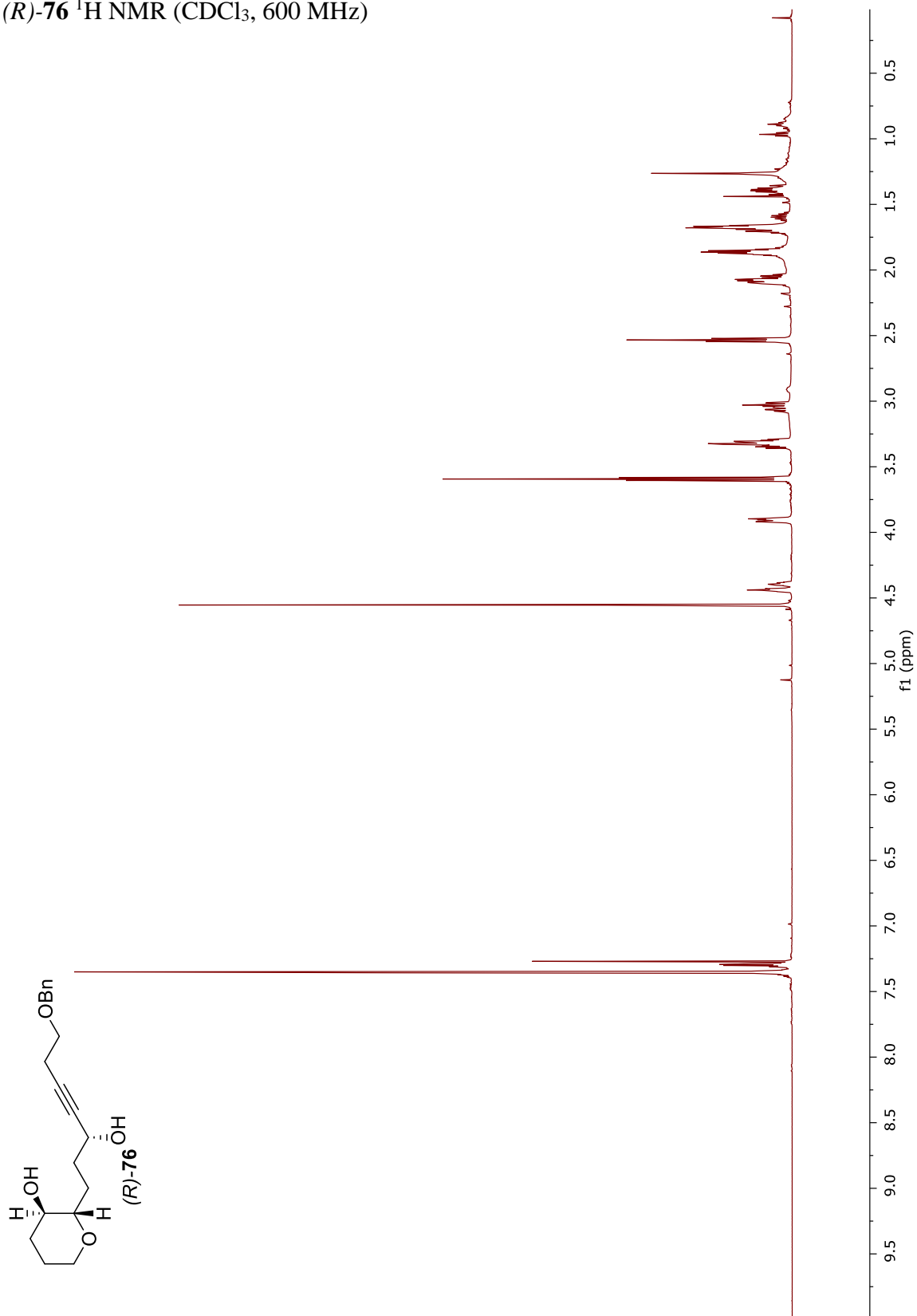
73 HMBC (C₆D₆)



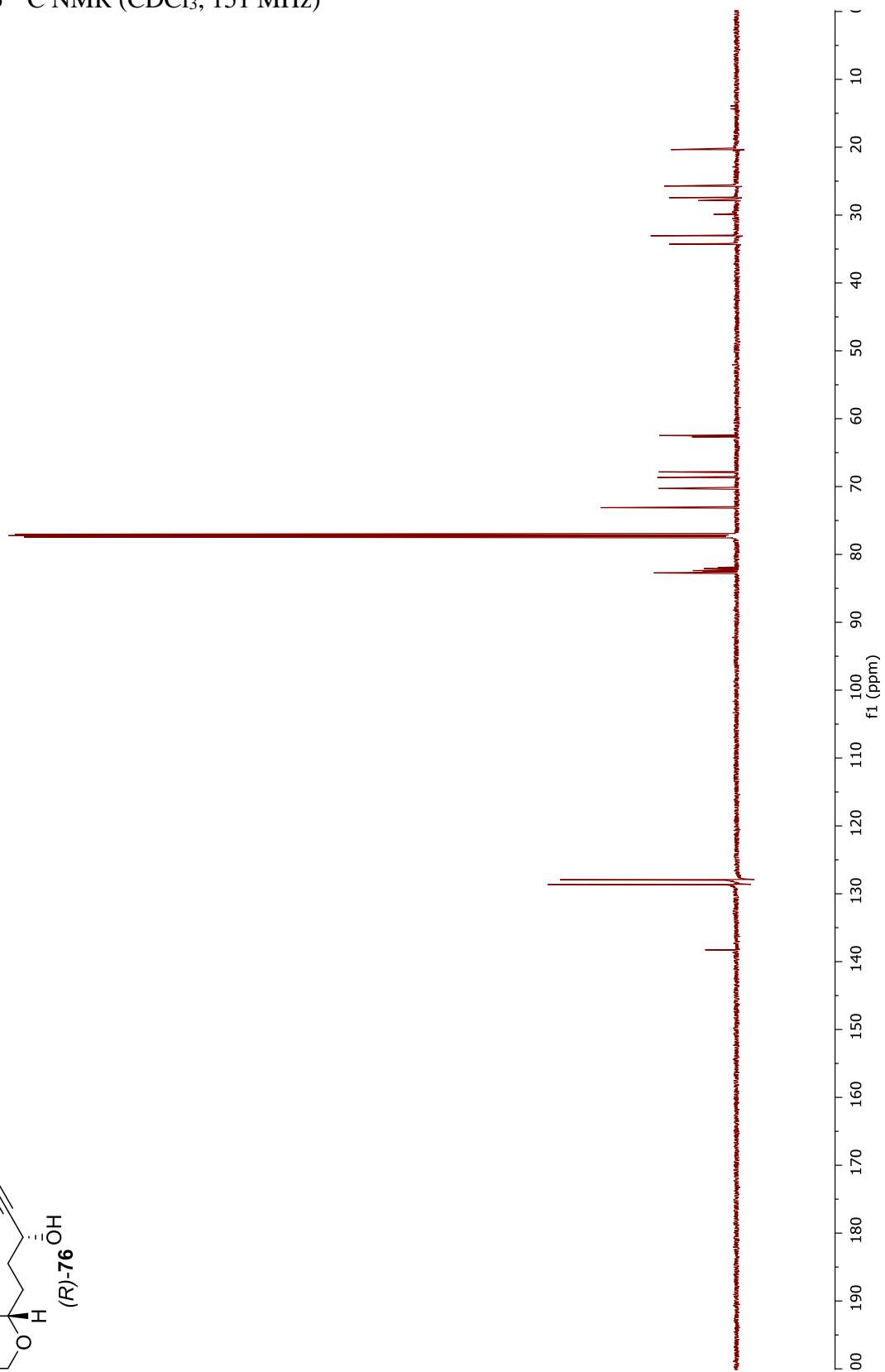
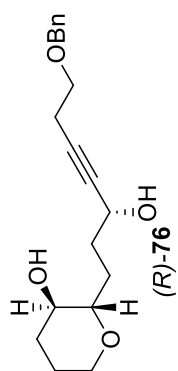
73 NOESY (C₆D₆, 600 MHz)



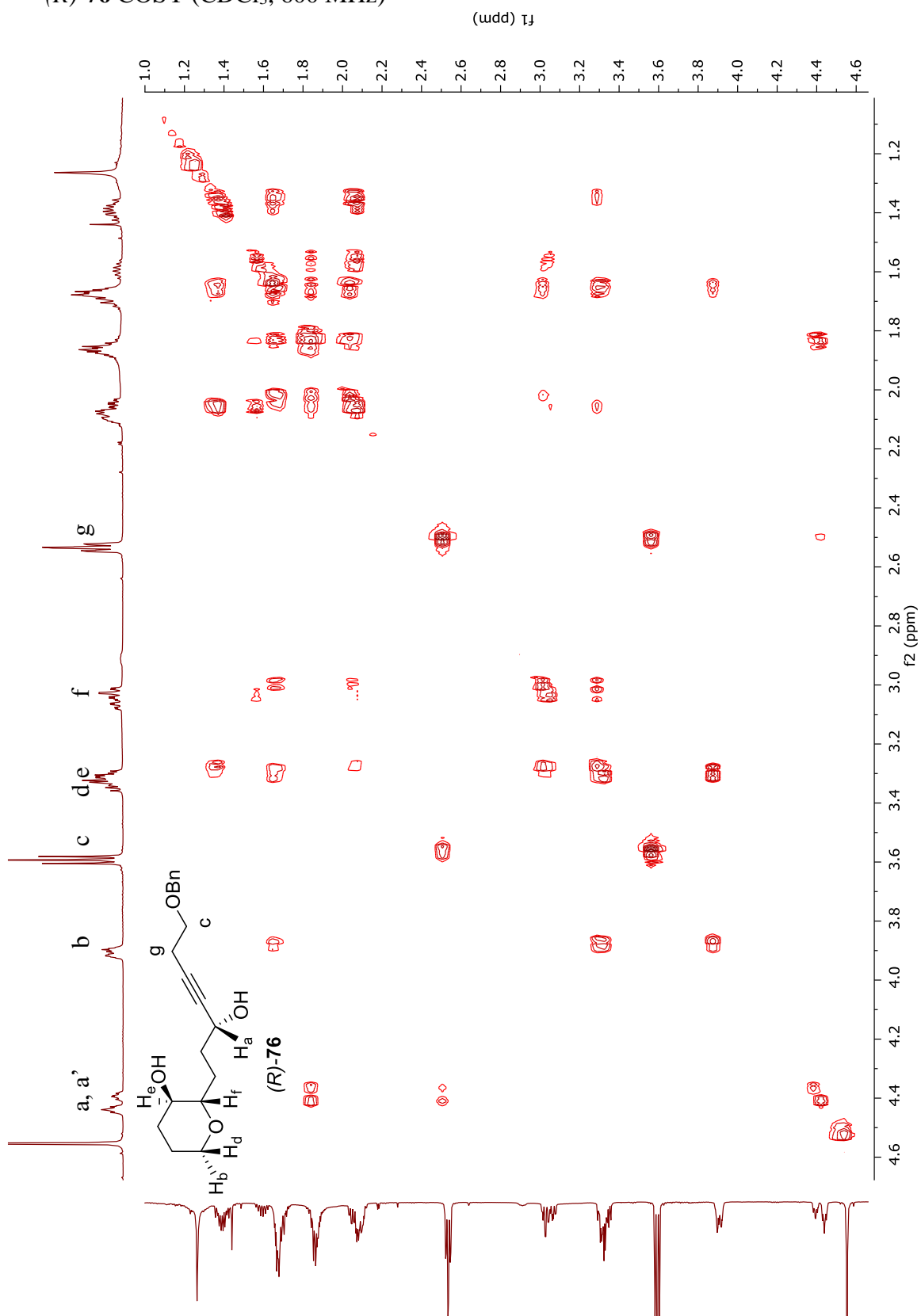
(*R*)-**76** ^1H NMR (CDCl_3 , 600 MHz)



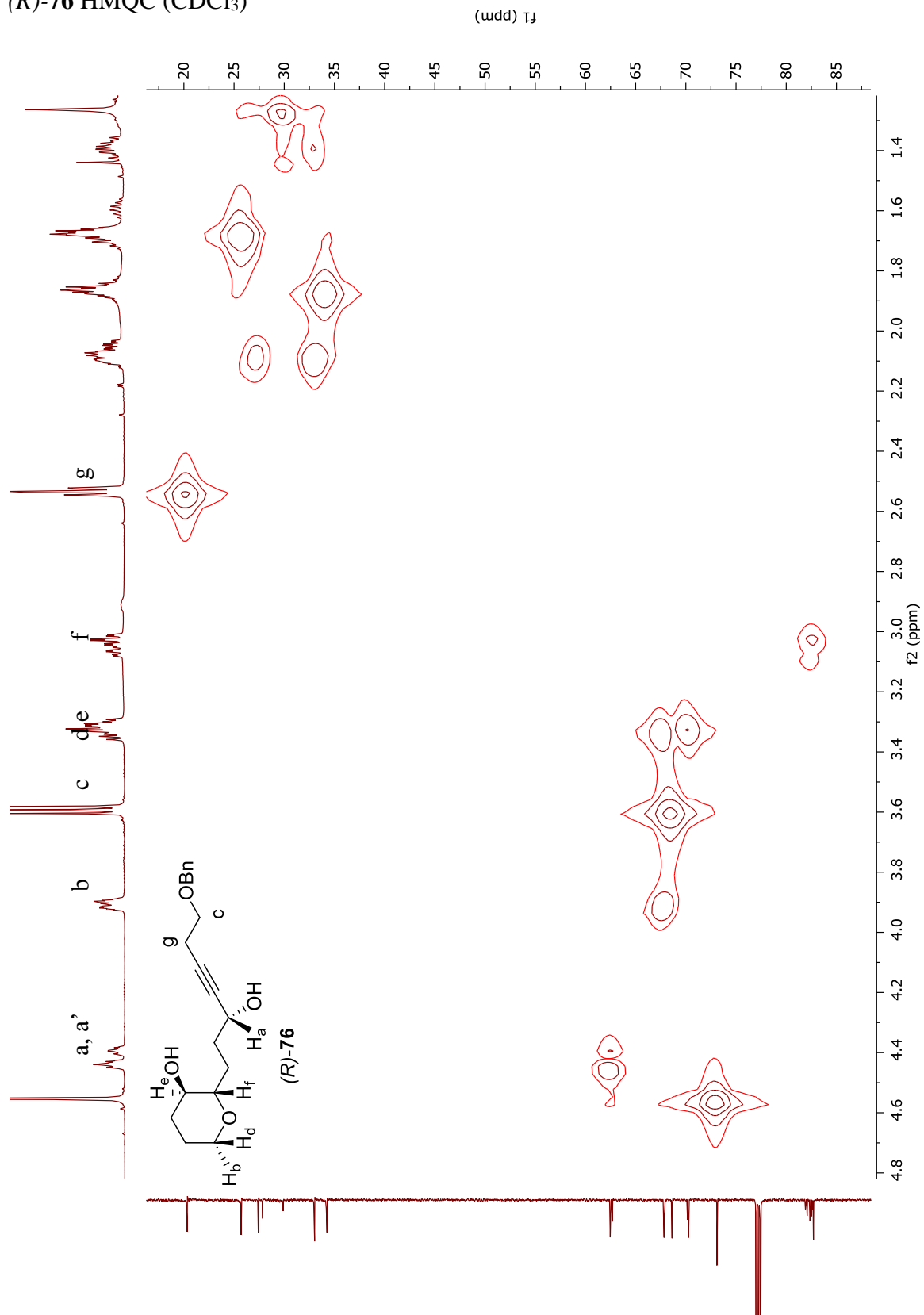
(*R*)-**76** ^{13}C NMR (CDCl_3 , 151 MHz)



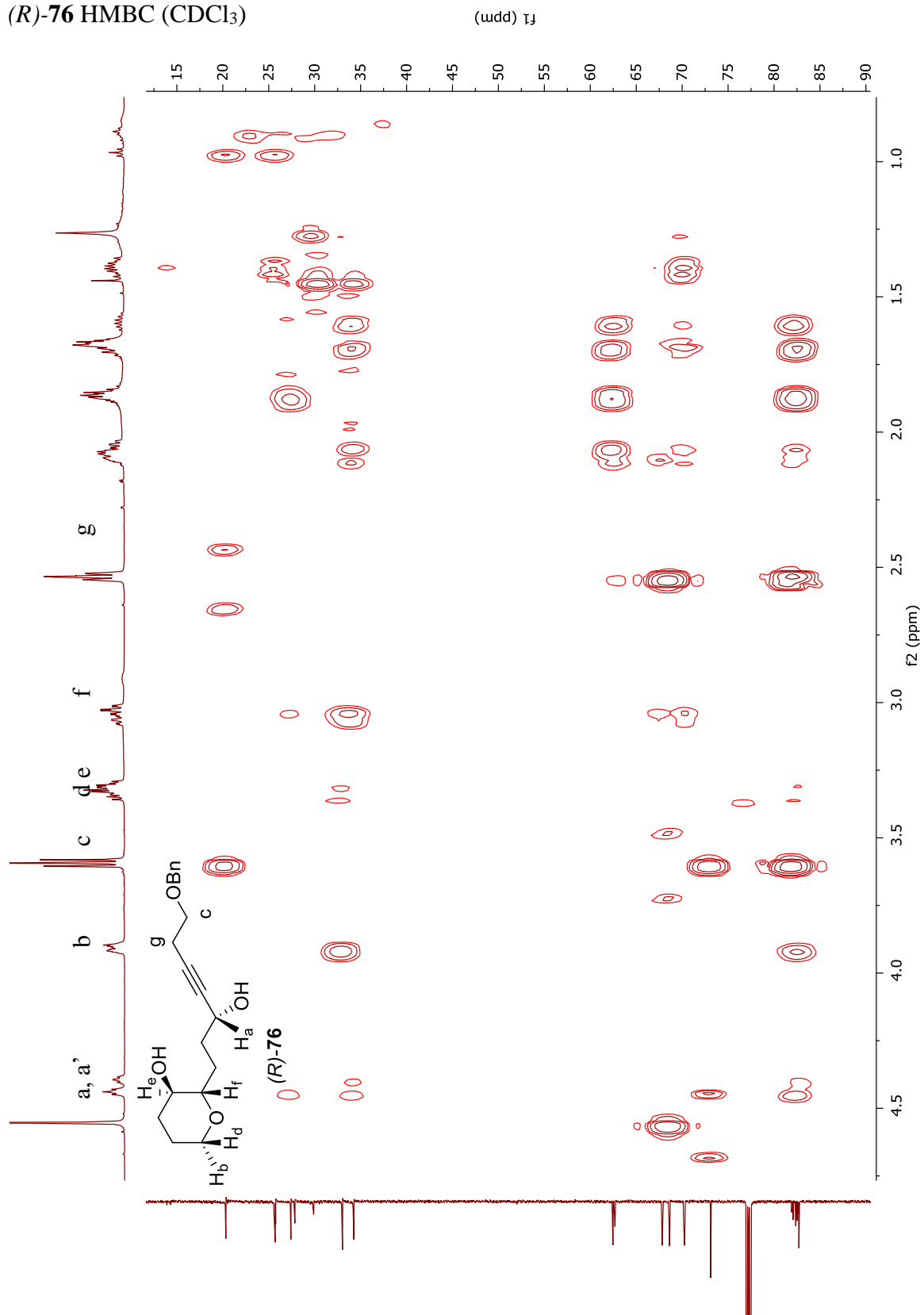
(R)-76 COSY (CDCl₃, 600 MHz)



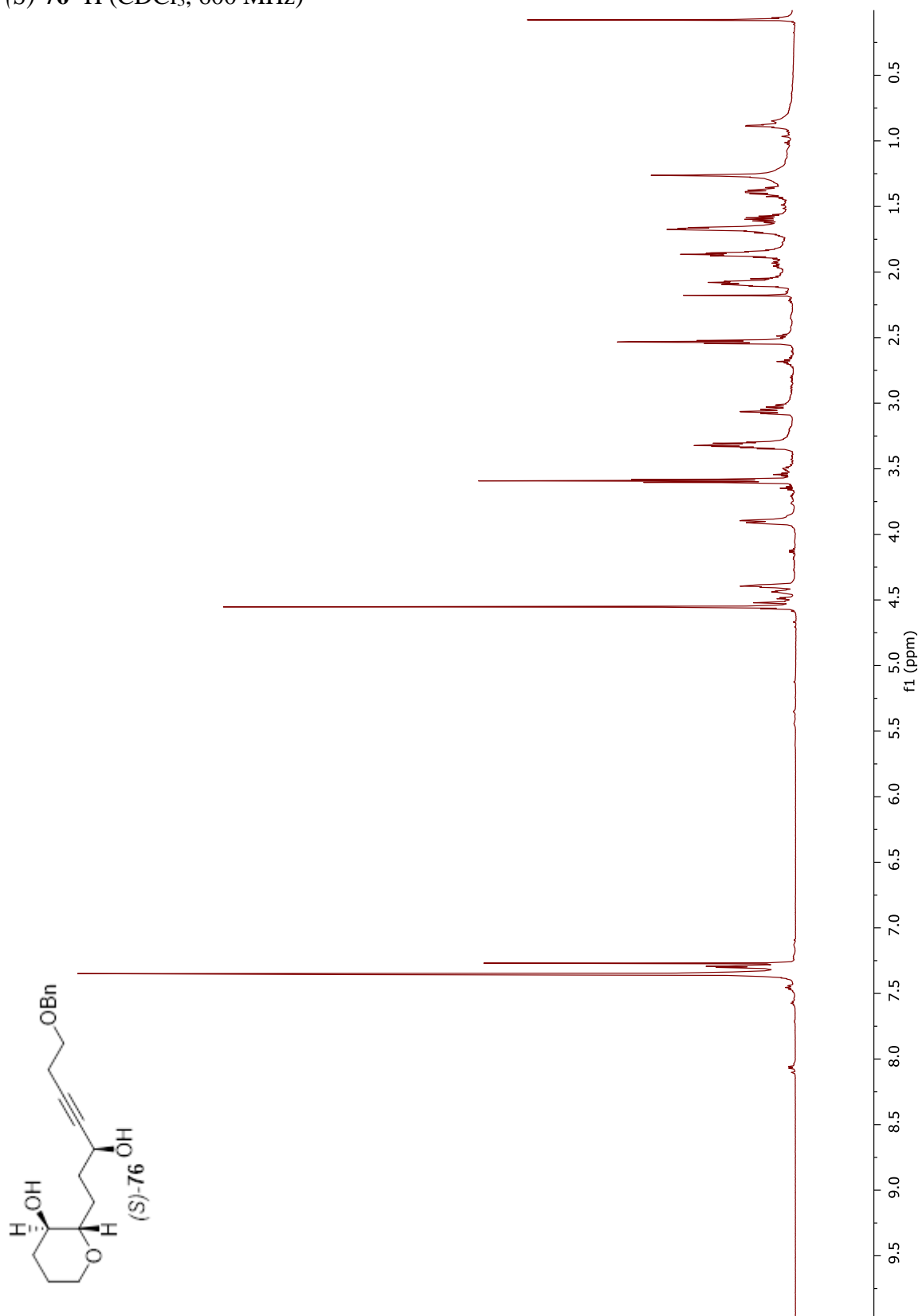
(R)-76 HMQC (CDCl₃)



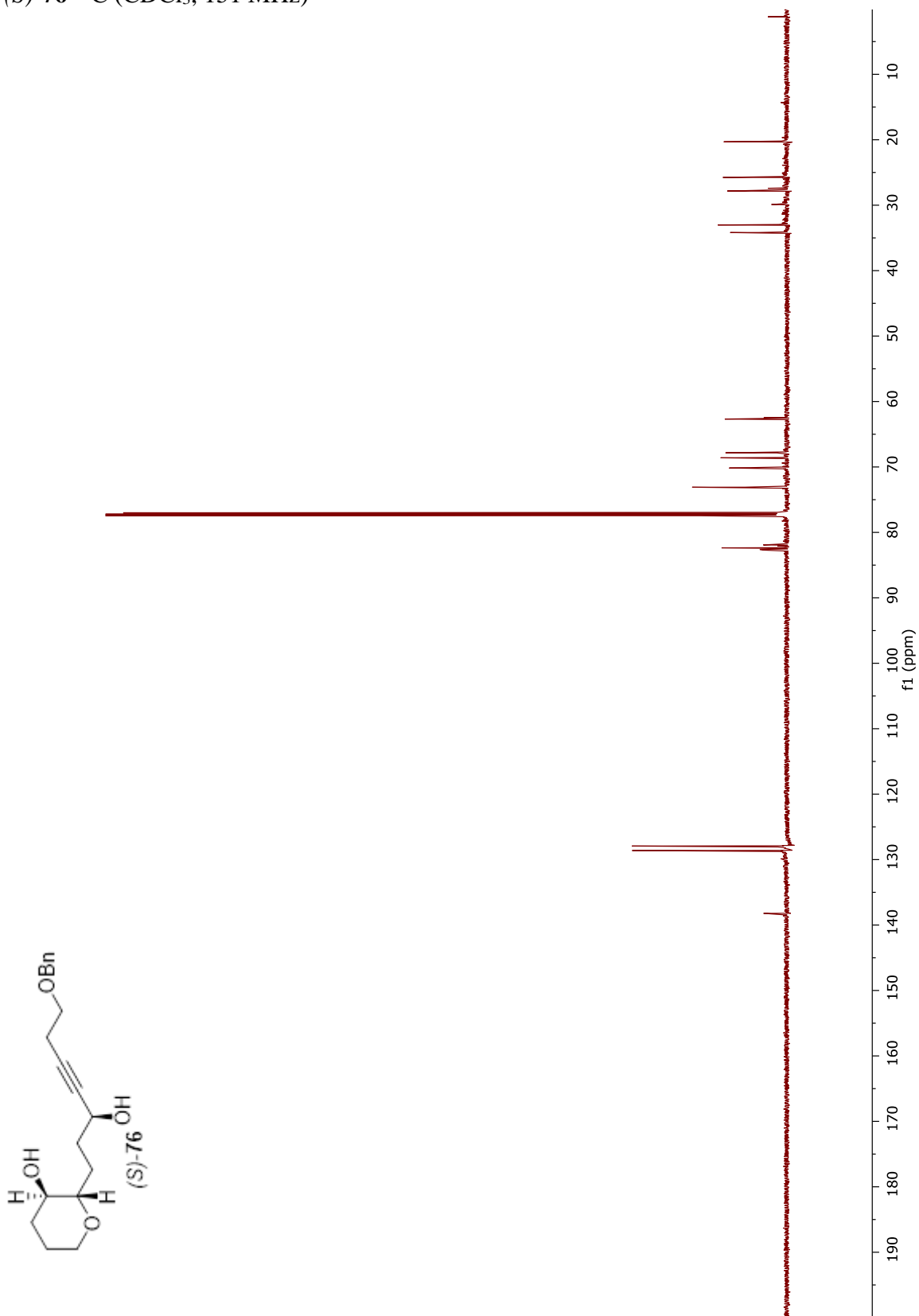
(R)-76 HMBC (CDCl₃)



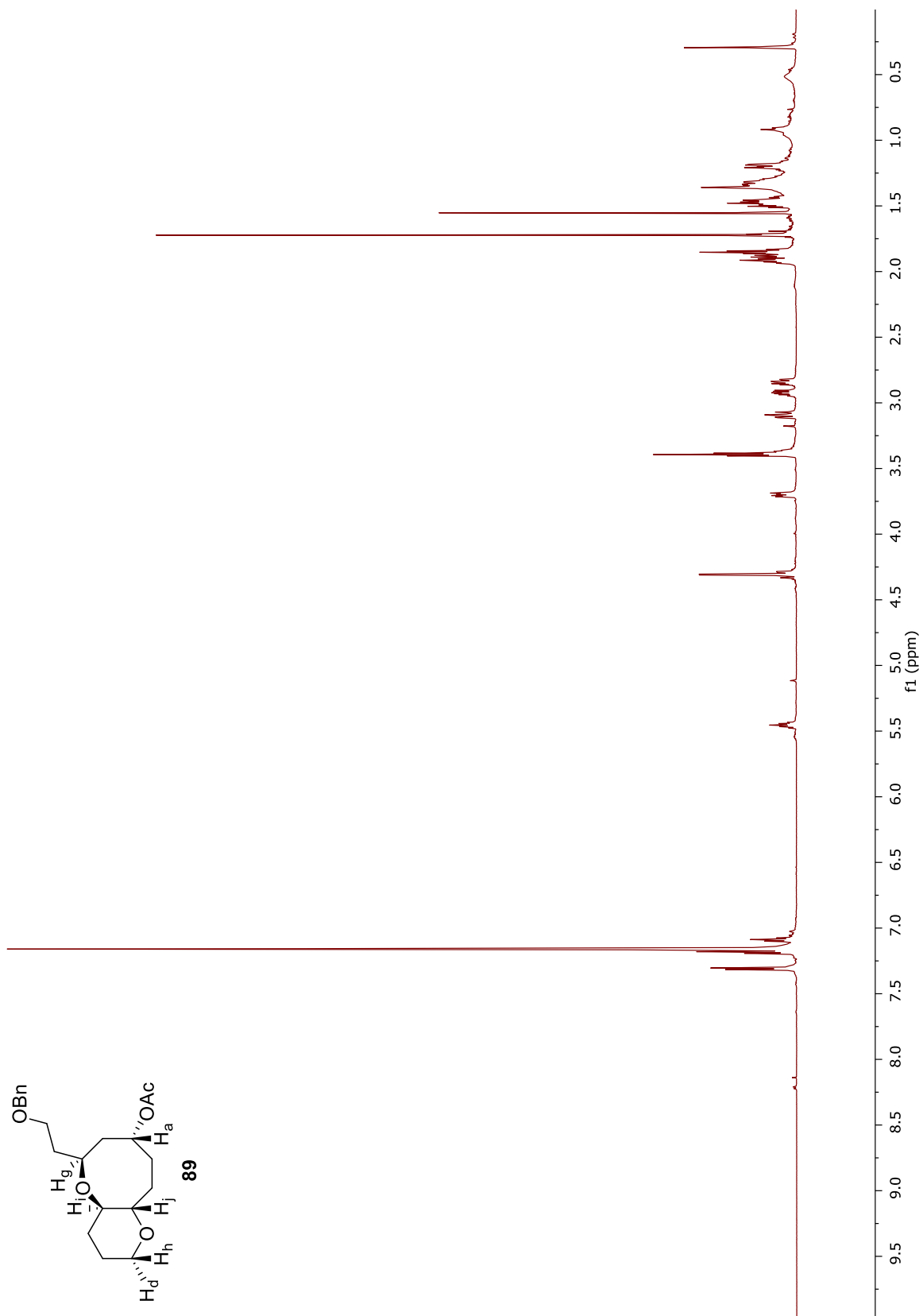
(S)-76 ¹H (CDCl₃, 600 MHz)



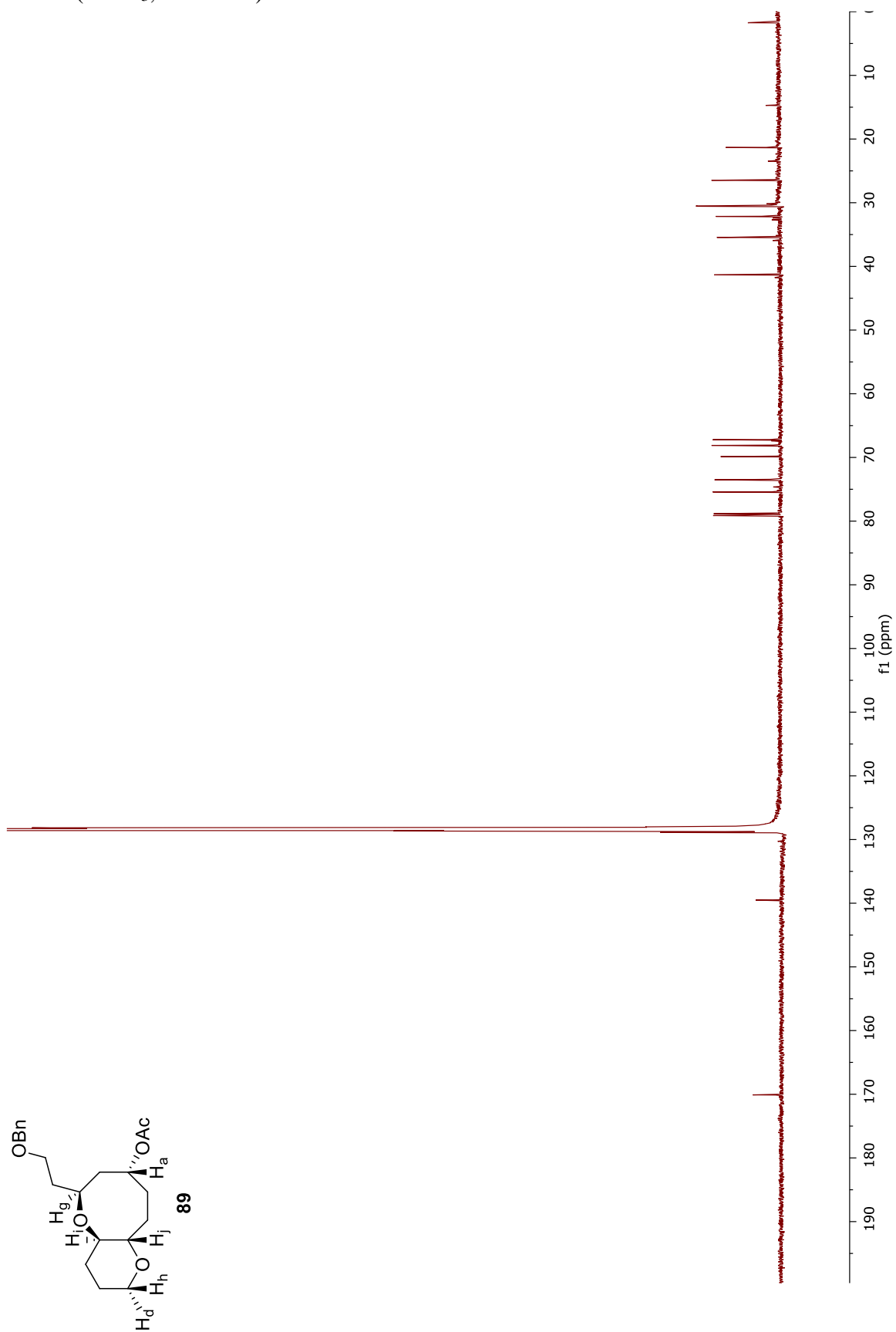
(*S*)-**76** ^{13}C (CDCl_3 , 151 MHz)



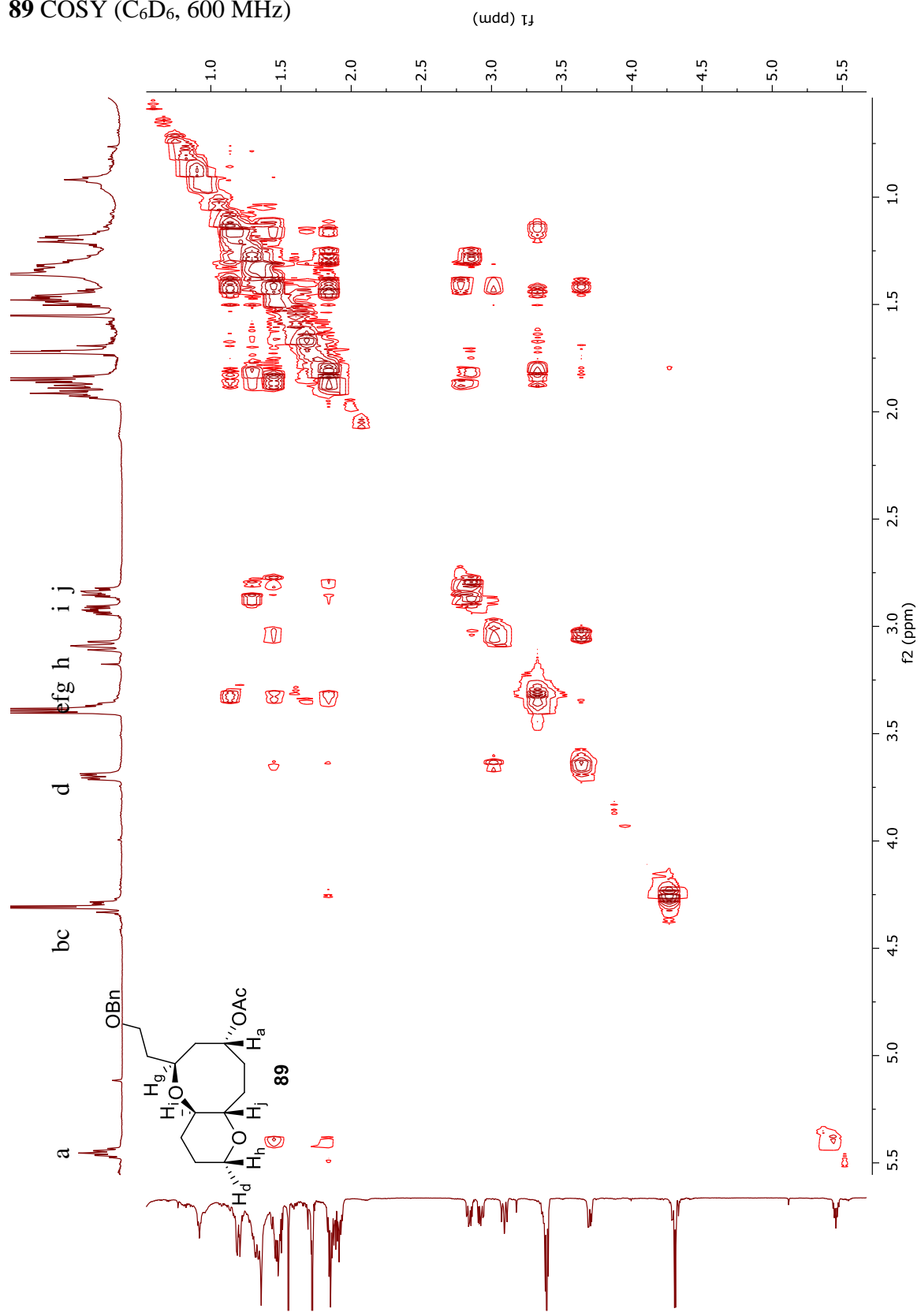
89 ^1H (C_6D_6 , 600 MHz)



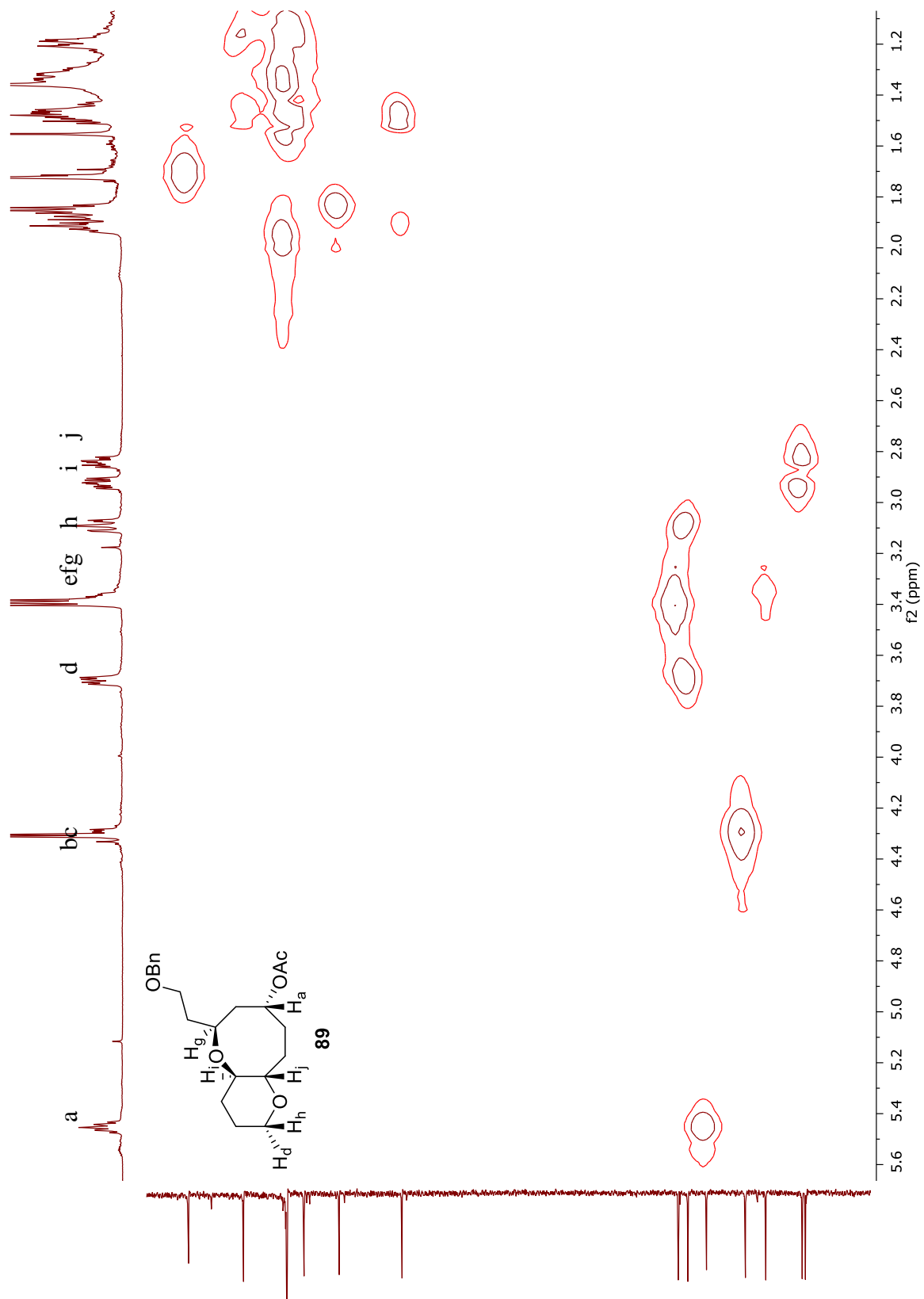
89 ^{13}C (CDCl_3 , 151 MHz)



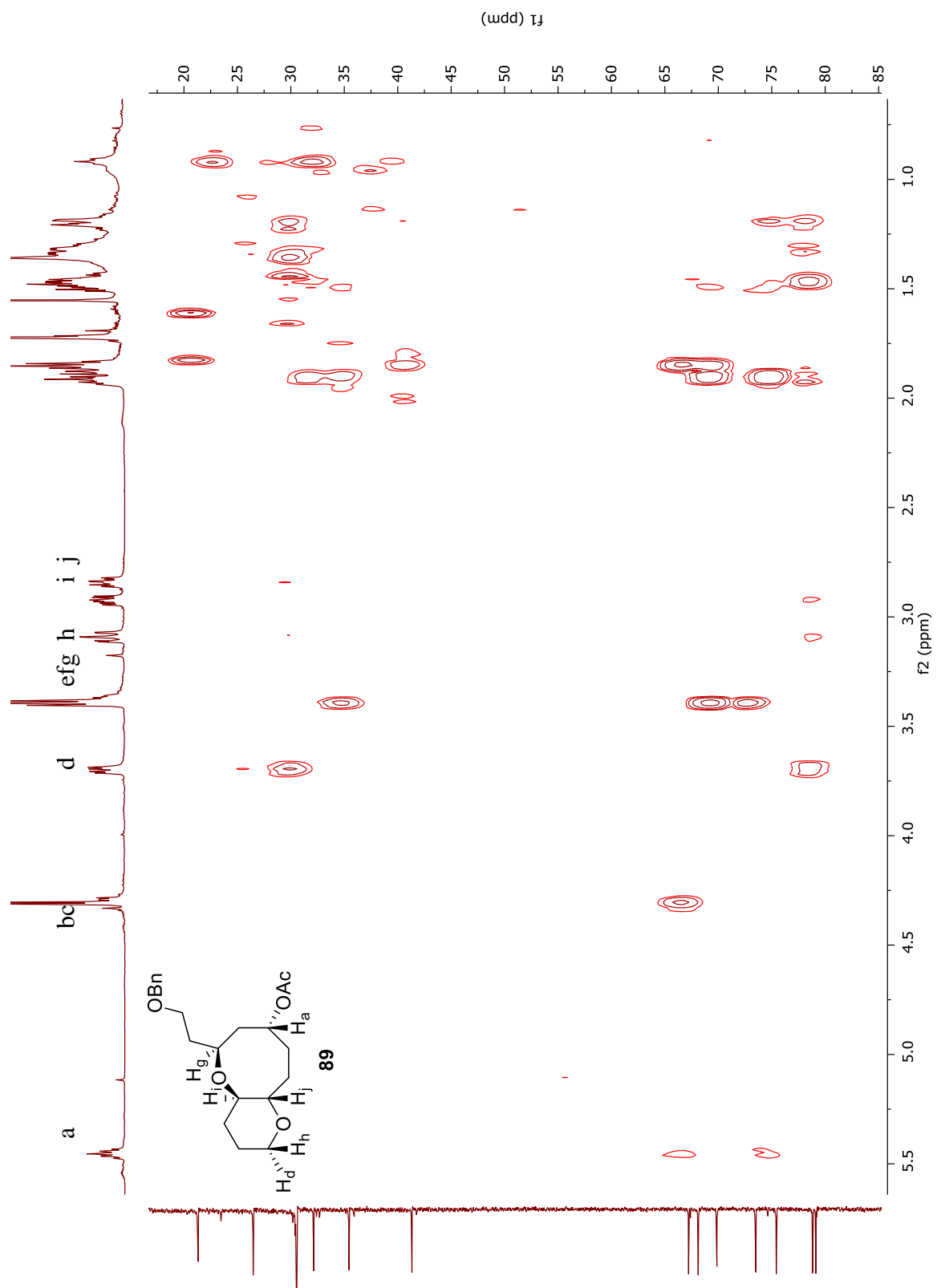
89 COSY (C₆D₆, 600 MHz)



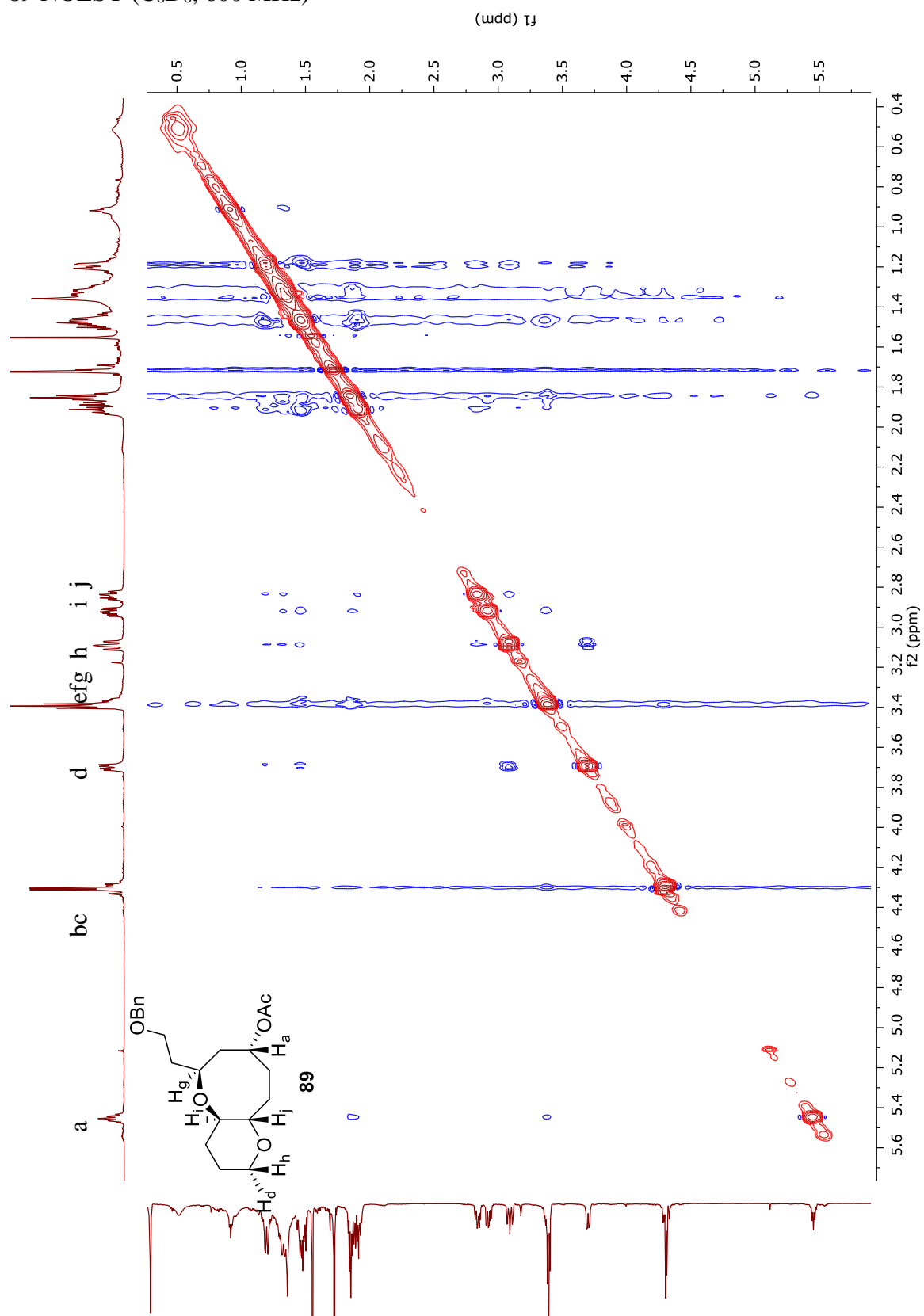
89 HMQC (C₆D₆)



89 HMBC (C₆D₆)



89 NOESY (C₆D₆, 600 MHz)



**Chapter 3. Alkenol oxacyclizations: Synthesis of the
ABC ring substructure of brevenal**

Chapter 3. Alkenol oxacyclizations: Synthesis of the ABC ring substructure of brevenal

3.1. Background and Introduction

3.1.1 Background

The overarching goal of our laboratory's research is harnessing stereo- and regioselective cascades of ring-forming reactions in order to efficiently prepare structurally complex members of the polycyclic ether natural products family. Our goal is to extend oxacyclization methodology developed in our laboratory to polycyclization processes, forming two or more cyclic ether rings in sequential transformations, controlling regio- and stereoselectivity. As precedents, our laboratory has uncovered the regio- and diastereoselectivities of various oxacyclization reactions on simple acyclic alkenes bearing allylic oxygen substituents as elements of stereinduction. Complementary to our previous work on *endo*-selective polyepoxide cyclization, the herein described *exo*-selective oxacyclization reactions may offer more generality. With this new approach, we hope to overcome some of the restrictions imposed by polyepoxide cascade approaches in chemical synthesis with regard to substitution pattern¹²⁴ and ring size.^{35,36} This chapter discusses our efforts at extending these new *exo*-mode reactions to the ABC sector (**27**) of the pentacyclic core of brevenal (**1**) (Figure 9). Chapter 1 contained background on the natural product and previous efforts in its total synthesis.

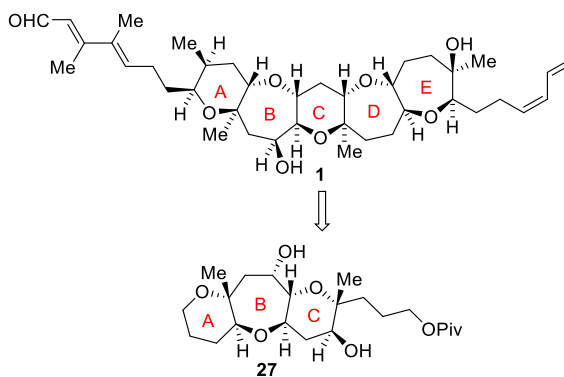


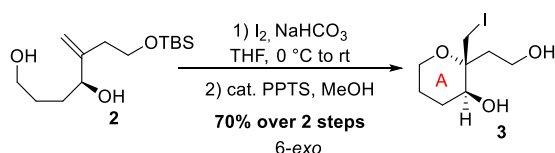
Figure 9. Pentacyclic marine natural product brevenal and ABC substructure **27**

3.1.2 Individual ring precedents: A and B rings

3.1.2.1 Individual ring precedent: A ring

The A-ring model of brevenal is formed through 6-*exo* iodocyclization. As described in Chapter 2, Dr. Kento Ishida discovered that 1,1-disubstituted alkenyl diol **2** undergoes iodine-promoted oxacyclization to afford *trans*-fused tetrahydropyran **3**⁶⁴ (Scheme 46). The observed diastereoselectivity is consistent with Chamberlin's model¹²⁵, with the allylic hydroxyl in the plane of the alkene (**4**, Figure 10). In this model, coordination of iodine on the face of the alkene with the allylic hydrogen attracted the tethered alcohol from the opposite face of the alkene, resulting in the desired stereochemistry, observed in product **6**. A notable aspect of this approach is in its ability to accommodate the methyl substituents.

Scheme 46. Iodine-promoted oxacyclization of 1,1-disubstituted alkenyldiol **2**



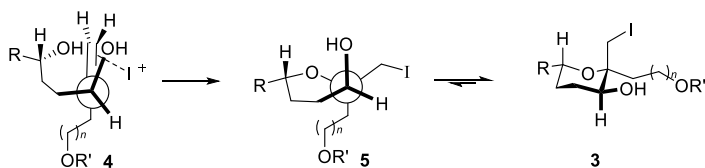
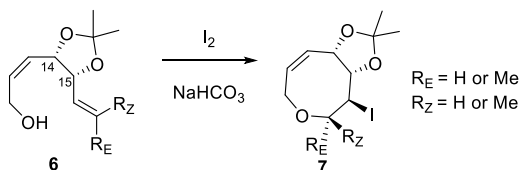


Figure 10. Conformational model for A-ring cyclization

3.1.2.2 Individual ring precedent: B ring

Initially, we hoped to synthesize oxepane **9**, our B-ring model, through 7-*exo* halocyclization of hydroxy-diene **6** (Scheme 47). Drs. Andre Roig Alba and Kristen Stoltz observed that iodocyclization of hydroxy-alkene derivatives of **6** exclusively proceeded through 8-*endo* cyclization, resulting in oxocene product **7**¹²⁶. Variations in both the conformational restrictions of the substrate and choice of electrophile to promote cyclization were unsuccessful in producing the desired 7-*exo* regioisomeric product, oxepane **9**.

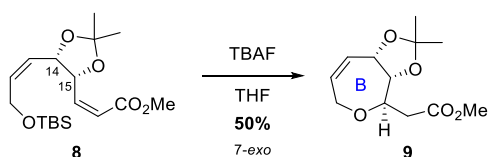
Scheme 47. 8-*Endo* iodocyclization cyclizations of hydroxy-alkenes **6**



Dr. Stoltz observed that unsaturated ester **8** underwent intramolecular conjugate addition upon desilylation to furnish the desired *trans*-fused oxepane **9**¹¹⁹ (Scheme 48). Although Nicolaou and Kishi synthesized tetrahydropyran rings through *oxa*-Michael

addition reactions in the syntheses of natural products brevetoxin B^{33,127} and the halichondrin B series¹²⁸, the corresponding reactions to form oxepanes are less-developed^{129–133} due to the enthalpic and entropic barriers of seven-membered ring formation, which are exacerbated by low reactivity of oxygen nucleophiles, the potential reversibility of the reaction, and the challenge in controlling stereoselectivity. Hydroxy ester **8** features an acetonide-protected *cis*-1,2-diol at C₁₄ and C₁₅. The inclusion of the cyclic protecting group serves as a conformational restraint to favor cyclization, and also provides an element of stereocontrol in the ring-closing reaction. To mimic the rigidity of the fused A-ring, favoring cyclization, a *cis*-alkene was installed in the tether¹³⁰. The ester electron-withdrawing substituent enforces the regioselectivity, and the acetonide-protected diol provides the opportunity for diastereoselectivity *via* stereoinduction. We propose a reactive conformation in which allylic acetonide-protected oxygen is perpendicular to the electrophilic alkene, which is oriented to minimize the steric interactions with the tether relative to the allylic hydrogen^{134,135}, resulting in the observed *trans*- orientation of protons at the site of ring-closure (Figure 11).

Scheme 48. Intramolecular *oxa*-Michael addition on unsaturated ester **8**



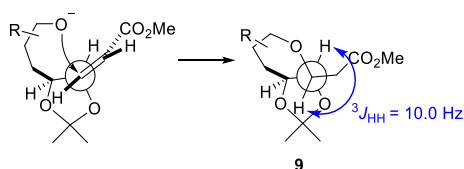


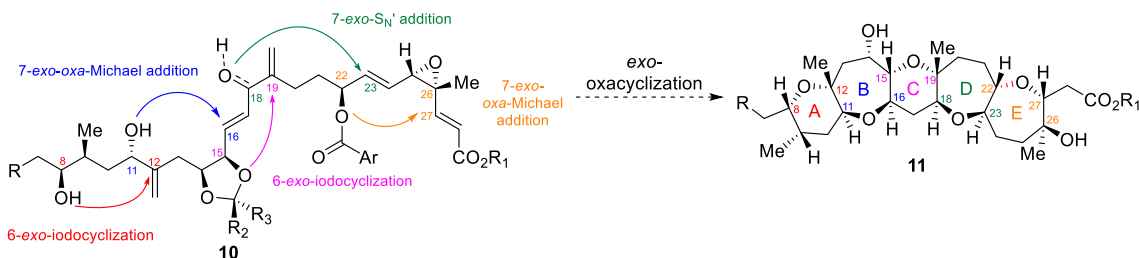
Figure 11. Conformational model for B-ring cyclization

3.1.3 *Exo*-mode oxacyclization strategy for brevenal

Building off the individual ring precedents for the A and B rings from our laboratory, we proposed sequential formation of each ring through an *exo*-mode cyclization of polyene substrate **10** to synthesize the pentacyclic core of brevenal **11** (Scheme 49). Each oxacyclization reaction is reliant upon stereinduction from the oxygen group at the allylic position of the tether to set the new chiral center at the site of ring closure. All cyclizations proposed are *exo*-mode, which is favored by Baldwin's rules⁴⁶. Alternative competitive 3-*exo* or 4-*exo* cyclization pathways should be disfavored relative to the competitive 6-*exo* and 7-*exo*. To execute such a transformation, the cyclization events must favor one direction of reactivity (A→E) to obtain the desired regioselectivity and diastereoselectivity. A major challenge of this approach is setting the new chiral center from an sp²-hybridized carbon with the desired diastereoselectivity in synthesis of polyene **10**. Another major challenge will be controlling against competing reaction pathways such as dehydrative cyclization and *endo*-mode cyclization, which have been observed in development of the A- and B-ring models. Due to the complexity of polyene **10** and core **11**, we decided that constructing model systems of first the individual rings and then of

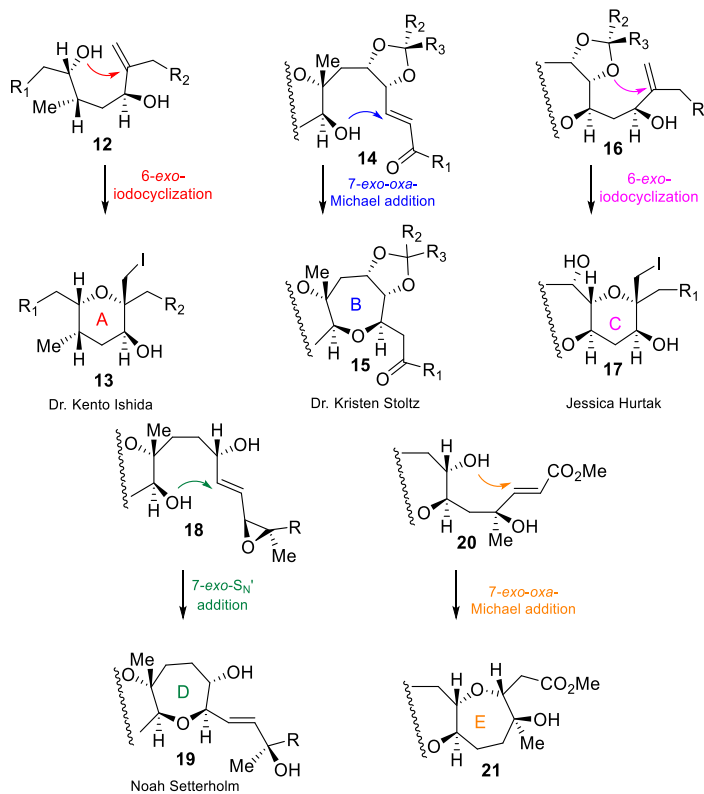
two- and three- ring substructures would be essential to inform the ultimate pentacyclization sequence.

Scheme 49. Proposed *exo*-oxacyclizations of polyene **10** to synthesize pentacyclic core **11**



Prior to my efforts on this project, our laboratory had developed precedents for the A ring and B ring. Dr. Kento Ishida formed A ring **13** through iodocyclization of alkene **12**⁶⁴, and Dr. Kristen Stoltz formed B ring **15** through intramolecular conjugate addition onto unsaturated ester **14**¹¹⁹ (Scheme 50). We hoped to close the C ring (**17**) through iodine promoted 6-*exo* cyclization from acetal-protected diol **16** (Scheme 50). In separate work performed by Mr. Noah Setterholm, formation of D-ring model **19** was pursued through a Pd- or acid-mediated 7-*exo* addition to vinyloxirane **18**. We planned to extend the successful 7-*exo*-intramolecular conjugate addition which formed B ring model **15** to form E-ring **21** from unsaturated methyl ester **20** (Scheme 50). The A-ring iodocyclization served as a precedent for the C-ring iodocyclization, and likewise the B-ring conjugate addition served a precedent for the E-ring conjugate addition. My work has focused sequential cyclization of a triene precursor to synthesize tricyclic ABC sector **27** of the brevenal core **11**, building off precedents for the A and B rings.

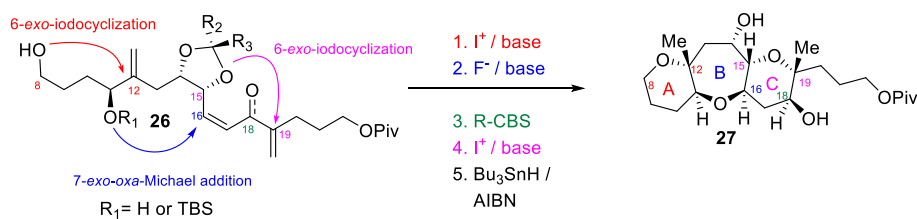
Scheme 50. Individual ring models: *exo*-oxacyclization



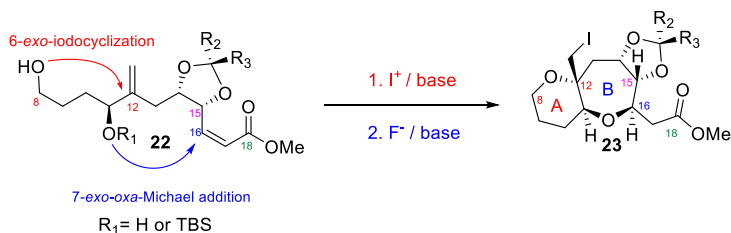
Our overall goal for the stage of the project disclosed in this dissertation is construction of the ABC ring sector of brevenal **27** from sequential oxacyclization of an acyclic precursor, such as triene **26** (Scheme 51). Prior to studies on tandem cyclization, we investigated iodine-promoted cyclization of acetal-protected diol **16** to form C-ring model **17** (Scheme 50). Before attempting the tricyclization sequence, we first investigated bicyclization sequences forming the AB and BC ring substructures individually. First, we investigated tandem cyclization of diene **22** to form the AB ring model system **23** (Scheme 52). In this system, we probed the effect of the preformed A-ring on the diastereoselectivity of the B-ring cyclization. Then, we investigated intramolecular *7-exo oxa*-Michael addition onto dienylketone **24** at C₁₆ in the BC ring model system **25** (Scheme 53). In this

system, we attempted to extend the successful B-ring conjugate addition from a simple methyl ester to a dienyl ketone. We used the results from the bicyclization studies to inform the synthesis of triene **26** and oxacyclizations to form the ABC ring subsector of brevenal **27** (Scheme 51).

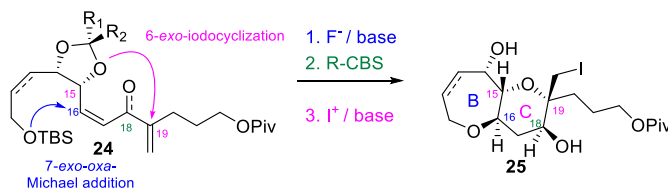
Scheme 51. Proposed cyclizations of triene **26** to synthesize ABC compound **27**



Scheme 52. Proposed bicyclization sequence of diene **22** to synthesize AB compound **23**



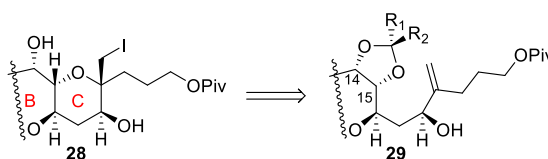
Scheme 53. Proposed cyclizations of triene **24** to synthesize BC compound **25**



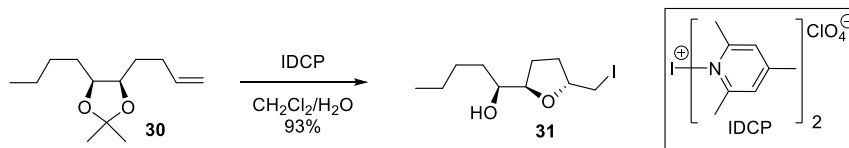
3.1.3 C ring

Before embarking on tandem cyclization studies, we pursued closing C-ring **28** through iodocyclization of acetal-alkene **29** (Scheme 54). In the B-ring model, we learned that a cyclic protecting group on oxygens at C₁₄ and C₁₅ increased the diastereoselectivity of the ring-closing reaction. With this knowledge, we proposed a one-step cyclization-deprotection reaction from the cyclic acetal, which should be regioselective and obviate the need for a separate deprotection step. Iodocyclization of acetal-alkene systems have been reported by Fraser-Reid^{136,137} and Mootoo¹³⁸⁻¹⁴⁰, although their findings are limited to the synthesis of five-membered cyclic ethers. For example, halocyclization of acetal-alkene **30**, promoted by iodonium di-*syn*-collidine perchlorate (IDCP)¹⁴¹, formed *trans*-tetrahydrofuran **31**¹³⁹ (Scheme 55).

Scheme 54. C-ring retrosynthetic analysis

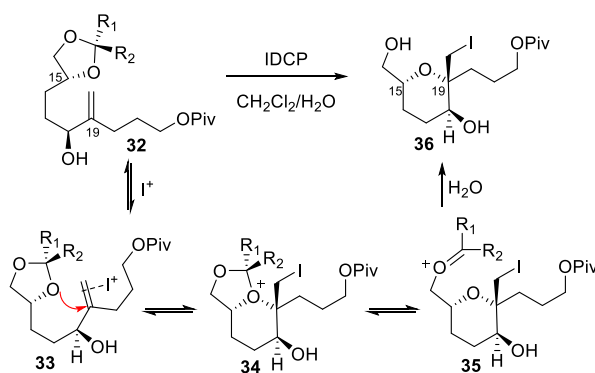


Scheme 55. Mootoo's iodocyclization of acetal alkene **30** to form *trans*-**31**



We planned to construct acetal-alkene **32** as a test substrate to explore the C-ring cyclization with the masked nucleophilic oxygen at C₁₅ (Scheme 56). We proposed this would occur through nucleophilic addition of the C₁₅-oxygen to activated alkene **33** at C₁₂, resulting in 6-*exo* cyclization to form oxonium **34**. Oxonium **34** would undergo elimination to form isopropenyl ether oxocarbenium **35**, followed by hydrolysis to furnish tetrahydropyran **36**. We proposed elimination of cyclic acetal **34** to isopropenyl ether oxocarbenium **35** as the driving force for this reaction, as Rychnovsky noted in his laboratory's work on the partial deprotection of acetonides¹⁴².

Scheme 56. Iodocyclization of acetal **32** to furnish C-ring model **36**



3.2. Results and Discussion

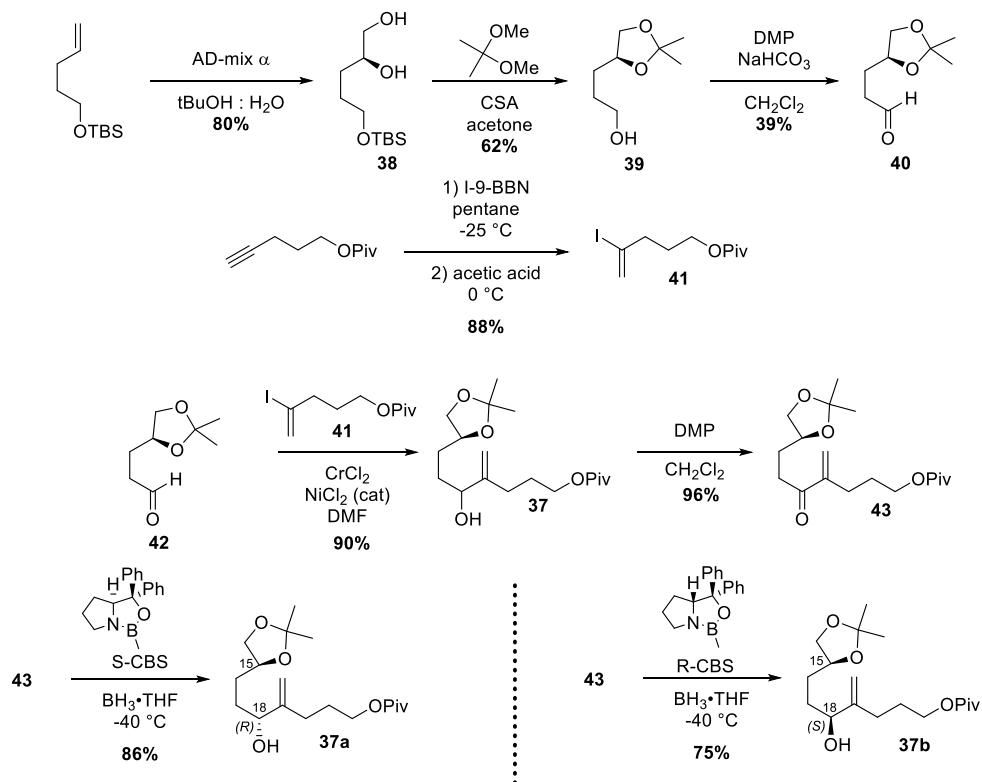
3.2.1 Electrophile-promoted oxacyclization of alkenyl alcohols

3.2.1.1 Synthesis of acetonide-protected diol 37

Keeping most closely to literature precedents, we first set out to make isopropylidene acetal **37** (Scheme 57). We planned on constructing the allylic alcohol through the Nozaki-Hiyama-Kishi (NHK) coupling^{143–145} of aldehyde **42** with vinyl iodide

41 and setting the stereochemistry through oxidation and CBS-reduction^{146,147}. Synthesis of aldehyde **42** began with 4-penten-1-ol. Although Sharpless asymmetric dihydroxylation¹⁴⁸ of 4-penten-1-ol proceeded to acceptable conversion, mass recovery of the triol was very low (less than 10%) due to the water solubility of the product. By silylating the primary alcohol, recovery of vicinal diol from the aqueous reaction mixture **38** increased to 80%. Next, the vicinal diol was protected as the isopropylidene acetal. The acid used in the protection cleaved the silyl protecting group, resulting in primary alcohol **39**. Dess-Martin periodinane oxidation¹⁴⁹ furnished aldehyde **40**. Vinyl iodide **41** was synthesized from the corresponding terminal alkyne using regioselective iodo-boration and subsequent protonolysis of the C-B bond.¹⁵⁰ Initial attempts at NHK coupling of aldehyde **40** with vinyl iodide **41** to access allylic alcohol **37** using DMF dried over sieves were low-yielding (10-15%). Upon switching to solvent distilled from CaSO₄ and sparged with argon, we increased the yield significantly. With the carbon backbone of the cyclization substrate intact, we needed to set the final stereocenter. DMP oxidation of allylic alcohol **37** to enone **43** followed by CBS-reduction allowed us separate access to both the diastereomers of the allylic alcohol, the R-diastereomer, **37a**, and the S-diastereomer, **37b**. Brevenal has *R*- stereochemistry at C₁₅ and *S*- stereochemistry at C₁₈. We used AD-mix α to set the stereocenter at C₁₅, resulting in the *S*-stereoisomer, yielding compound **37a**, the enantiomer of the natural product. We also synthesized C₁₈ diastereomer **37b** to investigate a potential conformational effect on cyclization.

Scheme 57. Synthesis of acetonide-protected C-ring cyclization substrates **37a** and **37b**



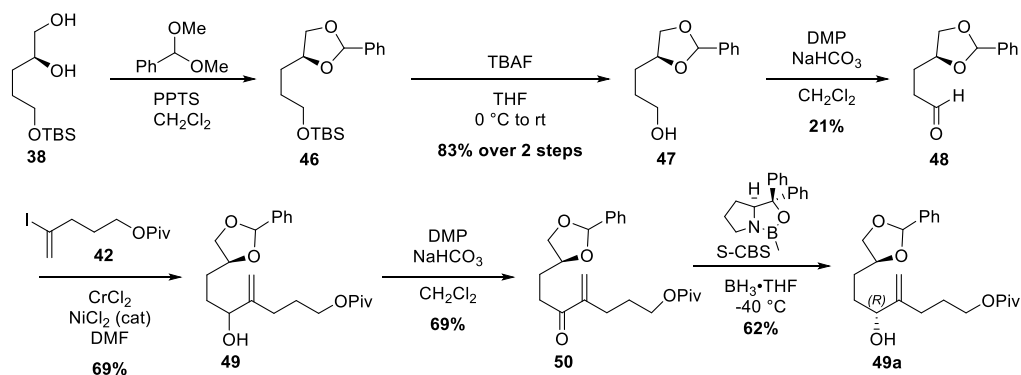
3.2.1.2 Synthesis of benzylidene protected diol **49**

We reasoned that if the isopropylidene acetal **37** was not able to sufficiently stabilize oxonium **34**, the equilibrium would not favor fragmentation of the acetal to isopropenyl ether **35** (Scheme 56). We proposed that the presence of electron donating substituent on the acetal protecting group, such as *p*-methoxyphenyl (PMP; $\text{R}_1 = p\text{-OMe-C}_6\text{H}_5$, $\text{R}_2 = \text{H}$), would stabilize oxonium intermediate **34**, favoring fragmentation of the acetal, and drive the equilibrium towards cyclic product **36** (Scheme 56). To synthesize the PMP protected diol, we planned on using the same disconnection at the allylic alcohol that we used to synthesize isopropylidene acetal **37**. We encountered significant difficulty with synthetic manipulation of the 1,2-PMP-acetal and were unable to synthesize the PMP

protected aldehyde corresponding to aldehyde **42**. The *p*-methoxybenzylidene acetal undergoes acid hydrolysis 10 times faster than the benzylidene acetal¹⁵¹, with the 1,3-derivative being thermodynamically favored over the 1,2-derivative^{152,153}. In our hands, the benzylidene acetal underwent hydrolysis upon silica gel column chromatography. Due to the labile nature of the 1,2-PMP acetal, we opted instead to synthesize the benzylidene acetal derivative, which was expected to be more stable toward synthetic manipulations. Although the benzylidene would not stabilize oxonium **34** as well as the proposed PMP-acetal, it would better stabilize oxonium **34** than isopropylidene acetal **37**.

We planned on synthesizing benzylidene-protected cyclization substrate **49a** in similar fashion to the isopropylidene acetal **37a** (Scheme 58). Benzylidene protection of vicinal diol **38** followed by desilylation furnished primary alcohol **47**. Dess-Martin periodinane oxidation resulted in aldehyde **48**, albeit in low yield. NHK coupling of aldehyde **48** with vinyl iodide **42** resulted in allylic alcohol **49**. Subsequent oxidation to enone **50** and CBS reduction allowed access to the *R*-allylic alcohol, **49a** (2.3:1 dr at benzylidene).

Scheme 58. Synthesis of benzylidene acetal C-ring cyclization substrate **49a**



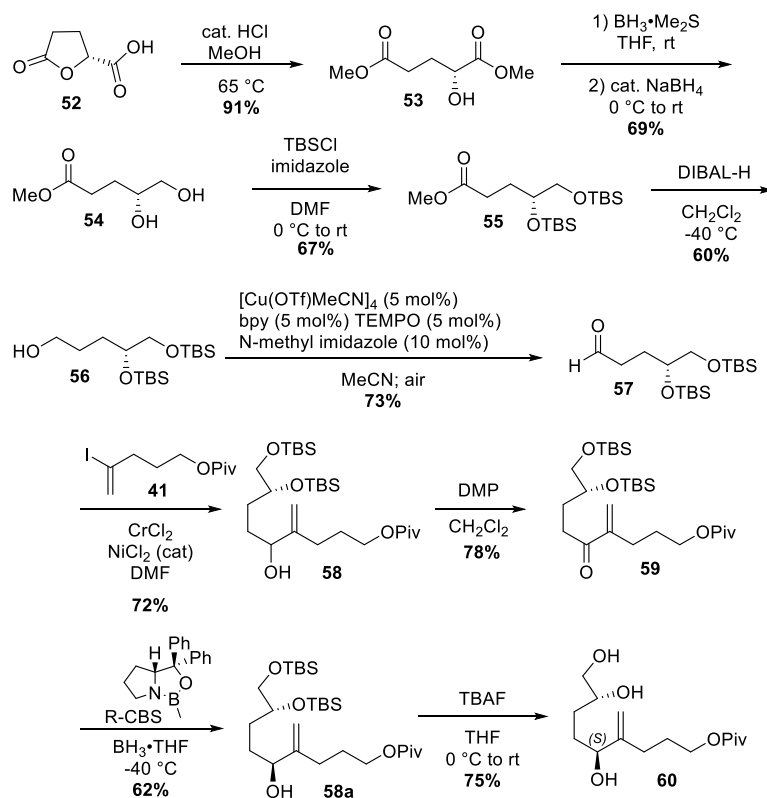
3.2.1.3 Synthesis of vicinal diol **60**

As a conservative approach, we also prepared the free diol for cyclization. Initially we attempted to access the diol through oxidative removal of the benzylidene on substrate **49a** but were unsuccessful. We instead synthesized triol **60** from the bis-silylated diol (Scheme 59). Rather than setting the stereochemistry of the vicinal diol through Sharpless asymmetric dihydroxylation, the chiral center came from *D*-glutamic acid. Treatment of *D*-glutamic acid with nitrous acid furnished *R*-butyrolactone **52**.^{154,155} Ring opening of lactone **52** under acid-catalyzed methanolic conditions resulted in diester **53**.¹⁵⁶ Selective reduction of the ester adjacent to the hydroxyl group was accomplished through use of borane dimethylsulfide and catalytic sodium borohydride, allowing access to diol **54**.¹⁵⁷ Bis-silylation resulted in adduct **55**, which underwent reduction of the ester to furnishing alcohol **56**. Treatment of alcohol **56** with Stahl's copper-mediated aerobic oxidation reaction conditions resulted in aldehyde **57**.¹⁵⁸ NHK coupling of aldehyde **57** with vinyl iodide **41** forged allylic alcohol **58**. Subsequent oxidation to enone **59** and *R*-CBS reduction allowed access to the *S*-allylic alcohol **58a** in 93:7 dr. The absolute

stereochemistry of the newly formed chiral center was confirmed by Mosher ester analysis.

Deprotection of the silyl groups afforded triol **60**, our desired cyclization substrate.

Scheme 59. Synthesis of vicinal diol C-ring cyclization substrate **60**

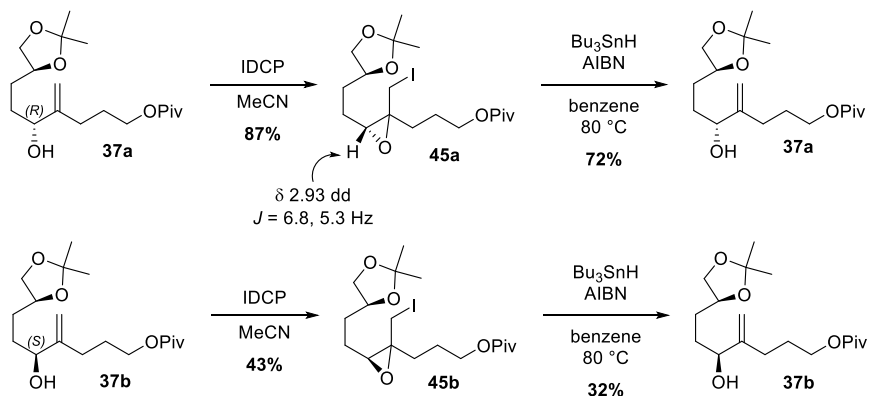


3.2.1.4 Cyclization of acetonide protected diol **37**

Keeping most closely to precedents, we started our cyclization studies with the isopropylidene acetal **37a**. Treatment of **37a** with IDCP¹⁴¹ resulted in a single less polar product by TLC with full consumption of starting material after three hours (Scheme 60). Treatment of **37a** with iodine and bicarbonate resulted only in recovery of starting material after 8 hours. The product is tentatively assigned as α -iodoepoxide **45a**. Proton and COSY

spectra were obtained in *d*-chloroform, *d*-acetone, *d*-benzene, and *d*-methanol to deconvolute the spectra. Although no single solvent cleanly resolved all the signals, the structural motifs were identifiable and spin systems were traceable. In the product, the acetonide remained unchanged, the alkene was consumed, and CH₂-I protons appeared in an isolated spin system at δ 3.30 (d, J = 10.2 Hz) and δ 3.07 (d, J = 10.2 Hz). The key diagnostic feature was the appearance of a proton proposed to be on the epoxide at δ 2.93 (dd, J = 6.8, 5.3 Hz) which shows COSY correlations to δ 1.77 and δ 1.67. The proposed structure is supported by HRMS, which shows a major molecular ion at 447.11103 (C₁₈H₃₁O₅I_na), which corresponds to α -iodoepoxide **45a**. In the literature, α -iodoepoxides have been synthesized from allylic alcohols using various iodine reagents, including IDCP,¹⁵⁹ often under photochemical conditions^{160–162}.

Scheme 60. Cyclization of acetonide-protected nucleophile



Upon treatment of **45a** with Bu₃SnH and AIBN in refluxing benzene, allylic alcohol **37a** was isolated as the major product (Scheme 60). Generation of a carbon radical α - to an epoxide by various methods is known to result in radical fission of the epoxide C-O

bond, result in an allylic alkoxy radical^{160,161}. Presumably, β -scission of the C-O bond of α -iodoepoxide **45a** furnished allylic alcohol **37a**. The same sequence of reactions was executed on the *S*-distereomer, **47b**, to a similar outcome, albeit in lower yield for both the cyclization step and the deiodination step (Scheme 60).

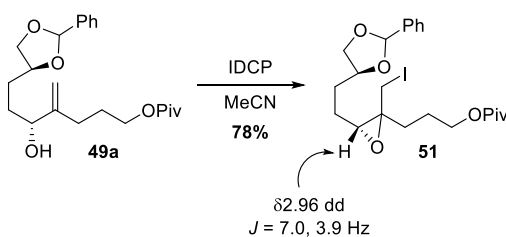
In summary, α -iodoepoxides **45a** and **45b** likely resulted from addition of the allylic alcohol to the iodonium intermediate in absence of a more suitable nucleophile. As the acetonide functional group masked the C₁₅ nucleophile for 6-*exo*-tet cyclization, the C₁₈ alcohol nucleophile participated in 3-*exo*-tet cyclization. After radical deiodination, the carbon-centered radical α - to the epoxide underwent C-O fission to give allylic alkoxy radical, which upon quenching furnished allylic alcohols **37a** and **37b**. This finding suggests that Mootoo's precedent for five-membered ring ether synthesis did not extend to forming the six-membered ring.

3.2.1.5 Cyclization benzylidene protected diol 49

We reasoned that isopropylidene acetal **37** was not able to sufficiently stabilize oxonium **34**, resulting in the equilibrium favoring the starting acetal-alkene. We proposed that the benzylidene acetal **49a** would better stabilize oxonium **34** than isopropylidene acetal **37**, thereby favoring the fragmentation and driving the reaction to the desired tetrahydropyran product. Treatment of **49a** with IDCP resulted in three less polar spots, close in R_f, with full consumption of starting material after two hours by TLC (Scheme 61). By proton NMR, the isolated product is consistent with α -iodoepoxide **51**, analogous

to reaction with isopropylidene acetal **37a**. Starting material **49a** was a 2.3:1 mixture of diastereomers at the benzylidene acetal, which complicated product analysis. In product **51**, the benzylidene acetal remained unchanged, the alkene was consumed, and CH₂-I protons appeared in an isolated spin system at δ 3.27 (d, $J = 10.6$ Hz) and δ 3.10 (d, $J = 10.6$ Hz). Additionally, notable was the appearance of a proton proposed to be on the epoxide at δ 2.96 (dd, $J = 7.0, 3.9$ Hz). Attempted deiodination under radical conditions resulted in decomposition of the material. As seen with cyclization attempts on acetonide protected **37a**, 3-*exo* cyclization of the allylic alcohol at C₁₈ outcompeted 6-*exo* cyclization from the masked nucleophile at C₁₅.

Scheme 61. Cyclization of benzylidene acetal C-ring cyclization substrate **49a**



3.2.1.6 Cyclization of vicinal diol **60**

We decided to cyclize the free vicinal diol to determine if 6-*exo* cyclization of the deprotected nucleophile would outcompete the 3-*exo* cyclization observed in cyclization reactions of isopropylidene acetal **37a** and benzylidene acetal **49a**. Iodocyclization of vicinal diol **60** with both iodine and sodium bicarbonate and with IDCP furnished exclusively 6-*exo* cyclization product **61** in 7:1 *dr* (Scheme 62). Both iodine reagents went

to similar conversion with similar dr. Several signals in the proton NMR of diol **61** overlapped, so the compound was derivitized as bis-acetate ester **62**, which supported the structural assignment and simplified the spectra. NOESY spectroscopy showed a correlation between protons labeled g and f (Figure 12), which indicate a *syn*-relationship of protons across the C-O-C of the pyran. Although we have no direct spectroscopic evidence of the *trans*-relationship between the carbinol proton a and the CH₂-I group, we have validated the *S*-stereochemistry at C₁₈ of cyclization substrate **60** though Mosher ester derivatization and analysis¹⁰⁷ of compound **58a**. Although we attempted radical deiodination to confirm the NOE with the corresponding methyl singlet, no material was recovered from attempted deiodination.

Scheme 62. Cyclization of vicinal diol C-ring cyclization substrate **60**

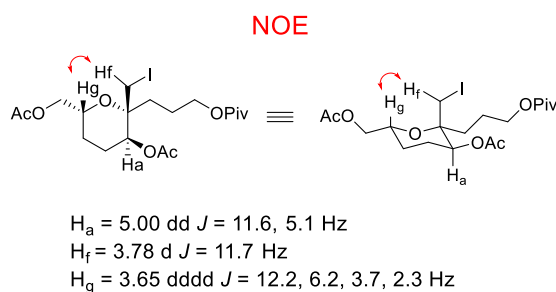
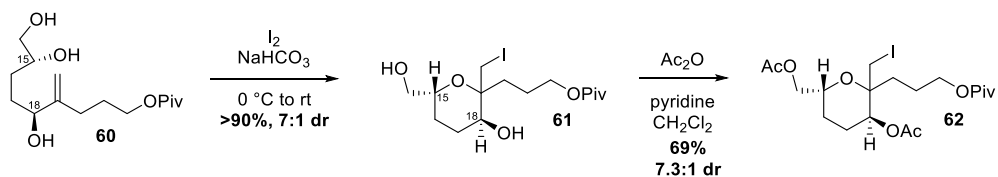
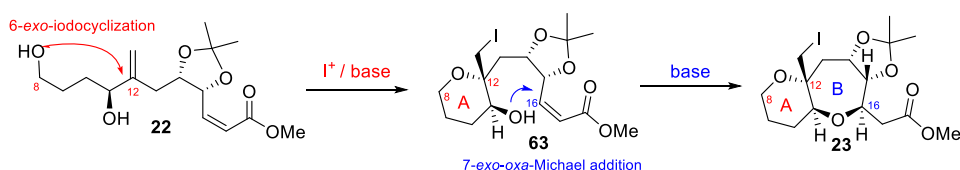


Figure 12. NOE correlations of tetrahydropyran **62**

3.2.2 AB ring model

With methods for forming the A, B, and C rings, we set out to explore tandem cyclization of diene **22** to form AB ring domain **23** (Scheme 63) before investigating BC bicyclization and ultimately ABC tricyclization sequences. With the AB ring model, we would determine the effect of a preformed A-ring on conjugate addition of the methyl ester **63**, which is more closely related to the B-ring precedent of conjugate addition onto a methyl ester, before building on this result to synthesize ABC tricyclic compound **27** through conjugate addition onto a dienyl ketone (Scheme 51).

Scheme 63. Proposed synthesis of AB bicyclic compound **23** through tandem cyclization of diene **22**

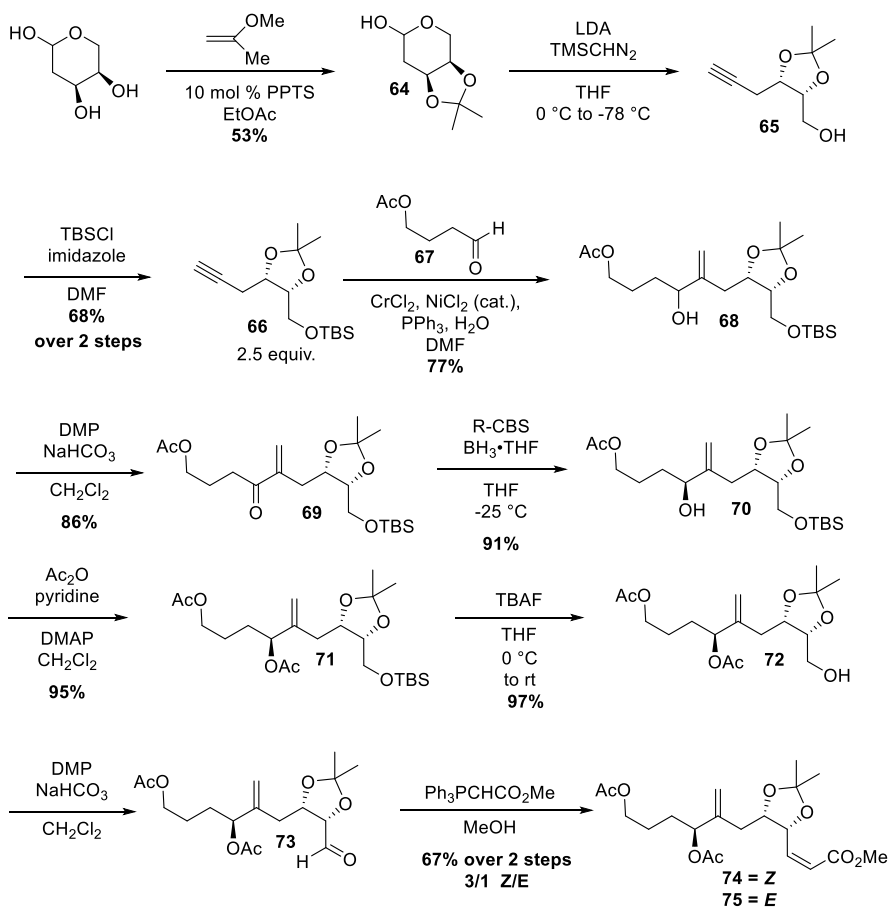


3.2.2.1 Synthesis of bis-acetate-diene **74**

Synthesis of AB tandem cyclization substrate **22** began from 2-deoxy-D-ribose (Scheme 64). Terminal alkyne **65** was prepared a one-carbon homologation of acetonide-protected 2-deoxy-D-ribose **64** (in a sequence adapted from the literature)¹⁶³. Silylation of the alcohol afforded alkyne **66**. Carbon-carbon bond formation to synthesize allylic alcohol **68** through Cr(II)/Ni(II)-mediated coupling with aldehyde **67** presented a significant synthetic challenge, and was the bottleneck of the entire synthetic route. Construction of the allylic alcohol directly from terminal alkyne **66** and an aldehyde **67** was not our first approach. Initially, we explored coupling of corresponding vinyl iodide

or triflate. The acid-sensitive acetonide and silyl group on alkyne **66** limited the methodology available for accessing the vinyl iodide¹⁵⁰. Ni-catalyzed hydroalumination of the terminal alkyne followed by exchange to the iodide¹⁶⁴ allowed access to the desired vinyl iodide, but efforts to scale up the reaction lead to incomplete conversion and regioisomeric mixtures of vinyl iodides (4:1), which were only partially separable by column chromatography. The corresponding vinyl triflate, synthesized through the kinetic enolate of the methyl ketone, underwent rapid decomposition, and when employed in the subsequent NHK coupling, resulted in low yields. Metalation of the iodide for participation in various coupling reactions was complicated by enolization of the aliphatic aldehyde, and chemoselectivity issues due to the acetate ester. In our hands, the direct method for the preparation of the 2-substituted allylic alcohol from a terminal alkyne and an aldehyde using chromium(II) under nickel catalysis¹⁶⁵ featured reproducible yields and regioselectivity, even with the requirement for excess alkyne.

Scheme 64. Synthesis of *bis*-acetate dienes **74** and **75**



Reductive coupling of alkyne **66** with aldehyde **67** provided allylic alcohol **68** as a mixture of diastereomers, which were converted to a single diastereomer *via* oxidation to enone **69** and CBS reduction¹⁴⁶ to (*S*)-alcohol **70** (93:7 dr). The absolute stereochemistry of the newly formed chiral center was confirmed by Mosher ester analysis. Next, the alcohol was protected as acetate ester **71** before selectively deprotecting the silyl group with buffered TBAF, resulting in primary alcohol **72**. Oxidation of the primary alcohol to aldehyde **73**, followed by Wittig olefination³ resulted in *Z*-α,β-unsaturated ester **74** and *E*-α,β-unsaturated esters **75**. The isomers were separated by silica gel column chromatography. Although stabilized Wittig reagents usually result in the *E*-isomer as the

major product, it is typical to observe *Z*-selectivity from reaction of a stabilized ylide in substrates with an electron-withdrawing substituent alpha to the carbonyl. The electron-withdrawing group decreases the lifetime of the oxaphosphetane intermediate sufficiently to restrict thermodynamic equilibration to the *trans* compound, as is the case with the electron withdrawing groups on the phosphonate in the Still-Gennari modification of the Horner-Wadsworth-Emmons olefination.¹⁶⁶

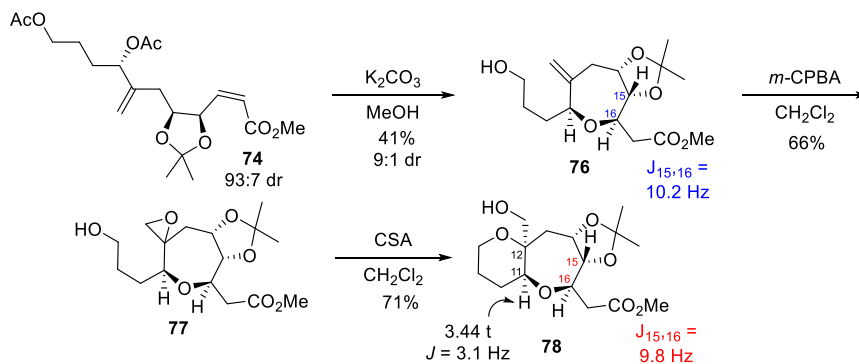
3.2.2.2 Cyclization of bis-acetate-diene 74

Upon deprotection of the acetate esters of the *Z*-unsaturated ester diene **74** with potassium carbonate in methanol, the secondary alcohol unexpectedly underwent conjugate addition, resulting in formation of B ring oxepane **76** (Scheme 65). A particularly suggestive spectroscopic feature of oxepane **76** was the 10.2 Hz coupling constant between the protons at C₁₅ and C₁₆ (brevenal numbering scheme), which is consistent with a *trans* orientation. Deprotection of the *E*-unsaturated ester diene **75** resulted in 10% recovery of the deprotected diol with no observation of cyclized product.

Although we had planned to deprotect the acetate esters to reveal diol **22**, our intended tandem cyclization substrate, with B ring oxepane **76** in hand, we were curious as to the effect of a reversed cyclization sequence, in which we would form the A ring tetrahydropyran through oxacyclization onto the exocyclic 1,1-disubstituted alkene of B ring oxepane **76**. We tried to form the A ring through iodocyclization onto the exocyclic alkene of oxepane **76** with iodine and sodium bicarbonate and with IDCP, which both failed to any any induce reaction. We then attempted to cyclize the compound though acid-

promoted epoxide-opening (Scheme 65). We successfully epoxidized exocyclic alkene **76** with *m*-CPBA, resulting in *spiro*-epoxide **77** as a single stereoisomer. Epoxide **77** underwent regioselective ring-opening with CSA, resulting in bicyclic compound **78**. The coupling constant between the protons at C₁₅ and C₁₆ is 9.8 Hz, consistent with *trans* orientation. As was the case with the C-ring model compound, obtaining direct evidence for the relationship of the substituents across the AB ring fusion with the quaternary carbon was difficult by NMR spectroscopy, although the proton at the ring fusion appeared as a triplet with a 3.2 Hz coupling constant, which is suggestive of a boat conformation of the six-membered ring. (If it were in a chair conformation, as would be expected from the *trans*-fused product, the proton would appear a doublet of doublets with one small and one large coupling constant). Fortunately, could grow crystals of bicyclic compound **78** via vapor-diffusion recrystallization from heptane and benzene, and obtained an X-ray crystal structure of bicyclic compound **78** (Figure 13). The crystal structure showed the desired *trans*-stereochemistry at C₁₅ and C₁₆ from conjugate addition to form the oxepane, but undesired *cis*-stereochemistry at C₁₁ and C₁₂ rather than the desired *trans*- AB ring fusion.

Scheme 65. Cyclization of diene **74** to afford *cis*-fused bicyclic product **78**



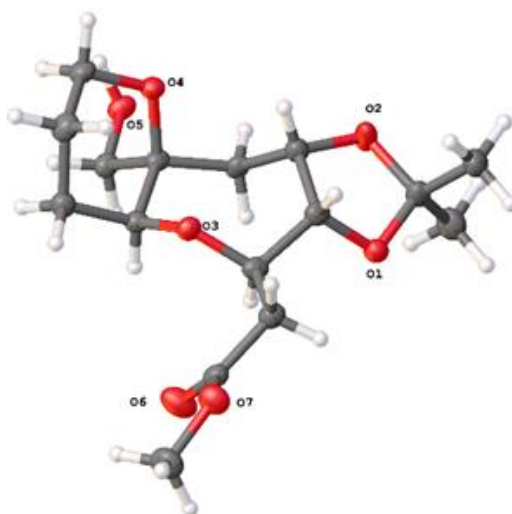


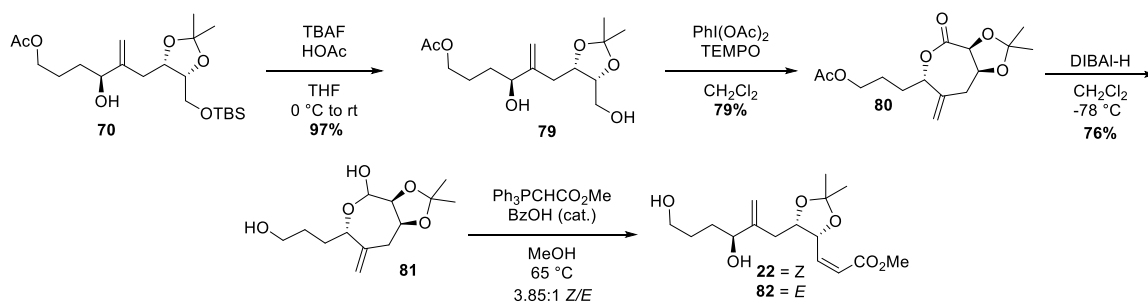
Figure 13. X-ray crystal structure of *cis, trans*- fused bicyclic compound **78**

3.2.2.3 Synthesis of diene **22**

Realizing that spontaneous cyclization to form B-ring oxepane would occur in basic media, we revised our synthetic strategy to minimize synthetic manipulation the α,β -unsaturated ester functionality (Scheme 66). This involved avoiding protection of the secondary alcohol, which would require selective oxidation of the primary alcohol. Desilylation of **70** with buffered TBAF furnished diol **79**. We successfully and selectively oxidized the primary alcohol with Ley oxidation¹⁶⁷, but participation from the nearby secondary hydroxyl resulted in formation of the 7-membered ring lactone **80**. Recognizing the substrate's propensity to undergo oxidative lactonization, the procedure was optimized though treatment of the 1,6 diol with Sasaki's method of oxidative lactonization using TEMPO and $\text{PhI}(\text{OAc})_2$ ^{168,169}. At this stage, the minor diastereomeric impurity from CBS reduction was removed, resulting in compound **80** as a single stereoisomer. Treatment of lactone **80** with three equivalents of DIBAL-H resulted in partial reduction to the hemiacetal with concomitant reductive removal of the acetate protecting group, furnishing lactol **81**. The substrate synthesis concluded with Wittig

olefination of lactol **81** to afford unsaturated ester as a mixture of alkene isomers (3.85 : 1 favoring *Z*, **22**) which were only partially separable by silica gel flash column chromatography, and contained a triphenylphosphine oxide impurity.

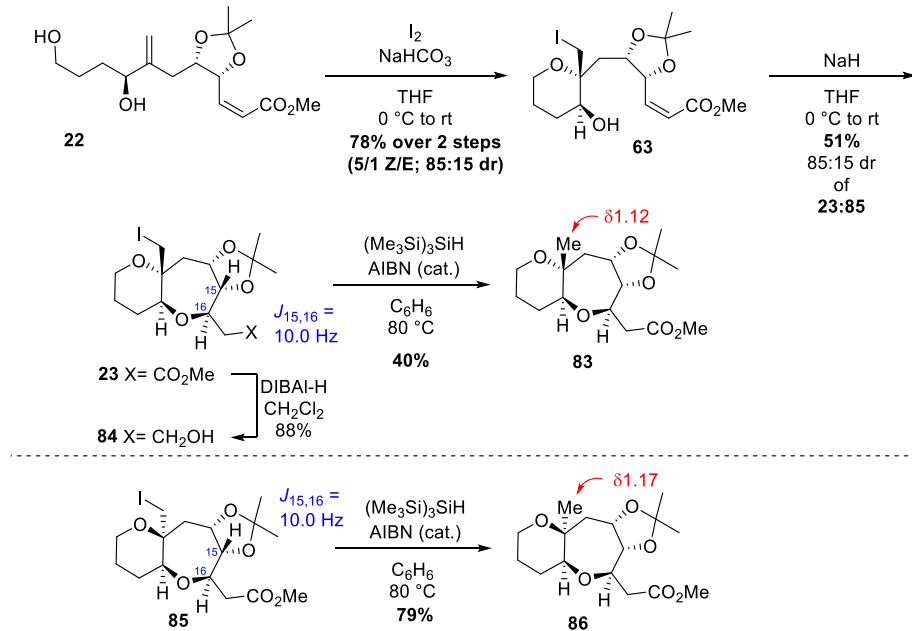
Scheme 66. Synthesis of AB tandem cyclization substrate, diene **22**



3.2.2.4 Cyclization of diene **22**

With diene **22** in hand, we could now explore tandem cyclization to form AB bicyclic compound **23** in the direction we had originally intended ($A \rightarrow E$). Iodocyclization of diene **22** (5/1 *Z/E* from chromatography of **22**) resulted in formation desired tetrahydropyran **63** as an 85:15 dr (Scheme 67). At this stage, the diastereomers resulting from cyclization were inseparable but the alkene isomers were separable. Treatment of compound **63** (pure *Z*-alkene, 85:15 dr) with sodium hydride resulted in diastereoselective formation of desired *trans*-fused oxepane **23**, furnishing the AB ring system of brevenal in 2 steps from the acyclic diene **22**. At this stage, only the *trans*-fused diastereomer was formed through conjugate addition, and we could separate the 85:15 mixture of diastereomers across the AB ring fusion through careful silica gel column chromatography, resulting in *trans, trans*-fused compound **23**, and *cis, trans*-fused compound **85**.

Scheme 67. Tandem cyclization of diene **22**



Trans,trans-fused compound **23** and *cis,trans*-fused compound **85** both exhibited a 10.0 Hz coupling constant between the protons on C₁₅ and C₁₆ (Scheme 67). Similarly large coupling constants were also observed at between *trans* protons on C₁₅ and C₁₆ in Dr. Stoltz's B-ring model system **7** (9.9 Hz)¹¹⁹, oxepane **76** (10.2 Hz), and *cis, trans*-fused bicyclic compound **78** (9.8 Hz).

The stereochemistry at C₁₂ in both compound **23** and compound **85** was assessed after radical deiodination^{170,171}, furnishing *trans, trans*-fused AB ring analogue **83** and *cis, trans*-fused compound **86** (Scheme 67). The chemical shift of the axial methyl substituent in *trans*-fused compound **83** was $\delta 1.12$ ppm and the shift of the equatorial methyl substituent in *cis*-fused compound **86** was $\delta 1.17$ ppm (Scheme 67). NOESY of deiodinated compound **83** showed correlations between the C₁₂ methyl and the proton H_a,

confirming the axial orientation of the methyl substituent (Figure 14). Additionally, there was a correlation between H_g and H_c , confirming the *syn*-relationship across the C-O-C portion of the ether ring. NOESY of deiodinated compound **85** showed correlations between the methyl and the proton H_d , and between the methyl and H_g , confirming the equatorial orientation of the methyl substituent. In compound **83**, proton g appeared as a doublet of doublets with 11.4 and 3.9 Hz coupling constants, consistent with the desired chair conformation. In compound **86**, proton g appeared as a triplet with a 3.2 Hz coupling by proton NMR, consistent with a boat conformation of the tetrahydropyran ring, as seen with compound **78**, in which the comparable proton appeared as a triplet with a 3.1 Hz coupling constant.

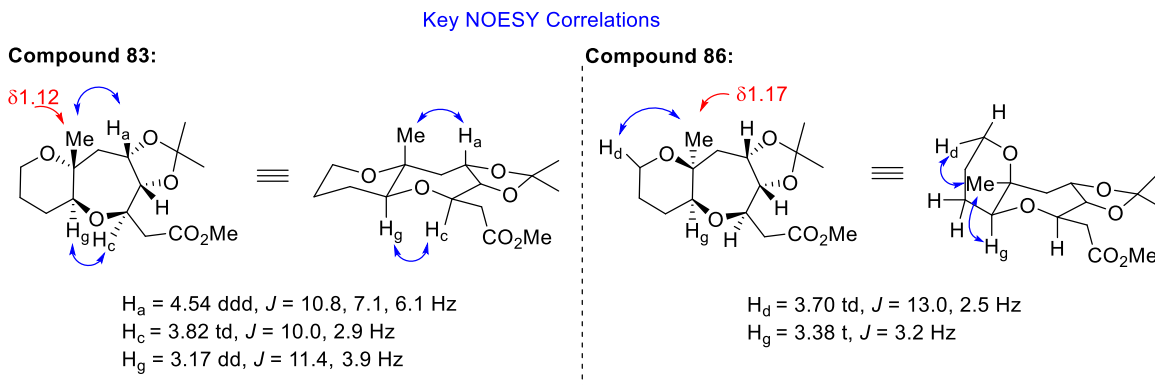


Figure 14. NOESY correlations of cyclic compounds **83** and **86**

The structural assignment of AB bicyclic compound **23** was confirmed by X-ray crystallography (recrystallized by slow evaporation from dichloromethane, Figure 15) of the corresponding primary alcohol, compound **118**, which was made through treatment of **23** with excess DIBAL-H (Scheme 67).

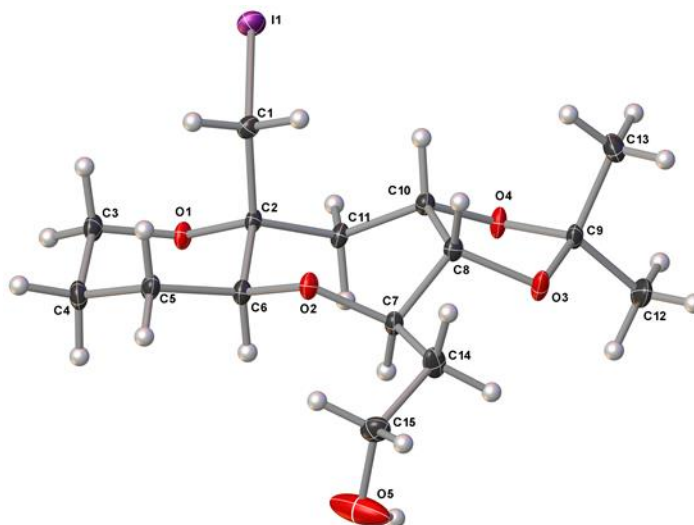
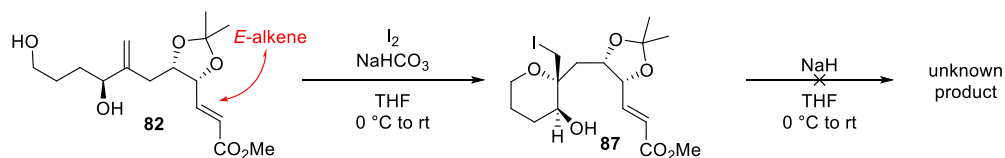


Figure 15. X-ray crystal structure of AB bicyclic compound **84**

Iodocyclization of *E*-alkene **82** resulted in tetrahydropyan **83** (85:15 dr, Scheme 68). However, attempted conjugate addition of *E*-alkene substrate **87** with sodium hydride failed to result in recovery of any organic material. By TLC, the starting material converged to a single polar spot. After aqueous workup, there was a yellow film on the inside of the reaction vessel, which was marginally soluble in chloroform. By proton NMR, there were no resolvable signals.

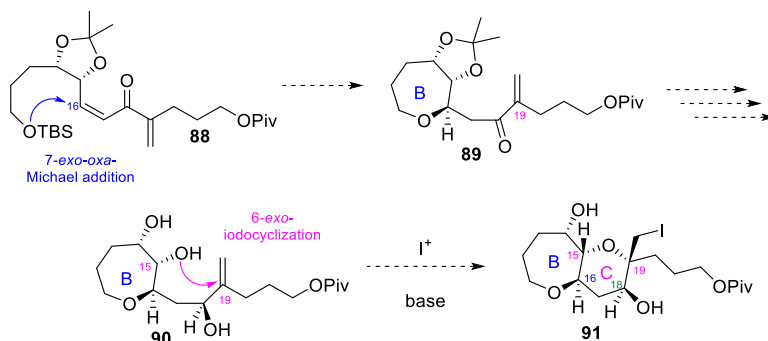
Scheme 68. Iodocyclization of *E*-alkenol **117** and attempted intramolecular conjugate addition



3.2.3 BC ring model

With regioselective, diastereoselective methods to form the AB ring system **23**, B ring **7**, and C-ring **61**, we began to investigate tandem cyclization of dienylketone substrates such as **88** in efforts to construct the bicyclic BC substructure of brevenal **91** (Scheme 69). The proposed system would allow us to investigate *7-exo* conjugate addition onto a dienylketone, an extension of the successful *7-exo* conjugate addition onto a simple methyl ester. It would also allow us to investigate the C-ring closure in a system closer to the real system.

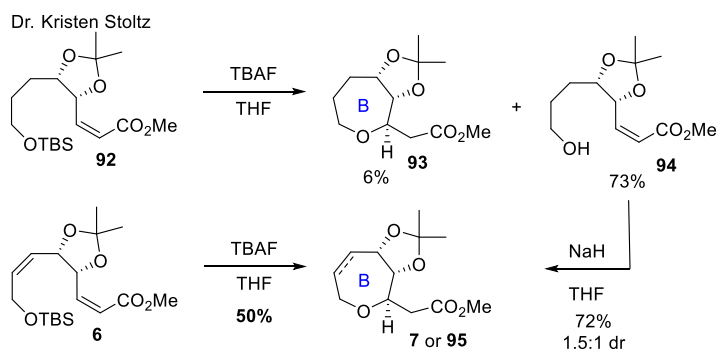
Scheme 69. Proposed cyclizations of diene **88** to synthesize BC compound **91**



We synthesized dienyl ketone **88** as the first BC cyclization substrate. We imagined that upon desilylation (as found to be most successful in Dr. Stoltz's B-ring model¹¹⁹) or upon treatment with base following desilylation, *7-exo oxa*-Michael addition onto dienyl ketone **88** would occur, resulting in oxepane **89**. Following synthetic manipulation to access triol **90**, we hoped to form the tetrahydropyran C ring through halocyclization, resulting in BC bicyclic compound **91**.

This work required extension of the B-ring conjugate addition methodology from the simple methyl ester **6** to the more reactive dienyl ketone **88**. Although dienyl ketone **88** could potentially undergo 11-*exo* cyclization, 7-*exo* cyclization should be more favorable. In the B-ring model system¹¹⁹, compound **6**, featuring an unsaturation in the tether, spontaneously cyclized upon desilylation to form oxepane **7** (Scheme 70). Compound **92**, having a fully saturated tether, did not cyclize to an appreciable degree under desilylation conditions, and resulted in mostly recovery of deprotected alcohol **94**, which underwent cyclization upon treatment with sodium hydride to form tetrahydropyran **95**, albeit without significant diastereoselectivity (Scheme 70). We decided to begin our investigation with synthesis of the dienyl ketone substrate with saturated tether thinking that the diminished reactivity of the saturated compound compared to the unsaturated compound would be advantageous in a system we were expecting to be reactive. At the time of this work (prior to unsuccessful *E*-alkenol conjugate addition of compound **87**, Scheme 68) we were unsure of the effects of having a *cis*- or *trans*- unsaturation at the site of conjugate addition. As a result, we were interested in synthesizing both *cis*-alkene **88** and the corresponding *trans*-alkene **96**. At the time of this work, we were initially interested in the *trans*-alkene as we did not know how it would react in conjugate addition reactions. We planned to access BC model substrates through diverging from the route to synthesize B ring substrates **92** and **6**.

Scheme 70. Saturated (**92**) and unsaturated (**6**) tether in B ring model system

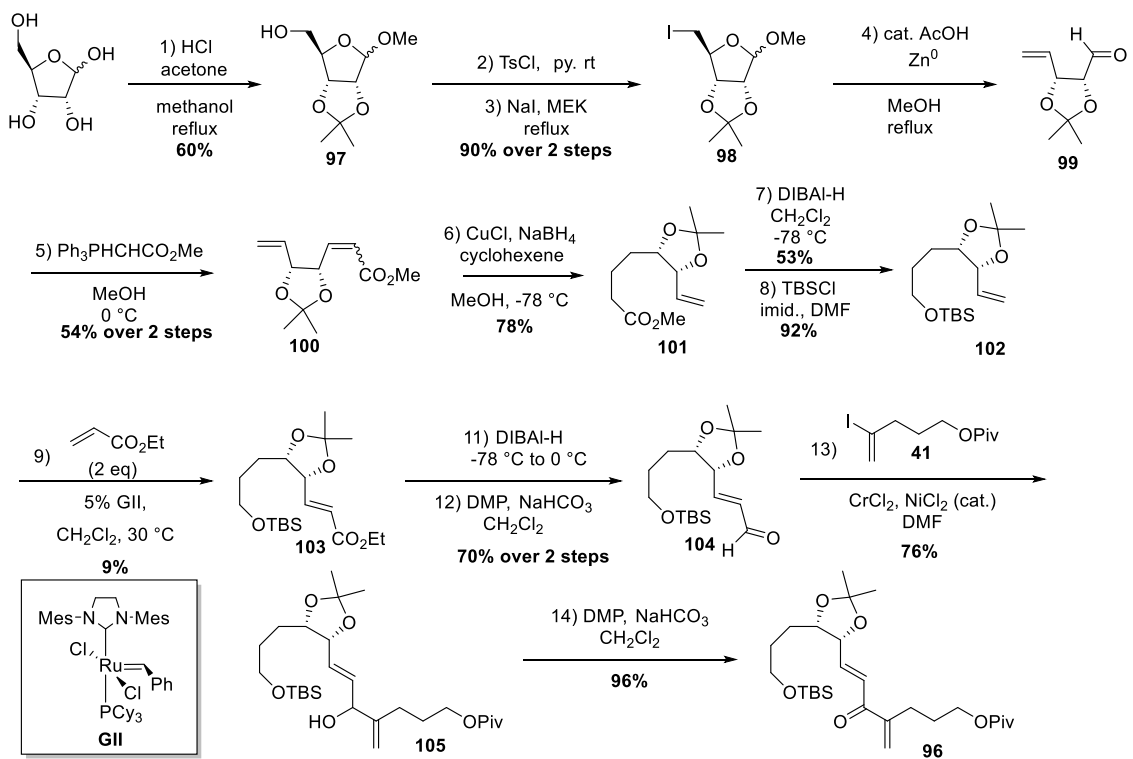


3.2.3.1 Synthesis of dienyl ketone **96**

Synthesis of BC model substrate with the saturated tether, compound **96** began from D-ribose (Scheme 71). Acetonide protection of the cis-1,2-diol followed by Finkelstein reaction of primary alcohol **97** furnished to iodide **98**. Zinc-promoted ring opening/elimination (Boord olefination) of iodide **98** provided aldehyde **99**, which was immediately subjected to Wittig olefination to form unsaturated ester **100** as a mixture of alkene isomers. The α,β -unsaturation of methyl ester **100**, resulting from Wittig reaction, was reduced to provide saturated ester **101**. Reduction of ester **101** to the primary alcohol followed by TBS protection produced terminal alkene **102**. Up until this point, the synthetic route followed the route employed by Dr. Kristen Stoltz in her synthesis of the B ring model substrates¹²⁶. We were initially interested in the *trans*-alkene as we did not know how it would react in conjugate addition reactions and were hopeful it would exhibit diminished reactivity compared to the *cis*-unsaturated substrates, which we hoped would translate to increased selectivity. To access the *trans*-alkene, we attempted cross-metathesis of terminal alkene **102** with ethyl acrylate using Grubbs-II as a catalyst, which resulted mostly in homodimer of **102**, although we obtained the desired alkene **103** in 9%

yield. With Grubbs-II, terminal olefin **102** is a type 1 olefin and ethyl acrylate is a type 2 olefin, which accounts for the low yield¹⁷². This was not optimized as the reactivity of the adduct was undesired. Nevertheless, the large scale this sequence (20 g) allowed us to carry material forward despite the low yield of the cross-metathesis reaction. Reduction of ester **103** to the alcohol and oxidation to the aldehyde furnished compound **104**, which underwent NHK coupling with vinyl iodide **41** to forge bis-allylic alcohol **105**. Dess-Martin oxidation furnished *trans*-dienyl ketone **96**.

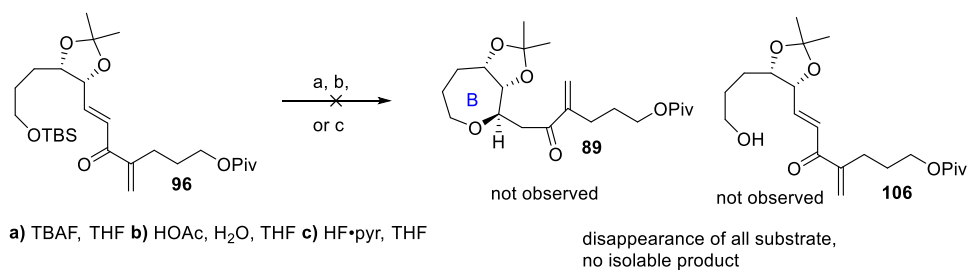
Scheme 71. Synthesis of BC cyclization substrate **96**



3.2.3.2 Cyclization of saturated dienyl ketone **96**

Keeping most closely to the B-ring precedence we had at the time, we first treated *trans*-dienyl ketone **96** with TBAF in efforts to induce conjugate addition upon desilylation under the basic reaction conditions (Scheme 72). Upon treatment with TBAF, compound **96** was fully consumed within 20 minutes with the appearance of a single polar spot by TLC (Scheme 72). Crude NMR showed no identifiable signals, only polymerized THF and TBAF salts. Following column chromatography, no product was visible by NMR. We had hoped the *trans*-unsaturation and lack of saturated tether would diminish the reactivity of dienyl ketone **96** such that we might be able to isolate deprotected starting material in the even in which cyclization did not occur (as seen in Dr. Stoltz's B-ring model, Scheme 70). We next attempted to deprotect the silyl group under milder, non-basic reaction conditions (Scheme 72). Attempts at deprotection with acetic acid in THF/water and with HF • pyridine also failed to result in any isolable material.

Scheme 72. Attempted conjugate addition and deprotection of saturated tether **96**



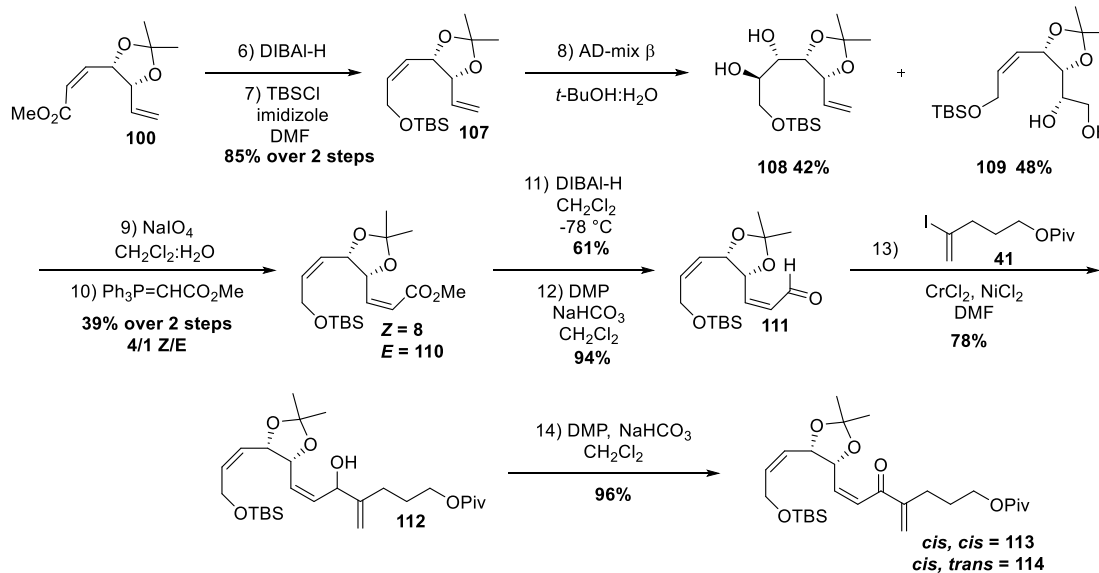
We observed rapid decomposition of dienyl ketone **96** under basic, acidic, and neutral desilylation conditions with no detection of either oxepane **89** or desilylated product **106**. At the outset of our work, we hypothesized that attempts at desilylation accompanied by spontaneous conjugate addition of a less reactive substrate (without an unsaturated tether) could allow us to isolate deprotected material in even that cyclization did not occur. We could then treat the deprotected material with base in efforts to access the oxepane conjugate addition adduct. After observing the reactivity of dienyl ketone **96**, we re-evaluated our hypothesis. In the B-ring model system, the unsaturated tether oriented the nucleophile in a reactive conformation, biasing the system towards conjugate addition. Perhaps, if instead of trying to diminish the reactivity of the substrate by removing the unsaturation, we should take advantage of the reactivity of the system and try to bias the conjugate addition through incorporation of a *cis*-alkene in the tether. Not only would the unsaturation mimic the conformation restriction of the A ring, it may also orient the nucleophile in a reactive conformation to favor the desired conjugate addition onto the dienyl ketone.

3.2.3.3 Synthesis of unsaturated dienyl ketones 113 and 114

Synthesis of *cis, cis*-dienyl ketone **113** and *cis, trans*-dienyl ketone **114**, featuring a *cis*-unsaturation in the tether, are outlined in Scheme 73. Fortunately, substrate **96** and substrates **113** and **114** differ only in the *Z*-unsaturation in the alkyl tether, which was reduced in the synthesis of dienyl ketone **96**. Starting with *Z*- α,β -unsaturated methyl ester **100** (Scheme 73), the methyl ester was reduced and the resulting primary alcohol silylated to afford diene **107**. At this point we attempted to selectively dihydroxylate the terminal

olefin to gain access to the aldehyde through periodate cleavage. Although osmium tetroxide dihydroxylation of simple non-conjugated dienes is expected to selectively oxidize the more substituted, internal olefin, Danishefsky has reported selective oxidation of the less substituted, terminal olefin using stoichiometric osmium tetroxide¹⁷³. Andrus has also reported selective oxidation of the less substituted, terminal olefin, using AD-mix, reasoning that larger ligand on osmium favors selectivity of the less hindered alkene¹⁷⁴. On diene **107**, both alkenes underwent dihydroxylation with AD-mix β . Although the reaction was not selective for the terminal olefin, the reaction provided access to synthetically useful quantities of vicinal diol **109**. Periodate cleavage of the diol to the aldehyde followed immediately by Wittig olefination resulted in a 4:1 mixture of alkene isomers of compounds **8:110**, which were separable by column chromatography. The *Z*-methyl ester **8** was reduced to the primary alcohol and oxidized to furnish aldehyde **111**. Aldehyde **111** underwent NHK coupling with vinyl iodide **41** to forge bis-allylic alcohol **112**. Dess-Martin oxidation furnished *cis, cis*-dienyl ketone **113**. From *E*-methyl ester **110**, the same transformations were conducted to produce *cis, trans*-dienyl ketone **114**.

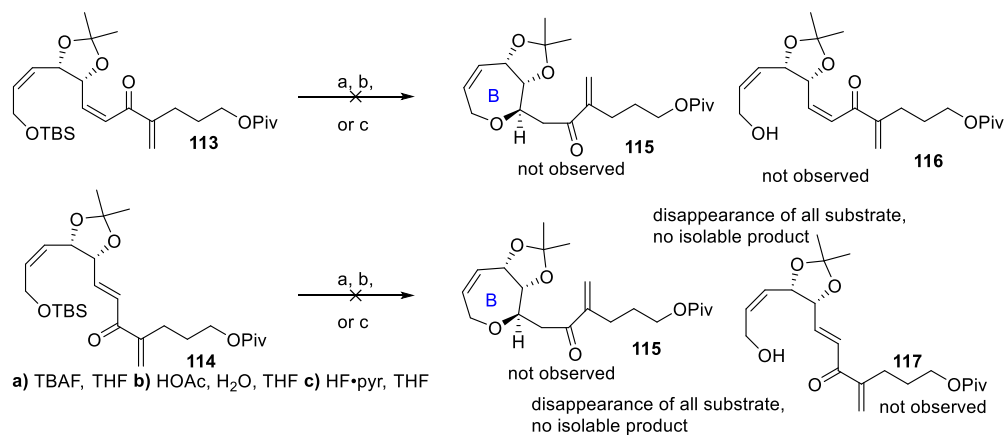
Scheme 73. Synthesis of BC ring models with unsaturated tether **81** and **89**



3.2.3.4 Cyclization of unsaturated dienyl ketones **113** and **114**

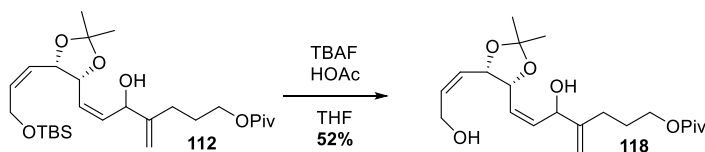
Upon treatment with TBAF, *cis, cis*- dienyl ketone **113** was consumed within 30 minutes by TLC with the appearance of a single polar spot (Scheme 74), similar to the observed reactivity seen with dienyl ketone **96**, which exhibited the unsaturated tether. Crude NMR showed no identifiable substrate signals, only polymerized THF and tetrabutyl ammonium residues. Following column chromatography, no product was visible by NMR. As with dienyl ketone **96**, we next attempted to deprotect the silyl group of *cis, cis*- dienyl ketone **11** under milder, non-basic reaction conditions (Scheme 74). Attempts at deprotection with acetic acid in THF/water and with HF • pyridine failed to result in any isolable material. We attempted these series of transformations on both *cis, cis*- dienyl ketone **113** and *cis, trans*- dienyl ketone **114** with similar disappointments. In no cases were traces of products **115**, **116**, or **117** detected.

Scheme 74. Attempted conjugate addition and deprotection of unsaturated tethers **113** and **114**



All attempts at synthetic manipulation of the dieny ketone functionality resulted in decomposition in systems **96**, **113**, and **114**. Next, we decided to investigate reactivity of the corresponding *cis*, *cis*- bis-allylic alcohol **118**. We successfully deprotected the silyl group of bis-allylic alcohol **112** with buffered TBAF to afford triene **118** (Scheme 75).

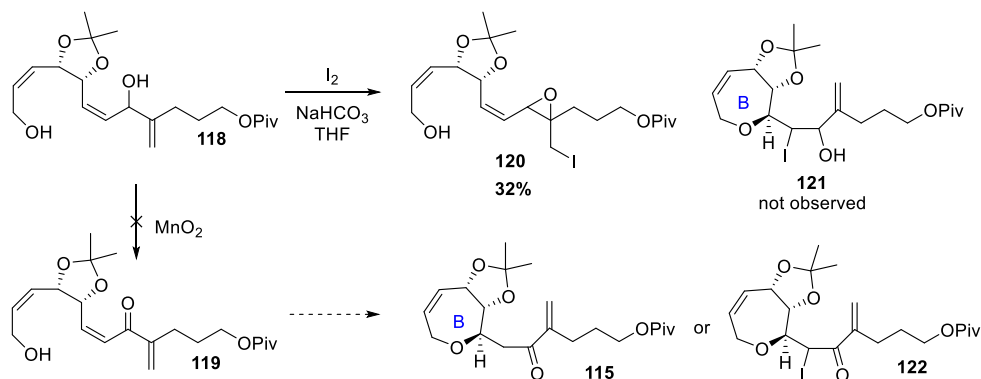
Scheme 75. Deprotection of 112 to afford bis-allylic alcohol substrate **118**



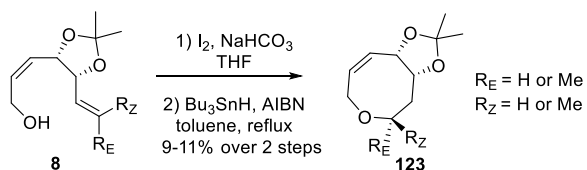
Prior to the development of the B-ring model through conjugate addition, we envisioned accessing the B-ring through iodocyclization of either bis-allylic alcohol **118** or dieny ketone **119**, resulting in oxepane **121** or oxepane **122**, or conjugate addition of **119** resulting in oxepane

115. Although Kristen Stoltz observed 8-*endo* selectivity for iodocyclization in B-ring model in substrate **8**,¹²⁶ these results were limited to either terminal olefins and trisubstituted olefins with a methyl substituent and were often low yielding (Scheme 77). We had no knowledge about what would happen with a sterically and/or electronically altered alkene, which made iodocyclization of **118** and **119** an enticing prospect. Iodocyclization of compound **118** resulted in formation α -iodoepoxide **120** from 3-*exo*-tet cyclization (Scheme 76). We also observed 3-*exo*-tet cyclization in studies toward the C-ring in cases where the 1,2-diol nucleophiles were protected. A limited number of attempts at MnO₂ oxidation of bis-allylic alcohol **118** on small scale failed to result in recovery of any material. Conjugate addition of **119** was an appealing prospect, as the dienyl ketone would be generated immediately prior to cyclization under mild reaction conditions.

Scheme 76. Attempts to cyclize bis-allylic alcohol triene **118**

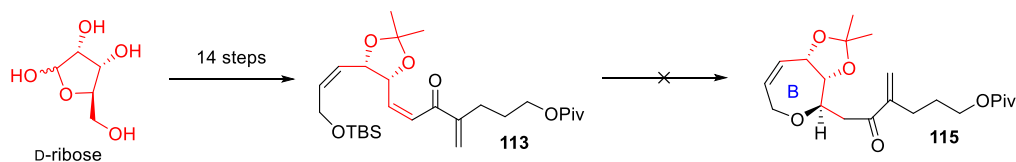


Scheme 77. 8-*Endo* selectivity observed on substrate **8**

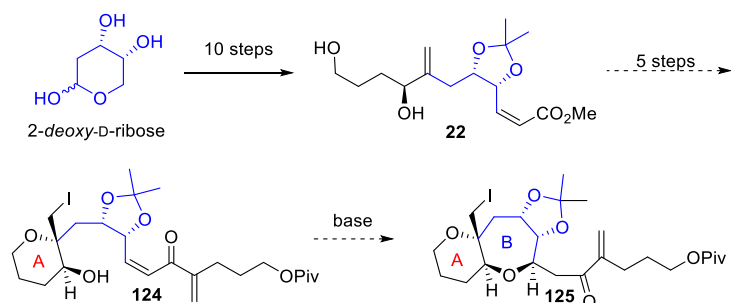


In summary, we were unable to extend conjugate addition from a methyl-ester substrate to a dienyl ketone substrate in the BC model studies. At 14 steps, the substrate synthesis for the BC ring model had selectivity issues due to the requirement for a *cis*-alkene in the tether in the presence of other unsaturations (Scheme 78). We would need to rework the synthesis of the substrate to be able to liberate primary alcohol under milder conditions or selectively oxidize the bis-allylic alcohol over the primary alcohol to access a suitable substrate to explore conjugate addition. Rather than pursue selective oxidation of bis-allylic alcohol **118** to dienyl ketone **119**, we decided to investigate the conjugate addition on a dienyl ketone in the ABC system with dienylketone **124**. By incorporating the A ring instead of an unsaturation in the tether, not only would we be working with a substrate closer to the real system, we would avoid the synthetic challenges introduced by working with the extra *cis*-alkene in the tether. Additionally, we would be able to generate the dienyl ketone immediately before use under mild conditions. We proposed a 15-step synthetic route to access dienylketone **124** from 2-*deoxy*-D-ribose (5 steps from known diene **22**, Scheme 79). We have found through the course of this work that these polycyclic ether ring systems are not amenable to model systems, as outcome of the cyclization reactions are strongly influenced by conformational effects. For the remainder of our studies on the ABC ring sector of brevenal, we only investigated cyclizations on templated ring sectors, building the core from the A→C direction.

Scheme 78. Unsuccessful BC-model conjugate addition of dienylketone **113**



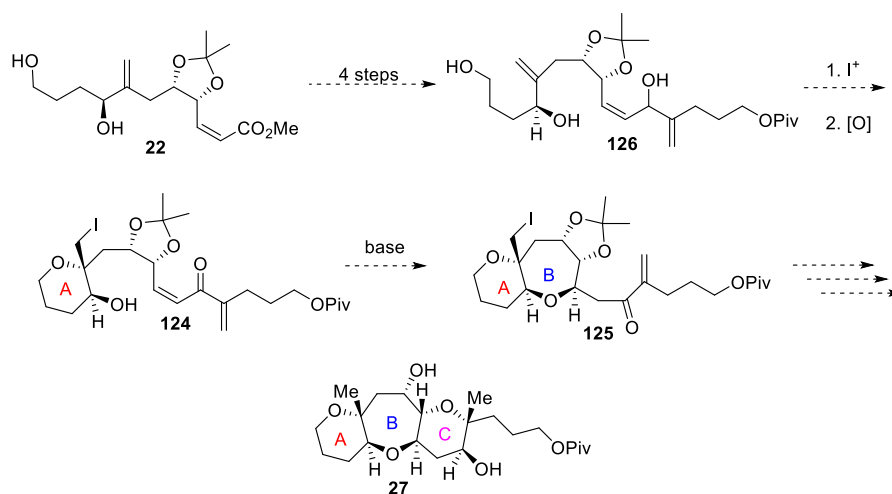
Scheme 79. Proposed ABC-model conjugate addition of dienylketone **124**



3.2.4 ABC linear precursor

Having established a synthetic route to diene **22**, we envisioned extending the carbon skeleton to accommodate a third site of unsaturation, forging dienyl ketone **126** (Scheme 80). We envisioned iodocyclization of triene **126** to form the A ring. By changing the cyclization substrate from dienylketone **113** to dienylketone **124**, we hoped to reinforce the conformational restriction provided by the isopropylidene acetal and better promote the conjugate addition. Bicyclic enone **125** could then undergo a series of synthetic manipulations to access the ABC tricyclic core **27** of brevenal.

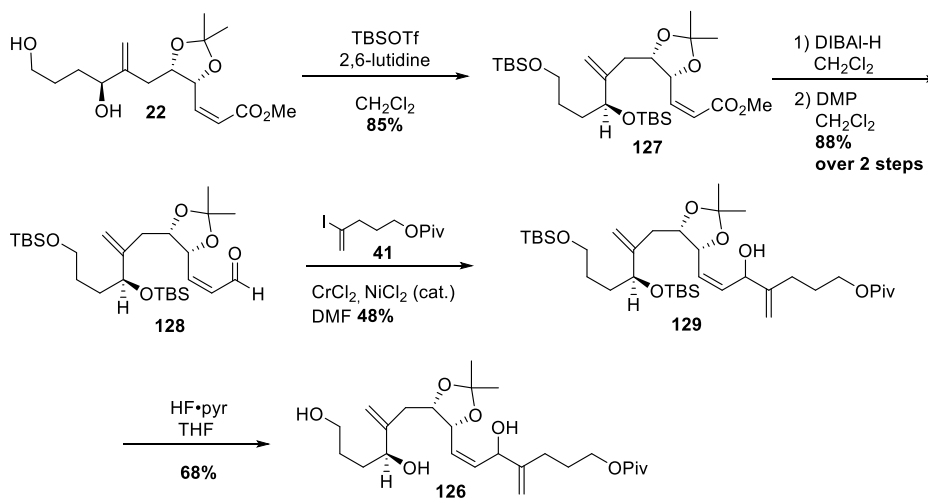
Scheme 80. Proposed ABC-model for conjugate addition of dienyketone **124**



3.2.4.1 Synthesis of triene 126

Synthesis of the triene substrate **126** from diene **22** is shown in Scheme 81. Bis-silylation of diene **22** afforded compound **127**, which underwent reduction of the ester to the alcohol followed by oxidation to provide aldehyde **128**. NHK coupling of aldehyde **122** and vinyl iodide **41** formed bis-allylic alcohol **129**, which upon desilylation with HF•pyridine resulted in triene **126**.

Scheme 81. Synthesis of ABC cyclization substrate, triene **126**

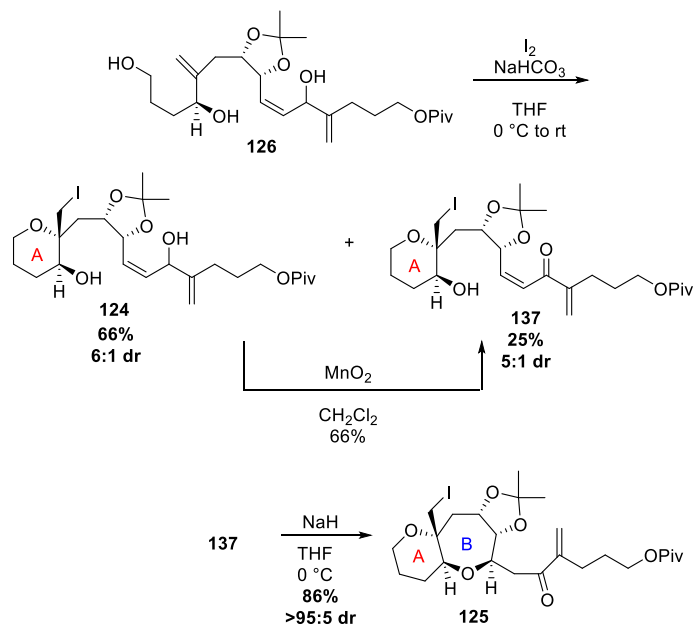


Although we have accessed allylic alcohol **129** through the $\text{Cr}^{\text{II}}/\text{Ni}^{\text{II}}$ coupling of dieny l aldehyde **128** with vinyl iodide **41** in a limited number of occasions, there is a major byproduct in the reaction that is difficult to distinguish from desired adduct **129**. The presence of alkene isomers and the diastereomeric alcohols further complicate the spectra. While there appear to be acetone signals in the NMR with CDCl_3 , the signals are not apparent in C_6D_6 . The byproduct is very difficult to purify by silica gel column chromatography as both the byproduct and triene **129** are very greasy, co-eluting at 0.5% ethyl acetate in hexanes. By proton NMR and COSY, the byproduct appears to exhibit a conjugated diene. By HRMS, the byproduct corresponds to compound **129** with loss of $\text{C}_3\text{H}_6\text{O}_2$. Further complicating structural assignment, the unidentified product undergoes iodocyclization, forming the desired tetrahydropyran. The byproduct does undergo oxidation to an enone with both MnO_2 and Stahl's copper-mediate aerobic oxidation, but the resulting enone does not undergo intramolecular conjugate addition.

3.2.4.2 Cyclization of triene 124

Treatment of triene **126** with iodine and bicarbonate resulted in iodocyclization accompanied by partial oxidation of the bis-allylic alcohol **124** to form dienyl ketone **137** (Scheme 82). Manganese dioxide oxidation of bis-allylic alcohol also furnished dienyl ketone **137**. Treatment of dienyl ketone **137** with sodium hydride resulted in diastereoselective 7-*exo* conjugate addition, resulting in AB bicyclic compound **125**. With this transformation, we achieved our goal of successfully extended oxepane-forming conjugate addition from a methyl ester to a dienyl ketone. This transformation provided AB bicyclic structure **125** from acyclic triene **126**, which contained the carbon backbone necessary to synthesize the ABC tricyclic structure of brevenal.

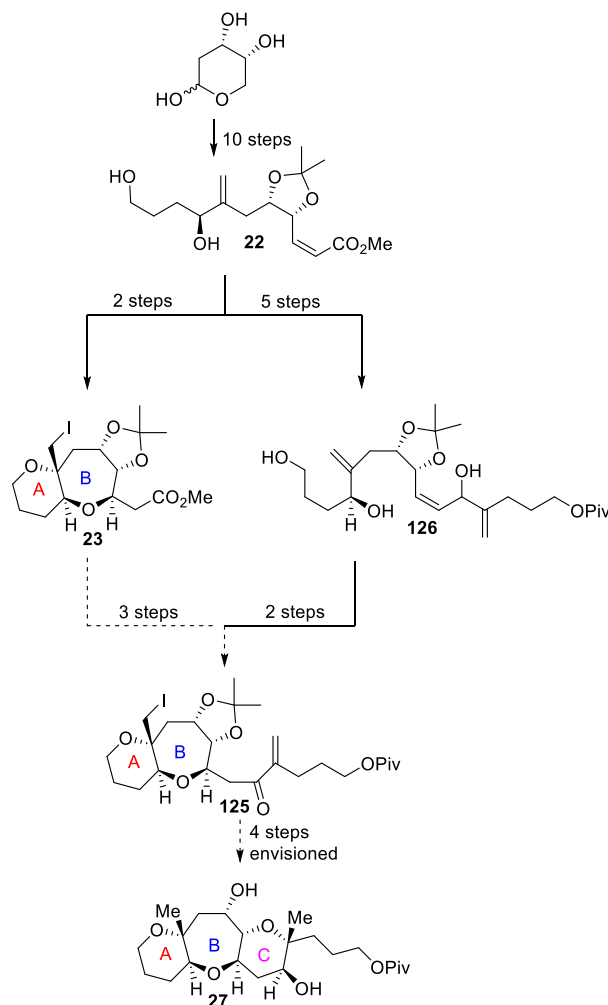
Scheme 82. Cyclization of triene **126** to form AB bicyclic compound **125**



3.2.5 ABC model

Although cyclization of triene **126** allowed access to AB-bicyclic compound **125**, the NHK coupling to synthesize triene **126** was plagued by an inseparable byproduct. The difficulties of reliably reproducing the coupling severely restricted the amount of material we could access through this route. To overcome this limitation, we envisioned supplementing our supplies of late-stage material through synthetic elaboration of AB-bicyclic compound **23** to intercept AB bicyclic enone **125** (Scheme 83). We hoped that by supplementing our supplies of AB bicyclic enone **125** through a more reliable synthetic route we would be able to work out the late-stage synthetic manipulations necessary to close the C-ring and complete synthesis of the ABC tricyclic core substructure **27** (Scheme 83).

Scheme 83. Proposal for alternative synthesis of AB enone **125** to investigate synthesis of tricyclic core substructure **27**

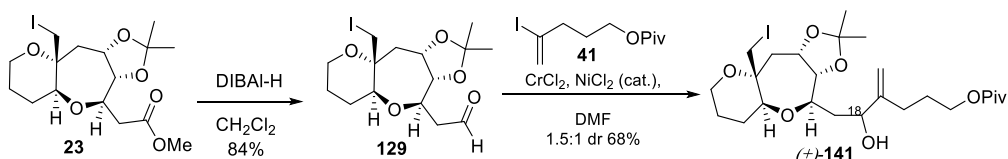


3.2.5.1 Synthesis of C-ring precursor **130**

Starting from the bicyclic ester **23**, reduction of the ester furnished aldehyde **129** (Scheme 84). NHK coupling of aldehyde **129** with vinyl iodide **41** resulted in allylic alcohol (\pm)-**141** as a mixture of diastereomers at C₁₈ (1.5:1 dr *S*:*R*). Following acetonide hydrolysis, the C₁₈ diastereomers were separable by careful silica gel flash column chromatography, resulting in isolation of both (*R*)-**141** and (*S*)-**141**. Alternatively, to increase the yield of the desired (*S*)-diastereomer, Luche reduction¹⁷⁵ of the ketone of

compound **125** was selective for the (*S*)-diastereomer at low temperature (32:1 *dr* at -78 °C; 5:1 *dr* at -40 °C) (Scheme 85). The observed 1,3-stereocontrol is consistent with the observations of Nelson from his synthesis of hemibrevetoxin B on a closely related compound¹⁷⁶, showing the generality of applying the Evans electrostatic model¹⁷⁷ to ketone reductions from β -cyclic ethers (Figure 16).¹⁷⁷ The absolute stereochemistry of the newly formed chiral center was confirmed by Mosher ester analysis.

Scheme 84. Synthesis of allylic alcohol (\pm)-**141**



Scheme 85. Setting stereochemistry at C₁₈

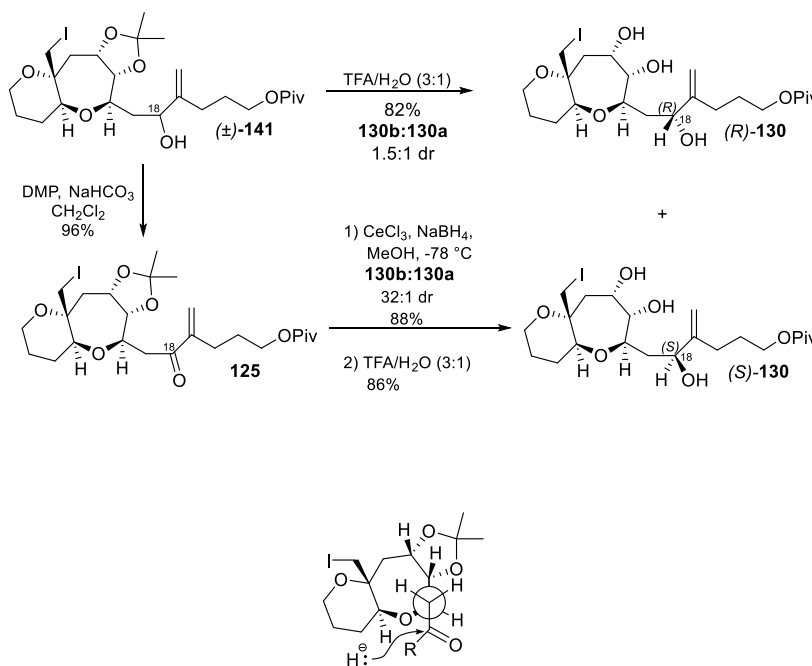
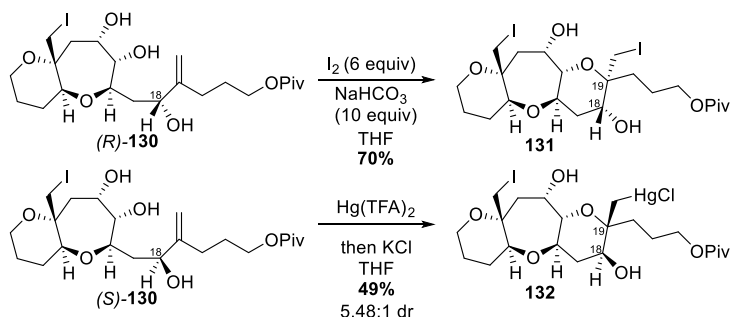


Figure 16. Model for 1,3-stereocontrol in ketone reduction of β -cyclic ether **125**

3.2.5.2 Cyclizations of C-ring precursor **130**

We expected to close the C-ring of brevenal through iodocyclization of compound (*S*)-**130**. Many attempts at iodo-etherification of (*S*)-**130** using iodine and bicarbonate and IDCP were unsuccessful. Reaction with iodine and bicarbonate resulted in full recovery of starting material and reaction with IDCP resulted in partial oxidation to the enone. However, (*R*)-**130**, the C₁₈ diastereomer, underwent iodo-etherification to afford tricyclic compound **131**, which has the opposite stereochemistry from the natural product at both C₁₈ and C₁₉ (Scheme 86). These results suggest diaxial orientation of the substituents in compound (*S*)-**130**, inhibiting attempts to cyclize. With precedents for inducing cyclization with mercuric-ion,^{75–77,82} treatment of (*S*)-**130** with mercuric trifluoroacetate⁸⁰ resulted in chemo- and diastereoselective closure of the C-ring, furnishing ABC tricyclic compound **132** (Scheme 86). The *dr* was determined from integration of the methyl substituents from the demercurated compound as it was not clear from the organomercurial compound. An electrostatic interaction between the Lewis acidic mercuric ion with a lone pair of the allylic oxygen may enable ring-closure by bringing the reactive groups into closer proximity⁶⁴. We have observed that the conformation of the B-ring oxepane changes significantly after cyclization has closed the C-ring.

Scheme 86. Electrophile-promoted cyclizations of (*R*)-**130** and (*S*)-**130**



3.2.5.3 Demercuration and deiodination of tricyclic compound 132

To complete synthesis of ABC tricyclic structure **127** we still needed to remove both the mercury and the iodine from tricyclic compound **132**. We decided to remove the mercury prior to removal of the iodide as we needed to remove the mercury to determine the stereoselectivity of the ring closure. Initially, we tried traditional reduction methods such NaBH₄ with NaOH¹⁷⁸ and NaBH₄ with BEt₃¹⁷⁹. Unfortunately, substrate **132** decomposed under these reaction conditions, although reactions on simple, unrestricted tetrahydropyran substrates were successful. Reductive demercuration has been noted to result in rearrangement and/or ring-cleavage, especially in the presence of a β -heteroatom¹⁸⁰. Furthermore, oxymercuration products bearing a β -heteroatom substituents can eliminate to starting unsaturated alcohols or amines under reductive demercuration conditions¹⁸⁰. Fortunately, we found reports of reductive cleavage of the C-Hg bond under phase-transfer conditions with NaBH₄¹⁸⁰. Organomercury compound **132** is water-soluble, which was used to our advantage in the demercuration. With short reaction times and concentrated reaction mixtures, we obtained nearly quantitative formation of cleanly demercurated compound **133** (Scheme 87). The axial methyl substituent appears at δ 0.88 in C₆D₆. Key NOE correlations are shown in Figure 17. Irradiation of the proton labeled i showed no NOE correlation, although NOE correlations did confirm the *syn* relationship of protons a and f across the C-O-C portion of the ether ring. The coupling constants of protons a and i (dd, J = 11.8, 4.9) are consistent with the desired chair conformations of the tetrahydropyran rings. The protons across the BC ring fusion shared a coupling constant of 9.5 Hz, consistent with the expected *trans*- orientation.

Scheme 87. Reduction of iodo-organomercury compound **132** to furnish ABC core substructure **27**

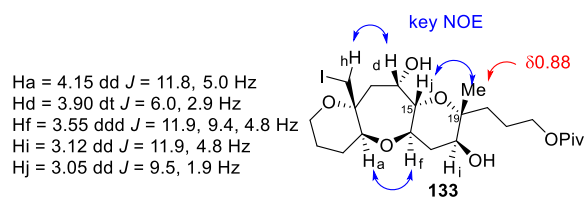
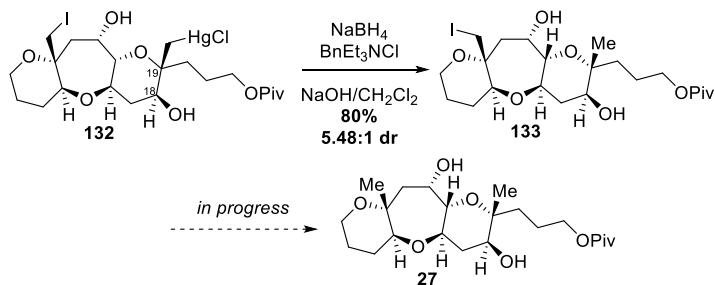


Figure 17. Key spectral data of tricyclic compound **133**

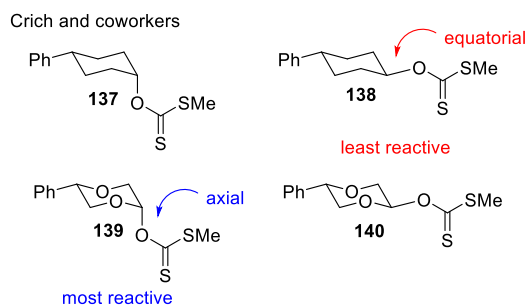
To complete the synthesis of the ABC core structure of brevenal, we attempted to remove the iodine from compound **133** to conclude our synthesis of the tricyclic substructure of brevenal (Scheme 897). We first tried classical methods of radical deiodination, with both tributyltin hydride and with *tris*-trimethyl silane¹⁷⁰, initiated by AIBN over a range of temperatures with varying equivalents of hydride source. We then attempted Stephenson's photocatalytic methodology for reduction of unactivated alkyl iodides using *fac*- $\text{Ir}(\text{ppy})_3$ and Hantzsch ester¹⁸¹. We expected that this milder system would be tolerant of our fused ether system, but reaction resulted in decomposition of starting material with trace iodomethylene protons still visible in the crude NMR. As observed with the radical demercuration reactions, all attempts at radical deiodination resulted in extensive decomposition of our substrate. We turned our attention to

hydrogenation. Attempts at hydrogenolysis of the alkyl iodide with 10% Pd/C with triethylamine at 30 bar for 22 hours resulted in no reaction, likely due to the steric congestion of the tricyclic compound.

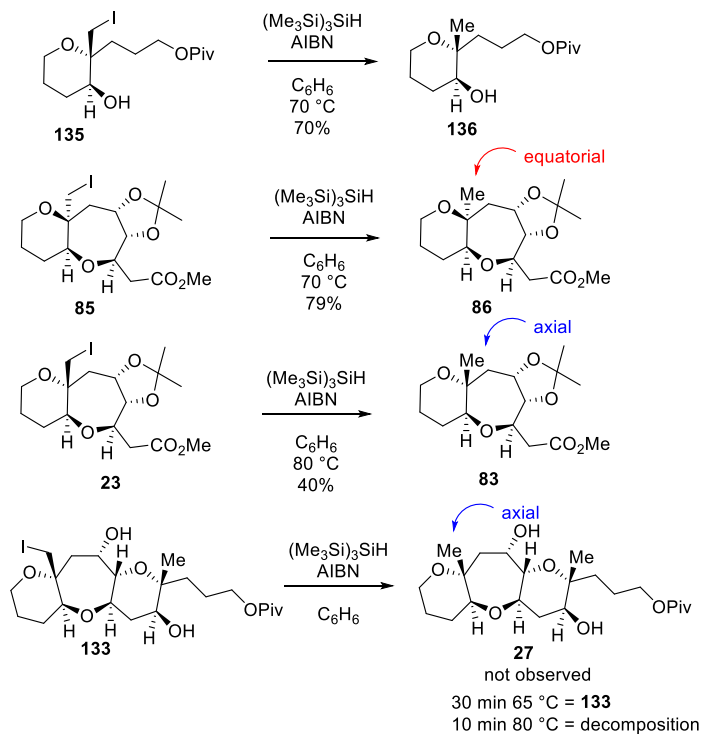
With our inability to deiodinate compound **133** we became curious about deiodination earlier in the synthesis, specifically on compound **23**. When we initially obtained this result, the low yield (40%) was not considered significant. However, with increased experience working on deiodination of compounds **135**, **85**, and **133** we became curious about a possible stereoelectronic effect to rationalize the observed reactivity. Although literature on stereoelectronic effects of alkyl iodide reductions is limited, there is discussion of β -oxygen effects in the related Barton-deoxygenation radical reactions^{182–186}. Barton reported various thiocarbonyl esters containing β -oxygen substituents undergoing deoxygenation at lower temperatures than corresponding substrates without heteroatom substitution¹⁸², which began a discussion involving experimental and computation contributions by several other laboratories, invoking a β -version of the Deslongchamp's well-documented α -stereoelectronic effect¹⁸⁷. The literature suggests that β -oxygen stabilizes carbon radicals, enabling unexpected homolytic bond cleavage. Notably, Crich¹⁸³ reported that in conformationally unrestricted systems there is a less significant β -oxygen effect, but with conformationally locked species orbital orientation has a marked effect. In a specific example from Crich and coworkers¹⁸³, a series of six reductions with tributyltin hydride were conducted on conformationally rigid xanthates **137–140**, and their relative rate constants were found to be in the order of $k_{139} > k_{140} > k_{137} > k_{138}$ (Scheme 88). From these studies, it was determined that the axial xanthate was more reactive than the

equatorial one, and the substrates with beta-oxygen substituents were more reactive than the corresponding substrates lacking oxygen substituents. This observation appears to be consistent with our observations (Scheme 89) wherein the equatorial substituent in compound **85** underwent deiodination in higher yield compared to compound **23** and **133** with axial substituents. We propose that not only is the barrier to the deiodination reaction lower for the axial iodomethyl compounds, the barrier to undesired reaction pathways is also lower, leading to more undesired reaction products in the more reactive, less selective system. If time permitted, the preferred route to access tricyclic compound **27** would involve deiodination of compound **23**, resulting in axial methyl compound **83**, which would then undergo the same synthetic sequence as **23** to ultimately afford tricyclic compound **27**.

Scheme 88. Relative rates of reduction of thiocarbonyl esters **137-140**



Scheme 89. Attempts at deiodination of cyclic compounds

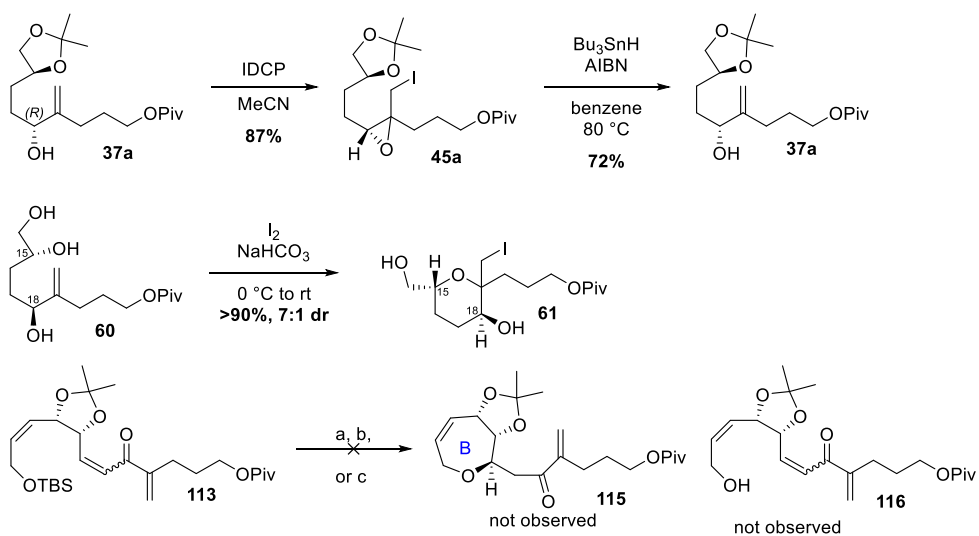


3.3 Conclusion

Although cyclization from acetal-protected nucleophiles such as **45a** resulted in 3-*exo*-tet cyclization forming α -iodoepoxides such as **45a**, cyclization of the vicinal diol resulted in diastereoselective formation of C ring model **61** (Scheme 90). Bis-acetate diene **78** spontaneously underwent intramolecular conjugate addition, forming the *trans*-fused oxepane, which underwent epoxidation and acid-promoted intramolecular cyclization to furnish *cis,trans*-fused bicyclic compound **78** (Scheme 91). Diene **22** undergoes tandem iodocyclization/ conjugate addition to afford the AB bicyclic product **23** (Scheme 9). Although we were unable to form the B-ring from conjugate addition onto dienyl ketones in the BC ring tandem cyclization studies (Scheme 90), we could effect conjugate addition

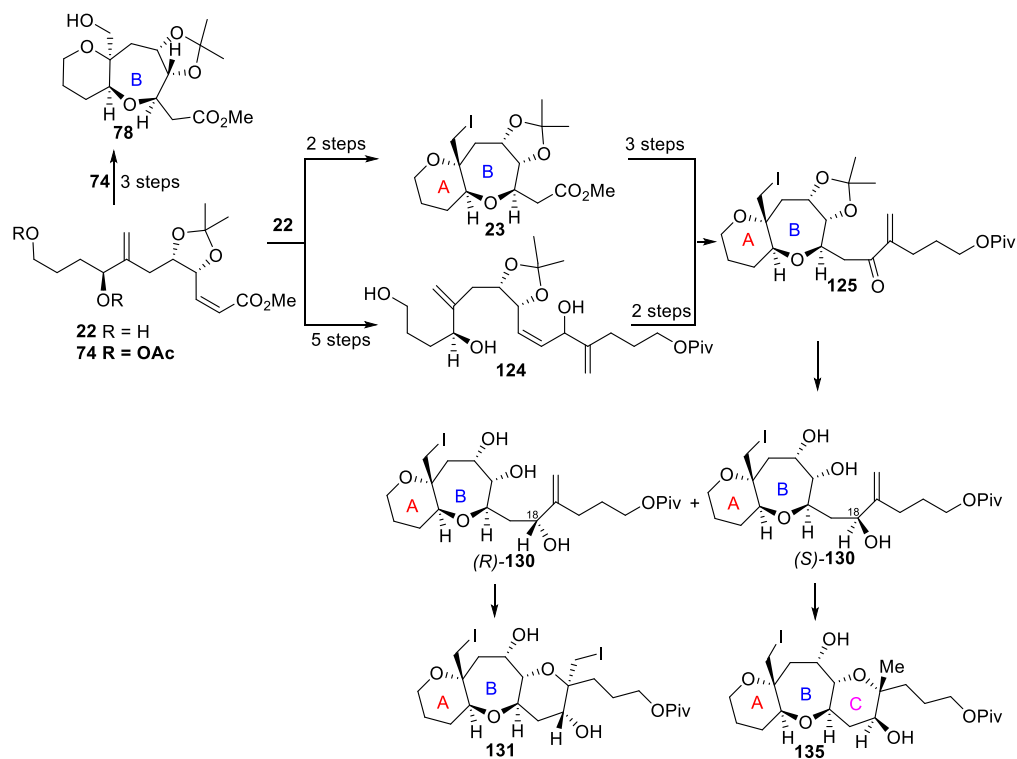
onto dienyl ketone **124** in the ABC model studies, furnishing bicyclic enone **125**. NHK coupling to synthesize triene **126** was plagued by difficulties in reproducibility, but we also synthesized bicyclic enone **125** through extending the carbon chain of AB bicyclic ester **23**, enabling the remaining synthetic studies to close the C ring.

Scheme 90. C-ring and BC-ring cyclization results



Although iodocyclization of alkenol alcohol (*S*)-**130** does not occur, iodocyclization of alkenol alcohol (*R*)-**130** resulted in tricyclic compound **131**. Mercury-promoted oxacyclization followed by reduction to the corresponding methyl group furnished ABC tricyclic compound **135**.

Scheme 91. AB and ABC cyclization results



For future synthetic studies of the brevenal core, we plan to build off the stoichiometric chemo-, regio- and diastereoselective halogen- and metal- promoted oxacyclization reactions described in this dissertation to access similar cyclic ether products through transition metal-promoted catalytic cycloisomerization reactions. Such catalytic methods will not only be beneficial in terms of atom economy, but will allow us to avoid the problematic dehalogenation and demercuration steps.

3.4 Experimental Details

^1H and ^{13}C NMR spectra were recorded on Varian INOVA 600, INOVA 400, and Bruker AVANCE 600 spectrometers. NMR spectra were generally measured from solutions of

deuterated chloroform (CDCl₃), with the residual chloroform (7.27 ppm for ¹H NMR and 77.23 ppm for ¹³C NMR) taken as the internal standard, and are reported in parts per million (ppm). Abbreviations for signal coupling are as follows: s, singlet; d, doublet; t, triplet; q, quartet; dd, doublet of doublet; ddd, doublet of doublet of doublet; dt, doublet of triplet; m, multiplet.

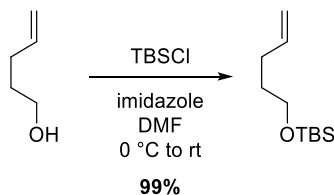
IR spectra were collected on a Thermo Scientific Nicolet iS10 FT-IR spectrometer as neat films. Mass spectra (high resolution ESI and APCI) were recorded on a Thermo LTQ FTMS Mass spectrometer. Optical rotations were measured using a Perkin-Elmer 341 polarimeter (concentration in g/100mL). Thin Layer Chromatography (TLC) was performed on a precoated glass backed plates purchased from Silacyle (silica gel 60F₂₅₄; 0.25mm thickness). Flash column chromatography was carried out with silica gel 60 (230-400 mesh ASTM) from Silacyle.

All reactions were carried out with anhydrous solvents in oven dried and argon-charged glassware. All anhydrous solvents were dried with 4Å molecular sieves purchased from Sigma Aldrich and tested for trace water content with Coulometric KF titrator from Denver Instruments. All solvents used in extraction procedures and chromatography were used as received from commercial suppliers without prior purification.

General procedure for preparing MTPA (Mosher) ester in NMR tube: The secondary alcohol (about 0.02 mmol) was added to a dried NMR tube. (+)- or (-)- MTPACl (1 drop), pyridine-d₅ (3 drops), and chloroform-*d* (0.5 mL) were added in that order. The

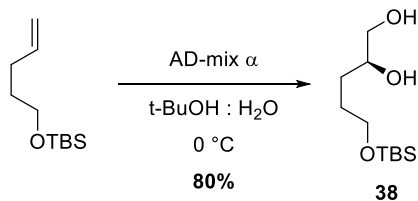
NMR tube was shaken and left overnight. Enantiomeric ratios were determined by integration of ^1H -NMR of the MTPA ester.

Synthesis of acetonide protected diol 37



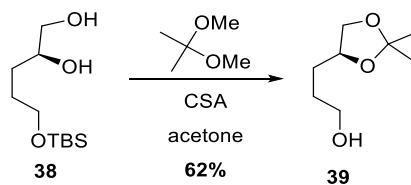
tert-Butyldimethyl(pent-4-en-1-yloxy)silane: To a solution of alcohol (4.79 g, 55.6 mmol) and TBSCl (18.30 g, 117 mmol) in DMF (55 mL) at 0 °C was added imidazole (21.1 g, 312 mmol) in one portion. The solution was slowly warmed to room temperature and after 4 hours was quenched with water (100 mL). The aqueous and organic layers were separated and the aqueous layer was extracted with Et_2O (20 mL x 7). The combined organic extracts were washed with H_2O (7 mL x 5), 5% aqueous LiCl (100 mL) and brine before being dried over MgSO_4 , filtered, and concentrated under reduced pressure. The residue was purified by flash column chromatography (hexanes) to yield the product as a clear oil (11.1 g, 55.6 mmol) in >99% yield. The ^1H NMR data is consistent with data reported in the literature.¹⁸⁸

^1H NMR (400 MHz, Chloroform-*d*) δ 5.93 – 5.74 (ddt, $J = 17.1, 10.1, 6.5$ Hz, 1H), 5.03 (m, 1H), 4.96 (m, 2H), 3.63 (t, $J = 6.5$ Hz, 2H), 2.12 (q, $J = 7.1$ Hz, 2H), 1.71 – 1.57 (p, $J = 7.5$ Hz, 2H), 0.91 (s, 9H), 0.06 (s, 6H).



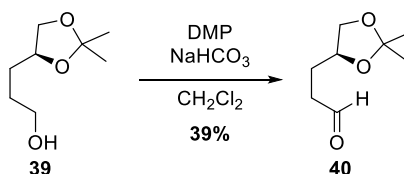
Diol 38: To a biphasic suspension of water (75 mL) and *t*-BuOH (75 mL) was added AD-mix α (21.2 g). The suspension was stirred at room temperature for 10 minutes before being cooled to 0 °C before addition of the alkene (3.03 g, 15.1 mmol). After 20 hours, the yellow-orange suspension was quenched with solid sodium sulfite (22.8 g) and stirred at room temperature for one hour, whereupon the suspension turned rusty brown in color. The suspension was diluted with water (50 mL) and extracted with CH_2Cl_2 (4 x 40 mL). The combined organic extracts were washed with 2M KOH (100 mL) and dried over Na_2SO_4 , filtered, and concentrated under reduced pressure. The resulting yellow oil was purified by silica gel flash column chromatography (40% EtOAc in hexanes) to afford product **38** as a clear oil (2.83 g, 12.1 mmol) in 80% yield. ^1H NMR data is consistent with data reported in the literature.¹⁸⁹

^1H NMR (400 MHz, CDCl_3) δ 3.82 – 3.68 (m, 2H), 3.68 – 3.61 (m, 2H), 3.58 – .41 (m, 2H), 2.03 (br s, 1H), 1.66 (m, 3H), 1.56 – 1.43 (m, 1H), 0.91 (s, 9H), 0.09 (s, 6H).



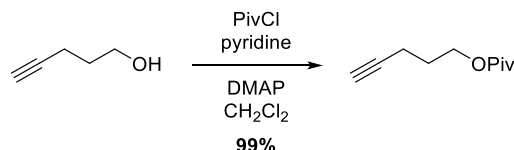
Acetal 39: Diol (878 mg, 3.75 mmol) was dissolved in acetone (20 mL). 2,2-Dimethoxypropane (2.36 mL, 31.2 mmol) and CSA (185 mg, 0.8 mmol) were added and the reaction was stirred at room temperature for two days, where it was quenched with solid NaHCO₃ and filtered. The crude material was concentrated under reduced pressure and the resulting oil was purified by silica gel flash column chromatography (15% to 20% EtOAc in hexanes) to afford the desilylated acetonide **39** (316 mg, 2.48 mmol) in 62% yield. ¹H NMR data is consistent with data reported in the literature.¹⁹⁰

¹H NMR (600 MHz, CDCl₃): δ 4.13 (m, 1H), 4.07 (dd, *J* = 7.5, 6.0 Hz, 1H), 3.72 – 3.66 (m, 2H), 3.54 (dd, *J* = 7.6 Hz, 1H), 1.78 – 1.60 (m, 5H), 1.42 (s, 3H), 1.37 (s, 3H).



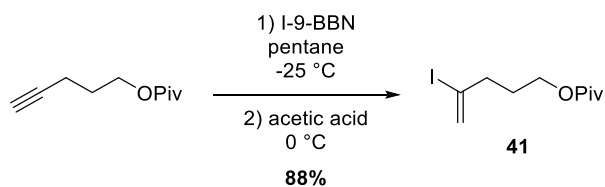
Aldehyde 40: To a stirred solution of alcohol (316 mg; 1.97 mmol) in CH₂Cl₂ (40 mL) was added DMP (1.00 g, 2.37 mmol) and NaHCO₃ (500 mg; 5.91 mmol). After 12 hours, additional DMP (2.00 g, 0.47 mmol) was added. After another 3 hours, the reaction was poured into a rapidly stirred solution of Na₂S₂O₃ (20 g) in 100 mL saturated aqueous NaHCO₃. The suspension was stirred for 30 minutes until the layers turned clear. The layers were separated and the organic layer was washed with water (15 mL x 3), dried over MgSO₄, filtered, and concentrated under reduced pressure. The resulting crude aldehyde **39** (120 mg, 0.76 mmol) was obtained in 39% yield and used without further purification. ¹H NMR data is consistent with data reported in the literature.¹⁹¹

¹H NMR (400 MHz, CDCl₃) δ 9.82 (t, *J* = 1.3 Hz, 1H), 4.14 (m, 1H), 4.07 (dd, *J* = 8.1, 6.0 Hz, 1H), 3.56 (dd, *J* = 7.9, 6.7 Hz, 1H), 2.72 – 2.53 (m, 2H), 1.99 – 1.89 (m, 1H), 1.89 – 1.78 (m, 1H), 1.41 (s, 3H), 1.35 (s, 3H).



Pent-4-yn-1-yl pivalate: Alcohol (9.62 g; 114 mmol) was dissolved in dichloromethane (375 mL) at 0 °C. PivCl (16.54 g; 137 mmol) was added slowly before addition of pyridine (13.57g; 172 mmol) and DMAP (200 mg). The reaction mixture was stirred overnight before further addition of PivCl (6.36 g; 52.8 mmol), pyridine (5.40 g; 68.2 mmol), and DMAP (100 mg). After an additional five hours, the reaction mixture quenched with saturated aqueous ammonium chloride (100 mL) and extracted with diethyl ether (5 x 75 mL). The combined organic layers were washed with brine (40 mL) and dried over magnesium sulfate before being filtered and concentrated under reduced pressure. The crude residue was purified by silica gel flash column chromatography (hexanes to 5% ethyl acetate in hexanes) to afford the product as clear oil (19.18 g; 114 mmol) in 99% yield. Spectra data of the alkyne match the literature.¹⁹²

¹H NMR (400 MHz, CDCl₃) δ 4.16 (t, *J* = 6.2 Hz, 2H), 2.30 (td, *J* = 7.1, 2.7 Hz, 2H), 1.98 (t, *J* = 2.7, 1H), 1.94 – 1.76 (p, *J* = 6.8 Hz, 2H), 1.21 (s, 9H).



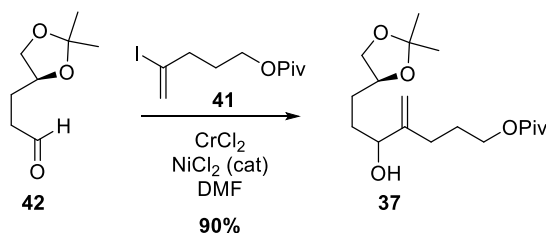
Vinyl iodide 41: I-9-BBN (1.0M in hexanes; 50 mL; 50.0 mmol) was diluted with pentane (80 mL) and cooled to -25 °C, at which point alkyne (3.36 g; 20.0 mmol) in pentane (35 mL) was added slowly and the reaction turned light yellow and clear. The reaction was stirred at -25 °C for 5 hours before addition of acetic acid (12 mL), which resulted in vigorous bubbling and white, cloudy precipitate. The suspension was then warmed to 0 °C, where it was stirred for 1 hour before addition of 3 M NaOH (280 mL) and 30% aqueous H₂O₂ (48 mL), resulting in vigorous bubbling upon addition. The suspension was then warmed to room temperature where it was stirred for 45 minutes. The layers turned clear and colorless. The aqueous layer was separated and extracted with dichloromethane (4 x 30 mL). The combined organic layers were dried over magnesium sulfate before being filtered and concentrated under reduced pressure. The crude residue was purified by silica gel flash column chromatography (hexanes to 2.5% ethyl acetate in hexanes) to afford compound **41** as light-yellow oil (5.17 g; 17.5 mmol) in 88% yield

HRMS (NSI): *m/z* calcd. for C₁₀H₁₈O₂I [M+H]⁺: 297.03460 found 297.03467.

IR (thin film): 2969, 2958, 1726, 1619, 1479, 1282, 1151, 892 cm⁻¹.

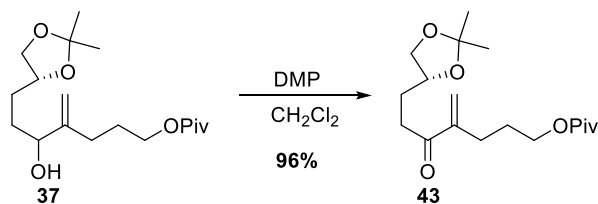
¹H NMR (500 MHz, CDCl₃) δ 6.06 (s, 1H), 5.74 (s, 1H), 4.08 (t, *J* = 6.3 Hz, 2H), 2.49 (t, *J* = 7.2 Hz, 2H), 1.91 – 1.83 (m, 2H), 1.21 (s, 9H).

¹³C NMR (126 MHz, CDCl₃) δ 178.66, 126.51, 110.75, 62.69, 42.03, 38.97, 28.30, 27.41.



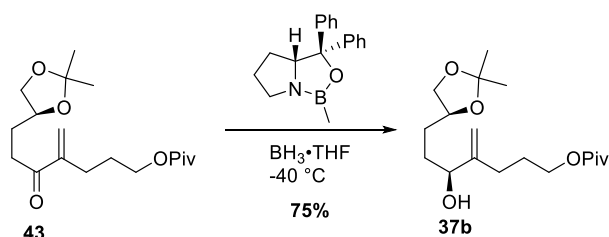
Allylic alcohol 37: In a glovebox, CrCl₂ (300 mg, 2.38 mmol) and NiCl₂ (1.7 mg, 0.012 mmol) were weighed into a dry round bottom flask. Out of the glovebox, the flask was cooled to 0 °C and salts were dissolved in DMF (7.5 mL, freshly distilled over CaSO₄) and stirred for 15 minutes before being warmed to room temperature. Vinyl halide **41** (355 mg, 1.19 mmol) in DMF (3.6 mL) was added to the dissolved salts, followed by aldehyde **42** (97 mg, 0.60 mmol) in DMF (1 mL) dropwise. The reaction mixture was stirred for 2 hours before being poured into water (50 mL). The aqueous and organic layers were separated and the aqueous layer was extracted with EtOAc (20 mL x 5) and concentrated under reduced pressure. The resulting yellow liquid was dissolved in Et₂O (25 mL) washed with H₂O (7 mL x 5), 5% aqueous LiCl (10 mL) and brine before being dried over MgSO₄, filtered, and concentrated under reduced pressure. The residue was purified by flash column chromatography (20% to 30% EtOAc in hexanes) to yield product **37** as a light yellow, clear oil (178 mg, 0.54 mmol) in 90% yield as a mixture of diastereomers.

¹H NMR (600 MHz, CDCl₃) δ 5.09 (d, *J* = 1.90 Hz, 1H), 4.89 (d, *J* = 2.5Hz, 1H), 4.15 – 4.08 (m, 4H), 4.08 – 4.04 (m, 1H), 3.56 – 3.50 (m, 1H), 2.22 – 2.13 (m, 1H), 2.12 – 2.03 (m, 2H), 1.88 – 1.80 (m, 2H), 1.71 – 1.64 (m, 2H), 1.64 – 1.55 (m, 2H), 1.42 (s, 3H), 1.36 (s, 3H), 1.21 (s, 9H).



Enone 43: To a stirred solution of alcohol (178 mg, 0.54 mmol) in CH₂Cl₂ (11 mL) was added DMP (361 mg, 0.85 mmol). After 3 hours, additional DMP (114 mg, 0.27 mmol) was added. After another 2 hours, the reaction was poured into a rapidly stirred solution of Na₂S₂O₃ (18 g) in 100 mL saturated aqueous NaHCO₃. The suspension was stirred for 30 minutes, until the layers turned clear. The layers were separated and the organic layer was extracted with dichloromethane (4 x 10 mL), washed with water (5 mL x 3), dried over MgSO₄, filtered, and concentrated under reduced pressure. The resulting crude enone **43** (170 mg, 0.52 mmol) was obtained in 96% yield and used without further purification.

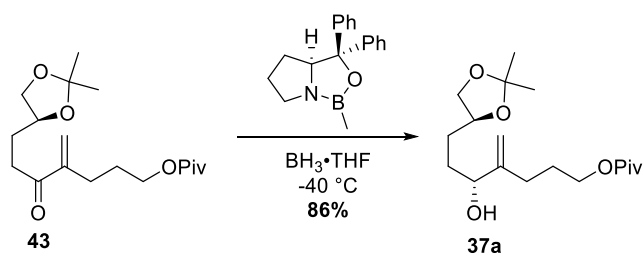
¹H NMR (600 MHz, CDCl₃) δ 6.09 (s, 1H), 5.79 (d, *J* = 1.3 Hz, 1H), 4.12 (dtd, *J* = 8.1, 6.5, 4.1 Hz, 1H), 4.08 – 4.04 (m, 3H), 3.56 (dd, *J* = 7.9, 6.9 Hz, 1H), 2.89 (ddd, *J* = 17.3, 8.9, 5.6 Hz, 1H), 2.81 (ddd, *J* = 17.3, 8.8, 6.4 Hz, 1H), 2.38 – 2.33 (m, 2H), 1.96 – 1.86 (m, 1H), 1.85 – 1.79 (m, 1H), 1.76 (m, 2H), 1.41 (s, 3H), 1.35 (s, 3H), 1.21 (s, 9H).



(S)-allylic alcohol 37b: A solution of (R)-2-methyl-CBS-oxazaborolidine in toluene (1.0 M, 0.52 mL, 0.52 mmol) and a solution of BH₃·THF (1.0 M, 0.52 mL, 0.52 mmol) were

added to THF (15 mL) at room temperature. After being stirred for 45 min at room temperature, the solution was cooled to -40 °C where a solution of ketone (170 mg, 0.52 mmol) in THF (10 mL) was slowly added, and the resulting reaction mixture was stirred at -40 °C for 5 hours. The reaction was quenched with MeOH (4.5 mL), warmed to room temperature, and concentrated under reduced pressure. The resulting oil was dissolved in ethyl acetate, washed with saturated aqueous NH₄Cl (15 mL), and extracted with ethyl acetate (3 × 15 mL). The combined organic layers were washed with brine (5 mL), dried over MgSO₄, filtered, and concentrated in under reduced pressure. The residue was purified by flash column chromatography (25% EtOAc in hexanes) to yield product **37b** as a light yellow clear oil (128 mg, 0.39 mmol) in 75% yield as the predominately the *S* alcohol in a mixture of diastereomers that could not be resolved by ¹H NMR.

¹H NMR (400 MHz, CDCl₃) δ 5.10 (s, 1H), 4.89 (s, 1H), 4.18 – 3.98 (m, 5H), 3.53 (td, *J* = 7.5, 3.4 Hz, 1H), 2.23 – 2.13 (m, 1H), 2.12 – 1.99 (m, 1H), 1.84 (m, 2H), 1.76 – 1.54 (m, 5H), 1.42 (s, 3H), 1.37 (s, 3H), 1.21 (s, 9H).



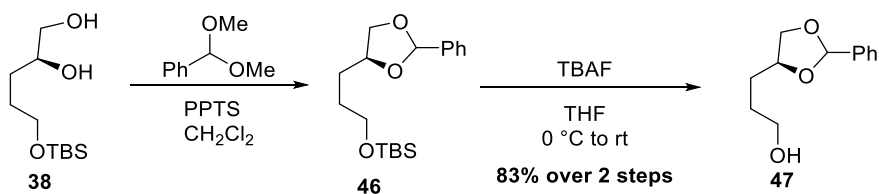
(*R*)-allylic alcohol 37a: A solution of (*S*)-2-methyl-CBS-oxazaborolidine in toluene (1.0 M, 0.25 mL, 0.22 mmol) and a solution of BH₃ · THF (1.0 M, 0.22 mL, 0.22 mmol) were added to THF (3 mL) at room temperature. After being stirred for 45 min at room

temperature, the solution was cooled to $-40\text{ }^{\circ}\text{C}$ where a solution of ketone (80 mg, 0.21 mmol) in THF (5 mL) was slowly added, and the resulting reaction mixture was stirred at $-40\text{ }^{\circ}\text{C}$ for 6 hours. The reaction was quenched with MeOH (2.2 mL), warmed to room temperature, and concentrated under reduced pressure. The resulting oil was dissolved in ethyl acetate, washed with saturated aqueous NH_4Cl (10 mL), and extracted with ethyl acetate ($3 \times 15\text{ mL}$). The combined organic layers were washed with brine (5 mL), dried over MgSO_4 , filtered, and concentrated in under reduced pressure. The residue was purified by flash column chromatography (20% to 30% EtOAc in hexanes) to yield product **37a** as a light yellow clear oil (60 mg, 0.18 mmol) in 86% yield as predominately the R alcohol in a mixture of diastereomers that could not be resolved by ^1H NMR.

^1H NMR (400 MHz, CDCl_3) δ 5.06 (s, 1H), 4.86 (s, 1H), 4.11 – 3.99 (m, 5H), 3.48 (m, 1H), 2.15 (m, 1H), 2.12 – 1.99 (m, 1H), 1.84 (m, 2H), 1.76 – 1.54 (m, 5H), 1.39 (s, 3H), 1.33 (s, 3H), 1.18 (s, 9H).

^{13}C NMR (101 MHz, CDCl_3) δ 178.746, 150.580, 110.341, 109.074, 76.200, 76.085, 75.093, 74.880, 69.553, 64.021, 38.907, 31.932, 31.795, 29.986, 29,704, 27.788, 27.750, 27.361, 27.048, 25.865.

Synthesis of benzylidene protected diol 49

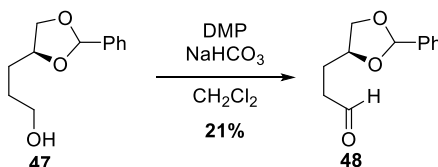


Alcohol 47: To a solution of diol (472 mg, 2.0 mmol) in dichloromethane (11 mL) were added benzaldehyde dimethylacetal (0.75 mL, 5 mmol) and PPTS (25 mg, 0.1 mmol). The reaction mixture was stirred at room temperature for 3 days before being quenched with saturated aqueous sodium bicarbonate (11 mL). The organic layer was separated and the aqueous layer was extracted with Et₂O (11 mL x 4, washed with brine (10 mL), dried over MgSO₄, filtered, and concentrated in under reduced pressure. The residue was purified by flash column chromatography (5% ethyl acetate in hexanes) to afford the product as a light-yellow oil as a 1: 2 mixture of diastereomers. The benzylidene acetal hydrolyzes on the column, resulting in an inseparable mixture of diastereomers of protected diol **46**, benzaldehyde, and benzaldehyde dimethylacetal. The purified mixture was subjected to further reaction. The diastereomers are spectroscopically dissimilar at the acetal proton.

¹H NMR (600 MHz, CDCl₃) δ 7.52 – 7.44 (m, 2H), 7.42 – 7.33 (m, 3H), 5.94 (s, 0.32 H), 5.81 (s, 0.68 H), 4.32 – 4.21 (m, 1H), 4.12 (ddd, $J = 7.4, 6.6, 0.7$ Hz, 1H), 3.77 – 3.61 (m, 1H), 1.87 – 1.67 (m, 4H), 1.67 – 1.54 (m, 2H), 0.90 (s, 9H), 0.06 (s Hz, 6H).

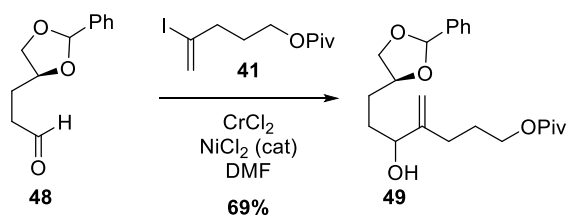
Silyl ether **46** was dissolved in THF (17 mL) and cooled to 0 °C before addition of TBAF in THF (1.0 M; 3.5 mL; 3.50 mmol). The resulting solution was gradually warmed to room temperature and stirred for 5 hours before removal of solvent under reduced pressure. The resulting oil was purified by silica gel flash column chromatography (40% ethyl acetate in hexane) to afford the product as a light-yellow oil (344 mg; 1.65 mmol) as a 1: 2 mixture of diastereomers of benzylidene acetal alcohol **47** in 83% yield over two steps. The diastereomers are spectroscopically dissimilar at the acetal proton.

¹H NMR (400 MHz, CDCl₃) δ 7.52 – 7.45 (m, 2H), 7.42 – 7.35 (m, 3H), 5.95 (s, 0.31 H), 5.83 (s, 0.69 H), 4.28 (m, 1H), 4.14 (ddd, *J* = 8.0, 6.5, 1.1 Hz, 1H), 3.72 (td, *J* = 6.3, 1.4 Hz, 3H), 1.90 – 1.69 (m, 4H), 1.70 – 1.65 (m, 1H).



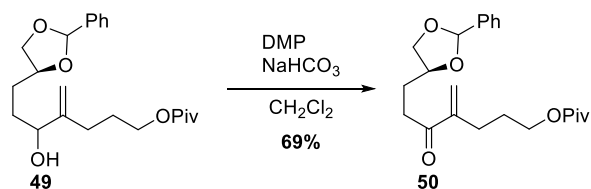
Aldehyde 48: To a stirred solution of alcohol **47** (1.62 g, 7.78 mmol) in CH₂Cl₂ (150 mL) was added DMP (4.95 g, 11.7 mmol) and NaHCO₃ (23.3 mmol, 1.96 g). After 15 hours, the reaction was poured into a rapidly stirred solution of Na₂S₂O₃ (30 g) in 200 mL saturated aqueous NaHCO₃. The suspension was stirred for 30 minutes until the layers turned clear. The layers were separated and the organic layer was extracted with dichloromethane (4 x 30 mL), washed with water (10 mL x 3), dried over MgSO₄, filtered, and concentrated under reduced pressure. The resulting residue was purified by silica gel flash column chromatography (10% to 20% EtOAc in hexanes) to afford product **48** as a yellow oil (346 mg, 1.66 mmol) in 21% yield as a 1:2 mixture of diastereomers, with clearly resolvable protons at the aldehyde and the acetal.

¹H NMR (600 MHz, CDCl₃) δ 9.85 (t, *J* = 1.3 Hz, 0.33H), 9.82 (t, *J* = 1.3 Hz, 0.67 H), 7.52 – 7.43 (m, 2H), 7.39 (m, 3H), 5.91 (s, 0.33H), 5.80 (s, 0.67H), 4.35 – 4.23 (m, 1H), 4.14 (m, 1H), 3.75 (m, 1H), 2.80 – 2.61 (m, 1H), 2.12 – 2.04 (m, 1H), 2.01 – 1.91 (m, 2H).



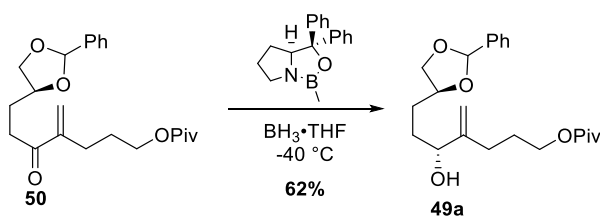
Allylic alcohol 49: In a glovebox, CrCl_2 (815 mg; 6.60 mmol) and NiCl_2 (4.4 mg; 0.033 mmol) were weighed into a dry round bottom flask. Out of the glovebox, the flask was cooled to 0 °C and salts were dissolved in DMF (freshly distilled over CaSO_4 , 20 mL) and stirred for 15 minutes before being warmed to room temperature. Vinyl iodide **41** (981 mg; 3.30 mmol) in DMF (9 mL) was added to the dissolved salts, followed by the aldehyde **48** (346 mg; 1.65 mmol) in DMF (1.7 mL) dropwise. The reaction mixture was stirred for 1.5 hours before being poured into water (50 mL). The aqueous and organic layers were separated and the aqueous layer was extracted with EtOAc (20 mL x 5) and concentrated under reduced pressure. The resulting yellow liquid was dissolved in Et_2O (25 mL) washed with H_2O (7 mL x 5), 5% aqueous LiCl (40 mL) and brine before being dried over MgSO_4 , filtered, and concentrated under reduced pressure. The residue was purified by flash column chromatography (20% to 25% EtOAc in hexanes) to yield the product **49** as a light yellow, clear oil (430 mg, 1.14 mmol) in 69% yield as a mixture of diastereomers. Vinyl iodide (530 mg; 1.79 mmol) was recovered. Except for the distinct diastereomeric acetal protons (2:1 dr) and the alkene, the diastereomers are not clearly resolvable.

^1H NMR (600 MHz, CDCl_3) δ 8.02 (s, 1H), 7.48 (m, 2H), 7.38 (m, 3H), 5.93 (s, 0.35 H), 5.82 (s, 0.65 H), 5.15 – 5.02 (m, 1H), 4.93 – 4.82 (m, 1H), 4.26 (m, 2H), 4.21 – 4.06 (m, 4H), 2.24 – 2.14 (m, 1H), 2.06 (m, 1H), 2.02 – 1.89 (br s, -OH), 1.89 – 1.79 (m, 3H), 1.79 – 1.71 (m, 1H), 1.71 – 1.57 (m, 2H), 1.20 (s, 9H).



Enone 50: To a stirred solution of alcohol **49** (428 mg; 1.14 mmol) in CH_2Cl_2 (23 mL) was added DMP (727 mg; 1.71 mmol). After stirring at room temperature for 14 hours, the reaction was poured into a rapidly stirred solution of $\text{Na}_2\text{S}_2\text{O}_3$ (25 g) in 100 mL saturated aqueous NaHCO_3 . The suspension was stirred for 30 minutes, until the layers turned clear. The layers were separated and the aqueous phase was extracted with dichloromethane (25 mL x 4) and the combined organic layers were washed with water (15 mL x 3), dried over MgSO_4 , filtered, and concentrated under reduced pressure. The resulting crude product **50** (338 mg; 0.79 mmol) was obtained in 69% yield and used without further purification. Except for the distinct diastereomeric acetal protons (2:1 dr), the diastereomers are not clearly resolvable by proton NMR.

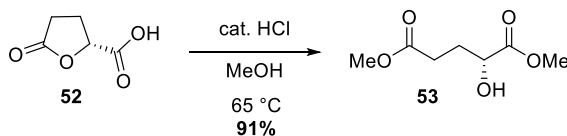
^1H NMR (600 MHz, CDCl_3) δ 7.54 – 7.44(m, 2H), 7.39 (m, 3H), 6.10 (s, 1H), 6.06 (s, 2H), 5.90 (s, 0.35 H), 5.80 (s, 0.65H), 4.32 – 4.24 (m, 2H), 4.14 (dd, $J = 7.8, 6.8$ Hz, 1H), 4.05 (m, 2H), 2.95 – 2.85 (m, 2H), 2.43 – 2.29 (m, 2H), 2.07 (m, 1H), 2.00 – 1.88 (m, 1H), 1.75 (m, 2H), 1.21 (s, 9H).



(R)-Allylic alcohol 49a: A solution of (S)-2-methyl-CBS-oxazaborolidine in toluene (1.0 M, 0.22 mL, 0.22 mmol) and a solution of $\text{BH}_3 \cdot \text{THF}$ (1.0 M, 0.22 mL; 0.22 mmol) were added to THF (0.8 mL) at room temperature. After being stirred for 45 min at room temperature, the solution was cooled to $-40\text{ }^\circ\text{C}$ where a solution of ketone **50** (80 mg, 0.21 mmol) in THF (4.2 mL) was slowly added, and the resulting reaction mixture was stirred at $-40\text{ }^\circ\text{C}$ for 2 hours. The reaction was quenched with MeOH (2.2 mL), warmed to room temperature, and concentrated under reduced pressure. The resulting oil was dissolved in ethyl acetate, washed with saturated aqueous NH_4Cl (20 mL), and extracted with ethyl acetate ($3 \times 7\text{ mL}$). The combined organic layers were washed with brine (10 mL), dried over MgSO_4 , filtered, and concentrated in under reduced pressure. The residue was purified by flash column chromatography (25% to 30% EtOAc in hexanes) to yield product **49a** as a light yellow clear oil (49 mg; 0.13 mmol) in 62% yield as the R alcohol in a 2:1 mixture of diastereomers, distinct at both the acetal and the alkene.

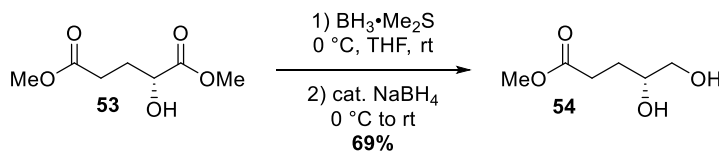
$^1\text{H NMR}$ (600 MHz, CDCl_3) δ 7.48 (m, 2H), 7.41 – 7.36 (m, 3H), 5.93 (s, 0.3H), 5.82 (s, 0.7H), 5.11 (s, 0.3H), 5.09 (s, 0.7H), 4.91 (d, $J = 1.4\text{ Hz}$, 0.3H), 4.89 (d, $J = 1.4\text{ Hz}$, 0.7H), 4.26 (m, 2H), 4.22 – 4.02 (m, 4H), 2.21 – 2.14 (m, 1H), 2.06 (m, 1H), 1.83 (m, 2H), 1.77 – 1.55 (m, 4H), 1.20 (d, $J = 2.0\text{ Hz}$, 9H).

Synthesis of vicinal diol 60



Dimethyl (R)-2-hydroxypentanedioate: To a solution of (R)- butyrolactone **52** (5.0g; 38.5 mmol) in MeOH (40 mL) was added 4 drops of concentrated HCl and heated to reflux overnight. The reaction was cooled to 0°C and quenched with NaHCO₃ (7 mL) and filtered. The solvent was removed under reduced pressure and the crude oil was purified via silica gel flash column chromatography (50% EtOAc in hexanes) to afford di-ester **53** as a viscous and colorless oil (6.18 g; 35.0 mmol) in 91% yield. The ¹H NMR data was consistent with reported data for the other enantiomer¹⁵⁶.

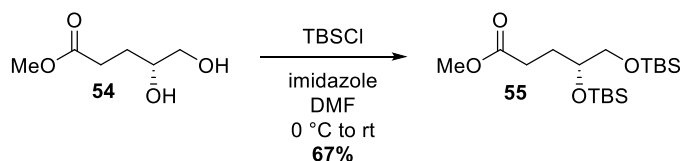
¹H NMR (400 MHz, CDCl₃): δ 4.25 (ddd, *J* = 7.9, 4.2 Hz, 1H), 3.81 (s, 3H), 3.69 (s, 3H), 2.90 (br s, -OH), 2.64 – 2.38 (m, 2H), 2.25 – 2.12 (m, 1H), 1.95 (m, 1H).



Diol 54: To a solution of diester (6.18 g, 35.0 mmol) in THF (55 mL) was added BH₃·Me₂S (37.6 mmol; 3.56 mL) dropwise maintaining a temperature of 0 °C. After stirring at 0 °C one hour, NaBH₄ (18 mg, 0.42 mmol) was added and the reaction was stirred for an additional hour in an ice bath. The reaction mixture was quenched with MeOH (20 mL) and stirred for an additional 30 minutes. The solvent was removed under reduced pressure

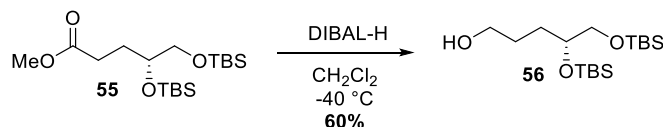
and the crude was purified via silica gel flash column chromatography (EtOAc) to afford diol **54** as a viscous colorless oil (3.60 g, 24.3 mmol) in 69% yield. The ^1H NMR data was consistent with reported data for the other enantiomer¹⁵⁶.

^1H NMR (600 MHz, CDCl_3) δ 3.78 – 3.71 (m, 1H), 3.69 (s, 3H), 3.65 (dd, $J = 11.0, 3.3$ Hz, 1H), 3.47 (dd, $J = 11.0, 7.0$ Hz, 1H), 2.84 – 2.65 (br s, -OH), 2.56 – 2.41 (m, 2H), 2.36 – 2.12 (br s, -OH), 1.98 – 1.63 (m, 2H).



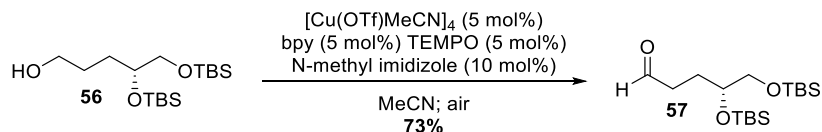
Bis-silyl ether 55: To a solution of alcohol **54** (3.60 g, 24.3 mmol) and TBSCl (16.0 g, 102 mmol) in DMF (25 mL) at 0° C was added imidazole (19.0 g, 279 mmol) in one portion. The solution was slowly warmed to room temperature and was quenched with water (50 mL) after 18 hours. The aqueous and organic layers were separated and the aqueous layer was extracted with Et_2O (25 mL x 7). The combined organic extracts were washed with H_2O (15 mL x 5), 5% aqueous LiCl (50 mL) and brine before being dried over MgSO_4 , filtered, and concentrated under reduced pressure. The residue was purified by flash column chromatography (hexanes) to yield product **55** as a clear oil (6.08 g, 16.1 mmol) in 67% yield. The ^1H NMR data was consistent with reported data for the other enantiomer¹⁵⁶.

^1H NMR (600 MHz, CDCl_3) δ 3.71 (m, 1H), 3.68 (s, 3H), 3.54 (dd, $J = 10.0, 5.2$ Hz, 1H), 3.40 (dd, $J = 10.0, 6.8$ Hz, 1H), 2.40 (qdd, $J = 16.0, 9.4, 6.2$ Hz, 2H), 1.94 (m, 1H), 1.71 (m, 1H), 0.92 (s, 18H), 0.11 (s, 12H).



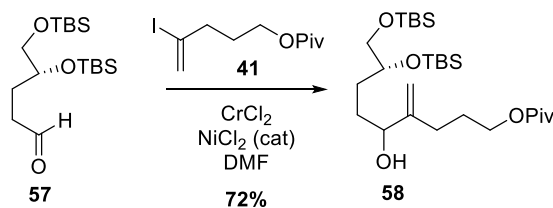
Alcohol 56: Ester **55** (6.08 g; 16.1 mmol) was dissolved in dichloromethane (40 mL) and cooled to -40 °C. DIBAL-H (1.0 M in hexanes; 19.4 mL; 19.4 mmol) was added dropwise and the reaction mixture stirred at -40 °C for 8 hours, where it was warmed to 0 °C and stirred for 1.5 hours. The reaction was diluted with ether and quenched by dropwise addition of water (1.2 mL). After five minutes, 15% aqueous NaOH (1.2 mL) was added dropwise, followed by additional water (1.8 mL). The reaction mixture became cloudy and was stirred at room temperature for 15 minutes before addition of MgSO_4 and stirring for an additional 30 minutes. The reaction mixture was filtered through a medium frit and concentrated under reduced pressure to afford crude primary alcohol **56**, which was purified by silica gel flash column chromatography (10% to 20% EtOAc in hexanes) to afford primary alcohol **56** as a clear oil (3.34g; 9.57 mmol) in 60% yield. Starting ester (2.12 g; 6.1 mmol) was recovered in 38% yield.

^1H NMR (600 MHz, CDCl_3) δ 3.75 (qd, $J = 6.2, 3.7$ Hz, 1H), 3.64 (qd, $J = 10.8, 5.9$ Hz, 2H), 3.56 (dd, $J = 10.0, 5.6$ Hz, 1H), 3.46 (dd, $J = 10.0, 6.7$ Hz, 1H), 1.73 – 1.48 (m, 5H), 0.92 (s, 9H), 0.90 (s, 9H), 0.11 (s, 6H), 0.08 (d, $J = 2.0$ Hz, 3H), 0.06 (d, $J = 2.9$ Hz, 3H).



Aldehyde 57: To a solution of primary alcohol **56** (3.33 g; 9.72 mmol) in acetonitrile (10 mL) were added the following reagents in order, each as a solution in acetonitrile (10 mL): [Cu(OTf)MeCN]₄ (185 mg; 0.49 mmol); 2,2'-bipyridine (77 mg; 0.49 mmol); TEMPO (79 mg; 0.49 mmol); N-methyl imidazole (80 μ L). The reaction was stirred open to air and turned from reddish-brown to teal and clear when complete, after 1.5 hours. The solvent was removed under reduced pressure and the residue filtered through a pad of silica gel (15% EtOAc in hexanes) to afford aldehyde **57** as an amber oil (2.45 g; 7.03 mmol) in 73% yield.

¹H NMR (400 MHz, CDCl₃) δ 9.79 (t, J = 1.70 Hz, 1H), 3.80 – 3.67 (m, 1H), 3.55 (dd, J = 10.0, 5.1 Hz, 1H), 3.39 (dd, J = 10.0, 7.2 Hz, 1H), 2.51 (dd, J = 8.4, 6.5 Hz, 2H), 1.96 (m, 1H), 1.76 (m, 1H), 0.89 (d, J = 4.8 Hz, 18H), 0.06 (d, J = 2.2 Hz, 12H).



Allylic alcohol 57: In a glovebox, CrCl₂ (3.48 g; 28.2 mmol) and NiCl₂ (76 mg; 0.57 mmol) were weighed into an oven-dried round bottom flask. Out of the glovebox, the flask was cooled to 0 °C and salts were dissolved in DMF (freshly distilled over CaSO₄, 88 mL)

ethyl acetate, washed with saturated aqueous NH_4Cl (20 mL), and extracted with ethyl acetate (3×25 mL). The combined organic layers were washed with brine (15 mL), dried over MgSO_4 , filtered, and concentrated in under reduced pressure. The residue was purified by flash column chromatography (15% to 25% EtOAc in hexanes) to yield the product as a light yellow clear oil (770 mg, 1.49 mmol) in 38% yield as the (*S*)- alcohol with a 93:7 dr determined by Mosher ester analysis (^{19}F -NMR and ^1H NMR). Starting ketone (1.18 g; 2.27 mmol) was recovered in 58% yield.

^1H NMR (600 MHz, CDCl_3) δ 5.08 (s, 1H), 4.87 (s, 1H), 4.09 (t, $J = 6.5$ Hz, 2H), 4.06 (dd, $J = 7.6, 4.7$ Hz, 1H), 3.73 (m, 1H), 3.55 (dd, $J = 10.0, 5.6$ Hz, 1H), 3.44 (dd, $J = 10.0, 6.9$ Hz, 1H), 2.22 – 2.14 (m, 1H), 2.12 – 2.02 (m, 1H), 1.88 – 1.79 (m, 2H), 1.78 – 1.62 (m, 3H), 1.61 – 1.52 (m, 1H), 1.52 – 1.45 (m, 1H), 1.21 (s, 9H), 0.89 (s, 18H), 0.06 (m, 9H).

The enantioselectivity was determined to be 93:7 er, by formation of the Mosher esters of compound **58a**. Specifically, an NMR tube containing the alcohol (ca. 10 mg) and pyridine- d_5 (2 - 3 drops) was dissolved in CDCl_3 (ca. 0.5 mL), and 2 – 3 drops of (*S*)- or (*R*)-methoxy(trifluoromethyl)- phenylacetyl chloride (MTPA-Cl) were added. The tube was gently shaken and then allowed to stand overnight, to afford a solution of the (*R*)- or (*S*)-MTPA ester, respectively. NMR data in CDCl_3 (600 MHz):

(*S*)-ester: ^1H NMR (600 MHz, CDCl_3) δ 5.38 (t, $J = 6.7$ Hz, 1H), 5.09 (s, 1H), 4.94 (q, $J = 1.4$ Hz, 1H), 3.98 (t, $J = 6.4$ Hz, 2H), 3.43 (m, 1H), 3.27 (dd, $J = 10.0, 6.7$ Hz, 1H), 2.05

(m, 2H), 1.81– 1.70 (m, 2H), 1.66 (m, 1H), 1.53 – 1.44 (m, 1H), 1.29 – 1.18 (m, 2H), 1.10 (s, 9H), 0.83 – 0.79 (m, 18H), -0.02 – -0.05 (m, 12H).

(R)-ester: ¹H NMR (600 MHz, CDCl₃) δ 5.34 (t, *J* = 6.7 Hz, 1H), 4.95 (s, 1H), 4.86 (t, *J* = 1.4 Hz, 1H), 3.92 (q, *J* = 6.3 Hz, 2H), 3.47 (dd, *J* = 9.9, 5.2 Hz, 1H), 3.30 (dd, *J* = 10.0, 6.9 Hz, 1H), 1.93 (ddd, *J* = 16.0, 9.5, 6.1 Hz, 2H), 1.82 (m, 1H), 1.74 – 1.55 (m, 4H), 1.36 – 1.24 (m, 2H), 1.12 (s, 9H), 0.81 (d, *J* = 2.3 Hz, 18H), 0.01 – -0.08 (m, 12H).

Table 4. MTPA-ester data for compound **58a**

MTPA-ester data JAH-5-234	δ <i>S</i> -ester (ppm)	δ <i>R</i> -ester (ppm)	ppm	Hz (600 MHz)
b	5.09	4.95	0.14	+84
g	2.05	1.93	0.12	+72
c	4.94	4.86	0.08	+48
d	3.98	3.91	0.07	+42
a	5.38	5.34	0.04	+24
f	3.27	3.3	-0.03	-18
e	3.42	3.47	-0.05	-30

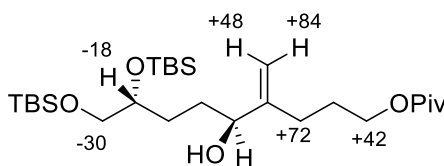
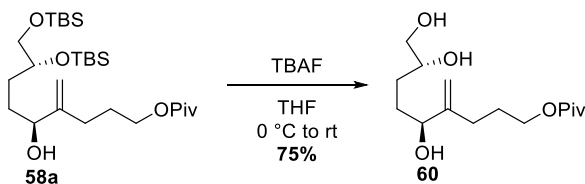


Figure 18. MTPA-ester data for **58a**



Triol 60: Silylated alcohol **58a** (770 mg; 1.49 mmol) was dissolved in THF (12 mL) and cooled to 0 °C before addition of TBAF in THF (1.0 M; 4.5 mL; 4.5 mmol). The resulting solution was gradually warmed to room temperature and stirred for 2 hours before removal of solvent under reduced pressure. The resulting oil was purified by silica gel flash column chromatography (ethyl acetate) to afford product **60** as a yellow oil (309 mg; 1.07 mmol) in 75% yield. D₂O was added to the NMR sample to sharpen signals.

$[\alpha]_D^{25}$: -9.3 (c = 1.21, CHCl₃)

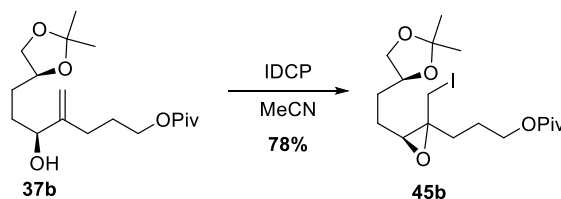
IR (neat): 3357, 2957, 2934, 2872, 1725, 1710, 1285, 1157, 1035, 901 cm⁻¹.

HRMS (ESI): *m/z* calcd. for C₁₅H₂₈O₅Na [M+Na⁺]: 311.18290 found 311.18318.

¹H NMR (600 MHz, CDCl₃) δ 5.10 (s, 1H), 4.90 (s, 1H), 4.15 (dd, *J* = 7.6, 4.2 Hz, 1H), 4.10 (t, *J* = 6.5 Hz, 2H), 3.80 – 3.71 (m, 1H), 3.63 (dd, *J* = 11.1, 3.2 Hz, 1H), 3.47 (dd, *J* = 11.1, 7.6 Hz, 1H), 2.14 (m, 1H), 2.06 (m, 1H), 1.83 (m, 2H), 1.80 – 1.74 (m, 1H), 1.66 (m, 1H), 1.59 (m, 1H), 1.51 (m, 1H), 1.20 (s, 9H).

¹³C NMR (151 MHz, CDCl₃) δ 178.96, 150.54, 110.39, 74.97, 72.20, 66.87, 64.06, 38.98, 31.41, 29.19, 27.98, 27.41, 27.20.

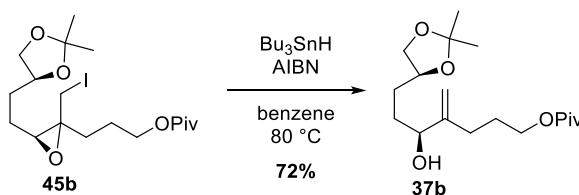
Cyclization of acetonide protected diol 37



Iodoepoxide 45b: A solution of **37a** (59 mg, 0.18 mmol) in acetonitrile (7 mL) was stirred at room temperature. The reaction mixture turned clear and golden yellow upon addition of IDCP (128 mg, 0.27 mmol). The reaction was stirred at room temperature for 3 hours, converging to a single less polar spot by TLC, before being quenched with addition of saturated aqueous sodium thiosulfate (5 mL). The resulting aqueous solution was extracted with ethyl acetate (4 x 7 mL). The combined organic layers were washed with brine (5 mL), dried over MgSO₄, filtered, and concentrated in under reduced pressure. The residue was purified by flash column chromatography (20% EtOAc in hexanes) to afford iodoepoxide **45b** as a light-yellow oil (66 mg, 0.14 mmol) in 87% yield. Proton NMR and COSY spectroscopy were conducted in chloroform, acetone, benzene, and methanol, with little improvement in separation of signals.

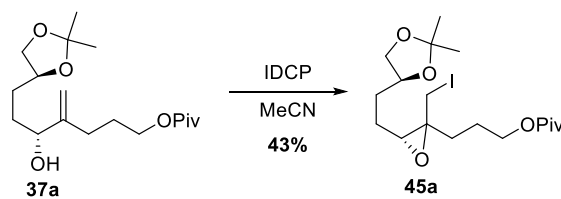
HRMS (ESI): *m/z* calcd. for C₁₈H₃₁O₅Na (M+Na⁺): 477.11084 found 477.11103.

¹H NMR (600 MHz, CDCl₃) 4.21 – 4.15 (m, 1H), 4.15 – 4.03 (m, 3H), 3.59 – 3.51 (m, 1H), 3.37 (dd, *J* = 10.5, 2.0 Hz, 1H), 3.12 – 3.04 (m, 1H), 2.93 (dd, *J* = 6.8, 5.3 Hz, 1H), 2.00 (m, 1H), 1.96 – 1.87 (m, 2H), 1.82 – 1.69 (m, 2H), 1.69 – 1.65 (m, 2H), 1.63 – 1.53 (m, 2H). 1.41 (d, *J* = 5.7 Hz, 3H), 1.36 (d, *J* = 4.4 Hz, 3H), 1.21 (d, *J* = 3.9, 9H).



Allylic alcohol 37b: Alkyl iodide **45b** (49 mg, 0.10 mmol) was dissolved in benzene (2 mL). One crystal of AIBN was added followed by Bu₃SnH (55 μL, 0.21 mmol). The reaction mixture was heated to 90 °C for 2 hours and was cooled to room temperature before being diluted with saturated aqueous KF (2 mL). The aqueous layer was extracted with Et₂O (3 x 5mL). The combined organic layers were washed with saturated aqueous KF (3 x 2mL), dried over MgSO₄, filtered, and concentrated under reduced pressure. The resulting crude oil was purified via silica gel flash column chromatography (20% to 30% ethyl acetate in hexanes) to afford the de-iodinated product **37b** (27 mg, 0.08 mmol) in 72% yield. Proton NMR and COSY spectroscopy matched that of the cyclization substrate.

¹H NMR (600 MHz, CDCl₃) δ 5.09 (s, 1H), 4.89 (s, 1H), 4.16 – 4.02 (m, 5H), 3.56 – 3.51 (m, 1H), 2.17 (m, 1H), 2.13 – 2.03 (m, 1H), 1.89 – 1.79 (m, 1H), 1.73 – 1.55 (m, 5H), 1.42 (s, 3H), 1.38 (s, 3H), 1.20 (s, 9H).



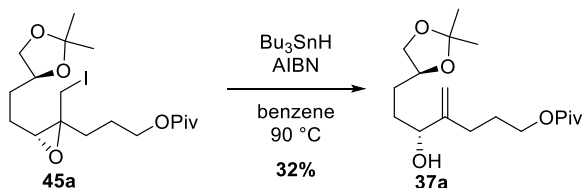
Iodoepoxide 45a: A solution of **37a** (60 mg, 0.18 mmol) in acetonitrile (8.5 mL) was stirred at room temperature. The reaction mixture turned clear and golden yellow upon addition of IDCP (174 mg, 0.37 mmol). The reaction was stirred at room temperature for 1.5 hours, converging to a single less polar spot by TLC, before being quenched with addition of saturated aqueous sodium thiosulfate (5 mL). The resulting aqueous solution was extracted with ethyl acetate (4 x 7 mL). The combined organic layers were washed

with brine (5 mL), dried over MgSO₄, filtered, and concentrated in under reduced pressure. The residue was purified by flash column chromatography (20% EtOAc in hexanes) to afford product **45a** as a light-yellow oil (37 mg, 0.08 mmol) in 43% yield. The proposed product is tentative.

HRMS (ESI): *m/z* calcd. for C₁₈H₃₁O₅Na (M+Na⁺): 477.11084 found 477.11099.

¹H NMR (600 MHz, CDCl₃) δ 4.20 – 4.15 (m, 1H), 4.15 – 4.02 (m, 3H), 3.54 (m, 1H), 3.36 (d, *J* = 10.5 Hz, 1H), 3.10 (d, *J* = 10.3 Hz, 1H), 2.92 (dd, *J* = 6.3, 5.0 Hz, 1H), 2.04 – 1.96 (m, 1H), 1.88 (m, 1H), 1.82 – 1.63 (m, 2H), 1.63 – 1.47 (m, 4H), 1.41 (d, *J* = 5.9 Hz, 3H), 1.35 (d, *J* = 4.6 Hz, 3H), 1.21 (d, *J* = 3.8 Hz, 9H).

¹³C NMR (101 MHz, CDCl₃) δ 178.644, 101.199, 75.793, 75.738, 75.167, 69.563, 69.508, 69.432, 66.812, 66.606, 65.526, 63.842, 62.370, 38.969, 31.075, 30.903, 30.862, 30.415, 27.437, 27.190, 25.849, 25.794, 25.705, 25.636, 25.058, 24.996, 24.639, 23.972, 11.40, 11.058.



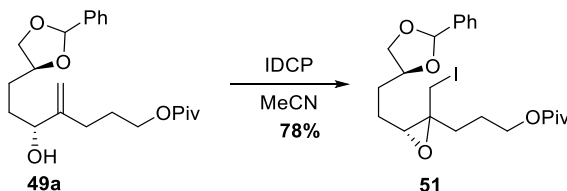
Allylic alcohol **37a**:

Alkyl iodide **45a** (37 mg, 0.80 mmol) was dissolved in benzene (2 mL). One crystal of AIBN was added followed by Bu₃SnH (43 μL, 0.16 mmol). The reaction mixture was heated to 90 °C for 5 hours and was cooled to room temperature before being diluted with

saturated aqueous KF (2 mL). The aqueous layer was extracted with Et₂O (3 x 5mL). The combined organic layers were washed with saturated aqueous KF (3 x 2mL), dried over MgSO₄, filtered, and concentrated under reduced pressure. The resulting crude oil was purified via silica gel flash column chromatography (20% to 30% ethyl acetate in hexanes) to afford the de-iodinated product **37a** (8 mg, 0.024 mmol) in 32% yield.

¹H NMR (600 MHz, CDCl₃) δ 5.10 (s, 1H), 4.90 (s, 1H), 4.20 – 4.01 (m, 5H), 3.60 – 3.46 (m, 1H), 2.23 – 2.14 (m, 1H), 2.07 (m, 1H), 2.02 (m, 1H), 1.88 – 1.81 (m, 2H), 1.80 – 1.73 (m, 3H), 1.73 – 1.58 (m, 2H), 1.42 (s, 3H), 1.37 (s, 3H), 1.21 (s, 9H).

Cyclization of benzylidene protected diol **49**

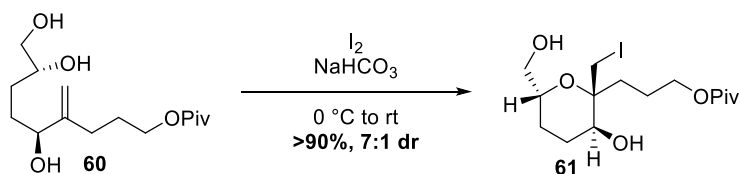


Iodoepoxide **51:** To a solution of benzylidene acetal **49a** (27.7 mg; 0.07 mmol) in acetonitrile (2.7 mL) was added IDCP (52 mg; 0.11 mmol). The solution immediately turned brown and remained clear. After stirring at room temperature for 3 hours, the reaction was quenched by addition of aqueous sodium thiosulfate (2 mL). The layers were separated and the aqueous layer was extracted with EtOAc (3 mL x 3). The combined organic layers were washed with brine (1.5 mL), dried over Na₂SO₄, decanted, and concentrated under reduced pressure to afford product **51** as a yellow oil (28 mg; 0.05

mmol) in 78% yield. The diastereomers were not able to be clearly resolved by proton NMR. The structure was tentatively assigned by proton NMR.

¹H NMR (600 MHz, CDCl₃) δ 7.52 – 7.45 (m, 2H), 7.39 (m, 3H), 5.95 (d, *J* = 4.2 Hz, 0.3H), 5.82 (d, *J* = 4.6 Hz, 0.7H), 4.36 – 4.21 (m, 1H), 4.24 – 4.02 (m, 2H), 3.79 – 3.71 (m, 1H), 3.71 – 3.63 (m, 1H), 3.28 (dd, *J* = 11.9, 10.3 Hz, 1H), 3.10 (dd, *J* = 10.4, 8.3 Hz, 1H), 2.97 (m, 1H), 2.03 – 1.82 (m, 3H), 1.82 – 1.61 (m, 5H), 1.20 (d, *J* = 1.1 Hz, 9H).

Cyclization of vicinal diol **60**



Tetrahydropyran **61:** To a solution of triol **60** (47 mg; 0.16 mmol) in THF (2 mL) at 0 °C were added I₂ (127 mg; 0.50 mmol) and NaHCO₃ (48 mg; 0.57 mmol). The solution immediately turned dark brown. After stirring at 0 °C for 1 hour, the reaction was warmed to room temperature, where it was stirred for 9 hours before being quenched by addition of aqueous sodium thiosulfate (2 mL). The layers were separated and the aqueous layer was extracted with EtOAc (3 mL x 3). The combined organic layers were washed with brine (1.5 mL), dried over Na₂SO₄, decanted, and concentrated under reduced pressure to afford cyclized iodo-compound in 96% yield (67 mg) as the only product. The compound was derivatized as the bis-acetate ester **62** to confirm the structural assignment.

[α]_D²⁵: -21.1 (c = 1.02, CHCl₃)

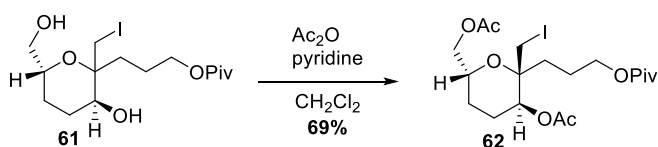
IR (neat): 3428, 2927, 2956, 2871, 1706, 1460, 1287, 1120, 1053 cm^{-1} .

HRMS (ESI): m/z calcd. for $\text{C}_{15}\text{H}_{27}\text{IO}_5\text{Na}$ [$\text{M}+\text{Na}^+$]: 437.07954 found 437.07947.

^1H NMR (600 MHz, CDCl_3) δ 4.17 – 4.05 (m, 2H), 3.90 (dd, $J = 11.4, 4.9$ Hz, 0.14H), 3.85 (dd, $J = 11.5, 5.0$ Hz, 0.86H), 3.77 (d, $J = 11.6$ Hz, 1H), 3.61 (d, $J = 10.0$ Hz, 1H), 3.51 (m, 2H), 3.41 (d, $J = 11.6$ Hz, 1H), 2.36 (broad, -OH), 1.96 – 1.80 (m, 2H), 1.79 – 1.59 (m, 4H), 1.49 – 1.36 (m, 1H), 1.31 – 1.24 (m, 1H), 1.21 (s, 9H).

^1H NMR (600 MHz, C_6D_6) δ 4.09 – 3.97 (m, 2H), 3.44 (dd, $J = 11.3, 3.3$ Hz, 1H), 3.40 (d, $J = 11.5$ Hz, 1H), 3.35 (dd, $J = 11.3, 6.1$ Hz, 1H), 3.28 (ddd, $J = 9.1, 6.9, 4.5$ Hz, 1H), 3.21 (d, $J = 11.5$ Hz, 1H), 3.07 – 3.00 (m, 1H), 1.84 (ddd, $J = 13.4, 10.4, 5.3$ Hz, 1H), 1.73 (ddtd, $J = 12.4, 10.3, 6.7, 6.3, 5.0$ Hz, 1H), 1.62 – 1.56 (m, 1H), 1.55 – 1.49 (m, 1H), 1.27 – 1.23 (m, 1H), 1.20 (s, 9H).

^{13}C NMR (151 MHz, C_6D_6) δ 178.54, 75.57, 71.10, 68.49, 66.11, 64.95, 39.23, 34.18, 28.52, 27.76, 26.67, 22.92, 13.67.

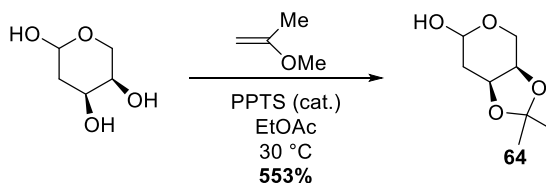


Bis-acetate ester 62: Tetrahydropyran diol **61** (67 mg; 0.16 mmol) was dissolved in dichloromethane (4 mL) and acetic anhydride (0.2 mL) and pyridine (0.2 mL) were added and stirred overnight. The crude was concentrated under reduced pressure and purified by silica gel flash column chromatography to afford the di-acetate ester as a bright yellow oil

(55 mg; 0.11 mmol) in 69% yield as an 88:12 mixture of diastereomers. COSY spectroscopy supports the structural assignment. NOESY spectroscopy showed a correlation between one of the CH₂-I proton (f) and the carbinol proton (g). The stereochemistry of the carbinol proton was confirmed through Mosher ester derivatization and analysis of compound **58a**. ¹H NMR and 2D spectra are in Section 3.6.

¹H NMR (600 MHz, CDCl₃) δ 5.00 (dd, *J* = 11.6, 5.1 Hz, 0.88H), 4.97 (d, *J* = 5.0 Hz, 0.12H), 4.12 (dd, *J* = 11.5, 3.7 Hz, 1H), 4.07 (dd, *J* = 11.7, 5.5 Hz, 1H), 4.04 – 3.97 (m, 2H), 3.78 (d, *J* = 11.7 Hz, 0.88H), 3.65 (dddd, *J* = 12.2, 6.2, 3.7, 2.3 Hz, 0.88H), 3.40 (d, *J* = 10.8 Hz, 0.12H), 3.31 (d, *J* = 11.7 Hz, 0.88H), 3.21 (d, *J* = 10.9 Hz, 0.12H), 2.09 (s, 3H), 2.04 (s, 3H), 2.01 (m, 1H), 1.86 (m, 1H), 1.82 – 1.70 (m, 2H), 1.70 – 1.59 (m, 2H), 1.51 – 1.38 (m, 2H), 1.19 (s, 9H).

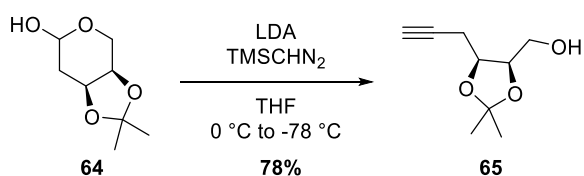
Oxepane forming cyclization of bis-acetate



Acetal 64: 2-Deoxy-D-ribose (25.0 g, 186 mmol) was dissolved in ethyl acetate (375 mL). 2-Methoxypropane (24.0 mL, 242 mmol) and PPTS (942 mg, 3.72 mmol) were added and the resulting suspension was stirred at 30 °C for 18 hours. By TLC, there was still starting material but extended reaction times, increased heating, and increased equivalencies of

reagent did not result in increased yield. Aqueous ammonium chloride (100 mL) was added to the pale yellow, clear reaction mixture and the resulting biphasic mixture was stirred for one hour. The layers were separated and the aqueous layer was extracted with ethyl acetate (25 mL x 3). The combined organic extracts were washed with brine and dried over sodium sulfate before being filtered and concentrated under reduced pressure to afford a crude yellow oil. The crude oil was purified by silica gel flash column chromatography (30% to 50% ethyl acetate in hexanes) to afford protected product **64** (17.9g, 102 mmol, 55%) as a clear, colorless oil in a 3:1 mixture of anomers by ^1H NMR. The spectra matched that of the published compound¹⁹³.

^1H NMR (500 MHz, CDCl_3) (major anomer) δ 5.26 (dd, $J = 7.1, 4.3$ Hz, 1H), 4.48 (dt, $J = 6.6, 4.2$ Hz, 1H), 4.22 – 4.09 (m, 1H), 3.98 – 3.92 (m, 1H), 3.74 – 3.67 (m, 1H), 3.06 (br s, OH), 2.24 (dt, $J = 14.8, 4.3$ Hz, 1H), 1.78 (ddd, $J = 14.8, 7.1, 4.2$ Hz, 1H), 1.50 (s, 3H), 1.35 (s, 3H).

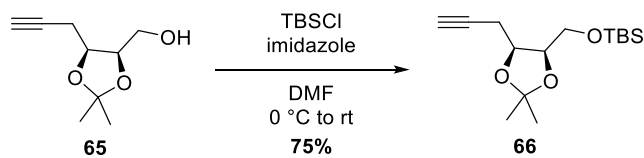


Alkyne 65: *n*-Butyllithium solution (61.2 mL, 2.45 M in hexanes, 150 mmol) was added dropwise to a stirred solution of diisopropylamine (20.0 mL; 150 mmol) in THF (36 mL) at $-78\text{ }^\circ\text{C}$. After stirring for 45 minutes, TMSCHN_2 solution (37.5 mL, 2.0M in ether, 75.0 mmol) was added dropwise. The reaction mixture was stirred at $-78\text{ }^\circ\text{C}$ for 30 minutes before slow addition of lactol **64** (8.71 g, 50.0 mmol) in THF (17 mL). The reaction

mixture was warmed to room temperature over a period of four hours and was stirred overnight before being quenched by addition of saturated aqueous ammonium chloride (40 mL). The aqueous phase was extracted with ethyl acetate (5 × 30 mL) and the combined organic phase was washed with water (2 x 30 mL), brine, and dried over Na₂SO₄, decanted, and concentrated under reduced pressure to afford an orange residue, which was dissolved in methanol (17 mL) and aqueous K₂CO₃ (10% w/w; 17 mL) and stirred for 30 minutes. The reaction mixture was then extracted with ethyl acetate (5 x 25 mL), washed with brine and dried over Na₂SO₄, and decanted before being concentrated under reduced pressure to afford the crude product as an orange syrup. The oil was purified by silica gel flash column chromatography (40% ethyl acetate in hexanes to 55% ethyl acetate in hexanes) to afford product **65** as a clear orange oil (6.62g, 38.9 mmol) in 78% yield. The spectra matched that of the published compound¹⁶³. This reaction was run with three batches in parallel around 50 mmol scale each, rather than scaling up, due to concerns of rapid nitrogen evolution as the reaction warmed to room temperature.

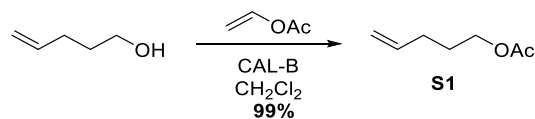
HRMS (NSI): *m/z* calcd. for C₁₅H₂₈O₃NaSi [M+Na]⁺: 307.16999 found 307.17002.

¹H NMR (600 MHz, CDCl₃) δ 4.38 (dt, *J* = 8.0, 6.1 Hz, 1H), 4.29 (td, *J* = 6.3, 4.4 Hz, 1H), 3.84 (dd, *J* = 11.7, 4.4 Hz, 1H), 3.77 (dd, *J* = 11.7, 6.4 Hz, 1H), 2.57 (ddd, *J* = 16.8, 6.1, 2.7 Hz, 1H), 2.51 (ddd, *J* = 16.7, 8.0, 2.7 Hz, 1H), 2.06 (t, *J* = 2.7 Hz, 1H), 1.94 (br s, -OH), 1.49 (s, 3H), 1.39 (s, 3H).



Silyl ether 66: To a solution alcohol **65** (6.62 g, 38.9 mmol) in DMF (40 mL) at 0° C were added TBSCl (7.02g, 46.6 mmol) and imidazole (3.32g, 48.6 mmol) in one portion. The solution was warmed to room temperature and stirred overnight at room temperature. Upon completion by TLC, the reaction mixture was diluted with water (300 mL) and Et₂O (50 mL). The aqueous and organic layers were separated and the aqueous layer was extracted with Et₂O (20 mL x 5). The combined organic extracts were washed with H₂O (10 mL x 2) and brine before being dried over MgSO₄, filtered, and concentrated under reduced pressure. The residue was purified by flash column chromatography (hexanes to 3% EtOAc in hexanes) to yield product **66** as a clear orange oil (7.20g, 29.0 mmol) in 75% yield. Although the ¹H NMR spectra of starting material matched the published compound¹⁶³, the silyl ether product was 0.14 ppm (+/- 0.2 ppm) higher in shift than the reported tabulated data. The image of the spectra did not have an apparent CDCl₃ signal. The discrepancies in shift between our spectra and the reported spectra are systematic. We believe the concentrated sample reported in the literature was referenced incorrectly, resulting in misreported tabulated data. The discrepancies in coupling constants can be explained by relatively low-resolution spectra in the literature spectra (300 MHz) compared to our spectra (600 MHz).

¹H NMR (600 MHz, CDCl₃) δ 4.35 (ddd, J = 7.9, 6.0, 5.2 Hz, 1H), 4.18 (ddd J = 7.0, 5.9, 5.1 Hz, 1H), 3.79 – 3.66 (m, 2H), 2.60 (ddd, J = 16.6, 5.3, 2.6 Hz, 1H), 2.50 (ddd, J = 16.9, 7.9, 2.7, 1H), 2.04 (t, J = 2.6 Hz, 1H), 1.47 (s, 3H), 1.37 (s, 3H), 0.90 (m, 9H), 0.08 (s, 6H).



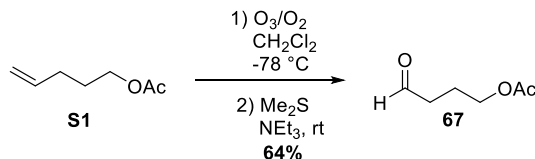
Acetate ester S1: 4-Penten-ol (10.54 g; 122.4 mmol) was dissolved in CH_2Cl_2 (300 mL). Vinyl acetate (16.9 mL; 183.6 mmol) and CAL-B (500 mg) were added. The reaction was stirred at room temperature for 3 hours before filtration over a pad of Celite (ether eluent) and concentration under reduced pressure to afford **S1** (15.46 g; 120.6 mmol) as a clear colorless liquid in 99% yield.

IR (thin film): 2922, 285, 1732, 1456, 1284 cm^{-1} .

HRMS (NSI): m/z calculated for $\text{C}_7\text{H}_{12}\text{O}_2\text{Na}$ $[\text{M}+\text{Na}]^+$: 151.07295 found 151.07294.

^1H NMR (500 MHz, CDCl_3) δ 5.82 (ddt, $J = 16.9, 10.2, 6.6$ Hz, 1H), 5.05 (dq, $J = 17.1, 1.7$ Hz, 1H), 5.00 (ddt, $J = 10.2, 1.9, 1.2$ Hz, 1H), 4.09 (t, $J = 6.7$ Hz, 2H), 2.18 – 2.10 (m, 2H), 2.06 (s, 3H), 1.81 – 1.68 (m, 2H).

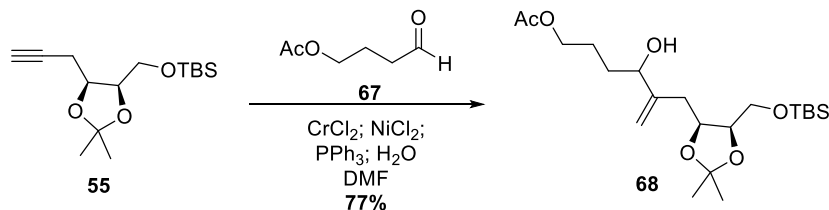
^{13}C NMR (126 MHz, CDCl_3) δ 170.97, 137.43, 115.22, 63.82, 30.05, 27.80, 20.89.



Aldehyde 67: Alkene 4 (8.19 g; 63.9 mmol) in CH_2Cl_2 (400 mL) was cooled to -78°C and sparged with O_2 for 10 minutes before being sparged with O_3 for 45 minutes, where the saturated solution took on a persistent pale blue color. The reaction was sparged with O_2 for an additional 10 minutes before the pale blue color faded and dimethyl sulfide (30 mL) was added. The reaction warmed to room temperature and after 1 hour, 20 mL NEt_3

was added. One hour later the reaction was complete by TLC and was diluted with water. The aqueous layer was separated and extracted with CH₂Cl₂ (25 mL x 3). The combined organic layer was washed with water (50 mL), washed with brine, and dried over MgSO₄ before filtration and concentration under reduced pressure to furnish aldehyde **67** (5.42 g; 41.7 mmol) as a yellow oil in 64% yield. ¹H NMR matched reported spectra from the literature from PCC oxidation ¹⁹⁴.

¹H NMR (400 MHz, CDCl₃) δ 9.80 (t, J = 1.0 Hz, 1H), 4.10 (t, J = 6.3 Hz, 2H), 2.55 (dt, J = 7.2, 1.3 Hz, 2H), 2.05 (s, 3H), 1.99 (td, J = 7.1, 6.4 Hz, 2H).



Allylic alcohol 68: CrCl₂ (3.30 g; 26.8 mmol) and NiCl₂ (71 mg; 0.54 mmol) were weighed out in a glovebox. The flask was removed from the glovebox and sparged with argon for 10 minutes before rapid addition of triphenylphosphine (707 mg; 2.68 mmol). After 10 additional minutes under argon, dry, degassed DMF (33 mL) was added. Aldehyde **67** (924 mg; 5.36 mmol) in DMF (21 mL) was added and reaction mixture was stirred for 15 minutes. Alkyne **55** (3.82 g; 13.4 mmol) and water (0.19 mL) in DMF (33 mL) were added via syringe pump over 4 hours and the resulting suspension was stirred at room temperature for 4 hours. The reaction mixture was diluted with saturated aqueous ammonium chloride (400 mL) and ethyl acetate (100 mL) and stirred for one hour. The layers were separated and the aqueous layer was extracted with ethyl acetate (50 mL x 6). The combined organic

phase was washed with water (50 mL x 2) and brine before being dried over Na₂SO₄, filtered, and concentrated under reduced pressure. The crude residue was purified by silica gel flash column chromatography (18% ethyl acetate in hexanes to 25% ethyl acetate in hexanes) to afford compound **68** (1.71 g, 4.10 mmol) as a clear pale yellow oil in 77% yield as a 60:40 *dr* (S:R).

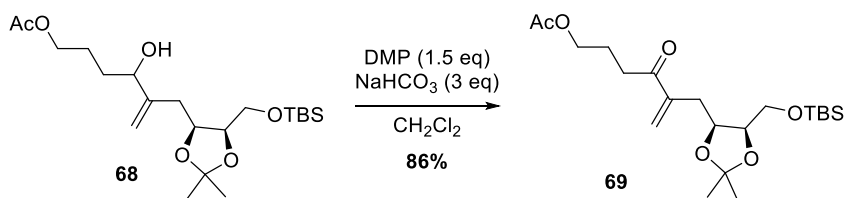
[α]_D²⁵: -25.6 (c=1.01, CHCl₃)

HRMS (NSI): *m/z* calcd. for C₂₁H₄₀O₆ClSi [M+Cl]⁻: 451.22882 found 451.22897.

IR (neat): 3464, 2930, 2857, 1739, 1471, 1367, 1246, 1163, 1096, 1071, 835, 777, 666 cm⁻¹.

¹H NMR (600 MHz, CDCl₃) δ 5.13 (s, 0.4H), 5.11 (d, *J* = 1.3 Hz, 0.6H), 5.02 (t, *J* = 1.3 Hz, 0.4H), 5.00 (t, *J* = 1.2 Hz, 0.6H), 4.40 (ddd, *J* = 9.6, 5.9, 3.5 Hz, 0.4H), 4.30 (ddd, *J* = 9.7, 6.1, 3.7 Hz, 0.6H), 4.21 – 4.15 (m, 1H), 4.15 – 4.05 (m, 3H), 3.71 (ddd, *J* = 10.5, 7.9, 1.7 Hz, 1H), 3.65 (ddd, *J* = 15.0, 10.5, 4.6 Hz, 1H), 3.19 (d, *J* = 4.4 Hz, 1H), 2.58 – 2.49 (m, 1H), 2.45 – 2.37 (m, 1H), 2.05 (s, 3H), 1.85 – 1.71 (m, 1H), 1.71 – 1.62 (m, 2H), 1.62 – 1.53 (m, 1H), 1.45 (s, 2H), 1.44 (s, 1H), 1.35 (s, 1H), 1.34 (s, 2H), 0.90 (s, 9H), 0.08 (s, 6H).

¹³C NMR (126 MHz, CDCl₃) δ 171.4, 148.8, 148.7, 114.3, 112.6, 108.4, 108.2, 78.3, 77.9, 77.9, 77.2, 75.2, 75.2, 75.0, 75.0, 64.6, 64.6, 62.1, 61.9, 32.5, 32.2, 31.6, 30.9, 28.3, 28.0, 26.0, 25.6, 25.5, 25.3, 25.2, 21.19, 18.42, 18.37, -5.3.



Enone 69: Allylic alcohol **68** (2.86 g; 6.86 mmol) was dissolved in CH₂Cl₂ (135 mL) before addition of NaHCO₃ (1.78 g; 21.0 mmol) and DMP (4.37 g; 10.3 mmol). The reaction mixture was stirred at room temperature for 3 hours. Aqueous Na₂S₂O₃ (80 mL) and aqueous NaHCO₃ (80 mL) were added and the biphasic mixture was stirred for one hour, at which point the layers became clear upon standing. The aqueous phase was separated and extracted with CH₂Cl₂ (3 x 30 mL) and the combined organic layers were dried over MgSO₄, filtered, and concentrated to afford enone **69** (2.44 g; 5.87 mmol) as a light yellow clear oil in 86% yield.

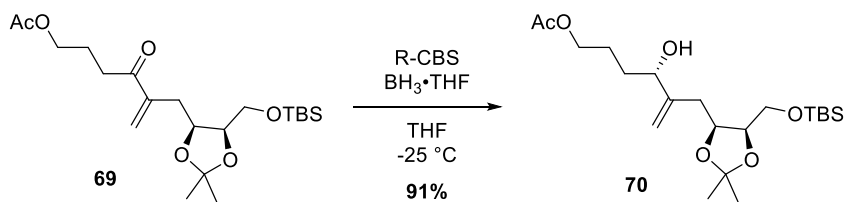
$[\alpha]_D^{25}$: -25.1 (c=1.00, CHCl₃)

HRMS (NSI): m/z calcd. for C₂₁H₃₈O₆NaSi [M+Na]⁺: 437.23299 found 437.23267.

IR (neat): 2984, 2930, 2857, 1740, 1679, 1471, 11380, 1245, 1165, 1045, 836, 777, 667 cm⁻¹.

¹H NMR (400 MHz, CDCl₃) δ 6.13 (s, 1H), 5.93 (d, $J = 1.3$ Hz, 1H), 4.29 (ddd, $J = 10.6, 6.0, 2.6$ Hz, 1H), 4.16 (dt, $J = 7.1, 5.6$ Hz, 1H), 4.10 (t, $J = 6.4$ Hz, 2H), 3.73 (dd, $J = 10.5, 7.1$ Hz, 1H), 3.68 (dd, $J = 10.5, 5.2$ Hz, 1H), 2.82 (td, $J = 7.1, 1.0$ Hz, 2H), 2.74 (ddd, $J = 14.7, 2.6, 1.2$ Hz, 1H), 2.37 (dd, $J = 14.8, 10.7$ Hz, 1H), 2.05 (s, 3H), 1.97 (p, $J = 7.0$ Hz, 2H), 1.43 (s, 3H), 1.32 (s, 3H), 0.91 (s, 9H), 0.09 (s, 6H).

¹³C NMR (126 MHz, CDCl₃) δ 200.2, 170.9, 145.2, 125.9, 107.9, 77.6, 75.4, 63.6, 61.7, 33.8, 30.9, 28.0, 25.8, 25.4, 23.1, 20.8, -5.6.



(S)-Alcohol 70: (*R*)-2-Methyl-CBS-oxazaborolidine in toluene (1.0 M, 2.90 mL, 2.90 mmol) and $\text{BH}_3 \cdot \text{THF}$ (1.0 M, 4.34 mL; 4.34 mmol) were added to THF (14 mL) at room temperature and stirred for 50 minutes before being cooled to $-40\text{ }^\circ\text{C}$, where a solution of enone **69** (1.12 g, 2.89 mmol) in THF (57 mL) was slowly added. The resulting reaction mixture was stirred at $-25\text{ }^\circ\text{C}$ for 2 hours. The reaction was quenched with MeOH (5 mL), warmed to room temperature, and concentrated under reduced pressure. The resulting oil was dissolved in ethyl acetate, washed with saturated aqueous NH_4Cl (20 mL), and extracted with ethyl acetate ($3 \times 25\text{ mL}$). The combined organic layers were washed with brine (15 mL), dried over MgSO_4 , filtered, and concentrated in under reduced pressure. The residue was purified by flash column chromatography (15% to 25% ethyl acetate in hexanes) to furnish compound **70** as a light yellow clear oil (1.10 g, 2.64 mmol) in 91 % yield as the (*S*)-alcohol (93:7 *dr* as determined by Mosher ester analysis).

$[\alpha]_{\text{D}}^{25}$: -32.8 ($c=1.10$, CHCl_3)

HRMS (NSI): m/z calcd. for $\text{C}_{21}\text{H}_{40}\text{O}_6\text{SiNa}$ $[\text{M}+\text{Na}]^+$: 439.24864 found 439.24833.

FT-IR (neat, cm^{-1}): 3485, 2953, 2930, 2857, 1738, 1649, 1471, 1367, 1245, 1094, 1045, 834, 776, 736, 703, 667, 607 cm^{-1} .

$^1\text{H NMR}$ (600 MHz, CDCl_3) δ 5.11 (s, 1H), 5.01 (t, $J = 1.2\text{ Hz}$, 1H), 4.31 (ddd, $J = 9.7$, 6.1, 3.7 Hz, 1H), 4.18 (ddd, $J = 7.8$, 6.1, 4.7 Hz, 1H), 4.16 – 4.12 (m, 1H), 4.10 (tt, $J = 6.4$, 3.3 Hz, 2H), 3.71 (dd, $J = 10.4$, 7.8 Hz, 1H), 3.67 (dd, $J = 10.4$, 4.7 Hz, 1H), 3.19 (d, $J =$

4.5 Hz, -OH), 2.45 – 2.36 (m, 2H), 2.06 (s, 3H), 1.80 – 1.71 (m, 1H), 1.71 – 1.55 (m, 3H), 1.46 (s, 3H), 1.35 (s, 3H), 0.90 (s, 9H), 0.05 (m, 6H).

¹³C NMR (126 MHz, CDCl₃) δ 171.3, 148.7, 114.2, 108.4, 78.3, 77.9, 75.2, 64.6, 61.9, 32.5, 30.9, 28.0, 26.0, 25.4, 25.2, 21.2, 18.4, -5.3, -5.3.

The enantioselectivity was determined to be 93:7 er, by formation of the Mosher esters of compound 70. Specifically, an NMR tube containing the alcohol (ca.10 mg) and pyridine-*d*₅ (2 - 3 drops) was dissolved in CDCl₃ (ca. 0.5 mL), and 2 – 3 drops of (S)- or (R)-methoxy(trifluoromethyl)- phenylacetyl chloride (MTPA-Cl) were added. The tube was gently shaken and then allowed to stand overnight, to afford a solution of the (R)- or (S)-MTPA ester, respectively. NMR data in CDCl₃ (600 MHz):

(S)-ester

¹H NMR (600 MHz, Chloroform-*d*) δ 5.41 (m, 1H), 5.16 (s, 1H), 5.12 (s, 1H), 4.31 (ddd, *J* = 10.0, 5.9, 2.9 Hz, 1H), 4.04 (dt, *J* = 7.6, 5.3 Hz, 1H), 4.00 – 3.87 (m, 2H), 3.56 (qd, *J* = 10.4, 6.3 Hz, 2H), 2.40 (dd, *J* = 16.3, 2.7 Hz, 1H), 2.27 (dd, *J* = 16.1, 10.0 Hz, 1H), 1.96 (s, 3H), 1.70 (dtd, *J* = 8.7, 6.1, 2.7 Hz, 2H), 1.47 (qdd, *J* = 13.8, 8.4, 6.7 Hz, 3H), 1.35 (s, 4H), 1.26 (s, 4H), 0.85 – 0.72 (m, 11H), -0.02 (d, *J* = 7.4 Hz, 6H).

(R)-ester

¹H NMR (600 MHz, Chloroform-*d*) δ 5.33 (t, *J* = 6.5 Hz, 1H), 5.03 (s, 1H), 4.99 (s, 1H), 4.26 (ddd, *J* = 10.0, 6.0, 2.9 Hz, 1H), 3.99 (dq, *J* = 17.2, 6.2 Hz, 3H), 3.52 – 3.46 (m, 5H),

2.38 – 2.25 (m, 1H), 2.16 (dd, $J = 16.0, 10.0$ Hz, 1H), 1.95 (s, 3H), 1.83 – 1.69 (m, 2H),
 1.69 – 1.54 (m, 2H), 1.33 (s, 3H), 1.25 (s, 3H), 0.80 (s, 11H), 0.12 – -0.11 (m, 6H).

Table 5. MTPA-ester data for compound **70**

MTPA-ester	δ S-ester (ppm)	δ R-ester (ppm)	ppm	Hz (600 MHz)
data JAH-9-8				
b	5.16	5.03	0.13	78
c	5.12	4.99	0.13	78
j	2.27	2.16	0.11	66
g	3.68	3.59	0.09	54
a	5.41	5.33	0.08	48
h	3.55	3.47	0.08	48
i	2.4	2.32	0.08	48
d	4.31	4.26	0.05	30
e	4.05	4.01	0.04	24
m	1.35	1.33	0.02	12
n	1.26	1.25	0.01	6
o	0.81	0.8	0.01	6
p	-0.02	-0.03	0.01	6
f	3.93	3.98	-0.05	-30
k	1.7	1.75	-0.05	-30
l	1.47	1.6	-0.13	-78

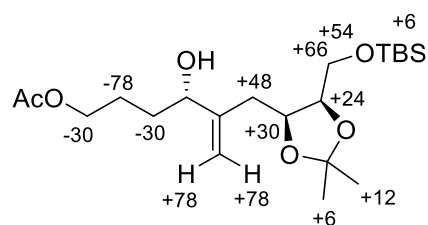
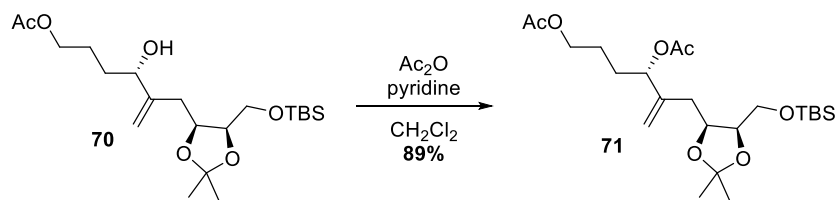


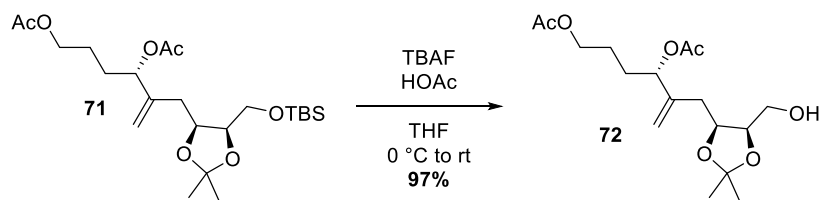
Figure 19. MTPA-ester data for compound **70**



Bis-acetate ester 71: Alcohol **70** (948 mg; 2.27 mmol) was dissolved in dichloromethane (25 mL) and acetic anhydride (0.9 mL) and pyridine (0.9 mL) were added and the reaction mixture was stirred overnight. The crude was concentrated under reduced pressure and purified by silica gel flash column chromatography (20% ethyl acetate in hexanes) to afford bis-acetate ester **71** as pale yellow, clear oil (929 mg; 2.09 mmol) in 89% yield.

HRMS (NSI): m/z calcd. for $C_2H_{42}O_7NaSi$ $[M+Na]^+$: 481.25920 found 481.25832.

1H NMR (600 MHz, $CDCl_3$): δ 5.21 (t, $J = 6.4$ Hz, 1H), 5.16 (s, 1H), 5.11 (q, $J = 1.4$ Hz, 1H), 4.39 (ddd, $J = 9.4, 5.9, 3.1$ Hz, 1H), 4.13 (ddd, $J = 7.8, 6.3, 4.8$ Hz, 1H), 4.07 (td, $J = 6.5, 1.7$ Hz, 2H), 3.68 (dd, $J = 10.4, 7.7$ Hz, 1H), 3.63 (dd, $J = 10.4, 4.7$ Hz, 1H), 2.44 (dd, $J = 16.3, 3.1$ Hz, 1H), 2.32 (dd, $J = 16.0, 9.8$ Hz, 1H), 2.07 (s, 3H), 2.05 (s, 3H), 1.80 – 1.70 (m, 2H), 1.69 (s, 3H), 1.44 (s, 3H), 1.35 (s, 3H), 0.90 (s, 9H), 0.08 (s, 6H).

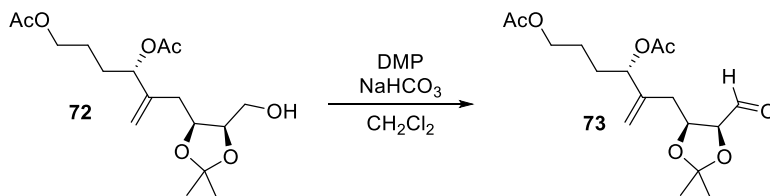


Alcohol 72: Silylated alcohol **71** (929 mg; 2.02 mmol) was dissolved in THF (20 mL) and cooled to 0 °C before addition of acetic acid (90 μ L; 1.5 mmol) TBAF in THF (1.0 M; 3.0 mL; 3.0 mmol). The resulting solution was gradually warmed to room temperature and

stirred for 2 hours before removal of solvent under reduced pressure. The resulting oil was purified by silica gel flash column chromatography (60% ethyl acetate in hexanes) to afford the product as a pale-yellow oil (675 mg; 1.96 mmol) in 97% yield.

HRMS (NSI): m/z calcd. for $C_{17}H_{28}O_7Na$ $[M+Na]^+$: 367.17272 found 367.17210.

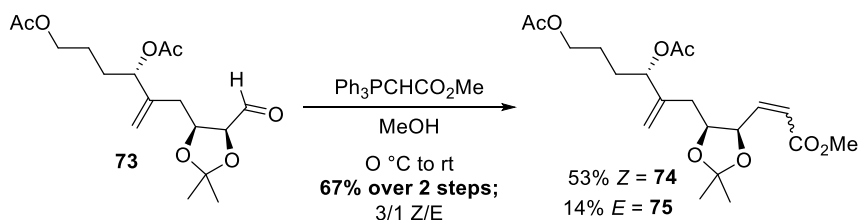
1H NMR (600 MHz, $CDCl_3$): δ 5.17 (t, $J = 6.4$ Hz, 1H), 5.16 (d, $J = 1.0$ Hz, 1H), 5.05 (t, $J = 1.5$ Hz, 1H), 4.46 (ddd, $J = 8.0, 6.2, 5.3$ Hz, 1H), 4.22 (td, $J = 6.3, 4.6$ Hz, 1H), 4.08 (td, $J = 6.4, 4.4$ Hz, 2H), 3.64 (m, 2H), 2.41 (ddt, $J = 16.2, 8.1, 1.3$ Hz, 1H), 2.28 (dd, $J = 16.0, 5.4$ Hz, 1H), 2.07 (s, 3H), 2.06 (s, 3H), 1.90 (s, 1H), 1.77 – 1.67 (m, 3H), 1.67 – 1.60 (m, 1H), 1.49 (s, 3H), 1.39 (s, 3H).



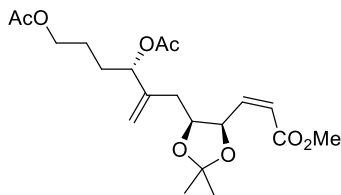
Aldehyde 73: To a stirred solution of primary alcohol **72** (675 mg; 1.96 mmol) in CH_2Cl_2 (40 mL) was added DMP (1.27 g; 3.03 mmol) and $NaHCO_3$ (503 mg; 6.05 mmol). After 2 hours, the reaction was poured into a rapidly stirred solution of $Na_2S_2O_3$ (25 g) in 100 mL saturated aqueous $NaHCO_3$. The suspension was stirred for 30 minutes until the layers turned clear. The layers were separated and the organic layer was washed with saturated aqueous $NaHCO_3$ (25 mL), water (15 mL x 2), dried over $MgSO_4$, filtered, and concentrated under reduced pressure. The resulting crude aldehyde **73** was used immediately without further purification.

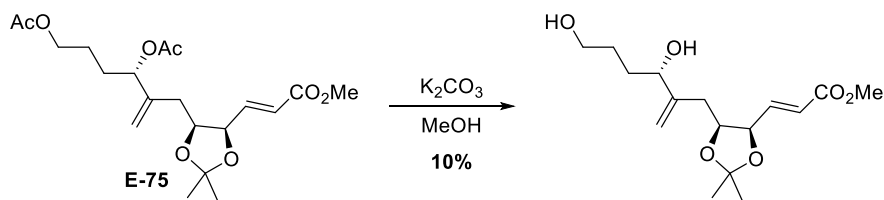
HRMS (NSI): m/z calcd. for $C_{17}H_{26}O_7Na$ $[M+Na]^+$: 365.157017 found 365.15667.

¹H NMR (400 MHz, CDCl₃): δ 9.68 (d, *J* = 3.3, Hz, 1H), 5.18 (s, 1H), 5.16 (m, 1H), 5.09 (s, 1H), 4.62 – 4.55 (m, 1H), 4.34 (dd, *J* = 7.0, 3.2 Hz, 1H), 4.08 (dt, *J* = 5.8, 2.8 Hz, 2H), 2.38 – 2.20 (m, 2H), 2.07 (s, 3H), 2.06 (s, 3H), 1.81 – 1.63 (m, 4H), 1.61 (s, 3H), 1.44 (s, 3H).



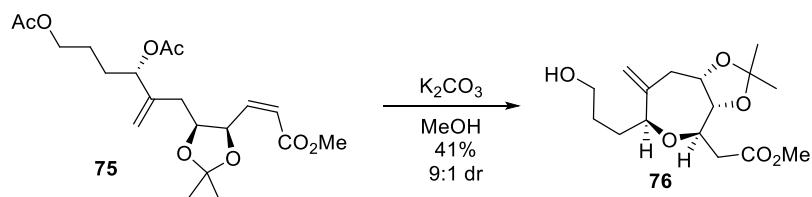
Esters **74 and **75**:** Crude aldehyde **73** (688 mg) was dissolved in MeOH (6.5 mL) and cooled to 0 °C before addition of Wittig reagent (803 mg; 2.4 mmol). The resulting mixture was stirred at 0 °C for two hours whereupon the solvent was removed under reduced pressure and the resulting viscous yellow oil was purified by silica gel flash column chromatography (15% ethyl acetate in hexanes). The alkene isomers were separated cleanly to afford **74**, Z- α , β unsaturated ester (398 mg; 1.07 mmol) in 53% yield over 2 steps and **75**, E- α , β unsaturated ester (107 mg; 0.29 mmol) in 14% yield over 2 steps (3/1 *E/Z*).





Bis-acetate (108 mg; 0.29 mmol) was dissolved in MeOH (3 mL) before addition of K_2CO_3 (8 mg; 0.06 mmol). The reaction mixture was stirred at room temperature for 6 hours. The MeOH was removed by rotary evaporation before immediate purification by silica gel flash column chromatography (40% ethyl acetate in hexanes to 60% ethyl acetate in hexanes) to afford the product as a light-yellow film (11 mg; 0.035 mmol) in 10% yield. The remaining mass was a thick yellow oil which was insoluble in organic solvent.

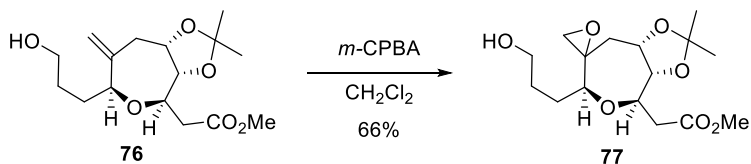
1H NMR (600 MHz, C_6D_6) δ 6.99 (dd, $J = 15.5, 5.3$ Hz, 1H), 6.27 (dd, $J = 15.6, 1.6$ Hz, 1H), 5.31 (dd, $J = 7.6, 5.8$ Hz, 1H), 5.16 (s, 1H), 4.83 (s, 1H), 4.38 (ddd, $J = 6.8, 5.3, 1.6$ Hz, 1H), 4.33 (dt, $J = 7.4, 6.0$ Hz, 1H), 3.39 (td, $J = 10.8, 4.4$ Hz, 2H), 3.36 (s, 3H), 2.41 (dd, $J = 7.5, 1.5$ Hz, 1H), 2.38 (dd, $J = 7.5, 1.3$ Hz, 1H), 2.15 (t, $J = 7.2$ Hz, 1H), 2.09 (dd, $J = 16.3, 5.9$ Hz, 1H), 1.71 (m, 1H), 1.65 (m, 1H), 1.64 – 1.58 (m, 2H), 1.43 (s, 3H), 1.24 (s, 3H).



Oxepane 76: Bis-acetate **75** (398 mg; 1.07 mmol) was dissolved in MeOH (11) before addition of K_2CO_3 (30 mg; 0.21 mmol). The reaction mixture was stirred at room temperature for 4 hours. The MeOH was removed by rotary evaporation before immediate

purification by silica gel flash column chromatography (40% ethyl acetate in hexanes to 60% ethyl acetate in hexanes) to afford oxepane **76** as a light-yellow oil (138 mg; 0.44 mmol) in 41% yield as a 9:1 mixture of diastereomers. ^1H NMR and COSY spectra are in Section 3.6.

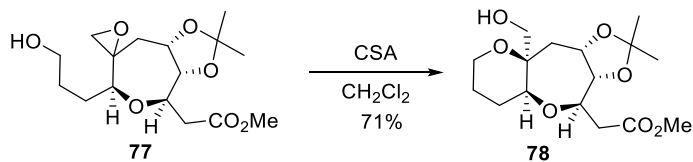
^1H NMR (600 MHz, C_6D_6) δ 5.06 (d, $J = 0.9$ Hz, 1H), 4.93 (t, $J = 1.3$ Hz, 1H), 4.31 (dd, $J = 8.4, 5.4$ Hz, 0.1 H), 4.26 (dd, $J = 8.6, 5.3$ Hz, 0.9 H), 4.04 (td, $J = 10.2, 2.7$ Hz, 1H), 3.99 (ddd, $J = 5.6, 4.5, 3.2$ Hz, 1H), 3.65 (dd, $J = 10.0, 5.8$ Hz, 0.1H), 3.52 (dd, $J = 10.2, 5.5$ Hz, 0.9H), 3.40 (dd $J = 12.4, 6.1$ Hz, 2H), 3.38 (s, 3H), 2.93 (dd, $J = 15.9, 2.6$ Hz, 0.1H), 2.89 (dd, $J = 16.0, 2.7$ Hz, 0.9H), 2.49 (dd, $J = 16.0, 10.3$ Hz, 1H), 2.41 (dd, $J = 14.0, 4.4$ Hz, 1H), 2.35 (ddd, $J = 14.0, 3.2, 1.0$ Hz, 1H), 1.69 – 1.61 (m, 1H), 1.58 – 1.45 (m, 2H), 1.43 – 1.37 (m, 1H), 1.36 (s, 3H), 1.24 (s, 3H).



Epoxide 77: Oxepane **76** (138 mg; 0.44 mmol) was dissolved in a rapidly stirred biphasic mixture of CH_2Cl_2 (9 mL) and aqueous pH 7 buffer (9 mL) before addition of *m*-CPBA (295 mg; 1.31 mmol). The suspension was stirred overnight before reaching completion, where it was diluted with ethyl acetate (20 mL). The organic layer was separated and washed with aqueous $\text{Na}_2\text{S}_2\text{O}_2$ (10 mL), aqueous NaHCO_3 (15 mL), water (15 mL), and brine before being dried over MgSO_4 , filtered, concentrated, and purified by silica gel flash column chromatography (50% ethyl acetate in hexanes) to afford the product with benzoic acid, which was re-subjected to column chromatography (40% ethyl acetate in hexanes) to

afford the product (95 mg; 0.29 mmol) as a light-yellow film in 66% yield. ^1H NMR and COSY spectra are in Section 3.6.

^1H NMR (600 MHz, C_6D_6) δ 4.26 (td, $J = 10.1, 2.4$ Hz, 1H), 4.14 (ddd, $J = 9.6, 6.8, 4.1$ Hz, 1H), 3.82 (dd, $J = 9.9, 6.8$ Hz, 1H), 3.71 (dd, $J = 10.7, 2.1$ Hz, 1H), 3.39 (m, 2H), 3.37 (s, 3H), , 2.84 (dd, $J = 15.9, 2.5$ Hz, 1H), 2.49 (dd, $J = 15.9, 10.3$ Hz, 1H), 2.38 (dd, $J = 4.5, 1.4$ Hz, 1H), 2.23 (ddd, $J = 14.0, 9.6, 1.5$ Hz, 1H), 2.08 (d, $J = 4.5$ Hz, 1H), 1.67 (dd, $J = 14.1, 4.1$ Hz, 1H), 1.65 – 1.60 (m, 1H), 1.44 (m, 1H), 1.40 (s, 3H), 1.36 (m, 2H), 1.19 (s, 3H).



Bicyclic compound 78: Starting material **77** (49 mg; 0.148 mmol) was dissolved in dry CH_2Cl_2 (3 mL) before addition of CSA (17.2 mg; 0.074 mmol). The reaction was stirred at room temperature for 14 hours before concentration under reduced pressure and silica gel flash column chromatography (40% ether in pentane to 50% ether in pentane) to afford bicyclic product **78** (35 mg; 0.106 mmol) as a white powder in 71% yield. The powder was recrystallized from heptane and benzene *via* vapor diffusion to afford clear needle-like crystals. ^1H NMR and COSY spectra are in Section 3.6.

$[\alpha]_{\text{D}}^{25}$: +5.4 ($c = 0.65$, CHCl_3)

IR (neat): 34356, 2924, 2854, 1739, 1439, 1370, 1263, 1209, 1106, 1044 cm^{-1} .

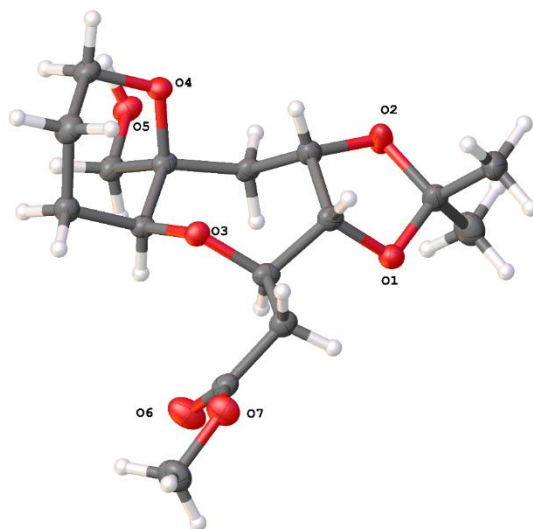
HRMS (NSI): m/z calcd. for $\text{C}_{16}\text{H}_{25}\text{O}_6\text{INa}$ $[\text{M}+\text{Na}]^+$: 463.05880 found 463.305845.

Melting point: 126-127 °C

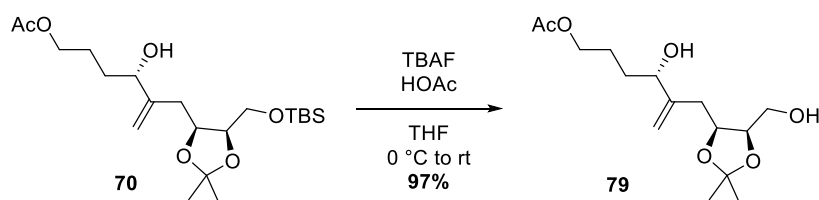
¹H NMR (600 MHz, CDCl₃) δ 4.68 (ddd, *J* = 11.6, 6.9, 3.1 Hz, 1H), 4.14 (dd, *J* = 9.6, 6.9 Hz, 1H), 4.02 (td, *J* = 10.2, 2.5 Hz, 1H), 3.96 (d, *J* = 11.3 Hz, 1H), 3.77 (dd, *J* = 11.6, 5.0 Hz, 1H), 3.70 (s, 3H), 3.62 (td, *J* = 12.9, 11.6, 2.5 Hz, 1H), 3.44 (t, *J* = 3.1 Hz, 1H), 3.24 (d, *J* = 11.3 Hz, 1H), 2.77 (dd, *J* = 16.3, 2.5 Hz, 1H), 2.55 (dd, *J* = 16.3, 10.4 Hz, 1H), 2.34 (dd, *J* = 14.6, 3.1 Hz, 1H), 1.92 – 1.82 (m, 2H), 1.82 – 1.71 (m, 3H), 1.68 (m, 1H), 1.45 (s, 3H), 1.35 (s, 3H).

¹H NMR (600 MHz, C₆D₆) δ 4.93 (ddd, *J* = 11.6, 6.9, 3.1 Hz, 1H), 4.15 (td, *J* = 10.0, 2.4 Hz, 1H), 4.07 (dd, *J* = 9.6, 6.9 Hz, 1H), 3.44 (d, *J* = 11.2 Hz, 1H), 3.39 (m, 2H), 3.33 (s, 3H), 3.11 (ddd, *J* = 13.1, 11.6, 2.5 Hz, 1H), 2.87 (d, *J* = 11.2 Hz, 1H), 2.79 (dd, *J* = 16.3, 2.4 Hz, 1H), 2.56 (dd, *J* = 16.3, 10.3 Hz, 1H), 2.47 (dd, *J* = 14.5, 3.1 Hz, 1H), 1.93 – 1.83 (m, 2H), 1.67 – 1.61 (m, 1H), 1.46 (s, 3H), 1.33 (tdd, *J* = 13.9, 4.6, 3.2 Hz, 2H), 1.21 (s, 3H), 0.94 – 0.90 (m, 1H), 0.77 (ddq, *J* = 13.2, 4.3, 2.3 Hz, 1H).

¹³C NMR (151 MHz, C₆D₆) δ 171.92, 128.67, 109.68, 79.79, 79.05, 76.73, 76.42, 74.83, 62.80, 61.79, 51.39, 40.49, 38.37, 30.55, 28.40, 27.13, 25.45, 20.49.



XRAY TABLES FOR COMPOUND 84 in Section 3.5.



Diol 70: Silylated alcohol **870** (1.78 g; 4.27 mmol) was dissolved in THF (40 mL) and cooled to 0 °C before addition of acetic acid (0.49 mL; 8.53 mmol), TBAF in THF (1.0 M; 6.40 mL; 6.40 mmol). The resulting solution was gradually warmed to room temperature and stirred for 18 hours before removal of solvent under reduced pressure. The resulting oil was purified by silica gel flash column chromatography (75% ethyl acetate in hexanes) to afford compound **79** as a clear colorless oil (1.248 g; 4.13 mmol) in 97% yield.

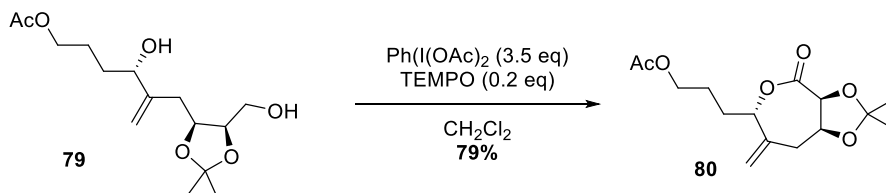
$[\alpha]_D^{25}$: -11.3 (c=0.981, CHCl₃)

HRMS (NSI): m/z calcd. for C₁₅H₂₆O₆Na [M+Na]⁺: 325.16216 found 325.16140.

IR (neat): 3425, 2985, 2931, 1734, 1648, 1454., 1368, 1243, 1164, 1037, 981, 899, 837, 734, 702, 607 cm^{-1} .

^1H NMR (600 MHz, Acetone- d_6) δ 5.09 (dt, $J = 1.9, 1.0$ Hz, 1H), 4.97 (q, $J = 1.6$ Hz, 1H), 4.42 (q, $J = 6.6$ Hz, 1H), 4.16 (q, $J = 5.9$ Hz, 1H), 4.10 (br s, 1H), 4.08 – 3.97 (m, 2H), 3.87 (s, 1H), 3.62 (dd, $J = 11.3, 5.9$ Hz, 1H), 3.57 (dd, $J = 10.9, 6.0$ Hz, 1H), 2.85 (d, $J = 11.6$ Hz, 1H), 2.37 (d, $J = 6.5$ Hz, 2H), 1.98 (s, 3H), 1.78 – 1.69 (m, 1H), 1.69 – 1.59 (m, 2H), 1.59 – 1.50 (m, 1H), 1.37 (s, 3H), 1.29 (s, 3H).

^{13}C NMR (126 MHz, CDCl_3) δ 171.4, 148.1, 114.0, 108.5, 78.0, 77.2, 75.1, 64.5, 61.6, 32.3, 30.9, 28.0, 25.4, 25.1, 21.2.



Lactone 80: In a procedure adapted from Forsyth et. al.¹⁶⁹, $\text{PhI}(\text{OAc})_2$ (1.67 g; 5.17 mmol) and TEMPO (47 mg; 0.30 mmol) were added to CH_2Cl_2 (25 mL) before diol (447 mg; 1.47 mmol) in CH_2Cl_2 (5 mL) was added in portion. The resulting mixture was stirred at room temperature for 8 hours before being diluted with diethyl ether and quenched with $\text{Na}_2\text{S}_2\text{O}_3$ (10 mL). The layers were separated and the aqueous phase was extracted with ethyl acetate (3 x 15 mL). The combined organic extracts were washed with aqueous NaHCO_3 (20 mL) and brine before being dried over MgSO_4 , filtered, and concentrated under reduced pressure. The resulting oil was purified by silica gel flash column chromatography (30%

to 45% diethyl ether in pentane) to afford lactone **80** (383 mg; 1.28 mmol) as an orange-yellow oil in 79% yield as a single stereoisomer.

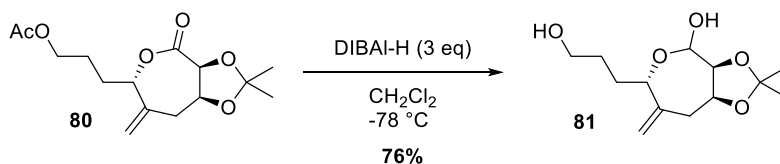
$[\alpha]_D^{25}$: -93.4 (c=1.10, CHCl₃)

HRMS (APCI): m/z calculated for C₁₅H₂₃O₆ [M+H]⁺ 299.1489 found 299.1490.

IR (neat): 3435, 2925, 2855, 1734, 1437, 1370, 1249, 1088, 1042, 980, 908 cm⁻¹.

¹H NMR (600 MHz, CDCl₃) δ 5.41 (d, J = 7.9 Hz, 1H), 5.11 (d, J = 1.8 Hz, 1H), 5.06 (d, J = 1.5 Hz, 1H), 4.83 (dd, J = 8.0, 0.8 Hz, 1H), 4.59 (ddd, J = 7.7, 5.0, 2.3 Hz, 1H), 4.21 – 4.05 (m, 2H), 2.78 (dd, J = 15.7, 5.0 Hz, 1H), 2.61 (d, J = 15.7 Hz, 1H), 2.06 (s, 3H), 1.98 – 1.86 (m, 2H), 1.86 – 1.73 (m, 2H), 1.55 (s, 3H), 1.37 (s, 3H).

¹³C NMR (100 MHz, CDCl₃) δ 171.3, 170.5, 141.4, 115.6, 111.3, 78.7, 78.2, 73.6, 64.0, 35.2, 29.5, 26.1, 24.6, 24.1, 21.1.



Lactol 81: Lactone **80** (383 mg; 1.28 mmol) was dissolved in CH₂Cl₂ (25 mL) and cooled to -78 °C where DIBAL-H (3.85 mL; 1.0 M in hexanes) was added dropwise. The reaction was stirred at -78 °C for 1.5 hours before being warmed to 0 °C and diluted with diethyl ether before quenching with H₂O (0.16 mL), 15% aqueous NaOH (0.16 mL), then more water (0.39 mL). The reaction was then allowed to warm to room temperature where it was stirred for 15 minutes before addition of MgSO₄. The mixture was stirred for 15

additional minutes before being filtered through a coarse frit and concentrated to afford crude lactol **81** (248 mg; 0.97 mmol) as a light-yellow oil in 76% yield.

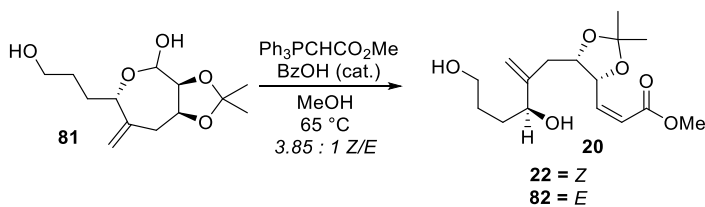
$[\alpha]_D^{25}$: -2.1 (c=0.975, CHCl₃)

HRMS (NSI): m/z calculated for C₁₃H₂₃O₅ [M+H]⁺ 259.15400 found 259.15402.

IR (neat): 3402, 2986, 2931, 2870, 1434, 1381, 1219, 1155, 1061, 909, 789, 733, 701 cm⁻¹.

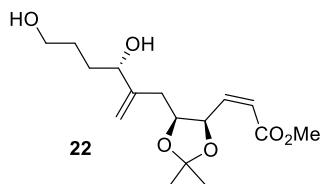
¹H NMR (400 MHz, CDCl₃) δ 5.03 (d, J = 13.8 Hz, 2H), 4.65 (d, J = 8.1 Hz, 1H), 4.33 (d, J = 5.3 Hz, 1H), 4.23 (d, J = 6.1 Hz, 1H), 3.91 – 3.79 (m, 1H), 3.75 – 3.60 (m, 2H), 2.70 – 2.55 (m, 2H), 2.45 (br s, OH), 1.86 – 1.64 (m, 3H), 1.56 (m, 1H), 1.44 (s, 3H), 1.37 (s, 3H).

¹³C NMR (101 MHz, CDCl₃) δ 144.2, 116.2, 108.6, 95.7, 82.2, 80.9, 74.6, 62.8, 32.2, 31.1, 29.4, 28.4, 25.9.



Z-Ester 22 and E-Ester 82: To a solution of lactol **81** (248 mg; 0.97 mmol) in methanol (5 mL) were added Wittig reagent (388 mg; 1.16 mmol) and benzoic acid (12 mg; 0.10 mmol). The reaction mixture was placed in an oil bath at 65 °C where it was heated for 4 hours. The reaction mixture was then cooled to room temperature before the solvent was removed under reduced pressure. The resulting oil was purified by silica gel flash column chromatography (75% ethyl acetate in hexanes) to afford the products **22** and **82** as a 3.85/1

mixture of Z/E alkene isomer with contamination by triphenylphosphine oxide. The impure material was partially separable at this point and subjected to further reaction, at which point the triphenylphosphine oxide and alkene isomers were completely separated.



$[\alpha]_D^{25}$: -96.9 (c=1.04, CHCl₃)

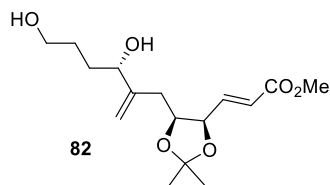
HRMS (NSI): m/z calcd. for C₁₆H₂₆O₆Na [M+Na]⁺: 337.16216 found 337.16174.

IR (neat): 3375, 2987, 2935, 1718, 1648, 1439, 1381, 1200, 1051, 902, 850, 826, 724, 542 cm⁻¹.

¹H NMR (600 MHz, CDCl₃, 5.7:1 Z/E major isomer reported) δ 6.28 (dd, J = 11.6, 7.8 Hz, 1H), 5.98 (dd, J = 11.6, 1.5 Hz, 1H), 5.66 (td, J = 8.1, 7.5, 1.6 Hz, 1H), 5.10 (s, 1H), 4.98 (d, J = 1.2 Hz, 1H), 4.57 (ddd, J = 10.2, 6.8, 3.7 Hz, 1H), 4.19 – 4.07 (m, 2H), 3.75 (s, 3H), 3.67 (m, 2H), 2.26 – 2.12 (m, 3H), 1.70 – 1.60 (m, 4H), 1.54 (s, 3H), 1.38 (s, 3H).

PPh₃O impurity: δ 7.68 (ddt, J = 10.8, 6.9, 1.4 Hz), 7.56 (td, J = 7.3, 1.4 Hz), 7.47 (td, J = 7.7, 7.2, 2.9 Hz).

¹³C NMR (151 MHz, CDCl₃) δ 166.14, 148.10, 146.72, 132.15 (PPh₃O), 128.50 (PPh₃O), 121.49, 113.98, 108.98, 78.79, 75.31, 75.19, 62.83, 51.65, 33.07, 32.25, 29.35, 27.82, 25.10.



$[\alpha]_D^{25}$: -32.0 (c=1.02, CHCl₃)

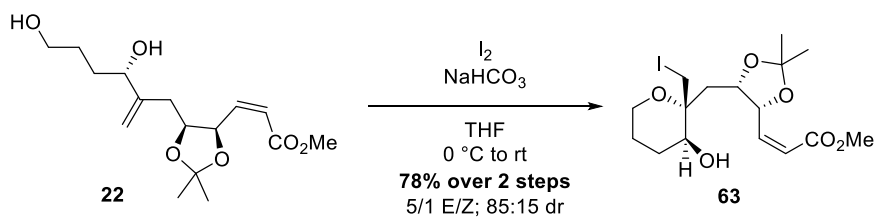
HRMS (NSI): m/z calcd. for C₁₆H₂₆O₆Na [M+Na]⁺: 337.16216 found 337.16202.

IR (neat): 3381, 2988, 2934, 1719, 1660, 1437, 1372, 1262, 1215, 1163, 1119, 1049, 984, 903, 734, 699, 541 cm⁻¹.

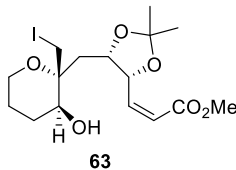
¹H NMR (600 MHz, CDCl₃ 5.2:1 E/Z major isomer reported) δ 6.86 (dd, J = 15.6, 5.7 Hz, 1H), 6.12 (dd, J = 15.6, 1.5 Hz, 1H), 5.13 (s, 1H), 4.95 (s, 1H), 4.78 (ddd, J = 7.0, 5.8, 1.5 Hz, 1H), 4.56 – 4.38 (m, 1H), 4.18 – 4.01 (m, 2H), 3.76 (s, 3H), 3.70 – 3.59 (m, 2H), 2.31 (dd, J = 14.9, 9.1 Hz, 1H), 2.17 (m, 1H), 2.11 (m, 1H), 2.10 – 2.07 (m, 2H), 1.70 – 1.59 (m, 2H), 1.53 (s, 3H), 1.38 (s, 3H).

PPh₃O impurity: δ 7.68 (ddt, J = 10.8, 6.9, 1.4 Hz), 7.56 (td, J = 7.3, 1.4 Hz), 7.47 (td, J = 7.7, 7.2, 2.9 Hz).

¹³C NMR (151 MHz, CDCl₃ 5.7:1 Z/E minor isomer denoted by *) δ 166.67, 166.34*, 148.30*, 148.10, 146.83*, 143.59, 132.34 (PPh₃O), 132.21 (PPh₃O), 132.20 (PPh₃O), 128.77 (PPh₃O), 128.69 (PPh₃O), 123.00, 121.70*, 114.17*, 113.57, 109.36, 109.18*, 78.98*, 78.21, 77.31*, 75.49, 75.39*, 63.03*, 62.99, 52.00, 51.86*, 33.26*, 33.08, 32.80, 32.45*, 29.55*, 29.49, 28.02*, 27.93, 25.45, 25.31*.



Tetrahydropyran 63: Diol **22** (338 mg; contaminated with PPh_3O) was dissolved in THF (10 mL) and cooled to $0\text{ }^\circ\text{C}$ before addition of $NaHCO_3$ (735 mg; 8.70 mmol) and I_2 (1.47 g; 5.80 mmol). The reaction warmed to room temperature and stirred for 2 hours. The reaction was quenched with addition of aqueous $Na_2S_2O_3$ and diluted with ethyl acetate. The organic layer was separated and the aqueous layer was extracted with ethyl acetate (3 x 5mL). The combined organic extracts were combined and washed with brine before being dried over $MgSO_4$, filtered and concentrated under reduced pressure. The resulting crude oil was purified by silica gel flash column chromatography (35% ether in pentane) to afford cyclized compound **63** (335 mg; 0.76 mmol) in 78% yield over 2 steps (85:15 *dr*; 5/1 *E/Z*). Although compound **87** was not isolated in this experiment, it can be separated by careful silica gel column chromatography (20% ether in pentane to 30% ether in pentane). The *Z*-alkenoate has been isolated as a single stereoisomer to investigate cyclization reactions on the *Z*-alkene alone. For analytical purposes the iodocyclization was first performed using each alkene isomer separately. On the preparative scale, a mixture of alkene isomers was used. When subjected to similar reaction conditions, both the *E*- and *Z*- isomers produced cyclized materials with 85:15 *dr*, although yields were not calculable due to PPh_3O impurities. The *Z*- isomer fully reacted in one hour, while the *E*- isomer required 4 hours to be fully consumed.



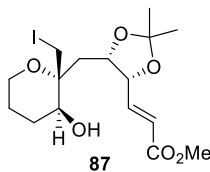
$[\alpha]_D^{25}$: -110.0 (c=1.00, CHCl₃)

HRMS (NSI): m/z calcd. for C₁₆H₂₆O₆I [M+H]⁺: 441.07686 found 441.07707.

IR (neat): 3469.61, 2983.48, 2939.13, 2869.51, 1723.08, 1660.17, 1437.33, 1305.97, 1255.46, 1216.48, 1164.36, 1080.38, 985.37, 860.97, 831.72 cm⁻¹.

¹H NMR (600 MHz, CDCl₃, major diastereomer) δ 6.19 (dd, $J = 11.7, 8.4$ Hz, 1H), 5.99 (dd, $J = 11.7, 1.4$ Hz, 1H), 5.69 (ddd, $J = 8.3, 6.7, 1.4$ Hz, 1H), 4.66 (ddd, $J = 10.5, 6.7, 1.2$ Hz, 1H), 3.99 (dd, $J = 9.3, 4.6$ Hz, 1H), 3.87 (d, $J = 11.5$ Hz, 1H), 3.74 (s, 3H), 3.65 (m, 1H), 3.39 (d, $J = 11.5$ Hz, 1H), 3.34 (m, 1H), 2.86 (d, $J = 4.9$ Hz, -OH), 2.00 (m, 1H), 1.87 (m, 2H), 1.68 (m, 3H), 1.52 (s, 3H), 1.41 (s, 3H).

¹³C NMR (126 MHz, CDCl₃) δ 206.99, 165.84, 146.35, 145.74, 121.93, 121.75, 109.29, 108.96, 75.86, 75.43, 75.13, 75.09, 73.80, 68.62, 68.44, 61.21, 60.84, 53.88, 51.68, 39.31, 30.99, 29.32, 28.27, 28.01, 27.34, 26.64, 25.56, 25.32, 12.59.



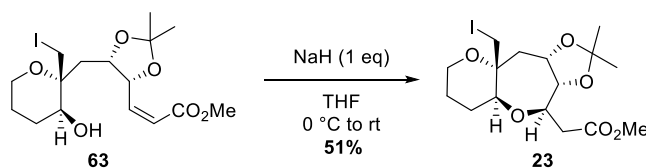
$[\alpha]_D^{25}$: -5.2 (c=1.01, CHCl₃)

HRMS (NSI): m/z calcd. for C₁₆H₂₅O₆INa [M+Na]⁺: 463.05880 found 463.05907.

IR (neat): 3475.93, 2984.45, 2938.16, 2865.30, 1719.84, 1649.92, 1438.25, 1407.87, 1380.70, 1219.08, 1198.21, 1163.11, 1084.05, 1042.99, 873.31, 832.84 cm^{-1} .

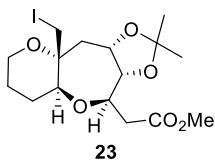
^1H NMR (600 MHz, CDCl_3) δ 6.86 (dd, $J = 15.5, 6.2$ Hz, 1H), 6.07 (dd, $J = 15.6, 1.3$ Hz, 1H), 4.67 (ddt, $J = 6.4, 5.1, 1.1$ Hz, 1H), 4.56 (ddd, $J = 9.7, 6.5, 1.3$ Hz, 1H), 3.99 (m, 1H), 3.86 (d, $J = 11.6$ Hz, 1H), 3.76 (s, 3H), 3.65 (m, 1H), 3.36 (d, $J = 11.7$ Hz, 1H), 2.03 (m, 1H), 1.88 (m, 1H), 1.78 – 1.60 (m, 4H), 1.53 (s, 3H), 1.42 (s, 3H).

^{13}C NMR (151 MHz, CDCl_3) δ 166.47, 144.01, 123.45, 109.43, 77.92, 77.02, 75.46, 73.62, 68.70, 61.21, 51.95, 39.30, 30.54, 28.16, 26.67, 25.76, 25.62, 12.14.



Bicyclic compound 23: Tetrahydropyran **63** (550 mg; 1.25 mmol) was dissolved in THF (20 mL) and cooled to 0 °C before addition of NaH (50 mg; 1.25 mmol; 60% in mineral oil). The reaction warmed to room temperature gradually and stirred for one hour. The reaction was diluted with diethyl ether and quenched by addition of MeOH (1 mL) and then concentrated under reduced pressure. The organic layer was separated and the aqueous layer was extracted with diethyl ether (3 x 7 mL). The combined organic extracts were combined and washed with brine before being dried over Na_2SO_4 , filtered and concentrated under reduced pressure. The resulting crude powder was purified by silica gel flash column chromatography (15% to 20% diethyl ether in pentane) to afford the cyclized compound **23** in (280 mg; 0.64 mmol) in 51% yield. At this stage, the AB cis-

fused isomer **85** (36 mg; 0.082 mmol) resulting from iodocyclization was isolated as a white powder in 7% yield. ^1H NMR and COSY spectra are in Section 3.6.



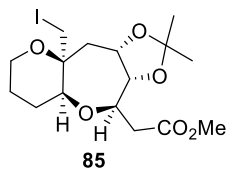
$[\alpha]_{\text{D}}^{25}$: +5.2 (c=0.78, MeOH); -0.7 (c=1.10, CHCl₃)

HRMS (NSI): m/z calcd. for C₁₆H₂₆O₆IH [M+H]⁺: 441.07686 found 441.07650.

IR (neat): 2983.15, 2947.25, 2874.57, 1736.44, 1437.02, 1380.95, 1301.53, 1265.74, 1211.65, 1166.08, 1120.78, 1104.86, 1043.27, 997.59, 882.81, 800.17, 736.67 cm⁻¹.

^1H NMR (400 MHz, CDCl₃) δ 4.50 (ddd, J = 10.8, 6.9, 6.0 Hz, 1H), 3.98 (dd, J = 10.0, 6.9 Hz, 1H), 3.90 (td, J = 9.9, 2.8 Hz, 1H), 3.77 (dd, J = 12.1, 2.0 Hz, 1H), 3.71 (s, 3H), 3.63 (ddt, J = 12.3, 4.6, 2.3 Hz, 1H), 3.52 (dd, J = 12.1, 4.2 Hz, 1H), 3.34 (td, J = 12.2, 5.3 Hz, 1H), 3.06 (d, J = 12.1 Hz, 1H), 2.78 (dd, J = 16.1, 2.8 Hz, 1H), 2.52 (dd, J = 14.0, 6.0 Hz, 1H), 2.42 (dd, J = 16.1, 9.9 Hz, 1H), 1.85 (ddd, J = 14.0, 10.8, 2.0 Hz, 1H), 1.79 – 1.64 (m, 3H), 1.51 (m, 1H), 1.42 (s, 3H), 1.35 (s, 3H).

^{13}C NMR (101 MHz, CDCl₃) δ 172.13, 108.96, 85.21, 79.15, 78.54, 73.98, 72.93, 59.96, 51.91, 42.06, 39.11, 27.32, 26.09, 25.53, 24.37, 8.14.



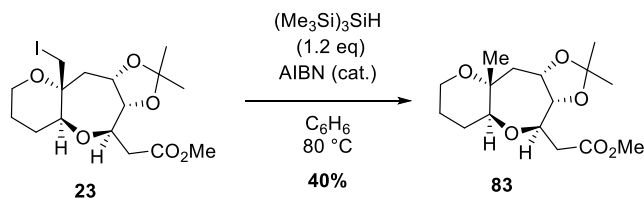
$[\alpha]_D^{25}$: -7.0 (c=0.772, CHCl₃)

HRMS (NSI): *m/z* calcd. for C₁₆H₂₆O₆IH [M+H]⁺: 441.07686 found 441.07727.

IR (neat): 2931, 2858, 1734, 1437, 1369, 1264, 1207, 1154, 1088, 1044, 1016, 995, 914, 870, 841, 800, 744, 648, 624, 589 cm⁻¹.

¹H NMR (400 MHz, CDCl₃) δ 4.66 (ddd, *J* = 11.4, 7.0, 3.3 Hz, 1H), 4.09 (dd, *J* = 9.7, 7.0 Hz, 1H), 3.96 (td, *J* = 10.0, 2.5 Hz, 1H), 3.77 – 3.65 (m, 2H), 3.71 (s, 3H), 3.57 (d, *J* = 11.1 Hz, 1H), 3.53 (app dd, *J* = 12.2, 2.9 Hz, 1H), 3.19 (d, *J* = 11.1 Hz, 1H), 2.73 (dd, *J* = 16.4, 2.4 Hz, 1H), 2.52 (dd, *J* = 16.4, 10.3 Hz, 1H), 2.22 (dd, *J* = 14.3, 3.3 Hz, 1H), 1.92 (dd, *J* = 14.3, 11.4 Hz, 1H), 1.85 – 1.75 (m, 4H), 1.42 (s, 3H), 1.31 (s, 3H).

¹³C NMR (151 MHz, CDCl₃) δ 172.20, 109.39, 78.66, 77.74, 76.37, 73.98, 73.20, 61.75, 51.86, 41.39, 39.88, 27.79, 26.75, 24.96, 19.60, 13.29.



Bicyclic compound 83: Alkyl iodide **23** (21 mg; 0.048 mmol) was dissolved in benzene (1 mL). A single crystal of AIBN was added along with (Me₃Si)₃SiH (18 μL; 0.057 mmol) and the reaction was heated to reflux, where it was stirred for 45 minutes before cooling

and solvent removal under reduced pressure. The resulting oil was purified by silica gel flash column chromatography (20% ethyl acetate in hexanes to 25% ethyl acetate in hexanes) to afford product **83** (6 mg; 0.019 mmol) in 40% yield. NOESY of this compound revealed correlations that allowed for assignment of the stereochemistry at the new stereocenters.

$[\alpha]_D^{25}$: +11.5 (c=0.609 CHCl₃)

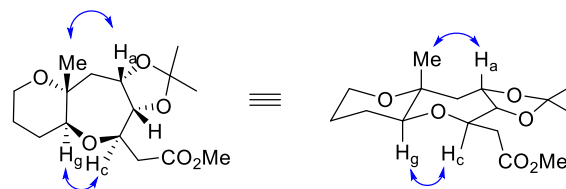
IR (thin film): 2983, 2875, 1737, 1383, 1221, 850 cm⁻¹.

HRMS (NSI): m/z calculated for C₁₆H₂₇O₆ [M+H]⁺ 315.18022 found 315.18045.

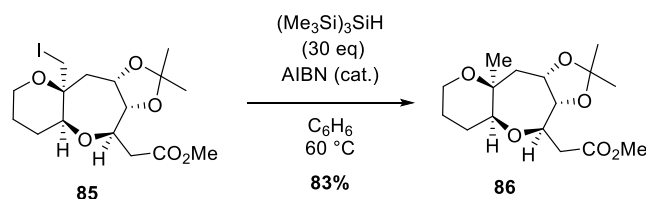
¹H NMR (400 MHz, Acetone-*d*₆) δ 4.54 (ddd, $J = 10.8, 7.1, 6.1$ Hz, 1H), 3.95 (dd, $J = 10.0, 7.1$ Hz, 1H), 3.82 (td, $J = 10.0, 2.9$ Hz, 1H), 3.64 (s, 3H), 3.59 – 3.50 (m, 1H), 3.46 (ddt, $J = 12.0, 4.7, 1.7$ Hz, 1H), 3.17 (dd, $J = 11.4, 3.9$ Hz, 1H), 2.67 (dd, $J = 15.8, 2.9$ Hz, 1H), 2.31 (dd, $J = 15.8, 10.1$ Hz, 1H), 2.15 – 2.10 (m, 1H), 1.85 (dd, $J = 13.4, 10.9$ Hz, 1H), 1.60 (m, 3H), 1.53 – 1.36 (m, 1H), 1.35 (s, 3H), 1.19 (s, 3H), 1.12 (s, 3H).

¹³C NMR (151 MHz, Acetone-*d*₆) δ 171.77, 109.00, 82.57, 80.13, 78.78, 74.73, 60.20, 51.79, 45.28, 40.18, 30.75, 27.72, 26.86, 24.45, 23.09, 21.23.

key NOESY Correlations



H_a = 4.54 ddd, $J = 10.8, 7.1, 6.1$ Hz
H_c = 3.82 td, $J = 10.0, 2.9$ Hz
H_g = 3.17 dd, $J = 11.4, 3.9$



Bicyclic compound 86: The minor *cis*-fused diastereomer was deiodinated to confirm the stereochemistry across the AB ring fusion. Alkyl iodide **85** (10 mg; 0.023 mmol) was dissolved in benzene (0.4 mL). $(\text{Me}_3\text{Si})_3\text{SiH}$ (18 μL ; 0.057 mmol) and a single crystal of AIBN were added and the reaction was heated to 60 °C, where it was stirred for 10 minutes before cooling and removal of solvent under reduced pressure. The resulting oil was purified by silica gel flash column chromatography (15% ethyl acetate in hexanes to 20% ethyl acetate in hexanes) to afford product **86** (6 mg; 0.019 mmol) in 83% yield as a 5.7:1 mixture of *cis* : *trans* fused diastereomers. NOESY of this compound revealed correlations that allowed for assignment of the stereochemistry at the *cis*-AB ring fusion.

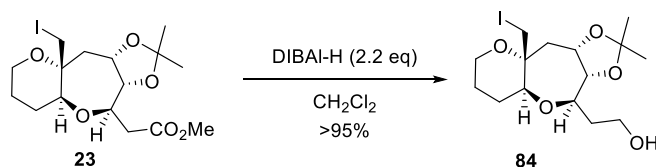
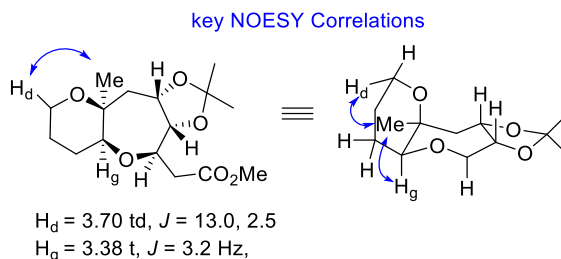
$[\alpha]_{\text{D}}^{25}$: +26.0 ($c=0.40$, CHCl_3)

IR (thin film): 2985, 2360, 1740, 1436, 1263, 1115, 1046 cm^{-1} .

HRMS (NSI): m/z calculated for $\text{C}_{16}\text{H}_{26}\text{O}_6\text{Na}$ $[\text{M}+\text{Na}]^+$: 337.16081 found 337.16171.

^1H NMR (600 MHz, Acetone- d_6) δ 4.62 (ddd, $J = 11.7, 6.9, 3.2$ Hz, 1H), 4.07 (dd, $J = 9.6, 6.9$ Hz, 1H), 3.92 (td, $J = 10.0, 2.6$ Hz, 1H), 3.70 (td, $J = 13.0, 2.5$ Hz, 1H), 3.65 (s, $J = 0.9$ Hz, 3H), 3.59 (dd, $J = 11.6, 5.1$ Hz, 1H), 3.38 (t, $J = 3.2$ Hz, 1H), 2.63 (dd, $J = 15.8, 2.7$ Hz, 1H), 2.42 (dd, $J = 16.1, 10.4$ Hz, 1H), 2.04 – 2.00 (m, 1H), 1.96 – 1.85 (m, 1H), 1.80 – 1.70 (m, 2H), 1.60 (dd, $J = 13.0, 3.8$ Hz, 1H), 1.35 (s, 3H), 1.28 (d, $J = 4.1$ Hz, 1H), 1.26 (s, 3H), 1.20 (s, 3H), 1.17 (s, 3H).

^{13}C NMR (151 MHz, Acetone- d_6) δ 172.2, 109.7, 82.5, 79.9, 77.2, 74.8, 74.3, 61.7, 51.7, 44.5, 40.7, 28.3, 27.3, 25.4, 23.0, 21.2.



Alcohol 84: To a solution of ester **23** (122 mg; 0.277 mmol) in CH_2Cl_2 (5.5 mL) was added DIBAL-H (0.61 mL; 1.0 M in hexanes) dropwise. After 2 hours, more DIBAL-H (0.3 mL) was added, and more (0.3 mL) was added after 7 hours. The reaction was cooled to 0°C , diluted with ether, and quenched by addition of Rochelle's salt (12 mL) and stirred for 4 hours at room temperature. The layers were separated and the aqueous layer was extracted with CH_2Cl_2 (3 x 8 mL). The combined organic layers were washed with water (10 mL x 2), dried over MgSO_4 , filtered, and concentrated under reduced pressure. The resulting crude powder **84** (113 mg; 0.277 mmol) recrystallized (details with crystal structure data).

$[\alpha]_D^{25}$: -8.1 ($c=1.02$ CHCl_3)

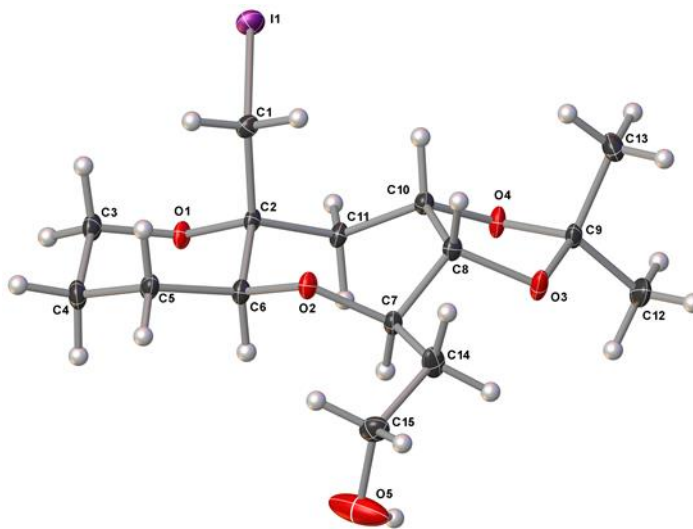
IR (neat): 3490, 2936, 2873, 1382, 1266, 1169, 1049, 882 cm^{-1} .

HRMS (NSI): m/z calcd. for $C_{15}H_{26}IO_5$ $[M+H]^+$: 413.08194 found 413.08197.

Melting point: dec. at 181-184 °C then melts at 187-188 °C

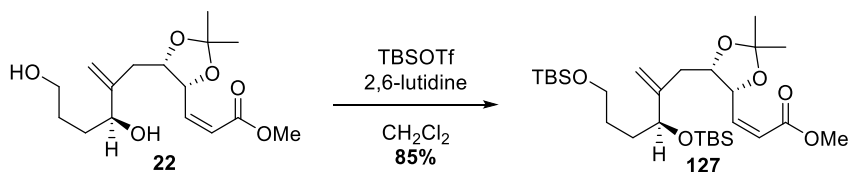
1H NMR (400 MHz, $CDCl_3$) δ 4.48 (ddd, $J = 10.9, 7.1, 5.8$ Hz, 1H), 4.03 (dd, $J = 9.7, 7.1$ Hz, 1H), 3.84 – 3.72 (m, 3H), 3.67 – 3.55 (m, 2H), 3.53 – 3.45 (m, 1H), 3.41 – 3.31 (m, 1H), 3.08 (d, $J = 12.1$ Hz, 1H), 2.53 – 2.47 (m, 1H), 2.09 – 1.96 (m, 1H), 1.87 – 1.77 (m, 2H), 1.77 – 1.64 (m, 2H), 1.63 – 1.52 (m, 1H), 1.42 (s, 3H), 1.36 (s, 3H), 0.91 – 0.87 (m, 1H).

^{13}C NMR (101 MHz, $CDCl_3$) δ 108.074, 85.30, 81.33, 79.73, 73.92, 72.97, 60.64, 59.89, 42.18, 36.13, 27.42, 26.35, 25.52, 24.39, 7.82.



X-ray crystal structure of AB bicyclic compound **84**

XRAY TABLES FOR COMPOUND 84 in Section 3.5.



Bis-silyl ether 127: To a stirred solution of diol **22** (256 mg; 0.82 mmol) in CH_2Cl_2 (6 mL) at -0°C were added 2,6-lutidine (350 μL ; 3.0 mmol) and TBSOTf (415 μL ; 1.80 mmol). The ice bath was removed the reaction was stirred at ambient temperature for 2 hours, whereupon it was quenched by addition of saturated aqueous ammonium chloride (2 mL). The organic layer was separated and the aqueous layer was extracted with CH_2Cl_2 (3 mL x 3). The combined organic extracts were washed with brine, dried over MgSO_4 , filtered, and concentrated under reduced pressure. The crude residue was purified by silica gel flash column chromatography (2% ethyl acetate in hexanes to 3% ethyl acetate in hexanes) to afford compound **127** (379 mg; 0.69 mmol) as a clear pale yellow oil in 85% yield.

Pure Z alkene:

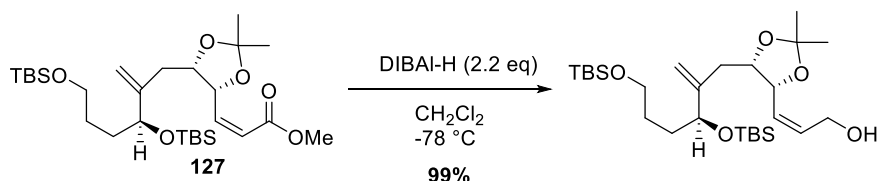
$[\alpha]_{\text{D}}^{25}$: -61.2 ($c=1.06$, CHCl_3)

HRMS (NSI): m/z calcd. for $\text{C}_{28}\text{H}_{54}\text{O}_6\text{Si}_2\text{Na}$ $[\text{M}+\text{Na}]^+$:565.33511 found 565.33598.

IR (neat): 2967, 2953, 2929, 2857, 1723, 1649, 1472, 1463, 1407, 1380, 1253, 1219, 1196, 1181, 1093, 1053, 1004, 939, 901, 835, 775, 740, 665 cm^{-1} .

^1H NMR (500 MHz, CDCl_3) δ 6.24 (dd, $J = 11.7, 8.4$ Hz, 1H), 5.94 (dd, $J = 11.7, 1.4$ Hz, 1H), 5.68 (ddd, $J = 8.2, 6.4, 1.4$ Hz, 1H), 5.05 (s, 1H), 4.95 (d, $J = 1.7$ Hz, 1H), 4.60 (ddd, $J = 9.4, 6.4, 3.9$ Hz, 1H), 4.08 (m, 1H), 3.72 (s, 3H), 3.59 (m, 2H), 2.18 – 2.05 (m, 2H), 1.51 (m, 8H), 1.39 (s, 3H), 0.89 (app. d, $J = 2.5$ Hz, 18H), 0.04 (app d, $J = 2.3$ Hz, 9H), 0.00 (s, 3H).

^{13}C NMR (126 MHz, CDCl_3) δ 166.11, 147.77, 146.60, 146.54, 121.59, 111.56, 108.86, 76.59, 76.55, 76.01, 75.93, 74.96, 74.92, 63.40, 32.95, 31.75, 28.92, 28.54, 28.51, 26.18, 26.05, 25.72, 25.69, 18.54, 18.40, -4.52, -4.80, -4.83, -5.05, -5.07.



Primary alcohol: DIBAL-H (0.76 mL; 1.0 M in hexanes) was added dropwise to a solution of ester **127** (193 mg; 0.35 mmol) in CH_2Cl_2 (7 mL) at $-78\text{ }^\circ\text{C}$. After 1.5 hours, the reaction was warmed to $0\text{ }^\circ\text{C}$ and diluted with ether before addition of water (30 μL), 15% aqueous NaOH (30 μL), and more water (75 μL). After stirring for 15 minutes, the ice bath was removed and magnesium sulfate was added. The slurry was stirred for 30 minutes at room temperature before filtration to remove the solids and concentration under reduced pressure. The resulting clear oil (182 mg; 0.35 mmol) was obtained in 99% yield and used without further purification.

$[\alpha]_{\text{D}}^{25}$: - 1.3 ($c=1.10$, CHCl_3)

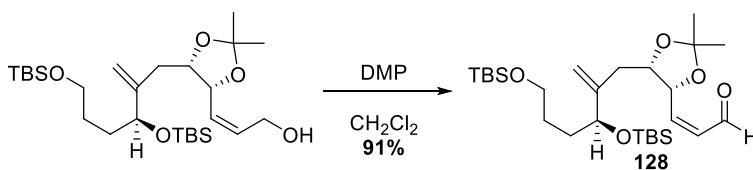
HRMS (NSI): m/z calcd. for $\text{C}_{27}\text{H}_{55}\text{O}_5\text{Si}_2$ $[\text{M}+\text{H}]^+$: 515.35825 found 515.35876.

IR (thin film): 3412, 2985, 2953, 2929, 2885, 2856, 1648, 1507, 1472, 1462, 1380, 1370, 1521, 1217, 1162, 1091, 1042, 106, 939, 896, 833, 773, 665, 542 cm^{-1} .

^1H NMR (500 MHz, CDCl_3) δ 5.83 (dddd, $J = 11.3, 7.1, 6.0, 1.2$ Hz, 1H), 5.58 (ddt, $J = 11.0, 9.3, 1.5$ Hz, 1H), 5.04 (q, $J = 1.2$ Hz, 1H), 4.93 (ddd, $J = 9.2, 6.0, 1.2$ Hz, 1H), 4.87

(q, $J = 1.6$ Hz, 1H), 4.45 (dt, $J = 7.7, 5.9$ Hz, 1H), 4.29 (ddd, $J = 13.3, 7.0, 1.4$ Hz, 1H), 4.15 (ddd, $J = 13.3, 6.1, 1.6$ Hz, 1H), 4.07 (t, $J = 5.7$ Hz, 1H), 3.59 (m, 2H), 2.34 (ddt, $J = 16.4, 7.8, 1.4$ Hz, 1H), 2.11 (ddt, $J = 16.0, 5.4, 1.1$ Hz, 1H), 1.82 (br s, -OH), 1.53 (m, 3H), 1.48 (s, 3H), 1.44 (m, 1H), 1.38 (s, 3H), 0.88 (s, 18H), 0.04 (s, 9H), 0.01 (s, 3H).

^{13}C NMR (126 MHz, CDCl_3) δ 147.94, 132.99, 128.19, 111.34, 108.35, 77.48, 77.22, 76.97, 76.42, 76.28, 73.99, 73.89, 63.35, 58.69, 32.89, 31.35, 28.57, 28.54, 26.06, 26.05, 25.88, 18.56, 18.39, -4.45, -4.78, -5.07.



Aldehyde 128: To a stirred solution of primary alcohol (182 mg; 0.35 mmol) in CH_2Cl_2 (7 mL) was added DMP (225 mg; 0.52 mmol) and NaHCO_3 (88mg; 1.04mmol). After 1.5 hours, the reaction was poured into a rapidly stirred solution of $\text{Na}_2\text{S}_2\text{O}_3$ (1 g) in 10 mL saturated aqueous NaHCO_3 . The suspension was stirred for 45 minutes until the layers turned clear. The layers were separated and the organic layer was washed with saturated aqueous NaHCO_3 (5 mL), water (8 mL x 2), dried over MgSO_4 , filtered, and concentrated under reduced pressure. The resulting crude oil was purified by silica gel flash column chromatography (8% ethyl acetate in hexanes) to furnish compound **128** (162 mg; 0.32 mmol) as a yellow oil in 91% yield.

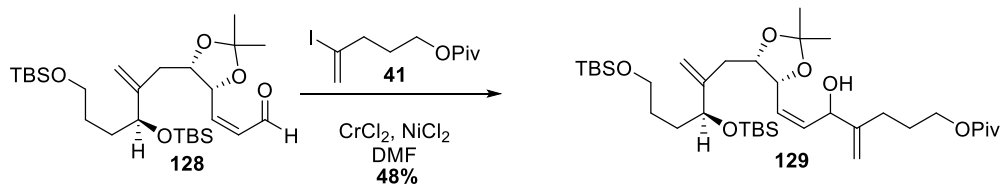
$[\alpha]_{\text{D}}^{25}$: -29.6. ($c=1.0$, CHCl_3)

HRMS (NSI): m/z calcd. for $\text{C}_{27}\text{H}_{52}\text{O}_5\text{Si}_2\text{Na}$ $[\text{M}+\text{Na}]^+$: 535.32455 found 353.32411.

IR (neat): 2953, 2929, 2886, 2856, 1697, 1686, 1253, 1217, 1093, 1054, 1005, 836, 776 cm^{-1} .

^1H NMR (500 MHz, CDCl_3) δ 10.09 (d, $J = 7.0$ Hz, 1H), 6.47 (dd, $J = 11.5, 8.8$ Hz, 1H), 6.10 (ddd, $J = 11.5, 7.0, 1.3$ Hz, 1H), 5.41 (ddd, $J = 8.9, 6.2, 1.3$ Hz, 1H), 5.05 (s, 1H), 4.88 (d, $J = 1.6$ Hz, 1H), 4.63 (dt, $J = 8.2, 5.9$ Hz, 1H), 4.06 (t, $J = 5.7$ Hz, 1H), 3.58 (t, $J = 5.8$ Hz, 2H), 2.35 (ddt, $J = 16.2, 8.2, 1.4$ Hz, 1H), 2.15 – 2.03 (m, 1H), 1.52 (s, 5H), 1.51 – 1.45 (m, 1H), 1.45 – 1.37 (m, 3H), 0.89 (s, 6H), 0.88 (s, 9H), 0.04 (s, 8H), -0.00 (s, 2H).

^{13}C NMR (126 MHz, CDCl_3) δ 190.77, 147.29, 146.08, 131.33, 112.01, 109.38, 77.22, 76.51, 76.47, 76.31, 76.24, 74.13, 74.10, 63.21, 32.93, 31.54, 28.86, 28.52, 26.17, 26.16, 26.05, 26.04, 25.73, 25.70, 18.54, 18.37, -4.45, -4.79, -5.05.



Bis-allylic alcohol 129: CrCl_2 (70 mg; 0.47 mmol) and NiCl_2 (0.3 mg; 0.02 mmol) were weighed out in a gloved box and the flask was sparged with argon for 10 minutes. The flask was cooled to 0°C and dry DMF (2 mL) was added. The ice bath was removed after 10 minutes and the solvated salts were warmed to room temperature. Vinyl iodide **41** (71 mg; 0.23 mmol) in DMF (0.7 mL) was added in one portion and the reaction was stirred for 10 minutes before aldehyde **128** (66 mg; 0.16 mmol) in DMF (0.33 mL+ 0.2 mL rinsate) was added over 30 minutes by syringe pump. The reaction mixture was stirred for at room temperature for 2 hours before being diluted with aqueous ammonium chloride (5 mL) and

ethyl acetate (5 mL). After stirring for one hour the layers were separated. The aqueous layer was extracted with ethyl acetate (10 mL × 6). The combined organic layers were washed with water (10 mL × 3), 10% aqueous LiCl, and brine before being dried over MgSO₄ and concentrated under reduced pressure. The crude residue was purified by silica gel flash column chromatography (6% ethyl acetate in hexanes to 14% ethyl acetate in hexanes) to afford compound **129** (52 mg; 0.077 mmol) as a clear pale yellow oil in 48% yield as a 1:1 mixture of diastereomers.

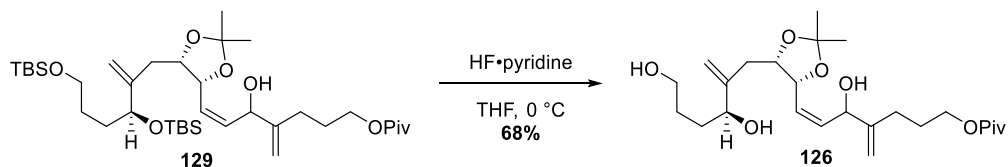
$[\alpha]_D^{25}$: +2.0 (c=1.00, CHCl₃)

HRMS (NSI): *m/z* calcd. for C₃₇H₇₀O₇Si₂Na [M+Na]⁺: 705.45523 found 705.45753.

IR (neat): 3412, 2954, 2928, 2856, 1729, 1253, 1159, 1095, 1054, 1006, 835, 775 cm⁻¹.

¹H NMR (600 MHz, C₆D₆) δ 5.87 – 5.71 (m, 2H), 5.17 (m, 1H), 5.12 (t, *J* = 1.1 Hz, 0H), 5.09 (t, *J* = 1.2 Hz, 1H), 5.03 (d, *J* = 1.6 Hz, 0.5H), 5.02 (d, *J* = 1.6 Hz, 0.5H) – 5.00 (m, 1H), 4.80 (d, *J* = 1.5 Hz, 1H), 4.52 (dt, *J* = 9.8, 6.6 Hz, 1H), 4.45 (m, 1H), 4.42 (m, 1H), 4.20 (t, *J* = 5.9 Hz, 1H), 4.04 (m, 2H), 3.60 (m, 2H), 2.53 (ddd, *J* = 20.5, 16.2, 8.4 Hz, 1H), 2.23 (td, *J* = 15.7, 5.0 Hz, 1H), 2.13 (m, 1H), 2.01 (m, 1H), 1.77 – 1.59 (m, 6H), 1.53 (s, 1.5H), 1.52 (s, 1.5H), 1.34 (s, 1.5H), 1.33 (s, 1.5H), 1.20 (s, 9H), 1.02 (s, 9H), 0.99 (m, 9), 0.13 (s, 6H), 0.08 (s, 6H).

¹³C NMR (151 MHz, C₆D₆) δ 177.75, 149.98, 149.91, 148.29, 135.13, 135.08, 128.35, 128.06, 111.89, 111.86, 110.82, 110.59, 108.24, 108.17, 79.09, 78.97, 76.65, 75.28, 75.21, 63.95, 63.93, 63.42, 63.39, 38.84, 33.38, 33.35, 32.52, 32.50, 30.23, 29.25, 28.58, 28.27, 28.13, 27.51, 27.49, 27.43, 26.23, 26.18, 25.79, -4.33, -4.75, -5.07.



Triene 126: HF·pyridine (1 mL) was added dropwise to a solution of bis-silylated compound **129** (52 mg; 0.077 mmol) in THF (5 mL) at 0 °C. The solution was warmed to room temperature gradually and stirred for 4 hours, at which point the reaction was cooled to 0 °C before addition of saturated sodium bicarbonate (10 mL in 1 mL portions). The mixture was stirred for 45 minutes before dilution with ethyl acetate (10 mL). The layers were separated and the aqueous layer was extracted with ethyl acetate (10 mL x 5). The combined organic layers were washed with saturated aqueous bicarbonate (10 mL) and brine (10 mL) before being dried over Na₂SO₄, filtered, and concentrated under reduced pressure. The crude oil was purified by silica gel flash column chromatography (50 % ethyl acetate in hexanes to ethyl acetate hexanes) to afford triene **126** (23 mg; 0.052 mmol) as a clear pale yellow oil in 68% yield as a 1:1 mixture of diastereomers.

$[\alpha]_D^{25}$: -5.5 (c=1.10, CHCl₃)

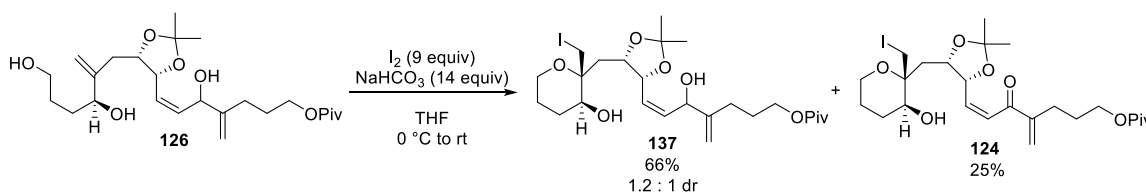
HRMS (NSI): m/z calcd. for C₂₅H₄₂O₇Na [M+Na]⁺: 447.28227 found 447.28259.

IR (neat): 3385, 2931, 2871, 1725, 1648, 1552, 1480, 1457, 1369, 1285, 1250, 1216, 1159, 1044, 976, 901, 795, 773 cm⁻¹.

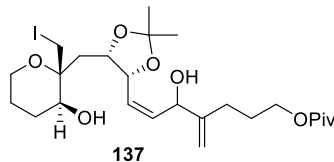
¹H NMR (600 MHz, CDCl₃) δ 5.82 – 5.72 (m, 2H), 5.16 (s, .05H), 5.15 (s, 1H), 5.13 (s, 0.5H), 4.95 (d, $J = 1.3$ Hz, 1H), 4.94 (s, 0.5H), 4.93 (s, 0.5H), 4.68 – 4.62 (m, 2H), 4.37 (dddd, $J = 17.5, 10.0, 6.2, 4.5$ Hz, 1H), 4.11 (m, 1H), 4.08 (td, $J = 6.8, 1.7$ Hz, 2H), 3.68

(m, 2H), 2.34 (ddd, $J = 20.2, 15.0, 9.2$ Hz, 1H), 2.18 – 2.08 (m, 3H), 1.89 – 1.78 (m, 2H), 1.76 – 1.60 (m, 4H), 1.52 (s, 1.5H), 1.51 (s, 1.5H), 1.38 (s, 3H), 1.20 (s, 9H).

^{13}C NMR (151 MHz, CDCl_3) δ 178.93, 149.23, 149.10, 148.35, 148.26, 135.36, 135.15, 127.49, 127.34, 113.20, 112.81, 111.15, 110.97, 108.68, 108.63, 78.75, 78.67, 78.40, 78.27, 75.38, 75.18, 75.04, 64.11, 64.09, 62.91, 38.95, 33.30, 33.26, 32.76, 32.74, 29.88, 29.36, 28.20, 28.16, 28.11, 27.39, 27.13, 27.11, 25.52.



Tetrahydropyrans 137 and 124: A solution of alcohol **126** (23 mg; 0.052 mmol) in THF (1 mL) was cooled to 0 °C before addition of sodium bicarbonate (60 mg; 0.71 mmol) and iodine (120 mg; 0.47 mmol). The reaction warmed to ambient temperature gradually. After 6 hours, the reaction was quenched by addition of saturated aqueous sodium thiosulfate (2 mL). The reaction mixture was diluted with ethyl acetate (2 mL) and the layers were separated. The aqueous layer was extracted with ethyl acetate (4 x 2 mL) and the combined organic extracts were washed with brine before being dried over sodium sulfate, filtered, and concentrated under reduced pressure. The crude oil was purified by silica gel flash column chromatography (15% ethyl acetate in hexanes) to afford iodo-alcohol **137** (20 mg; 0.034 mmol) as a clear light-yellow film in 66% yield a 1:1.2 mixture of diastereomers. COSY, HMBC, and HMQC confirmed the structure. Additionally, enone **124** (7 mg; 0.013 mmol) was obtained in 25% yield.



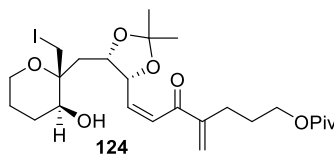
$[\alpha]_D^{25}$: -5.9 (c=1.02, CHCl₃)

HRMS (NSI): m/z calcd. for C₂₅H₄₁O₇INa [M+Na]⁺: 603.17892 found 603.17999.

IR (neat): 3457, 2956, 2925, 2853, 2152, 1726, 1558, 1457, 1371, 1286, 1215, 1162, 1084, 1036, 975, 943, 905, 802 cm⁻¹.

¹H NMR (600 MHz, C₆D₆ * denotes minor diastereomer) δ 5.75 (ddd, *J* = 15.4, 7.7, 1.4 Hz, 0.45H)*, 5.67 (dd, *J* = 15.6, 7.9 Hz, 0.55H), 5.57 (app. t, *J* = 6.2 Hz, 0.55H), 5.55 (app. t, *J* = 6.2 Hz, 0.45H)*, δ 5.16 (s, 0.45H)*, 5.11 (d, *J* = 3.5 Hz, .55H), 4.84 (s, 0.55H), 4.82 (d, *J* = 1.6 Hz, 0.45H)*, 4.52 (m, 1H), 4.38 (dd, *J* = 17.5, 6.8 Hz, 1H), 4.32 (m, 1H), 4.08 (m, 2H), 3.67 (d, *J* = 11.5 Hz, 1H), 3.41 (d, *J* = 11.6 Hz, 1H), 3.37 (m, 1H), 3.05 (br t, *J* = 11.9 Hz, 1H), 2.15 (m, 2H), 2.03 (m, 1H), 1.73 (m, 2H), 1.69 – 1.59 (m, 3H), δ 1.36 (s, 1.65H), 1.35 (s, 1.55H)*, 1.34 (m, 2H), 1.21 (s, 4H)*, 1.20 (s, 5H).

¹³C NMR (151 MHz, C₆D₆) δ 177.85, 149.62, 135.72, 135.50, 111.00, 110.72, 108.47, 79.69, 75.58, 75.32, 75.18, 74.05, 68.90, 64.07, 60.83, 40.33, 40.29, 38.85, 32.37, 32.37, 30.23, 28.37, 28.25, 28.08, 27.55, 27.45, 25.83, 25.60, 14.40, 13.34.

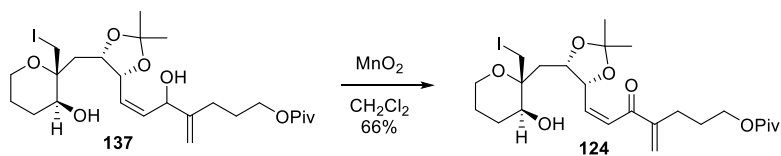


$[\alpha]_D^{25}$: +3.4 (c=0.62, CHCl₃)

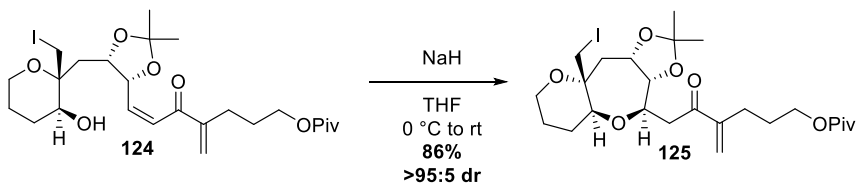
HRMS (APCI): m/z calcd. for C₂₅H₄₀O₇I [M+H]⁺: 579.18132 found 579.18135.

IR (neat): 2933, 2873, 234, 2481, 2365, 2230, 2183, 2046, 1725, 1674, 1561, 1510, 1479, 1370, 1285, 1215, 1162, 1081, 1046, 881 cm^{-1} .

^1H NMR (600 MHz, CDCl_3 5:1 dr major diastereomer reported) δ 6.79 (dd, $J = 11.7, 1.4$ Hz, 1H), 6.16 (dd, $J = 11.7, 8.1$ Hz, 1H), 6.06 (s, 1H), 5.84 (s, 1H), 5.36 (t, $J = 7.2$ Hz, 1H), 4.73 (dd, $J = 10.4, 6.8$ Hz, 1H), 4.25 (m, 1H), 4.06 (m, 2H), 3.87 (d, $J = 11.5$ Hz, 1H), 3.65 (m, 1H), 3.40 (d, $J = 11.5$ Hz, 1H), 3.36 (m, 1H), 2.44 – 2.34 (m, 2H), 1.88 – 1.76 (m, 4H), 1.72 – 1.64 (m, 2H), 1.59 – 1.55 (m, 2H), 1.53 (s, 3H), 1.41 – 1.38 (s, 3H), 1.21 (s, 9H).



Enone 124: Alcohol **137** (11 mg; 0.019 mmol) was dissolved in dichloromethane (2.5 mL) and activated MnO_2 (80 mg; 0.95 mmol) was added. The reaction was stirred at ambient temperature for 16 hours before it was filtered through a pad of Celite. By proton NMR of the crude, enone **124** and alcohol **137** were in a 2:1 ratio, which means that the reaction proceeded to roughly 66% conversion. The crude mixture was used in conjugate addition reactions at which point the alcohol was separated.



Enone 125: The starting dienyl ketone was obtained through iterative runs of iodocyclization and oxidation run on scales similar to scale in the given experimental to run a larger scale reaction. The iodocyclization and NHK coupling to access the triene precursor were not reliable transformations and did not scale up well. Dienyl ketone **124** (44 mg; 0.076 mmol) was dissolved in THF (5 mL) and cooled to 0 °C before addition of sodium hydride (3.3 mg; 0.083 mmol). The reaction was stirred at 0 °C for 2 hours before being quenched with methanol. The solvent was removed under reduced pressure and the resulting film was purified by silica gel column chromatography (40% diethyl ether in pentane) to afford enone **125** (37 mg; 0.65mmol) as a light-yellow oil in 86% yield as a single diastereomer at the newly formed chiral center, although an 85:15 mixture of diastereomers across the AB ring fusion.

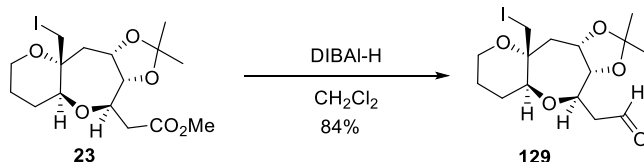
$[\alpha]_D^{25}$: +8.4 (c=1.06, CHCl₃)

HRMS (NSI): m/z calcd. for C₂₅H₃₉O₇INa [M+Na]⁺: 601.16327 found 601.16314.

IR (neat): 2954.01, 2872.79, 2196.07, 1725.88, 168.80, 1480.09, 1452.50, 1367.71, 1345.83, 1283.79, 1211.59, 1158.26, 1121.10, 1105.48, 1079.95, 1038.28, 972.64, 939.06, 884.08 cm⁻¹.

¹H NMR (600 MHz, CDCl₃) δ 6.04 (s, 1H), 5.79 (d, J = 1.3 Hz, 1H), 4.50 (dt, J = 10.4, 5.9 Hz, 1H), 4.04 (t, J = 6.5 Hz, 2H), 4.02 (app. dq, J = 3.3, 2.1, 1.4 Hz, 2H), 3.75 (dd, J = 12.0, 1.9 Hz, 1H), 3.61 (dd, J = 12.6, 5.2 Hz, 1H), 3.57 (dd, J = 12.1, 4.1 Hz, 1H), 3.33 (td, J = 12.3, 2.7 Hz, 1H), 3.05 (d, J = 12.0 Hz, 1H), 2.94 (m, 2H), 2.50 (dd, J = 14.0, 5.9 Hz, 1H), 2.35 (td, J = 7.4, 4.6 Hz, 2H), 1.87 (ddd, J = 13.4, 10.9, 1.9 Hz, 1H), 1.75 (p, J = 7.0 Hz, 2H), 1.72 – 1.62 (m, 3H), 1.41 (s, 3H), 1.35 (s, 3H), 1.20 (s, 9H).

^{13}C NMR (101 MHz, CDCl_3) δ 199.17, 178.71, 148.09, 125.41, 108.82, 84.99, 79.04, 77.76, 73.93, 73.03, 63.73, 59.96, 42.02, 41.83, 38.93, 27.56, 27.52, 27.39, 27.30, 25.93, 25.50, 24.34, 8.32.



Aldehyde 129: To a solution of ester **23** (445 mg; 1.01 mmol) in CH_2Cl_2 (25 mL) was added DIBAL-H (1.10 mL; 1.0 M in hexanes) dropwise. After stirring at room temperature for 2 hours the reaction was cooled to 0 °C, diluted with ether, and quenched by addition of Rochelle's salt (10 mL) and stirred for 4 hours at room temperature. The layers were separated and the aqueous layer was extracted with CH_2Cl_2 (3 x 8 mL). The combined organic layers were washed with water (10 mL x 2), dried over MgSO_4 , filtered, and concentrated under reduced pressure. The resulting crude powder **129** (443 mg; 1.00 mmol) was used without further purification.

$[\alpha]_{\text{D}}^{25}$: -6.4 ($c=1.00$, CHCl_3)

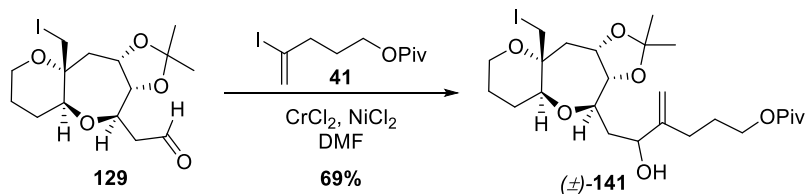
HRMS (NSI): m/z calcd. for $\text{C}_{15}\text{H}_{24}\text{O}_7$ $[\text{M}+\text{H}]^+$: 411.06629 found 411.06620.

IR (neat): 2938.98, 2870.07, 1970.58, 1725.13, 1453.98, 1381.98, 1212.07, 1078.42, 1049.57, 974.94, 880.67 cm^{-1} .

^1H NMR (399 MHz, CDCl_3) δ 9.79 (dd, $J = 2.0, 1.1$ Hz, 1H), 4.52 (dt, $J = 10.8, 6.2$ Hz, 1H), 4.09 – 3.86 (m, 2H), 3.77 (dd, $J = 12.1, 2.0$ Hz, 1H), 3.68 – 3.61 (m, 1H), 3.61 – 3.51 (m, 1H), 3.43 – 3.27 (m, 1H), 3.05 (d, $J = 12.1$ Hz, 1H), 2.91 – 2.71 (m, 1H), 2.61 (ddd, J

= 17.3, 9.0, 2.0 Hz, 1H), 2.54 (dd, $J = 14.0, 6.1$ Hz, 1H), 1.85 (ddd, $J = 14.1, 10.8, 2.0$ Hz, 1H), 1.80 – 1.73 (m, 1H), 1.73 – 1.65 (m, 1H), 1.51 (m, 4.9 Hz, 1H), 1.41 (s, 3H), 1.35 (s, 3H).

^{13}C NMR (101 MHz, CDCl_3) 200.33, 108.927, 85.110, 79.122, 76.543, 73.919, 72.744, 59.921, 47.845, 42.032, 27.286, 26.012, 25.470, 24.326, 7.955. JAH-12-150-C13



Allylic alcohol (\pm) -141: CrCl_2 (80 mg; 0.64 mmol) and NiCl_2 (0.5 mg; 0.03 mmol) were weighed out in a gloved box and the flask was sparged with argon for 10 minutes. The flask was cooled to 0°C and dry DMF (2 mL) was added. The ice bath was removed after 10 minutes and the solvated salts were warmed to room temperature, where vinyl iodide **41** (97 mg; 0.32 mmol) in DMF (0.6 mL) was added in one portion. The reaction mixture was stirred for 15 minutes and then a solution of aldehyde **25** (66 mg; 0.16 mmol) in DMF (0.33 mL) was added dropwise. The resulting suspension was stirred at room temperature for 4 hours. The reaction mixture was diluted with water (15 mL) and extracted with ethyl acetate (10 mL \times 6). The combined organic phase was washed with water (20 mL \times 2) and brine before being dried over Na_2SO_4 and concentrated under reduced pressure. The crude residue was purified by silica gel flash column chromatography (20% ethyl acetate in hexanes to 30% ethyl acetate in hexanes) to afford compound (\pm) -**141** (64 mg; 0.11 mmol) as a clear pale-yellow oil in 69% yield as a 1.5:1 mixture of diastereomers.

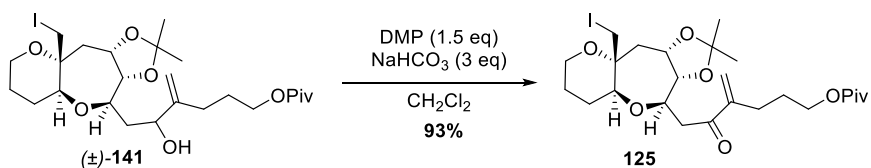
$[\alpha]_D^{25}$: -2.1 ($c=1.03$, CHCl_3)

HRMS (NSI): m/z calcd. for $\text{C}_{25}\text{H}_{42}\text{IO}_7$ $[\text{M}+\text{H}]^+$: 581.19697 found 581.19623.

IR (neat): 3485.11, 2954.03, 2936.96, 2872.07, 1724.85, 1645.51, 1479.99, 1455.78, 128.92, 1211.72, 1161.90, 1119.87, 1105.63, 1045.32, 996.94, 886.01, 799.79, 771.93 cm^{-1} .

^1H NMR (500 MHz, CDCl_3) δ 5.16 (d, $J = 1.3$ Hz, 0.4H), 5.10 (t, $J = 1.2$ Hz, 0.6H), 4.92 (t, $J = 1.3$ Hz, 0.4H), 4.88 (q, $J = 1.5$ Hz, 4.6H), 4.47 (dtd, $J = 11.0, 7.1, 5.9$ Hz, 1H), 4.31 (td, $J = 11.1, 9.6, 5.5$ Hz, 1H), 4.08 (dd, $J = 6.4$ Hz, 2H), 3.99 (ddd, $J = 9.7, 7.1, 5.8$ Hz, 1H), 3.76 (dt, $J = 12.2, 2.3$ Hz, 1H), 3.68 (dd, $J = 9.8, 2.4$ Hz, 0.4H), 3.63 (m, 1H), 3.57 (td, $J = 9.8, 2.6$ Hz, 0.6H), 3.48 (ddd, $J = 14.9, 11.8, 4.4$ Hz, 1H), 3.42 – 3.32 (m, 1H), 3.06 (dd, $J = 12.1, 6.0$ Hz, 1H), 2.49 (dt, $J = 14.0, 5.4$ Hz, 1H), 2.16 (qd, $J = 15.6, 14.4, 7.9$ Hz, 1H), 2.06 (m, 1H), 1.96 (m, 1H), 1.88 – 1.77 (m, 4H), 1.74 – 1.67 (m, 2H), 1.67 – 1.55 (m, 1H), 1.41 (s, 3H), 1.34 (s, 3H), 1.20 (s, 9H).

^{13}C NMR (126 MHz, CDCl_3) δ 178.73, 150.91, 150.08, 110.60, 109.66, 108.70, 108.67, 85.25, 85.01, 82.22, 79.83, 79.51, 79.33, 74.67, 73.88, 73.76, 72.92, 72.77, 71.76, 64.14, 64.01, 59.85, 53.95, 42.14, 42.07, 39.38, 38.93, 38.46, 31.94, 29.88, 29.45, 28.62, 27.54, 27.30, 27.18, 26.30, 25.52, 25.46, 24.37, 24.30, 7.90, 7.58.



Enone 125: To a stirred solution of allylic alcohol (\pm)-**141** (60 mg; 0.10 mmol) in CH₂Cl₂ (3 mL) was added DMP (44 mg; 0.10 mmol) and NaHCO₃ (17 mg; 0.21 mmol). After 2.5 hours, additional DMP (27 mg; 0.06 mmol) was added. After one hour, the reaction was poured into solution of aqueous Na₂S₂O₃ (5 g) and saturated aqueous NaHCO₃ (5 mL). The suspension was stirred for 30 minutes until the layers turned clear upon standing. The layers were separated and the aqueous layer was extracted with and CH₂Cl₂ (5 mL x 3). The combined organic extracts were washed with saturated aqueous NaHCO₃ (5 mL), water (5 mL), dried over MgSO₄, filtered, and concentrated under reduced pressure to afford enone **125** (54 mg; 0.09 mmol) in 93% yield.

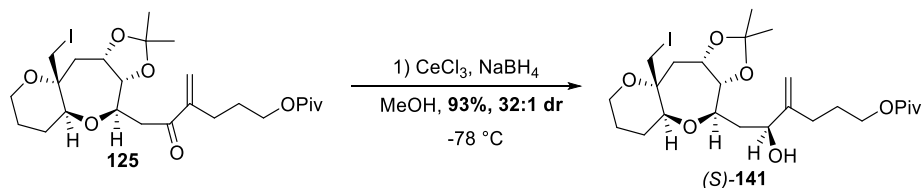
$[\alpha]_D^{25}$: +8.4 (c=1.06, CHCl₃)

HRMS (NSI): m/z calcd. for C₂₅H₃₉O₇INa [M+Na]⁺: 601.16327 found 601.16314.

IR (neat): 2954.01, 2872.79, 2196.07, 1725.88, 168.80, 1480.09, 1452.50, 1367.71, 1345.83, 1283.79, 1211.59, 1158.26, 1121.10, 1105.48, 1079.95, 1038.28, 972.64, 939.06, 884.08 cm⁻¹.

¹H NMR (600 MHz, CDCl₃) δ 6.04 (s, 1H), 5.79 (d, J = 1.3 Hz, 1H), 4.50 (dt, J = 10.4, 5.9 Hz, 1H), 4.04 (t, J = 6.5 Hz, 2H), 4.02 (dq, J = 3.3, 2.1, 1.4 Hz, 2H), 3.75 (dd, J = 12.0, 1.9 Hz, 1H), 3.61 (dd, J = 12.6, 5.2 Hz, 1H), 3.57 (dd, J = 12.1, 4.1 Hz, 1H), 3.33 (td, J = 12.3, 2.7 Hz, 1H), 3.05 (d, J = 12.0 Hz, 1H), 2.94 (m, 2H), 2.50 (dd, J = 14.0, 5.9 Hz, 1H), 2.35 (td, J = 7.4, 4.6 Hz, 2H), 1.87 (ddd, J = 13.4, 10.9, 1.9 Hz, 1H), 1.75 (p, J = 7.0 Hz, 2H), 1.72 – 1.62 (m, 3H), 1.41 (s, 3H), 1.35 (s, 3H), 1.20 (s, 9H).

^{13}C NMR (101 MHz, CDCl_3) δ 199.17, 178.71, 148.09, 125.41, 108.82, 84.99, 79.04, 77.76, 73.93, 73.03, 63.73, 59.96, 42.02, 41.83, 38.93, 27.56, 27.52, 27.39, 27.30, 25.93, 25.50, 24.34, 8.32.



Alcohol (S)-141: To a stirred solution of enone **125** (119 mg; 0.204 mmol) in MeOH (2 mL) at -78°C were added $\text{CeCl}_3 \cdot 7 \text{H}_2\text{O}$ (96 mg; 0.26 mmol) and NaBH_4 (9.8 mg; 0.26 mmol). After stirring at -78°C for 1.5 hours, the reaction was quenched at low temperature by addition of acetone (0.5 mL) and allowed to warm to room temperature. The reaction mixture was concentrated under reduced pressure before being diluted saturated aqueous ammonium chloride (2 mL) and ethyl acetate (2 mL). The layers were separated and the aqueous later was extracted with ethyl acetate (3 mL X 3). The combined organic extracts were washed with brine, dried over MgSO_4 , filtered, and concentrated under reduced pressure. The crude residue was purified by silica gel flash column chromatography (20% ethyl acetate in hexanes to 25% ethyl acetate in hexanes) to afford compound **(S)-141** (110 mg; 0.189 mmol) as a clear pale-yellow oil in 93% yield S-alcohol as a 32:1 mixture of diastereomers in 93% yield.

$[\alpha]_{\text{D}}^{25}$: -7.3 ($c=1.02$, CHCl_3)

HRMS (NSI): m/z calcd. for $\text{C}_{25}\text{H}_{42}\text{IO}_7$ $[\text{M}+\text{H}]^+$: 581.19697 found 581.19781.

IR (neat): 3504, 2954, 2935, 2872, 2360, 2342, 1726, 1457, 1381, 1285, 1080 cm^{-1} .

¹H NMR (500 MHz, CDCl₃) δ 5.10 (t, *J* = 1.2 Hz, 1H), 4.88 (q, *J* = 1.5 Hz, 1H), 4.46 (ddd, *J* = 11.0, 7.1, 5.9 Hz, 1H), 4.32 (dd, *J* = 8.4, 4.0 Hz, 1H), 4.09 (t, *J* = 6.5 Hz, 2H), 3.98 (dd, *J* = 9.7, 7.1 Hz, 1H), 3.76 (dd, *J* = 12.1, 1.9 Hz, 1H), 3.63 (dt, *J* = 12.7, 2.8 Hz, 1H), 3.57 (td, *J* = 9.9, 2.6 Hz, 1H), 3.50 (dd, *J* = 11.9, 4.5 Hz, 1H), 3.36 (ddd, *J* = 12.4, 8.3, 5.9 Hz, 1H), 3.09 (s, 1H), 3.05 (d, *J* = 12.1 Hz, 1H), 2.50 (dd, *J* = 14.0, 5.8 Hz, 1H), 2.23 – 2.18 (m, 1H), 2.09 – 2.02 (m, 2H), 1.88 – 1.78 (m, 4H), 1.71 (app. qd, *J* = 6.4, 2.5 Hz, 2H), 1.68 – 1.56 (m, 2H), 1.41 (s, 3H), 1.34 (s, 3H), 1.20 (s, 9H).

¹³C NMR (126 MHz, CDCl₃) δ 178.74, 150.08, 110.59, 108.69, 85.25, 82.21, 79.83, 74.66, 73.76, 72.77, 64.13, 59.83, 42.14, 39.39, 38.93, 27.41, 27.30, 26.30, 25.46, 24.30, 7.59.

Table 6. MTPA-ester data for compound (*S*)-**141**

#	δ <i>S</i> -ester (ppm)	δ <i>R</i> -ester (ppm)	ppm	Hz (600 MHz)
5.12	5.21	5.14	0.07	42
4.89	5.11	5.05	0.06	36
2.06	2.13	2.08	0.05	30
4.33	5.69	5.67	0.02	12
3.77	3.77	3.77	0	0
3.77	2.5	2.5	0	0
2.51	3.62	3.63	-0.01	-6
3.64	3.35	3.36	-0.01	-6
3.37	3.04	3.07	-0.03	-18
3.99	3.95	4	-0.05	-30

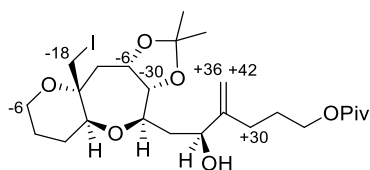
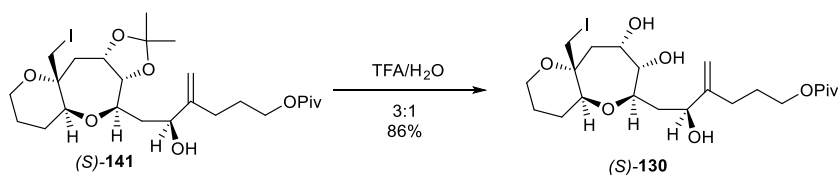


Figure 20. MTPA-ester data for compound (*S*)-**141**



Triol (*S*)-130: To a vial containing compound (*S*)-**141** (44 mg; .075 mmol) was added TFA/H₂O (3:1; 1 mL). The reaction was stirred for 15 minutes, at which point the reaction mixture was cooled to 0 °C before slow addition of saturated aqueous sodium bicarbonate solution (4 mL) and dilution with ethyl acetate (2 mL). The biphasic mixture was stirred for 30 minutes before the layers were separated. The aqueous layer was extracted with ethyl acetate (5 mL x 5). The combined organic extracts were washed with brine, and dried over Na₂SO₄ before being filtered and concentrated under reduced pressure. The crude residue was purified by silica gel flash column chromatography (50% ethyl acetate in hexanes to 75% ethyl acetate in hexanes) to afford compound (*S*)-**141** (35 mg; 0.065 mmol) as a clear pale-yellow film in 86% yield. The (*R*)-diastereomer was isolated from deprotection of the coupling adduct, without going through the oxidation-reduction sequence.

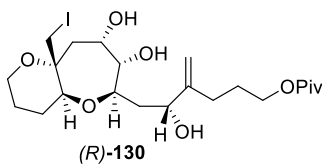
$[\alpha]_D^{25}$: +20.1 (c=1.01, CHCl₃)

IR (neat): 3479 (br), 1722, 1479, 1283, 1158, 802 cm⁻¹.

HRMS (NSI): m/z calcd. for $C_{22}H_{37}IO_7Na$ $[M+Na]^+$: 563.14762 found 563.14745.

1H NMR (600 MHz, $CDCl_3$) δ 5.11 (s, 1H), 4.88 (q, $J = 1.4$ Hz, 1H), 4.29 (dd, $J = 8.7, 3.5$ Hz, 1H), 4.09 (td, $J = 6.6, 2.5$ Hz, 2H), 3.96 (ddd, $J = 10.3, 3.7, 1.9$ Hz, 1H), 3.89 (ddd, $J = 9.8, 4.0, 2.6$ Hz, 1H), 3.86 (m, 2H), 3.79 (dd, $J = 11.9, 1.9$ Hz, 1H), 3.62 (ddd, $J = 10.8, 5.1, 3.0$ Hz, 1H), 3.45 (d, $J = 11.9$ Hz, 1H), 3.34 (d, $J = 11.8$ Hz, 1H), 3.33 (m, 1H), 2.23 – 1.99 (m, 4H), 1.91 – 1.75 (m, 4H), 1.75 – 1.64 (m, 2H), 1.51 (m, 2H), 1.21 (s, 9H).

^{13}C NMR (126 MHz, $CDCl_3$) δ 179.00, 149.69, 110.74, 83.74, 79.12, 77.88, 74.43, 73.39, 68.34, 64.14, 60.15, 42.23, 40.79, 38.97, 27.77, 27.24, 26.38, 25.18, 10.32.



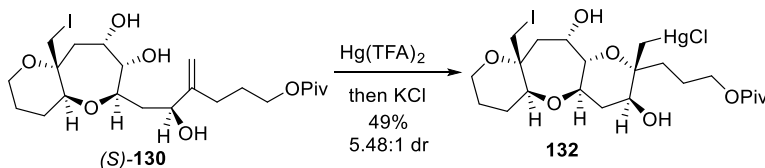
$[\alpha]_D^{25}$: -7.0 ($c=0.827$, $CHCl_3$)

IR (neat): 3406 (br), 2955, 2922, 1480, 1275, 1161, 763 cm^{-1} .

HRMS (APCI): m/z calcd. for $C_{22}H_{38}O_7I$ $[M+H]^+$: 541.16567 found 541.16433.

1H NMR (600 MHz, $CDCl_3$) δ 5.17 (t, $J = 1.2$ Hz, 1H), 4.96 (q, $J = 1.3$ Hz, 1H), 4.26 (dd, $J = 6.9, 2.6$ Hz, 1H), 4.13 (dt, $J = 10.9, 6.7$ Hz, 1H), 4.08 (dt, $J = 10.8, 6.4$ Hz, 1H), 3.96 (ddd, $J = 10.6, 3.2, 2.2$ Hz, 1H), 3.92 (dt, $J = 9.8, 3.1$ Hz, 1H), 3.85 (t, $J = 2.4$ Hz, 1H), 3.81 (ddd, $J = 11.9, 6.9, 3.4$ Hz, 2H), 3.62 (ddd, $J = 13.8, 4.9, 1.9$ Hz, 1H), 3.44 (d, $J = 11.9$ Hz, 1H), 3.34 (td, $J = 11.8, 4.1$ Hz, 1H), 2.18 – 2.09 (m, 3H), 2.09 – 1.99 (m, 1H), 1.91 – 1.78 (m, 4H), 1.67 (m, 3H), 1.57 – 1.42 (m, 1H), 1.21 (s, 9H).

^{13}C NMR (126 MHz, CDCl_3) δ 179.04, 149.93, 110.16, 81.66, 79.14, 78.23, 73.43, 72.27, 68.62, 64.01, 60.18, 42.47, 39.34, 39.01, 27.43, 27.11, 26.52, 25.26, 10.23.

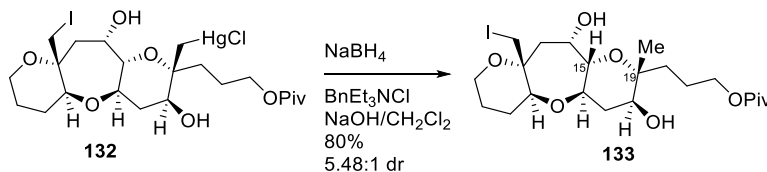


Organomercury 131: $\text{Hg}(\text{O}_2\text{CCF}_3)_2$ (48 mg; 0.088 mmol) was added to a solution of compound (*S*)-**130** (32 mg; 0.059 mmol) in THF (1.2 mL) at 0 °C. The ice bath was removed after 5 minutes and the reaction was stirred at ambient temperature for 2 hours before addition of saturated aqueous KCl (60 μL) and stirring for an additional 1.5 hours. The reaction mixture was diluted with water (1 mL) and ethyl acetate (2 mL). The layers were separated and the organic layer was extracted with ethyl acetate (2 mL x 3). The combined organic extracts were washed with brine, dried over Na_2SO_4 , filtered, and concentrated under reduced pressure. The crude oil was purified by silica gel flash column chromatography (35% ethyl acetate in hexanes to 45% ethyl acetate in hexanes) to afford organomercurial intermediate **132** (0.028 mmol; 22 mg) in addition another slightly more polar product in 45 % yield (calc'd assuming mercury incorporation, 21 mg; 0.027 mmol). The other product underwent decomposition upon attempted demercuration when following the same protocol that was successful for compound **132**. The *dr* was determined from integration of the methyl substituents from the demercurated compound as it was not clear from the organomercurial compound. ^1H NMR, ^{13}C NMR, and 2D spectra are in Section 3.6. HRMS was complicated by the multiple isotopes of mercury in high abundance.

IR (neat): 3426, 2957, 2854, 2360, 2342, 1725, 1554, 1480, 1285, 1160, 1082, 1014 cm^{-1} .

^1H NMR (600 MHz, C_6D_6) δ 4.13 (dd, $J = 11.9, 5.0$ Hz, 1H), 4.05 (dt, $J = 10.7, 7.1$ Hz, 1H), 3.93 (dt, $J = 10.6, 6.8$ Hz, 1H), 3.86 (t, $J = 4.8$ Hz, 1H), 3.73 (d, $J = 11.5$ Hz, 1H), 3.50 (ddd, $J = 11.6, 9.4, 4.7$ Hz, 1H), 3.43 (d, $J = 11.6$ Hz, 1H), 3.40 (dd, $J = 12.7, 5.0$ Hz, 1H), 3.10 (dd, $J = 12.0, 4.5$ Hz, 1H), 3.03 (dd, $J = 9.5, 1.8$ Hz, 1H), 2.95 (td, $J = 12.5, 2.4$ Hz, 1H), 2.39 (dd, $J = 16.1, 4.9$ Hz, 1H), 2.20 (dd, $J = 16.2, 4.4$ Hz, 1H), 1.75 (dt, $J = 12.0, 4.6$ Hz, 1H), 1.63 (d, $J = 14.5$ Hz, 1H), 1.49 (m, 2H), 1.42 – 1.24 (m, 3H), 1.21 (s, 9H), 1.11 – 1.06 (m, 1H), 1.01 – 0.89 (m, 1H), 0.82 (d, $J = 12.0$ Hz, 1H).

^{13}C NMR (151 MHz, C_6D_6) δ 178.3, 79.4, 77.1, 76.0, 75.3, 72.7, 70.1, 67.9, 64.3, 60.0, 46.0, 36.9, 35.0, 29.9, 27.1, 26.8, 26.1, 25.1, 22.3, 14.9.



Demercurated 133: Organomercury **132** (12 mg; 0.016 mmol) was added to a 0.3 mL conical vial containing CH_2Cl_2 (40 μL). Benzyl triethylammonium chloride (14 mg; 0.061 mmol) and 10% aqueous sodium hydroxide (150 μL) were added and the resulting biphasic mixture was rapidly stirred before addition of NaBH_4 (0.012 mmol in 25 μL in 10% aqueous NaOH). The biphasic mixture continued stirring for 10 minutes, at which time it was diluted with water (1 mL) and CH_2Cl_2 (1 mL). The layers were separated and the aqueous layer was washed with CH_2Cl_2 (3 x 1 mL). The combined organic extracts were dried over Na_2SO_4 , filtered, and concentrated under reduced pressure to afford a crude oil.

The crude compound was purified by silica gel flash column chromatography (30% - 40% ethyl acetate in hexanes) to afford **133** as a clear pale-yellow oil in 80 % yield as a 5.48:1 dr. COSY, HMBC, and HMQC support the structural assignment and NOE supports the axial methyl assignment. ^1H NMR, ^{13}C NMR, and 2D spectra are in Section 3.6.

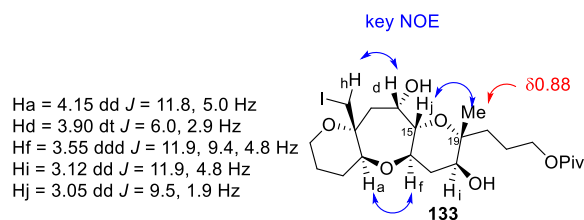


Figure 21. Key NOE correlations of compound **133**

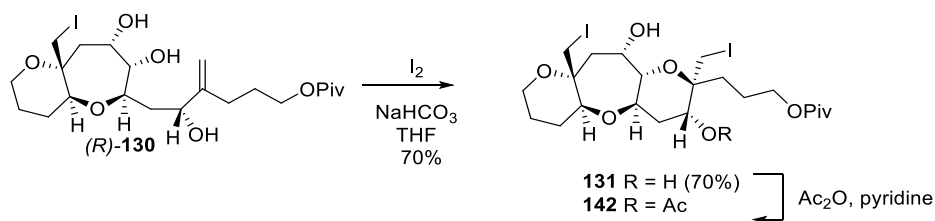
$[\alpha]_{\text{D}}^{25}$: -15.7 ($c=0.60$, CHCl_3)

IR (neat): 3465 (br), 2956, 2925, 2854, 1721, 1462, 1261, 1158, 1015, 798 cm^{-1} .

HRMS (NSI): m/z calcd. for $\text{C}_{22}\text{H}_{38}\text{IO}_7$ $[\text{M}+\text{H}]^+$: 541.16567 found 541.16631.

^1H NMR (600 MHz, C_6D_6) δ 4.18 – 4.11 (m, 2H), 3.98 (dt, $J = 10.6, 6.8$ Hz, 1H), 3.90 (dt, $J = 4.6, 3.0$ Hz, 1H), 3.68 (d, $J = 11.5$ Hz, 1H), 3.55 (ddd, $J = 11.6, 9.4, 4.7$ Hz, 1H), 3.40 (dd, $J = 12.2, 5.0$ Hz, 1H), 3.33 (d, $J = 11.5$ Hz, 1H), 3.12 (dd, $J = 11.7, 4.7$ Hz, 1H), 3.05 (dd, $J = 9.4, 1.9$ Hz, 1H), 2.93 (td, $J = 12.4, 2.5$ Hz, 1H), 2.36 (dd, $J = 16.0, 4.8$ Hz, 1H), 2.26 (dd, $J = 16.1, 4.6$ Hz, 1H), 1.92 (dt, $J = 11.8, 4.7$ Hz, 1H), 1.61 (p, $J = 7.2$ Hz, 3H), 1.55 – 1.44 (m, 2H), 1.42 – 1.27 (m, 5H), 1.19 (s, 9H), 0.87 (s, 3H).

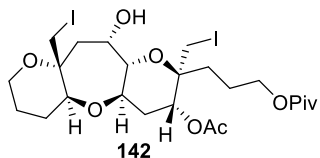
^{13}C NMR (151 MHz, C_6D_6) δ 178.5, 77.9, 76.9, 76.7, 76.3, 73.8, 71.1, 71.0, 65.2, 60.7, 46.6, 36.4, 35.9, 27.7, 27.4, 25.8, 23.2, 15.9.



Tetrahydropyran 131: A solution of alcohol (*R*)-**130** (9 mg; 0.017 mmol) in THF (1.5 mL) was cooled to 0 °C before addition of sodium bicarbonate (14 mg; 0.16 mmol) and iodine (26 mg; 0.10 mmol). The reaction warmed to ambient temperature gradually. After 10 hours, the reaction was quenched by addition of saturated aqueous sodium thiosulfate (2 mL). The reaction mixture was diluted with ethyl acetate (2 mL) and the layers were separated. The aqueous layer was extracted with ethyl acetate (4 x 2 mL) and the combined organic extracts were washed with brine before being dried over sodium sulfate, filtered, and concentrated under reduced pressure. The crude oil was purified by silica gel flash column chromatography (50% ethyl acetate in hexanes) to afford iodo-product **131** (7 mg; 0.012 mmol) in 70 % yield.

HRMS (NSI): m/z calcd. for $\text{C}_{22}\text{H}_{37}\text{O}_7\text{I}_2$ $[\text{M}+\text{H}]^+$: 667.06232 found 667.06346.

$^1\text{H NMR}$ (600 MHz, CDCl_3) δ 4.15 (dd, $J = 12.0, 4.9$ Hz, 1H), 4.11 (td, $J = 5.4, 2.0$ Hz, 2H), 4.04 (td, $J = 12.2, 11.0, 4.7$ Hz, 1H), 3.98 (t, $J = 3.2$ Hz, 1H), 3.87 (d, $J = 11.5$ Hz, 1H), 3.64 (dd, $J = 12.7, 4.7$ Hz, 1H), 3.41 (dd, $J = 10.0, 1.7$ Hz, 1H), 3.26 (dd, $J = 9.1, 2.8$ Hz, 1H), 3.25 (d, $J = 11.4$ Hz, 1H), 3.12 (d, $J = 10.1$ Hz, 1H), 2.26 – 2.21 (m, 1H), 2.21 – 2.15 (m, 2H), 2.09 – 2.02 (m, 1H), 1.95 – 1.75 (m, 4H), 1.68 (m, 2H), 1.58 (m, 2H), 1.25 (s, 9H).



Compound **131** was dissolved in CH₂Cl₂ (1 mL), and Ac₂O (0.1 mL) and pyridine (0.1 mL) were added. The reaction mixture was stirred overnight. The crude product was concentrated under reduced pressure and purified by silica gel flash column chromatography to afford the acetate ester **142** as a yellow oil.

$[\alpha]_D^{25}$: -10.5 (c=0.327, CHCl₃)

IR (neat): 3477, 2958, 2925, 2854, 1729, 1460, 1259, 1241, 1316, 1028, 797 cm⁻¹.

HRMS (APCI): m/z calcd. for C₂₄H₃₉O₈I₂ [M+H]⁺: 709.07288 found 709.07025.

¹H NMR (600 MHz, C₆D₆) δ 5.00 (t, J = 3.1 Hz, 1H), 4.19 (dd, J = 11.8, 4.9 Hz, 1H), 4.06 (ddd, J = 11.9, 9.3, 4.6 Hz, 1H), 3.85 (m, 3H), 3.67 (d, J = 11.4 Hz, 1H), 3.35 (dd, J = 12.5, 4.7 Hz, 1H), 3.28 (d, J = 11.4 Hz, 1H), 3.15 (app. ddd, J = 18.3, 9.9, 1.8 Hz, 2H), 2.91 (td, J = 12.5, 2.7 Hz, 1H), 2.85 (d, J = 10.2 Hz, 1H), 2.38 (dt, J = 14.5, 4.0 Hz, 1H), 2.31 (dd, J = 16.2, 4.4 Hz, 1H), 1.66 (s, 3H), 1.41 – 1.29 (m, 8H), 1.27 (s, 9H).

¹³C NMR (151 MHz, C₆D₆) δ 177.25, 168.87, 77.68, 77.32, 75.86, 75.78, 71.40, 70.72, 69.99, 63.16, 60.10, 45.94, 38.56, 29.85, 29.47, 27.28, 25.09, 22.77, 21.19, 20.16, 14.83, 6.92.

3.5 X-RAY data of compounds 78 and 84

X-RAY data of compound 78

Single colorless needle-shaped crystals of **78** (JAH-7-208-1) were recrystallized from a mixture of benzene and heptane by slow evaporation. A suitable crystal (1.14×0.19×0.09) was selected and mounted on a loop with paratone oil on a Bruker APEX-II CCD diffractometer. The crystal was cooled to $T = 110(2)$ K during data collection. The structure was solved with the **ShelXS-97** (Sheldrick, 2008) structure solution program using **Olex2** (Dolomanov et al., 2009), using the Direct Methods solution method. The structure was refined with version of **ShelXL-97** (Sheldrick, 2008) using Least Squares minimization.

Crystal Data. $C_{64}H_{106}O_{29}$, $M_r = 1339.48$, monoclinic, I2 (No. 5), $a = 19.911 \text{ \AA}$, $b = 5.551 \text{ \AA}$, $c = 30.35 \text{ \AA}$, $\beta = 95.908(8)^\circ$, $\alpha = \gamma = 90^\circ$, $V = 3337(3) \text{ \AA}^3$, $T = 110(2) \text{ K}$, $Z = 2$, $Z' = 0.5$, $\mu(\text{MoK}\alpha) = 0.105$, 16419 reflections measured, 8035 unique ($R_{int} = 0.0417$) which were used in all calculations. The final wR_2 was 0.1229 (all data) and R_I was 0.0530 ($I > 2(I)$).

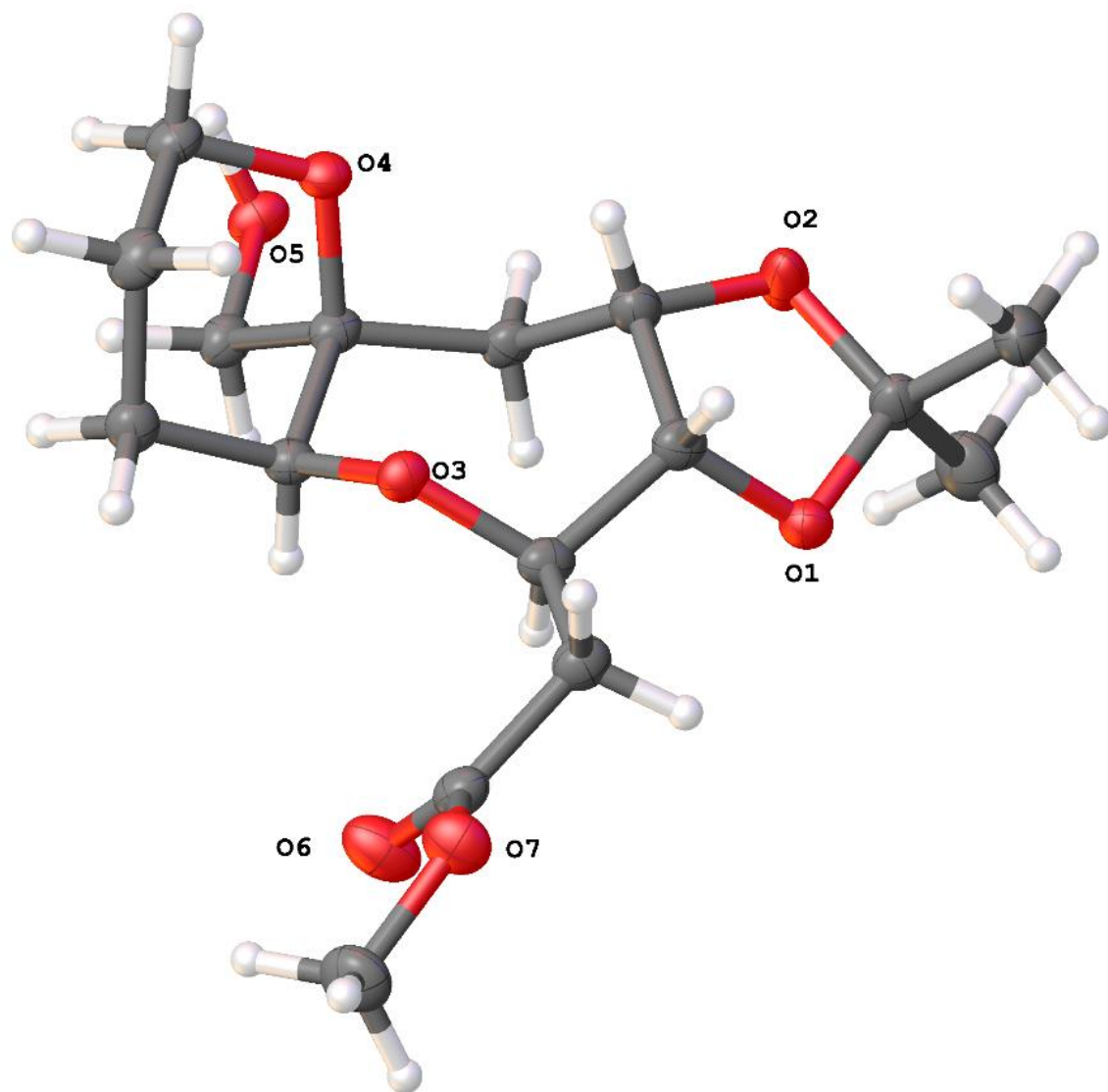


Table 7. Crystal data and structure refinement for compound **78**

Molecular formula	(C ₁₆ H ₂₆ O ₇) ₄ • H ₂ O
Empirical formula	(C ₁₆ H ₂₆ O ₇) ₄ • H ₂ O
<i>D</i> _{calc.} / g cm ⁻³	1.333
μ /mm ⁻¹	0.105
Formula Weight	1339.48
Colour	colorless
Shape	needle
Max Size/mm	1.14
Mid Size/mm	0.19
Min Size/mm	0.09
<i>T</i> /K	110(2)
Crystal System	monoclinic
Space Group	I2
<i>a</i> /Å	19.911(10)
<i>b</i> /Å	5.551(3)
<i>c</i> /Å	30.35(2)
ALPHA/°	90
BETA/°	95.908(8)
GAMMA/°	90
<i>V</i> /Å ³	3337(3)
<i>Z</i>	2
<i>Z'</i>	0.5

θ_{min}°	1.170
θ_{max}°	28.344
Measured Refl.	16419
Independent Refl.	8035
Reflections Used	6424
R_{int}	0.0417
Parameters	539
Restraints	88
Largest Peak	0.319
Deepest Hole	-0.245
Goof	1.064
wR_2 (all data)	0.1229
wR_2	0.1138
R_1 (all data)	0.0694
R_1	0.0530

Table 8. Fractional Atomic Coordinates ($\times 10^4$) and Equivalent Isotropic Displacement Parameters ($\text{\AA}^2 \times 10^3$) for compound **78**. U_{eq} is defined as 1/3 of the trace of the orthogonalized U_{ij} .

Atom	x	y	z	U_{eq}
O4B	4414.1(10)	4033(4)	5957.0(7)	18.9(4)
O1W	5000	4182(6)	5000	18.8(6)
O3B	3974.2(9)	2566(4)	6834.6(6)	18.9(4)

Atom	x	y	z	<i>U_{eq}</i>
O1B	5555.2(10)	3824(4)	7482.8(7)	23.3(5)
O4	7936.6(10)	4926(4)	9295.4(7)	20.1(5)
O1	6057.5(10)	2714(4)	10181.3(7)	22.7(5)
O3	6633.8(9)	2265(4)	9092.3(7)	19.8(5)
O5B	5308.0(11)	687(4)	5601.0(7)	23.5(5)
O5	8965.8(10)	2257(5)	9789.6(7)	22.5(5)
O2B	5875.7(10)	5864(5)	6885.1(7)	26.0(5)
O6	4940.2(11)	-787(5)	8626.2(7)	29.5(6)
O7B	3635.0(12)	-1455(5)	7473.5(9)	33.1(6)
O2	6932.3(11)	5235(5)	10372.9(8)	33.2(6)
O6B	3147.2(12)	997(6)	7927.6(8)	40.1(7)
O7	5848.5(12)	-2607(5)	8963.1(8)	36.8(6)
C14B	3610.0(15)	432(7)	7656.1(10)	25.5(7)
C4	6238.2(15)	1617(6)	9438.1(11)	21.0(7)
C14	5478.4(15)	-925(6)	8930.1(10)	22.6(7)
C5	7292.2(15)	1245(6)	9106.9(10)	18.9(6)
C6	7806.5(14)	2536(6)	9440(1)	18.7(6)
C5B	4071.3(15)	990(6)	6473.6(10)	19.3(6)
C1B	6097.7(15)	5182(6)	7334.7(10)	23.0(7)
C4B	4460.2(14)	2367(6)	7210.8(10)	19.3(6)
C3B	4958.8(15)	4399(6)	7202.8(10)	19.7(6)
C9	7478.5(16)	1443(6)	8633.7(11)	22.4(7)

Atom	x	y	z	U_{eq}
C2B	5222.8(14)	4840(6)	6759.6(10)	19.1(6)
C6B	4627.3(15)	1893(6)	6193.5(10)	19.1(6)
C3	6267.9(15)	3617(6)	9777.9(11)	21.4(7)
C10	7554.9(14)	2854(6)	9894.9(10)	19.9(7)
C10B	5279.9(14)	2632(6)	6474.2(10)	19.2(6)
C2	6973.1(15)	4600(6)	9917.4(11)	22.8(7)
C16	8463.4(15)	1092(6)	9496.5(10)	20.7(6)
C13B	4092.0(15)	2488(7)	7621.8(10)	22.6(7)
C13	5528.2(15)	1233(7)	9224.0(11)	24.1(7)
C9B	3388.4(15)	832(7)	6202.4(11)	23.0(7)
C16B	4802.4(16)	-73(6)	5867.3(10)	22.3(7)
C8B	3218.2(16)	3161(7)	5962.8(11)	24.9(7)
C7B	3783.9(16)	3842(7)	5689.9(11)	23.9(7)
C7	8133.7(16)	5089(6)	8854.3(11)	22.6(7)
C8	7595.2(17)	4055(7)	8520.5(11)	26.9(7)
C1	6314.7(15)	4349(7)	10514.7(11)	26.2(7)
C12	5833.6(18)	6427(7)	10549.5(12)	32.1(8)
C12B	6220.3(17)	7431(7)	7607.0(11)	29.3(7)
C11B	6707.2(16)	3599(7)	7342.6(12)	28.7(8)
C11	6465.8(18)	3010(8)	10941.2(11)	34.2(9)
C15	4813.5(19)	-2908(8)	8358.3(12)	35.4(9)
C15B	2655(2)	-849(10)	7996.4(16)	56.4(13)

Table 9. Anisotropic Displacement Parameters ($\times 10^4$) for compound **78**. The anisotropic displacement factor exponent takes the form: $-2\pi^2[a^{*2} \times U_{11} + \dots 2hka^* \times b^* \times U_{12}]$

Atom	U_{11}	U_{22}	U_{33}	U_{23}	U_{13}	U_{12}
O4B	19.4(10)	18.1(11)	18.9(10)	1.6(9)	-0.4(8)	1.2(9)
O1W	16.0(14)	18.7(16)	21.2(15)	0	-1.1(12)	0
O3B	17.6(10)	21.1(11)	17.7(10)	0.1(10)	0.7(8)	1.7(9)
O1B	20.1(11)	27.0(12)	21.8(11)	4.4(10)	-2.8(8)	-5.5(10)
O4	20.4(10)	17.1(11)	22.8(11)	1(1)	2.3(8)	-0.8(9)
O1	22.0(11)	22.0(12)	24.4(11)	-2.8(10)	3.2(8)	-3.0(9)
O3	15.5(10)	21.5(11)	22.1(10)	0.7(10)	0.7(8)	0.1(9)
O5B	26.3(11)	23.6(12)	21.6(11)	4.6(10)	7.1(9)	8(1)
O5	16.1(10)	25.6(12)	25.3(11)	5.6(11)	-1.1(8)	-1.1(9)
O2B	22.3(11)	31.1(14)	23.7(11)	7.6(11)	-1.4(9)	-6.6(10)
O6	28.2(12)	31.4(14)	26.9(12)	-2.4(11)	-6.2(9)	-0.4(11)
O7B	33.7(13)	23.5(13)	42.6(15)	0.2(12)	6.7(11)	-5.4(10)
O2	25.0(12)	44.3(16)	31.7(12)	-19.3(12)	10(1)	-12.2(11)
O6B	35.9(14)	53.8(18)	33.4(13)	-11.8(14)	16.7(11)	-18.9(13)
O7	35.2(14)	29.1(14)	43.5(15)	-7.0(13)	-8.5(11)	3.1(12)
C14B	22.1(16)	34(2)	20.2(16)	4.6(16)	-0.7(12)	-2.3(14)
C4	16.4(14)	19.2(16)	27.0(17)	1.5(14)	-0.5(12)	0.0(12)
C14	20.8(15)	25.5(18)	21.5(16)	1.6(15)	2.3(12)	-5.2(14)
C5	19.1(15)	17.5(16)	19.8(15)	1.3(13)	0.6(11)	-0.9(12)
C6	15.9(13)	16.9(15)	23.1(15)	3.0(14)	1.3(11)	0.4(12)
C5B	21.8(15)	16.9(16)	19.4(15)	0.3(13)	3.6(12)	0.5(12)

Atom	U_{11}	U_{22}	U_{33}	U_{23}	U_{13}	U_{12}
C1B	21.1(15)	26.3(17)	20.9(15)	2.6(15)	-1.6(12)	-3.3(13)
C4B	16.3(14)	20.5(16)	20.4(14)	0.1(14)	-1.4(11)	-0.8(13)
C3B	18.8(14)	19.6(16)	20.3(15)	-0.3(13)	-0.8(11)	0.4(12)
C9	19.2(15)	25.1(17)	22.5(16)	-1.4(14)	0.4(12)	0.0(13)
C2B	14.0(14)	21.1(16)	22.0(15)	5.2(14)	0.7(11)	-0.8(12)
C6B	20.1(15)	19.3(16)	18.3(15)	0.4(13)	3.4(12)	2.7(12)
C3	16.0(14)	21.7(17)	26.2(16)	0.2(14)	1.0(12)	0.6(12)
C10	14.9(14)	23.7(17)	20.6(15)	-0.1(14)	0.3(11)	-3.4(12)
C10B	16.7(14)	22.5(16)	18.7(15)	5.3(14)	3.7(11)	1.7(13)
C2	20.2(15)	23.9(18)	24.6(17)	-4.2(14)	3.2(12)	-2.7(13)
C16	18.0(14)	21.8(16)	22.3(16)	3.2(14)	2.0(12)	2.2(13)
C13B	22.1(15)	25.6(17)	19.7(15)	1.3(15)	0.8(12)	-0.5(14)
C13	20.0(16)	26.0(17)	26.0(17)	1.6(15)	1.2(12)	-1.1(13)
C9B	21.1(15)	27.3(18)	20.8(15)	-3.6(15)	3.7(12)	-5.5(13)
C16B	27.2(16)	20.7(16)	19.6(15)	-0.7(14)	4.5(12)	0.7(13)
C8B	16.3(15)	35(2)	22.1(16)	-4.3(15)	-3.6(12)	0.2(13)
C7B	25.6(16)	24.6(18)	20.2(16)	2.0(15)	-4.3(12)	0.4(14)
C7	23.0(15)	21.4(17)	23.4(16)	4.9(14)	2.8(12)	-1.7(13)
C8	27.2(17)	32(2)	20.8(16)	4.6(15)	1.4(13)	-0.7(15)
C1	19.8(15)	30.5(19)	28.6(17)	-6.8(15)	4.2(13)	-4.2(14)
C12	34.4(19)	28.6(19)	35.3(19)	-6.0(17)	13.5(15)	-1.2(15)
C12B	30.4(17)	25.1(18)	31.4(18)	-1.4(17)	-1.5(14)	-5.4(16)

Atom	U_{11}	U_{22}	U_{33}	U_{23}	U_{13}	U_{12}
C11B	24.0(17)	32(2)	29.5(18)	2.8(16)	-0.7(13)	-0.1(15)
C11	33.7(19)	40(2)	28.4(18)	-7.6(17)	-0.9(14)	-1.6(16)
C15	39(2)	38(2)	27.5(18)	-7.6(18)	-4.9(15)	-5.9(17)
C15B	47(2)	70(3)	56(3)	-5(3)	25(2)	-28(2)

Table 10. Bond Lengths in Å for compound **178**

Atom	Atom	Length/Å
O4B	C6B	1.430(4)
O4B	C7B	1.426(4)
O3B	C5B	1.431(4)
O3B	C4B	1.423(3)
O1B	C1B	1.427(4)
O1B	C3B	1.424(4)
O4	C6	1.429(4)
O4	C7	1.436(4)
O1	C3	1.425(4)
O1	C1	1.415(4)
O3	C4	1.422(4)
O3	C5	1.424(4)
O5B	C16B	1.418(4)
O5	C16	1.424(4)

Atom	Atom	Length/Å
O2B	C1B	1.441(4)
O2B	C2B	1.434(4)
O6	C14	1.342(4)
O6	C15	1.438(5)
O7B	C14B	1.188(4)
O2	C2	1.437(4)
O2	C1	1.431(4)
O6B	C14B	1.335(4)
O6B	C15B	1.447(5)
O7	C14	1.187(4)
C14B	C13B	1.502(5)
C4	C3	1.512(5)
C4	C13	1.509(4)
C14	C13	1.491(5)
C5	C6	1.540(4)
C5	C9	1.524(4)
C6	C10	1.527(4)
C6	C16	1.529(4)
C5B	C6B	1.547(4)
C5B	C9B	1.518(4)
C1B	C12B	1.503(5)
C1B	C11B	1.496(5)

Atom	Atom	Length/Å
C4B	C3B	1.504(4)
C4B	C13B	1.512(4)
C3B	C2B	1.514(4)
C9	C8	1.513(5)
C2B	C10B	1.512(5)
C6B	C10B	1.535(4)
C6B	C16B	1.537(4)
C3	C2	1.525(4)
C10	C2	1.517(5)
C9B	C8B	1.505(5)
C8B	C7B	1.513(5)
C7	C8	1.511(5)
C1	C12	1.510(5)
C1	C11	1.496(5)

Table 11. Bond Angles in ° for compound **78**

Atom	Atom	Atom	Angle/°
C7B	O4B	C6B	115.0(2)
C4B	O3B	C5B	115.7(2)
C3B	O1B	C1B	107.8(2)
C6	O4	C7	114.9(2)
C1	O1	C3	105.8(2)

Atom	Atom	Atom	Angle/°
C4	O3	C5	117.0(2)
C2B	O2B	C1B	109.2(2)
C14	O6	C15	115.0(3)
C1	O2	C2	109.9(2)
C14B	O6B	C15B	116.3(3)
O7B	C14B	O6B	124.0(3)
O7B	C14B	C13B	125.4(3)
O6B	C14B	C13B	110.5(3)
O3	C4	C3	109.4(3)
O3	C4	C13	106.5(2)
C13	C4	C3	111.5(3)
O6	C14	C13	111.4(3)
O7	C14	O6	123.2(3)
O7	C14	C13	125.4(3)
O3	C5	C6	112.5(3)
O3	C5	C9	104.7(2)
C9	C5	C6	112.0(2)
O4	C6	C5	111.1(2)
O4	C6	C10	104.9(3)
O4	C6	C16	109.9(2)
C10	C6	C5	112.9(2)
C10	C6	C16	108.4(2)

Atom	Atom	Atom	Angle/°
C16	C6	C5	109.4(3)
O3B	C5B	C6B	112.6(3)
O3B	C5B	C9B	105.5(2)
C9B	C5B	C6B	111.9(3)
O1B	C1B	O2B	105.6(2)
O1B	C1B	C12B	110.5(3)
O1B	C1B	C11B	108.9(3)
O2B	C1B	C12B	108.6(3)
O2B	C1B	C11B	109.8(3)
C11B	C1B	C12B	113.2(3)
O3B	C4B	C3B	108.9(3)
O3B	C4B	C13B	108.1(2)
C3B	C4B	C13B	110.9(3)
O1B	C3B	C4B	109.5(3)
O1B	C3B	C2B	102.8(2)
C4B	C3B	C2B	115.2(3)
C8	C9	C5	110.0(3)
O2B	C2B	C3B	102.5(2)
O2B	C2B	C10B	110.7(2)
C10B	C2B	C3B	115.6(3)
O4B	C6B	C5B	110.7(2)
O4B	C6B	C10B	104.3(2)

Atom	Atom	Atom	Angle/°
O4B	C6B	C16B	110.0(2)
C10B	C6B	C5B	113.2(2)
C10B	C6B	C16B	108.2(2)
C16B	C6B	C5B	110.3(3)
O1	C3	C4	109.5(3)
O1	C3	C2	103.4(2)
C4	C3	C2	115.0(3)
C2	C10	C6	115.9(3)
C2B	C10B	C6B	115.2(2)
O2	C2	C3	102.3(2)
O2	C2	C10	108.6(3)
C10	C2	C3	116.4(3)
O5	C16	C6	111.7(3)
C14B	C13B	C4B	113.0(3)
C14	C13	C4	111.9(3)
C8B	C9B	C5B	110.9(3)
O5B	C16B	C6B	112.2(3)
C9B	C8B	C7B	109.6(3)
O4B	C7B	C8B	111.6(3)
O4	C7	C8	111.0(3)
C7	C8	C9	109.1(3)
O1	C1	O2	105.3(2)

Atom	Atom	Atom	Angle/°
O1	C1	C12	110.8(3)
O1	C1	C11	109.0(3)
O2	C1	C12	109.2(3)
O2	C1	C11	109.2(3)
C11	C1	C12	113.0(3)

Table 12. Hydrogen Fractional Atomic Coordinates ($\times 10^4$) and Equivalent Isotropic Displacement Parameters ($\text{\AA}^2 \times 10^3$) for compound **78**. U_{eq} is defined as 1/3 of the trace of the orthogonalised U_{ij} .

Atom	x	y	z	U_{eq}
H12D	5764	7283	10259	50(4)
H12E	6028	7571	10783	50(4)
H12F	5392	5804	10630	50(4)
H12A	5798	8412	7589	44
H12B	6588	8392	7491	44
H12C	6357	6984	7922	44
H11A	6827	2975	7649	43
H11B	7094	4549	7248	43
H11C	6608	2217	7135	43
H11D	6038	2339	11036	50(4)

H11E	6674	4133	11174	50(4)
H11F	6786	1665	10899	50(4)
H15D	4462	-2545	8108	50(4)
H15E	4651	-4233	8543	50(4)
H15F	5240	-3419	8238	50(4)
H15A	2510	-1664	7709	85
H15B	2255	-98	8115	85
H15C	2862	-2061	8213	85
H5BA	4198(15)	-580(40)	6581(10)	14(2)
H10A	5592(13)	2970(60)	6264(8)	14(2)
H10B	5437(14)	1250(50)	6643(9)	14(2)
H4B	4723(14)	910(40)	7204(10)	14(2)
H16A	4407(12)	-660(60)	5690(9)	14(2)
H16B	4964(14)	-1470(50)	6035(9)	14(2)
H5B	5155(14)	1970(40)	5417(9)	17
H13A	4437(11)	2500(70)	7876(7)	18(6)
H13B	3831(14)	3980(40)	7615(11)	18(6)
H3B	4752(14)	5830(50)	7310(10)	14(2)
H7BA	3712(15)	5450(70)	5559(10)	14(2)
H7BB	3813(15)	2740(70)	5448(10)	14(2)
H9BA	3050(13)	390(60)	6405(9)	14(2)
H9BB	3408(15)	-470(50)	5983(9)	14(2)
H8BA	3175(15)	4360(50)	6177(9)	14(2)

H8BB	2805(12)	3060(60)	5783(9)	14(2)
H2B	4954(14)	6010(50)	6583(9)	14(2)
H7A	8205(15)	6830(20)	8806(10)	15(3)
H9A	7106(10)	730(60)	8436(8)	15(3)
H8A	7163(9)	4900(50)	8543(10)	15(3)
H9B	7896(10)	530(50)	8602(10)	15(3)
H8B	7760(14)	4090(60)	8225(5)	15(3)
H7B	8579(8)	4330(50)	8841(10)	15(3)
H5A	7279(15)	-370(40)	9203(10)	16(4)
H4	6386(14)	180(40)	9584(9)	16(4)
H2	7041(15)	6010(40)	9753(9)	16(4)
H3	5975(13)	4870(50)	9668(10)	16(4)
H16C	8645(14)	800(60)	9218(6)	15(3)
H10C	7923(11)	3480(60)	10095(8)	15(3)
H13C	5390(14)	2620(40)	9043(9)	15(3)
H13D	5231(12)	990(60)	9453(7)	15(3)
H16D	8380(15)	-450(30)	9630(9)	15(3)
H10D	7422(14)	1300(30)	10002(10)	15(3)
H5	9166(16)	3520(50)	9630(10)	30(10)
H1W	5362(14)	5310(60)	5054(12)	37(11)

Table 13. Hydrogen Bond information for compound **78**.

D	H	A	d(D-H)/Å	d(H-A)/Å	d(D-A)/Å	D-H-A/deg
O5B	H5B	O1W	0.938(13)	1.766(15)	2.690(3)	168(3)
O5	H5	O5B ¹	0.961(14)	1.786(15)	2.734(3)	168(3)
O1W	H1W	O5 ¹	0.955(14)	1.749(14)	2.700(3)	174(4)

¹3/2-X,1/2+Y,3/2-Z

X-RAY data of compound 84

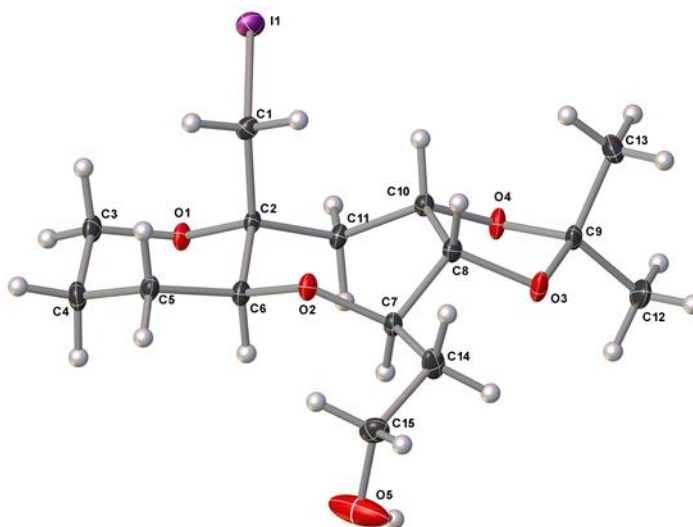


Table 14. Crystal data and structure refinement for compound **84** (JAH-11-102).

Identification code	84 (JAH-11-102)
Empirical formula	C ₁₅ H ₂₅ O ₅ I
Formula weight	412.25

Temperature	100(2) K
Wavelength	0.71073 Å
Crystal system	Orthorhombic
Space group	P2 ₁ 2 ₁ 2 ₁
Unit cell dimensions	a = 10.02693(17) Å α = 90.0°. b = 11.10793(17) Å β = 90.0°. c = 14.3797(3) Å γ = 90.0°.
Volume	1601.59(5) Å ³
Z	4
Density (calculated)	1.710 Mg/m ³
Absorption coefficient	2.021 mm ⁻¹
F(000)	832
Crystal size	0.74 x 0.334 x 0.322 mm ³
Theta range for data collection	2.317 to 30.507°.
Index ranges	-14 ≤ h ≤ 14, -16 ≤ k ≤ 16, -20 ≤ l ≤ 20
Reflections collected	20884
Independent reflections	4889 [R(int) = 0.0327]
Completeness to theta = 25.242°	99.9 %
Absorption correction	Sphere
Max. and min. transmission	0.33311 and 0.31215
Refinement method	Full-matrix least-squares on F ²
Data / restraints / parameters	4889 / 1 / 196
Goodness-of-fit on F ²	1.116
Final R indices [I > 2σ(I)]	R1 = 0.0238, wR2 = 0.0612
R indices (all data)	R1 = 0.0240, wR2 = 0.0613
Absolute structure parameter	-0.026(9)
Extinction coefficient	n/a
Largest diff. peak and hole	0.984 and -0.448 e.Å ⁻³

Table 15. Atomic coordinates ($\times 10^4$) and equivalent isotropic displacement parameters ($\text{\AA}^2 \times 10^3$) for compound **84**. $U(\text{eq})$ is defined as one third of the trace of the orthogonalized U^{ij} tensor.

	x	y	z	$U(\text{eq})$
I(1)	3476(1)	2896(1)	1400(1)	19(1)
O(3)	8962(2)	2844(2)	3270(2)	17(1)
O(2)	6147(2)	4708(2)	3998(1)	13(1)
O(1)	3286(2)	2655(2)	3714(2)	13(1)
O(4)	7559(2)	1471(2)	2668(2)	15(1)
O(5)	7965(5)	4895(3)	6133(2)	52(1)
C(5)	3877(3)	5016(2)	4455(2)	14(1)
C(15)	8094(3)	5580(3)	5318(2)	18(1)
C(9)	8913(2)	1862(2)	2624(2)	13(1)
C(2)	4496(2)	3244(2)	3408(2)	10(1)
C(8)	7723(3)	3486(2)	3169(2)	12(1)
C(10)	6760(2)	2542(2)	2735(2)	11(1)
C(11)	5490(2)	2211(2)	3267(2)	11(1)
C(3)	2196(3)	3478(2)	3921(2)	15(1)
C(7)	7345(2)	4018(2)	4108(2)	12(1)
C(6)	4943(2)	4090(2)	4207(2)	12(1)
C(12)	9807(3)	858(3)	2962(2)	21(1)
C(14)	8435(3)	4877(3)	4444(2)	18(1)
C(13)	9274(3)	2296(3)	1649(2)	20(1)
C(1)	4275(3)	3979(2)	2516(2)	13(1)
C(4)	2582(3)	4345(3)	4691(2)	17(1)

Table 16. Bond lengths [\AA] and angles [$^\circ$] for compound **84**.

I(1)-C(1)	2.158(3)
O(3)-C(9)	1.434(3)
O(3)-C(8)	1.439(3)
O(2)-C(7)	1.433(3)
O(2)-C(6)	1.421(3)
O(1)-C(2)	1.448(3)
O(1)-C(3)	1.455(3)
O(4)-C(9)	1.427(3)
O(4)-C(10)	1.438(3)
O(5)-C(15)	1.403(4)
O(5)-H(5)	0.96(2)
C(5)-H(5A)	0.9900
C(5)-H(5B)	0.9900
C(5)-C(6)	1.526(4)
C(5)-C(4)	1.535(4)
C(15)-H(15A)	0.9900
C(15)-H(15B)	0.9900
C(15)-C(14)	1.518(4)
C(9)-C(12)	1.510(4)
C(9)-C(13)	1.526(4)
C(2)-C(11)	1.533(3)
C(2)-C(6)	1.550(4)
C(2)-C(1)	1.536(4)
C(8)-H(8)	1.0000
C(8)-C(10)	1.556(4)
C(8)-C(7)	1.523(4)
C(10)-H(10)	1.0000
C(10)-C(11)	1.530(3)
C(11)-H(11A)	0.9900
C(11)-H(11B)	0.9900
C(3)-H(3A)	0.9900
C(3)-H(3B)	0.9900

C(3)-C(4)	1.518(4)
C(7)-H(7)	1.0000
C(7)-C(14)	1.529(4)
C(6)-H(6)	1.0000
C(12)-H(12A)	0.9800
C(12)-H(12B)	0.9800
C(12)-H(12C)	0.9800
C(14)-H(14A)	0.9900
C(14)-H(14B)	0.9900
C(13)-H(13A)	0.9800
C(13)-H(13B)	0.9800
C(13)-H(13C)	0.9800
C(1)-H(1A)	0.9900
C(1)-H(1B)	0.9900
C(4)-H(4A)	0.9900
C(4)-H(4B)	0.9900

C(9)-O(3)-C(8)	106.40(19)
C(6)-O(2)-C(7)	115.46(19)
C(2)-O(1)-C(3)	114.09(19)
C(9)-O(4)-C(10)	106.34(19)
C(15)-O(5)-H(5)	115(3)
H(5A)-C(5)-H(5B)	108.4
C(6)-C(5)-H(5A)	110.0
C(6)-C(5)-H(5B)	110.0
C(6)-C(5)-C(4)	108.5(2)
C(4)-C(5)-H(5A)	110.0
C(4)-C(5)-H(5B)	110.0
O(5)-C(15)-H(15A)	108.4
O(5)-C(15)-H(15B)	108.4
O(5)-C(15)-C(14)	115.6(3)
H(15A)-C(15)-H(15B)	107.4
C(14)-C(15)-H(15A)	108.4
C(14)-C(15)-H(15B)	108.4
O(3)-C(9)-C(12)	109.5(2)
O(3)-C(9)-C(13)	110.3(2)

O(4)-C(9)-O(3)	103.57(19)
O(4)-C(9)-C(12)	109.0(2)
O(4)-C(9)-C(13)	111.3(2)
C(12)-C(9)-C(13)	112.9(2)
O(1)-C(2)-C(11)	104.29(19)
O(1)-C(2)-C(6)	106.9(2)
O(1)-C(2)-C(1)	111.9(2)
C(11)-C(2)-C(6)	111.3(2)
C(11)-C(2)-C(1)	112.4(2)
C(1)-C(2)-C(6)	109.8(2)
O(3)-C(8)-H(8)	108.8
O(3)-C(8)-C(10)	104.0(2)
O(3)-C(8)-C(7)	108.5(2)
C(10)-C(8)-H(8)	108.8
C(7)-C(8)-H(8)	108.8
C(7)-C(8)-C(10)	117.6(2)
O(4)-C(10)-C(8)	103.77(19)
O(4)-C(10)-H(10)	108.9
O(4)-C(10)-C(11)	107.3(2)
C(8)-C(10)-H(10)	108.9
C(11)-C(10)-C(8)	118.5(2)
C(11)-C(10)-H(10)	108.9
C(2)-C(11)-H(11A)	108.5
C(2)-C(11)-H(11B)	108.5
C(10)-C(11)-C(2)	115.3(2)
C(10)-C(11)-H(11A)	108.5
C(10)-C(11)-H(11B)	108.5
H(11A)-C(11)-H(11B)	107.5
O(1)-C(3)-H(3A)	109.5
O(1)-C(3)-H(3B)	109.5
O(1)-C(3)-C(4)	110.9(2)
H(3A)-C(3)-H(3B)	108.1
C(4)-C(3)-H(3A)	109.5
C(4)-C(3)-H(3B)	109.5
O(2)-C(7)-C(8)	108.5(2)
O(2)-C(7)-H(7)	110.2

O(2)-C(7)-C(14)	107.5(2)
C(8)-C(7)-H(7)	110.2
C(8)-C(7)-C(14)	110.2(2)
C(14)-C(7)-H(7)	110.2
O(2)-C(6)-C(5)	108.6(2)
O(2)-C(6)-C(2)	112.4(2)
O(2)-C(6)-H(6)	107.8
C(5)-C(6)-C(2)	112.3(2)
C(5)-C(6)-H(6)	107.8
C(2)-C(6)-H(6)	107.8
C(9)-C(12)-H(12A)	109.5
C(9)-C(12)-H(12B)	109.5
C(9)-C(12)-H(12C)	109.5
H(12A)-C(12)-H(12B)	109.5
H(12A)-C(12)-H(12C)	109.5
H(12B)-C(12)-H(12C)	109.5
C(15)-C(14)-C(7)	114.9(2)
C(15)-C(14)-H(14A)	108.5
C(15)-C(14)-H(14B)	108.5
C(7)-C(14)-H(14A)	108.5
C(7)-C(14)-H(14B)	108.5
H(14A)-C(14)-H(14B)	107.5
C(9)-C(13)-H(13A)	109.5
C(9)-C(13)-H(13B)	109.5
C(9)-C(13)-H(13C)	109.5
H(13A)-C(13)-H(13B)	109.5
H(13A)-C(13)-H(13C)	109.5
H(13B)-C(13)-H(13C)	109.5
I(1)-C(1)-H(1A)	109.2
I(1)-C(1)-H(1B)	109.2
C(2)-C(1)-I(1)	112.19(17)
C(2)-C(1)-H(1A)	109.2
C(2)-C(1)-H(1B)	109.2
H(1A)-C(1)-H(1B)	107.9
C(5)-C(4)-H(4A)	109.4
C(5)-C(4)-H(4B)	109.4

C(3)-C(4)-C(5)	111.3(2)
C(3)-C(4)-H(4A)	109.4
C(3)-C(4)-H(4B)	109.4
H(4A)-C(4)-H(4B)	108.0

Table 17. Anisotropic displacement parameters ($\text{\AA}^2 \times 10^3$) for compound **84**. The anisotropic displacement factor exponent takes the form: $-2\pi^2 [h^2 a^{*2} U^{11} + \dots + 2 h k a^* b^* U^{12}]$

	U11	U22	U33	U23	U13	U12
I(1)	17(1)	24(1)	16(1)	-2(1)	-3(1)	-2(1)
O(3)	8(1)	20(1)	22(1)	-9(1)	-2(1)	3(1)
O(2)	8(1)	12(1)	18(1)	-1(1)	1(1)	-1(1)
O(1)	7(1)	12(1)	19(1)	2(1)	2(1)	-1(1)
O(4)	7(1)	13(1)	24(1)	-2(1)	2(1)	2(1)
O(5)	113(3)	24(1)	19(1)	0(1)	4(2)	17(2)
C(5)	10(1)	15(1)	16(1)	-2(1)	0(1)	3(1)
C(15)	22(1)	18(1)	16(1)	-4(1)	-4(1)	1(1)
C(9)	7(1)	18(1)	15(1)	-3(1)	0(1)	1(1)
C(2)	6(1)	10(1)	14(1)	1(1)	1(1)	0(1)
C(8)	9(1)	13(1)	15(1)	0(1)	1(1)	0(1)
C(10)	10(1)	12(1)	13(1)	-1(1)	0(1)	1(1)
C(11)	7(1)	10(1)	16(1)	0(1)	0(1)	1(1)
C(3)	8(1)	17(1)	18(1)	1(1)	2(1)	0(1)
C(7)	9(1)	12(1)	13(1)	-2(1)	1(1)	0(1)
C(6)	8(1)	12(1)	15(1)	-1(1)	1(1)	0(1)
C(12)	17(1)	26(1)	21(1)	-3(1)	0(1)	12(1)
C(14)	10(1)	21(1)	21(1)	-7(1)	1(1)	-5(1)
C(13)	16(1)	25(1)	18(1)	2(1)	6(1)	4(1)
C(1)	12(1)	12(1)	14(1)	-1(1)	-2(1)	0(1)
C(4)	10(1)	21(1)	19(1)	-1(1)	4(1)	2(1)

Table 18. Hydrogen coordinates ($\times 10^4$) and isotropic displacement parameters ($\text{\AA}^2 \times 10^3$) for compound **84**.

	x	y	z	U(eq)
H(5A)	3727	5566	3924	17
H(5B)	4170	5500	4996	17
H(15A)	8796	6193	5419	22
H(15B)	7245	6014	5210	22
H(8)	7855	4157	2714	15
H(10)	6510	2810	2094	14
H(11A)	5749	1896	3886	14
H(11B)	5034	1553	2930	14
H(3A)	1401	3012	4114	18
H(3B)	1962	3938	3354	18
H(7)	7204	3361	4574	14
H(6)	5106	3582	4770	14
H(12A)	10739	1124	2940	32
H(12B)	9693	152	2561	32
H(12C)	9569	649	3603	32
H(14A)	9256	4406	4562	21
H(14B)	8634	5456	3939	21
H(13A)	8677	2955	1469	30
H(13B)	9178	1630	1207	30
H(13C)	10198	2583	1644	30
H(1A)	5135	4333	2316	15
H(1B)	3652	4648	2649	15
H(4A)	2701	3894	5279	20
H(4B)	1854	4936	4785	20
H(5)	8240(50)	4070(30)	6080(40)	37(13)

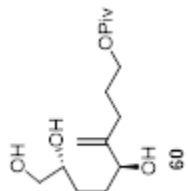
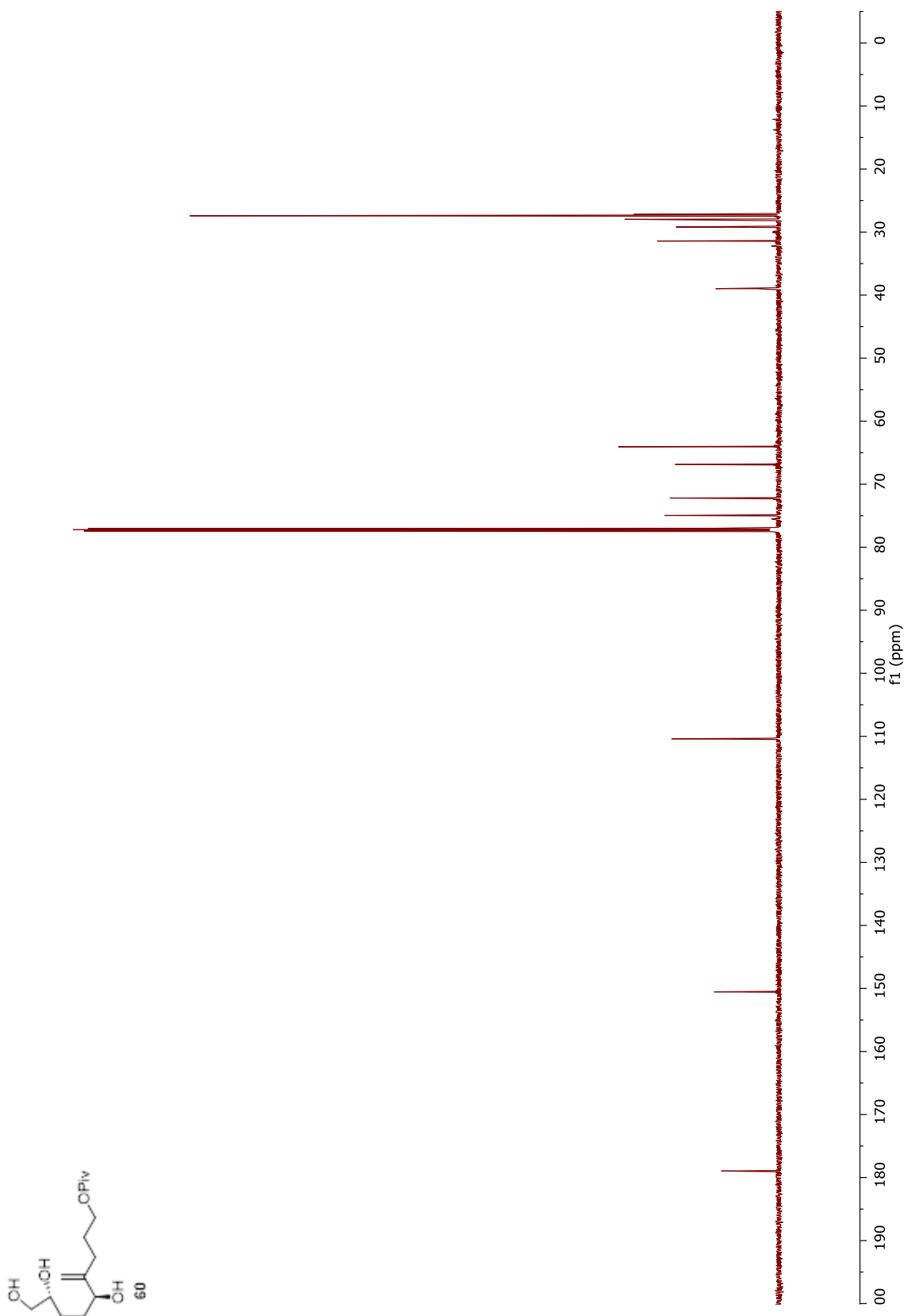
Table 19. Hydrogen bonds for compound **84** [Å and °].

D-H...A	d(D-H)	d(H...A)	d(D...A)	<(DHA)
O(5)-H(5)...O(1)#1	0.96(2)	1.94(3)	2.860(3)	160(5)

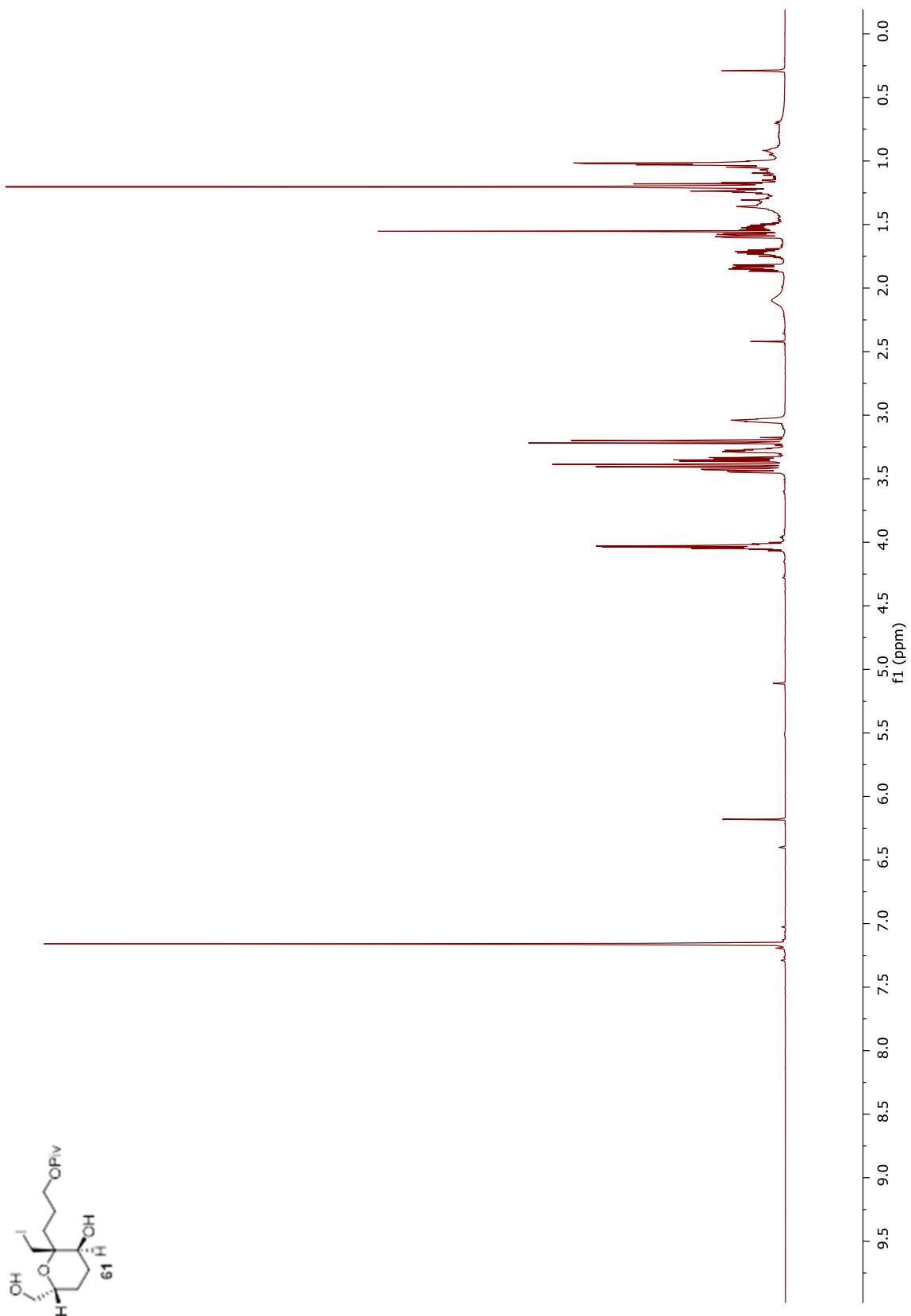
Symmetry transformations used to generate equivalent atoms:

#1 $x+1/2, -y+1/2, -z+1$

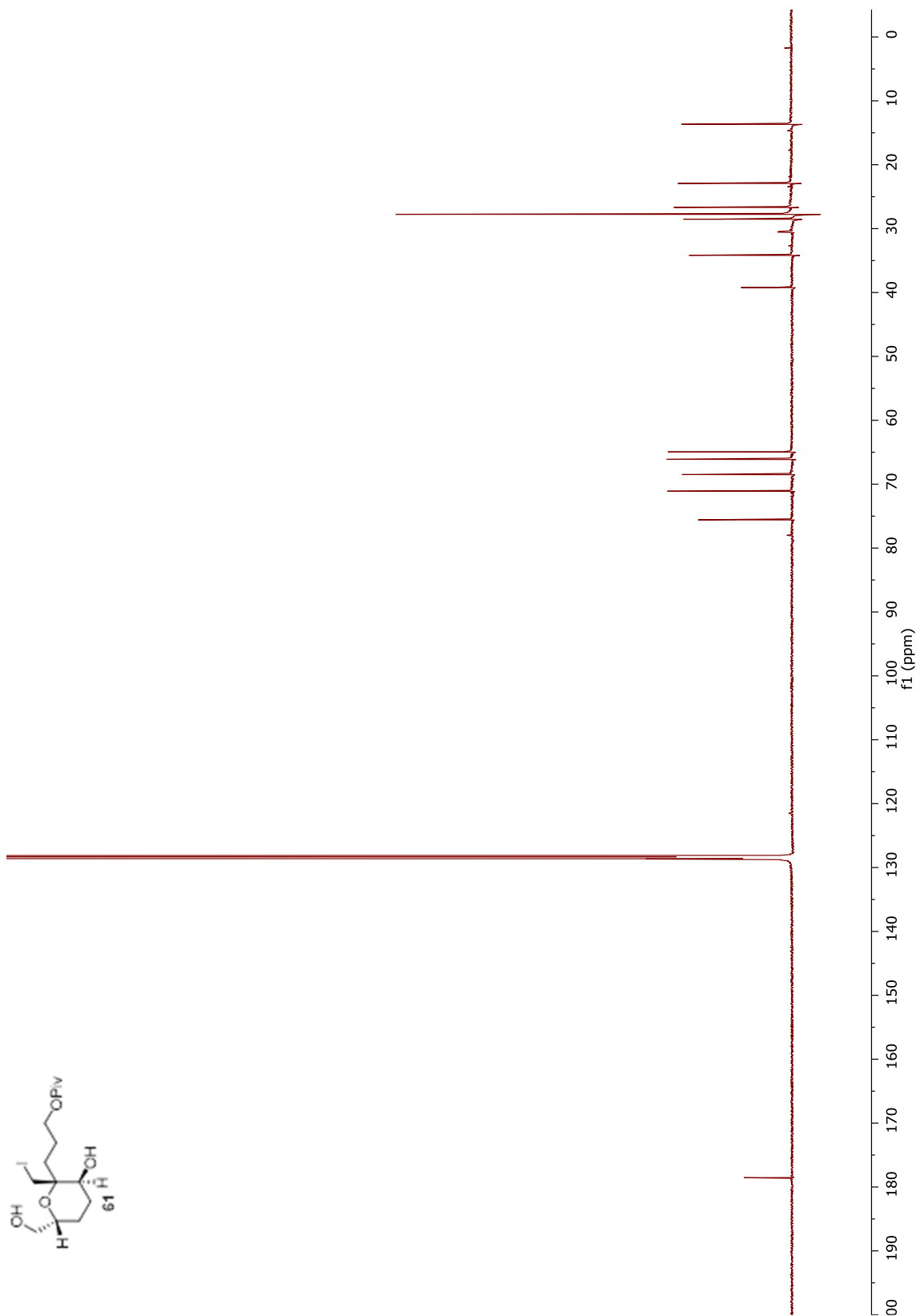
Compound **60** ^{13}C -NMR (151 MHz, CDCl_3) JAH-5-236-C13



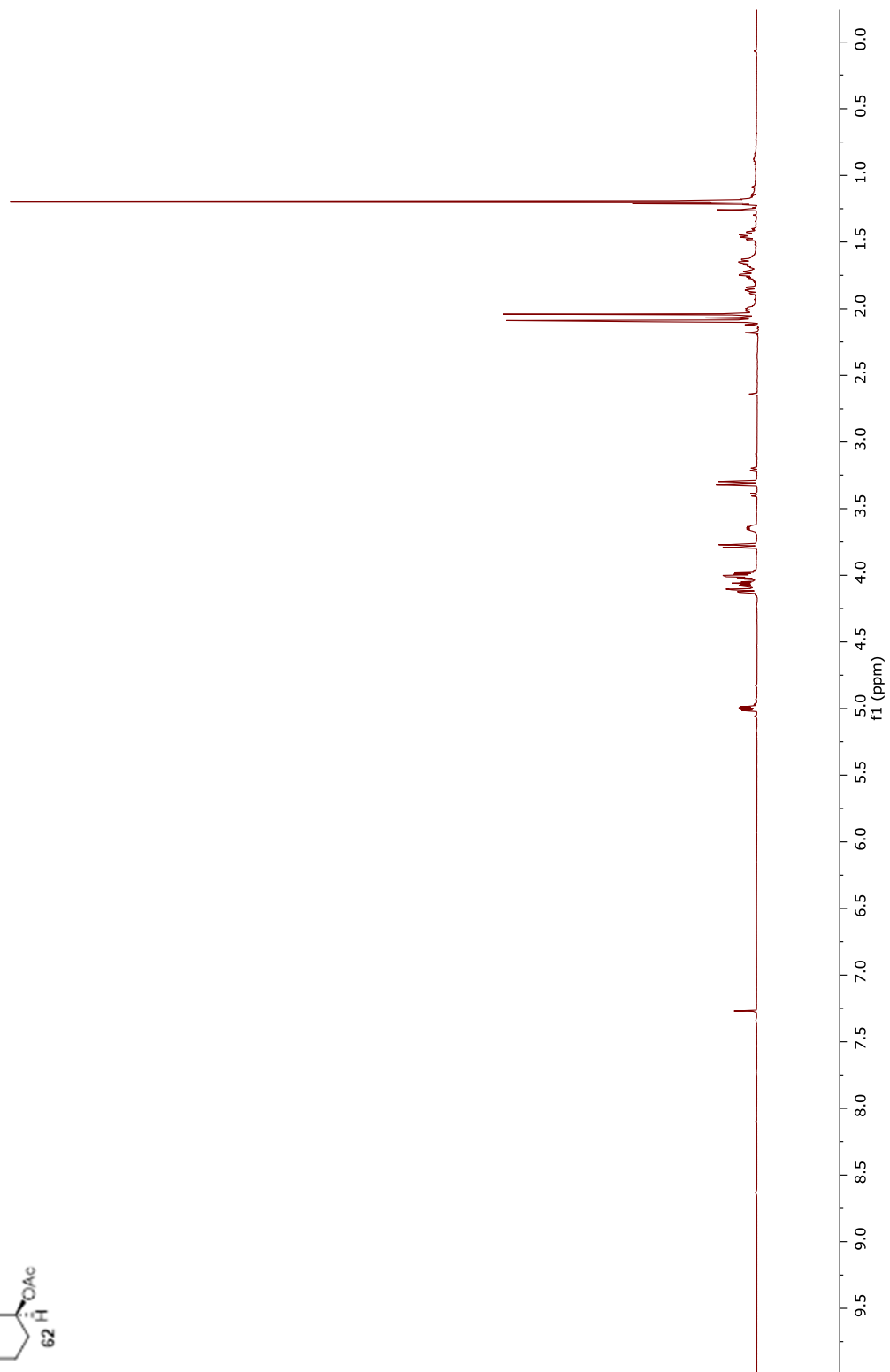
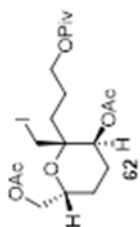
Compound **61** $^1\text{H-NMR}$ (600 MHz, C_6D_6) JAH-5-238



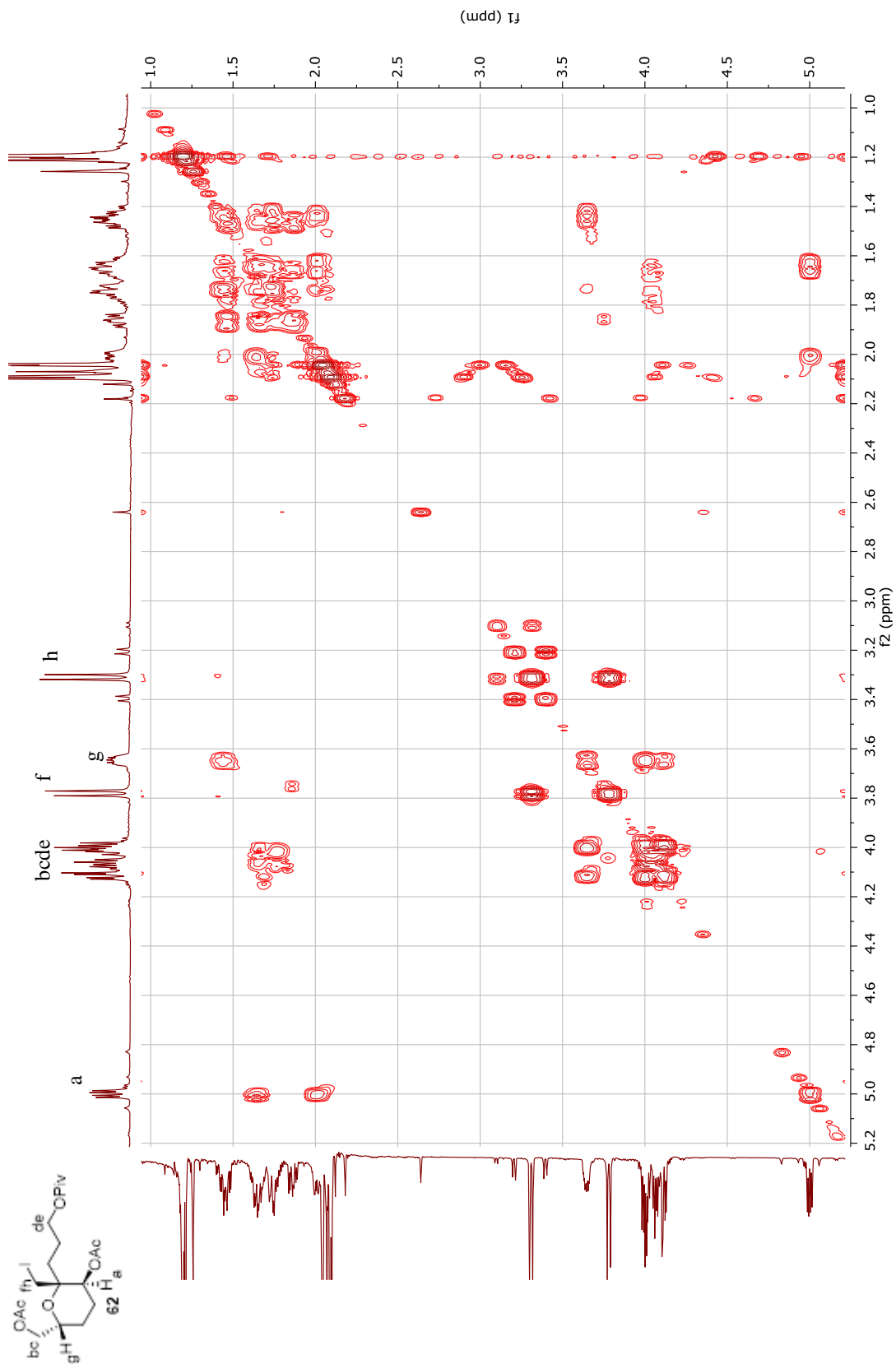
Compound **61** ^{13}C -NMR (151 MHz, C_6D_6) JAH-5-238-C13



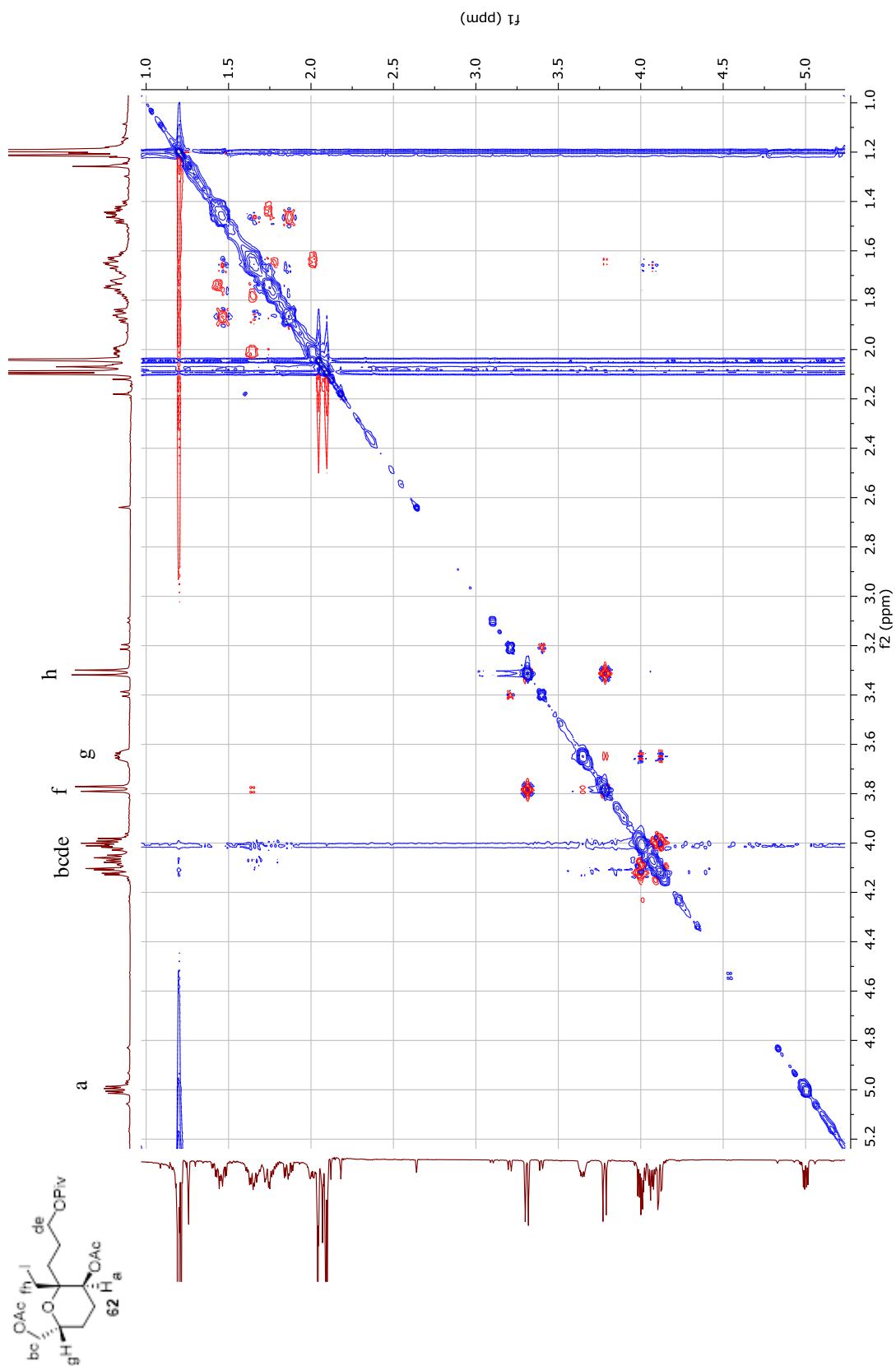
Compound **62** $^1\text{H-NMR}$ (600 MHz, CDCl_3) JAH-5-240-acetate



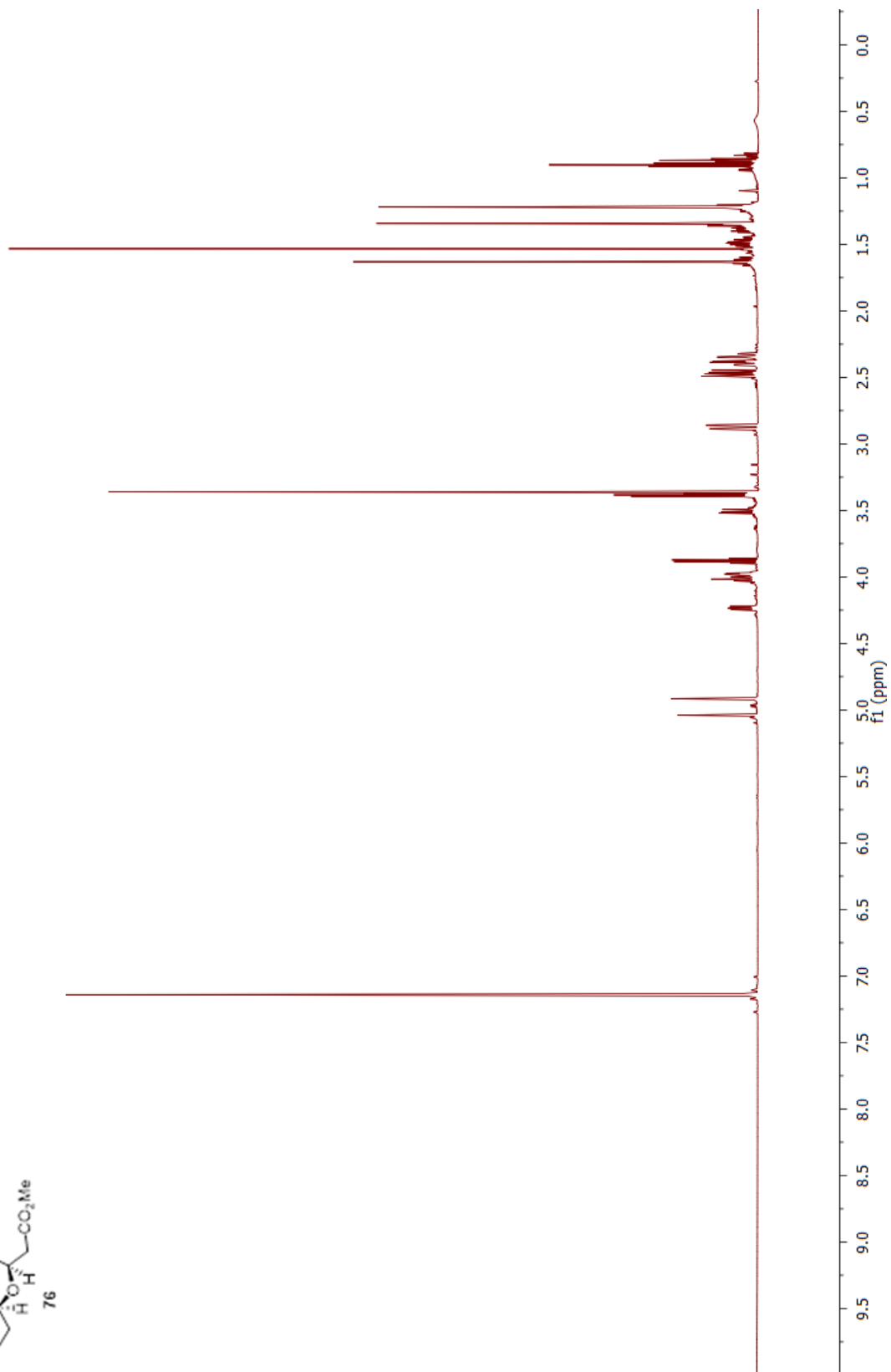
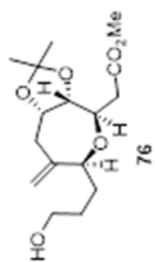
Compound **62** COSY (600 MHz, CDCl₃) JAH-5-240-acetate-COSY



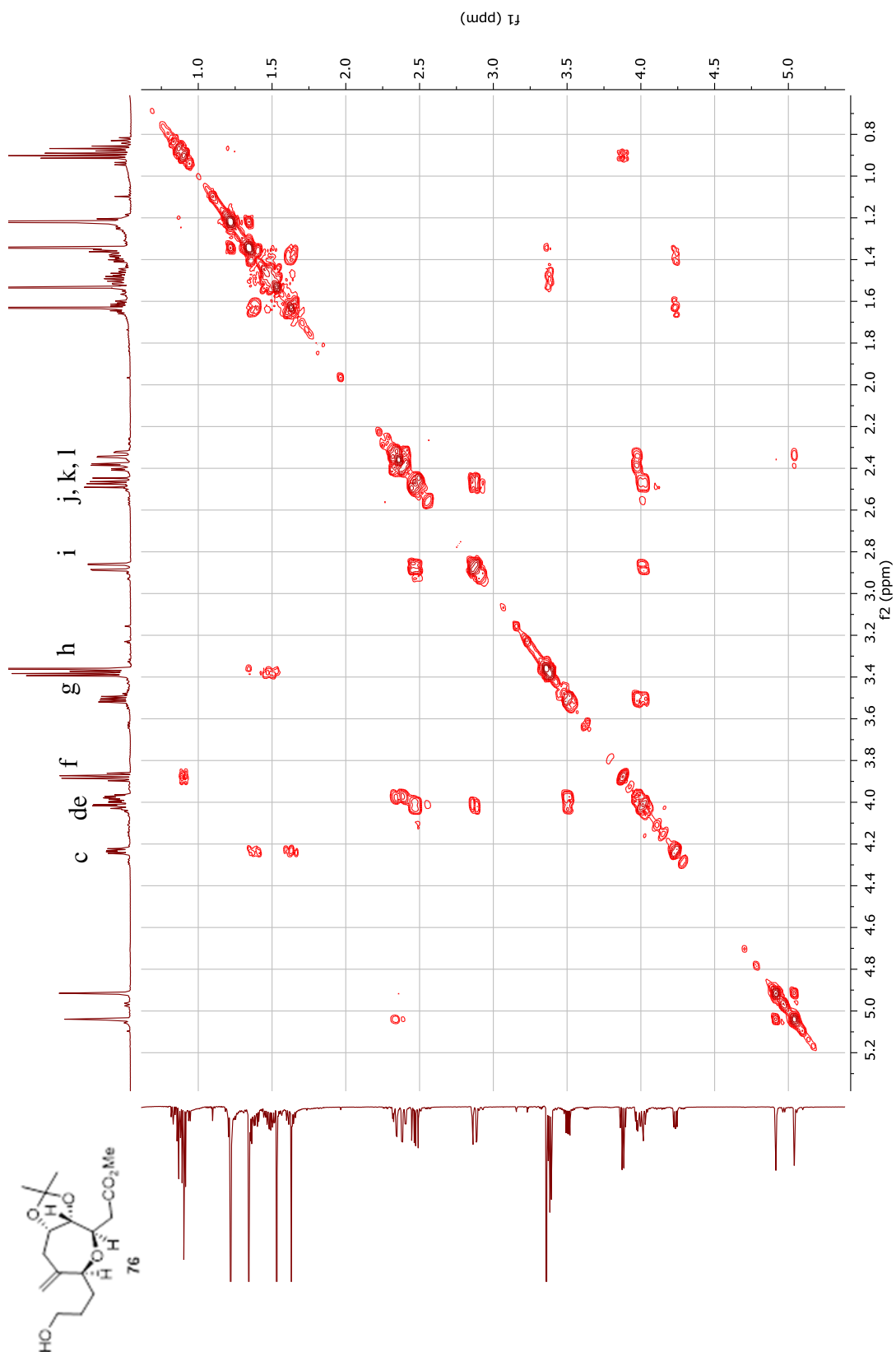
Compound **62** NOESY (600 MHz, CDCl₃) JAH-5-240-acetate-NOESY



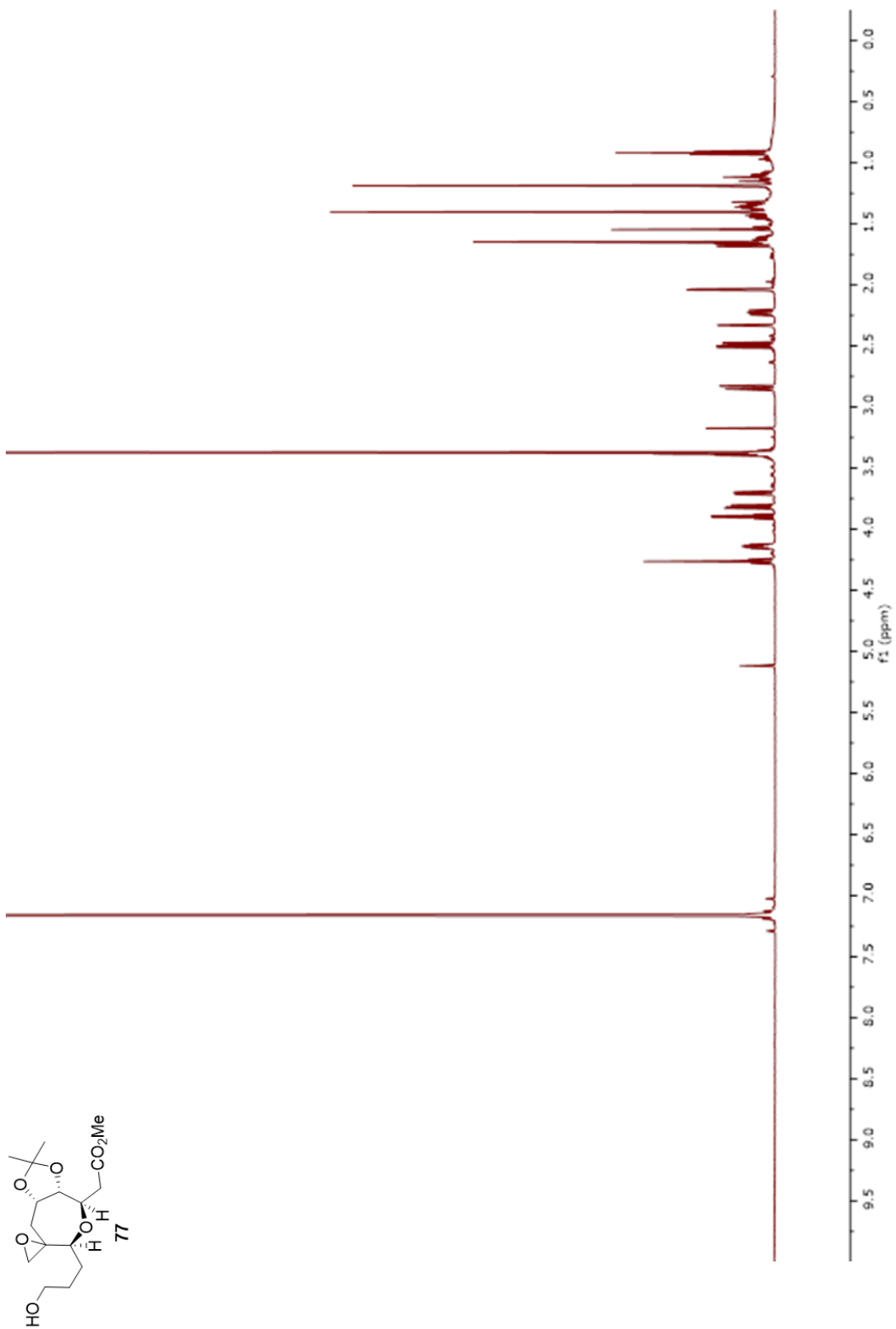
Compound **76** $^1\text{H-NMR}$ (600 MHz, C_6D_6) JAH-6-264-1-C6D6



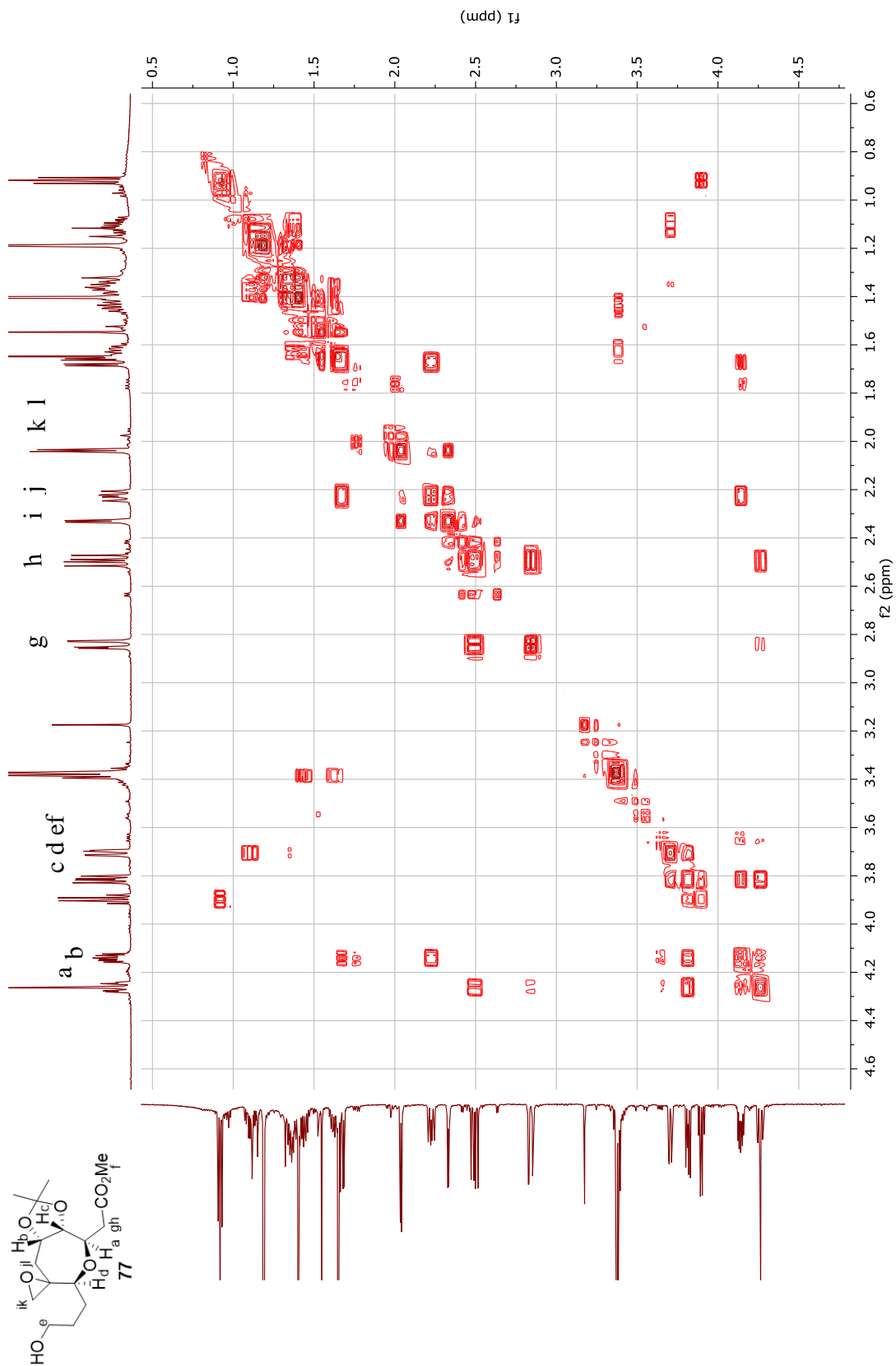
Compound **76** COSY (600 MHz, C₆D₆) JAH-6-264-1-COSY-C6D6



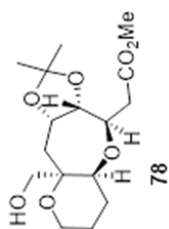
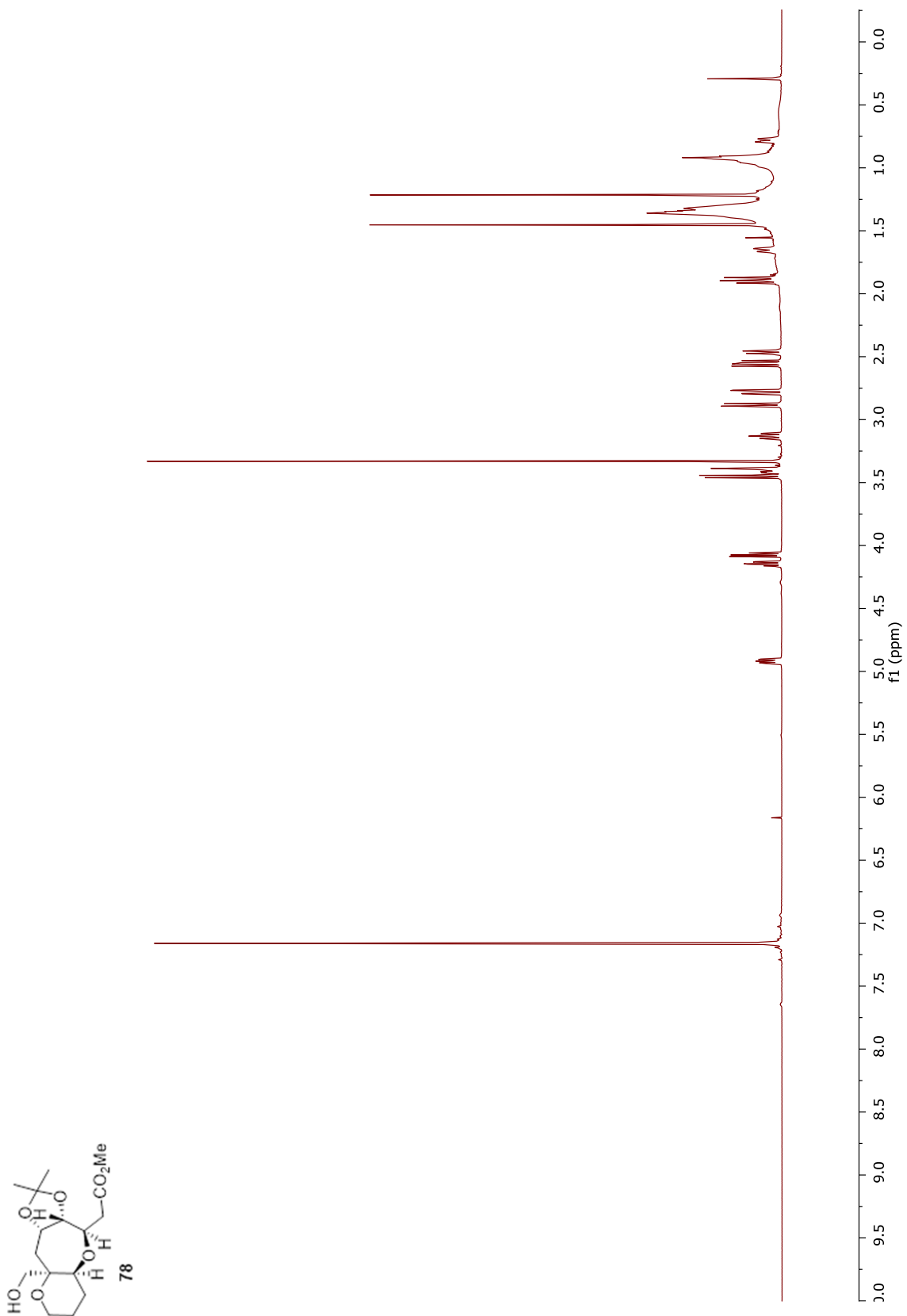
Compound **77** $^1\text{H-NMR}$ (600 MHz, C_6D_6) ^1H JAH-7-168-C6D6



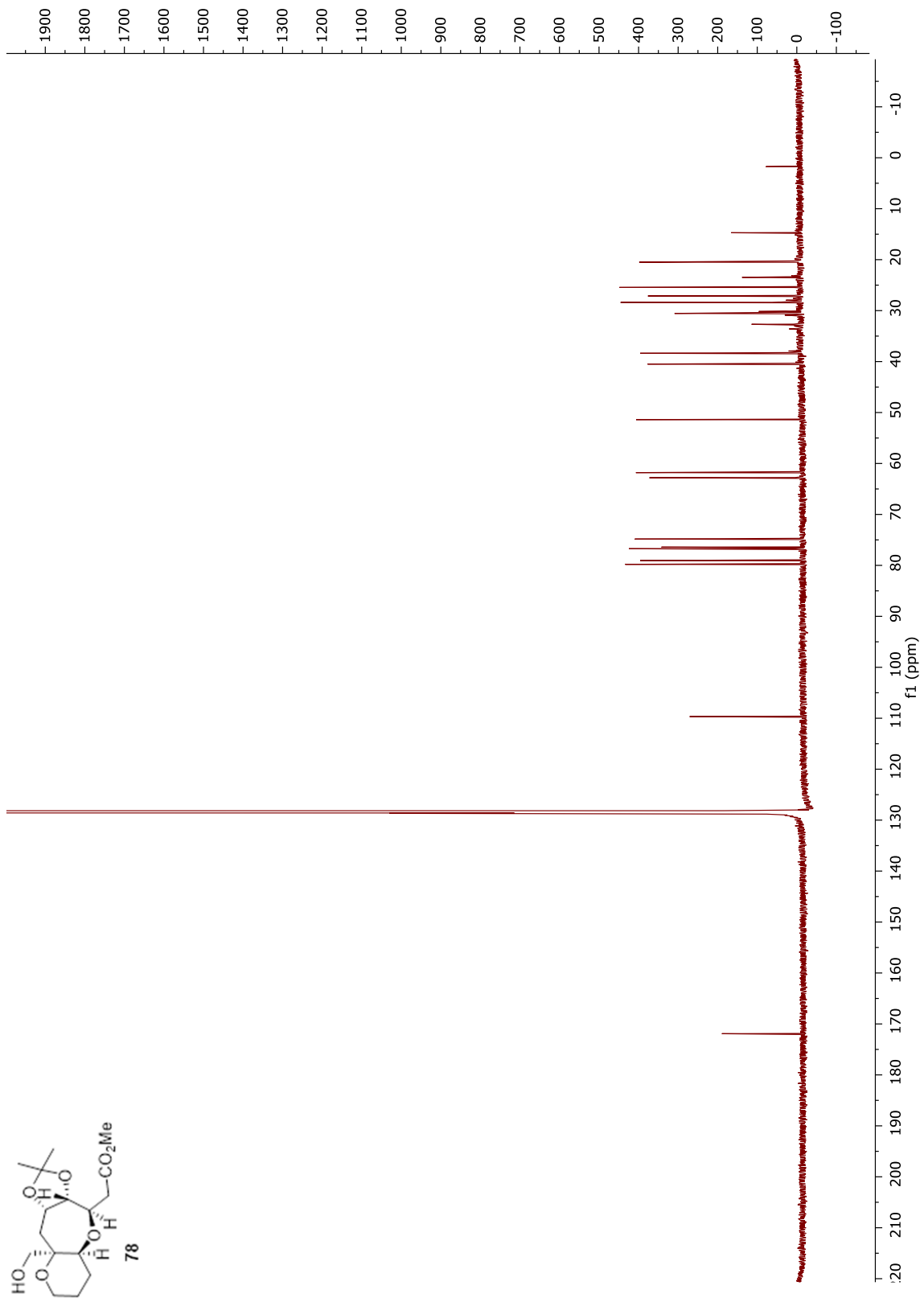
Compound **77** COSY (600 MHz, C₆D₆) JAH-7-168-C6D6-COSY



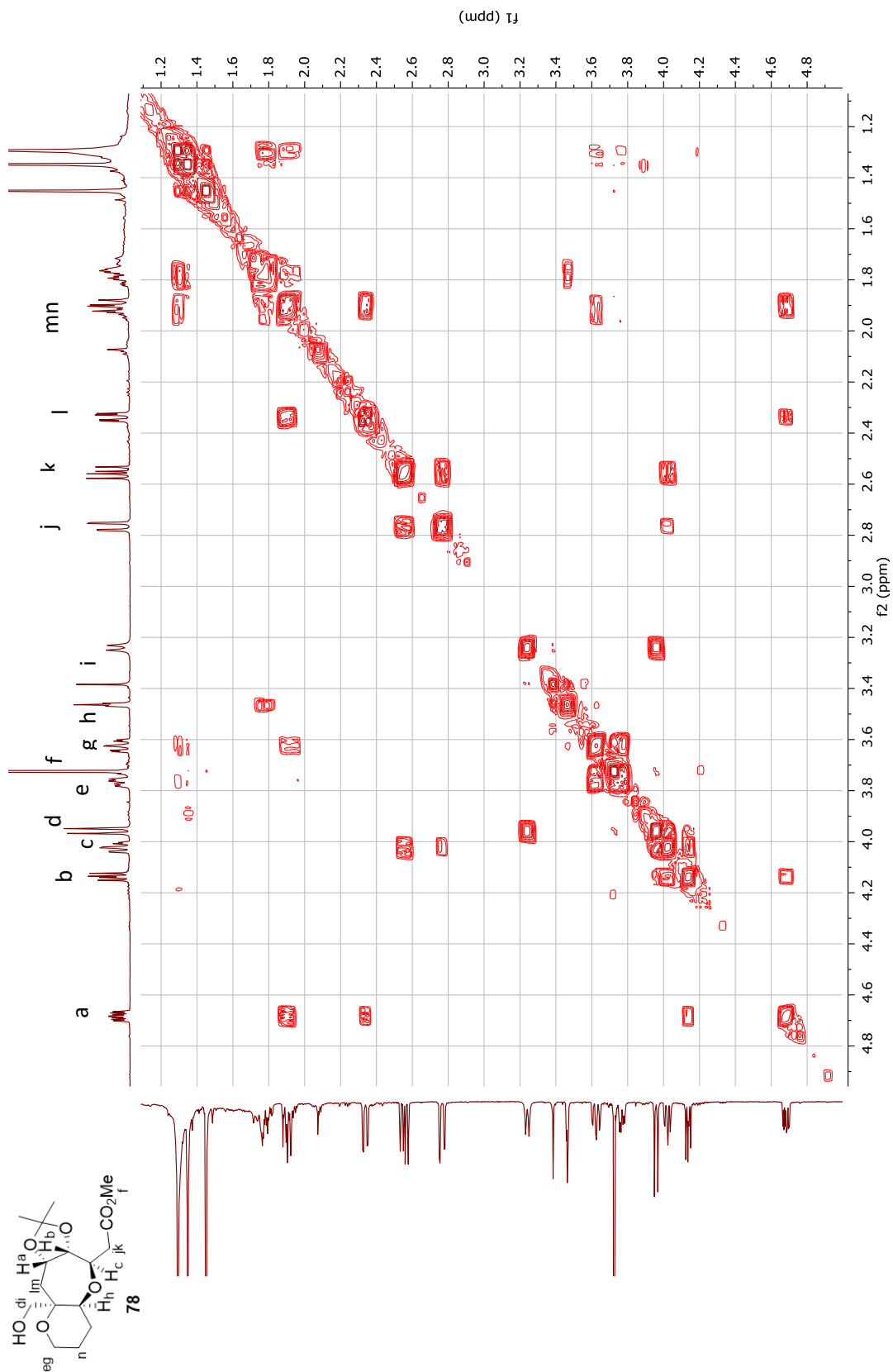
Compound **78** $^1\text{H-NMR}$ (600 MHz, CDCl_3) JAH-7-184- CDCl_3



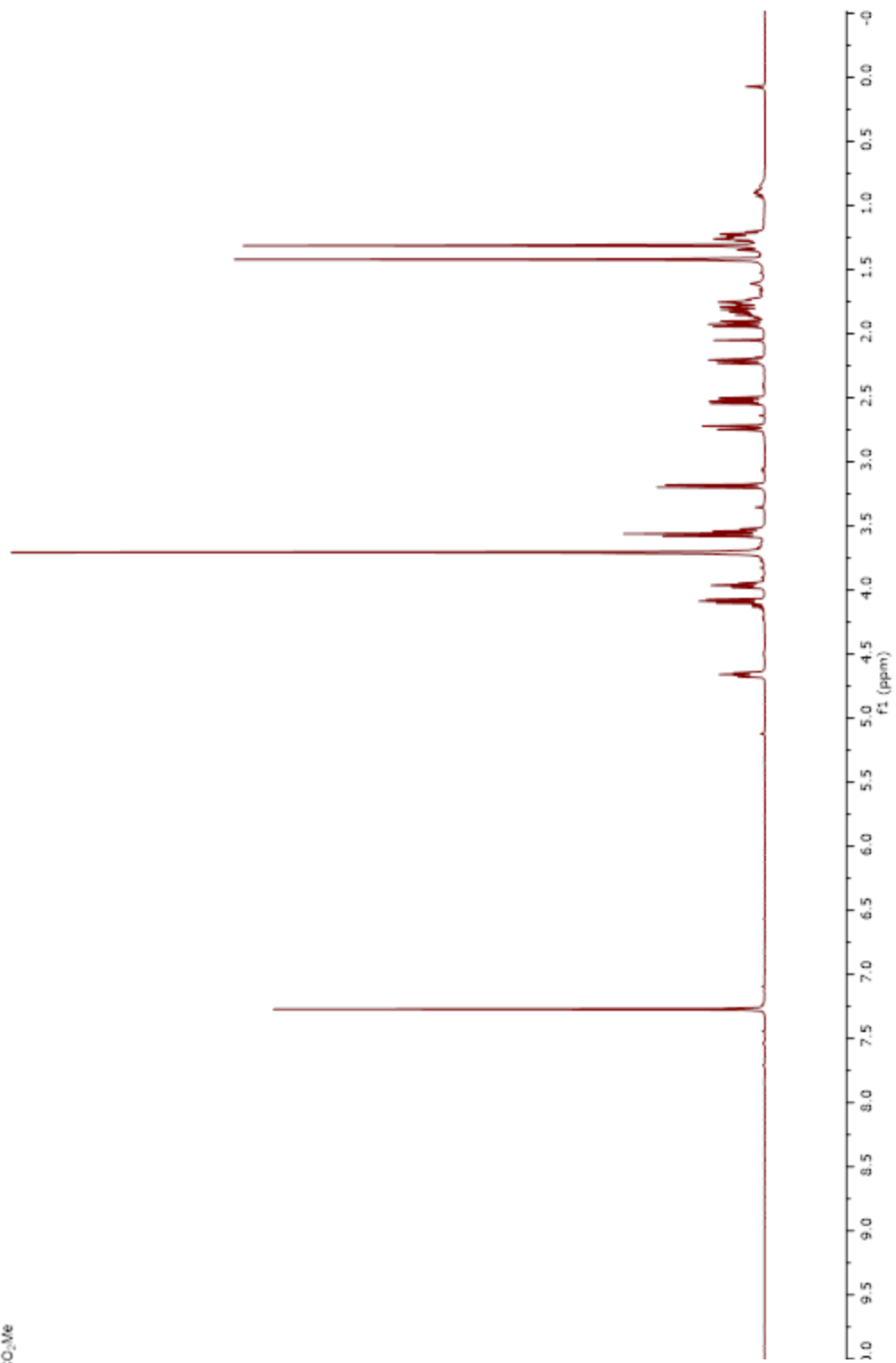
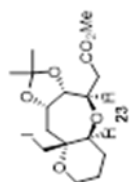
Compound **78** ^{13}C -NMR (151 MHz, CDCl_3) JAH-7-184-C13



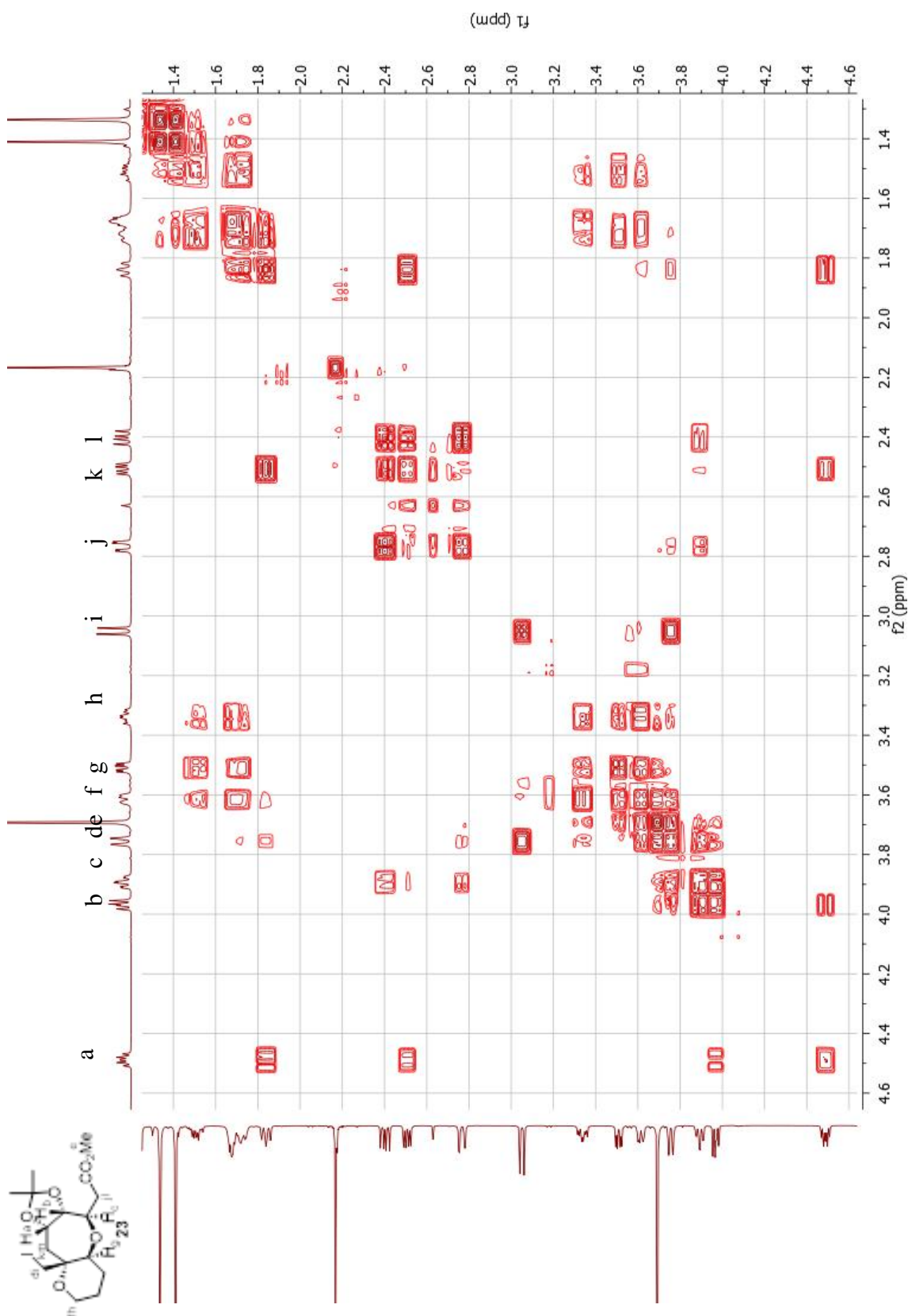
Compound **78** COSY (600 MHz, CDCl₃) JAH-7-184-C6D6-COSY



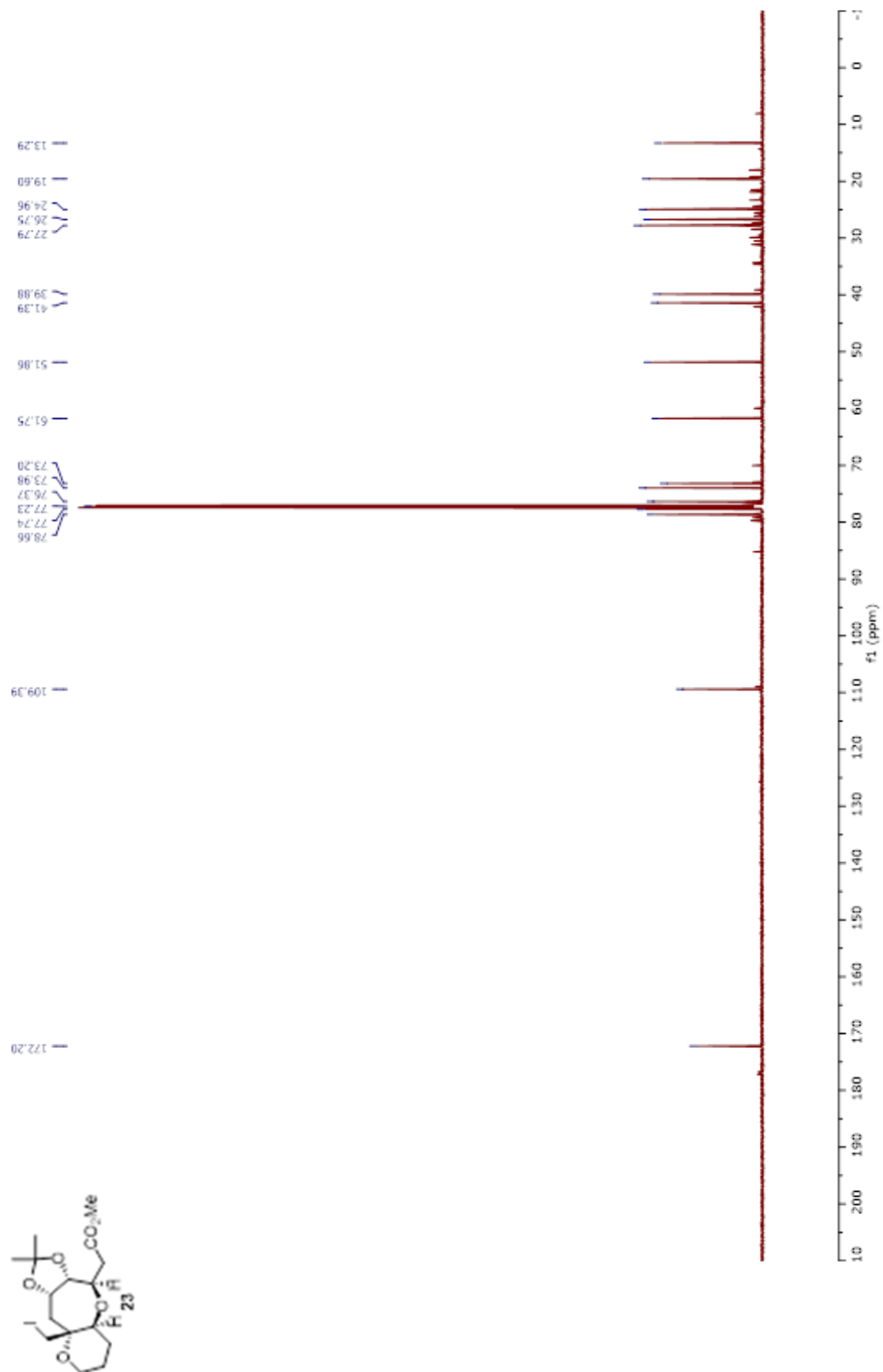
Compound **23** $^1\text{H-NMR}$ (600 MHz, CDCl_3) JAH-12-120-2



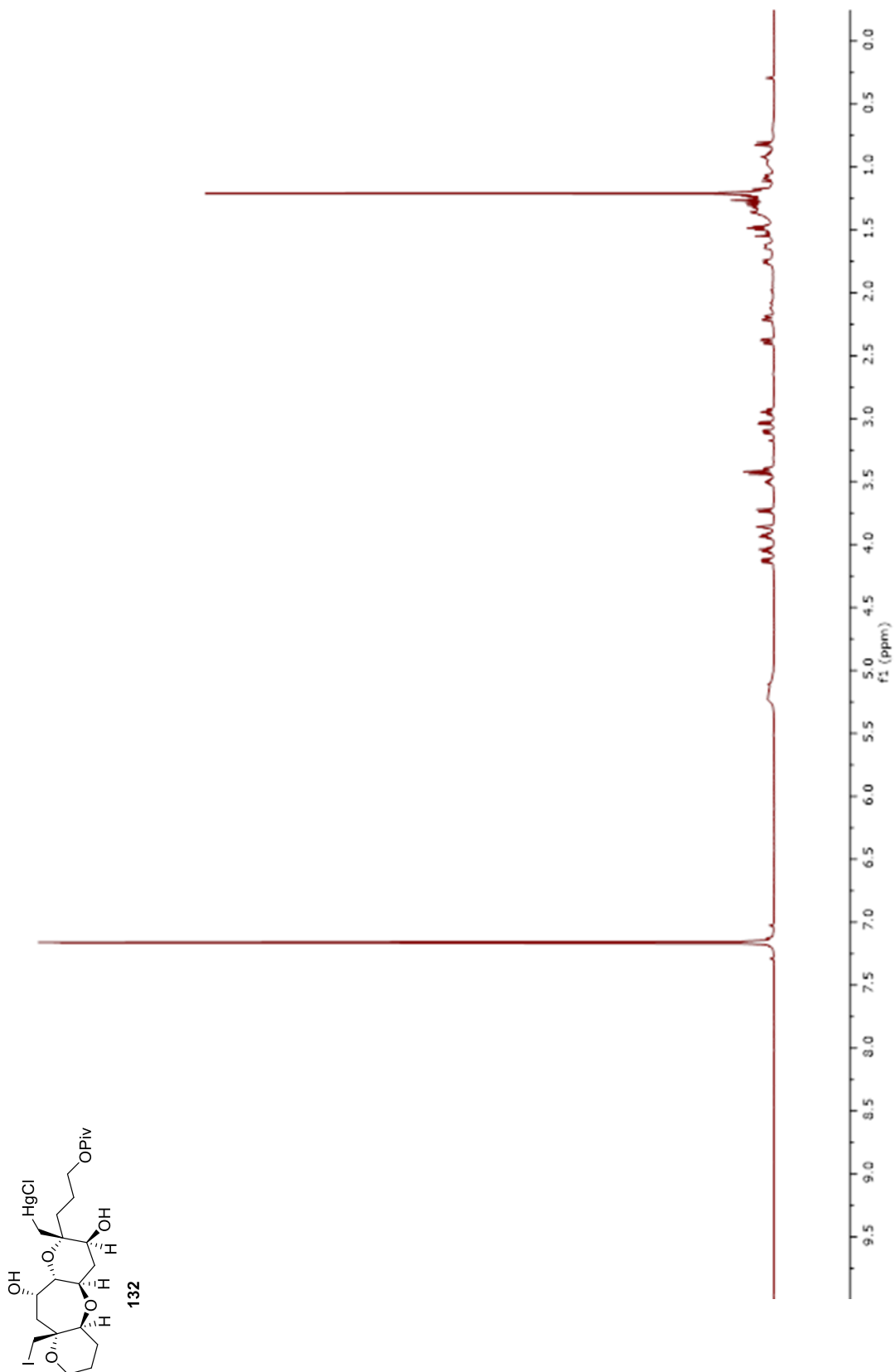
Compound **23** COSY (600 MHz, CDCl₃) JAH-12-120-2-COSY



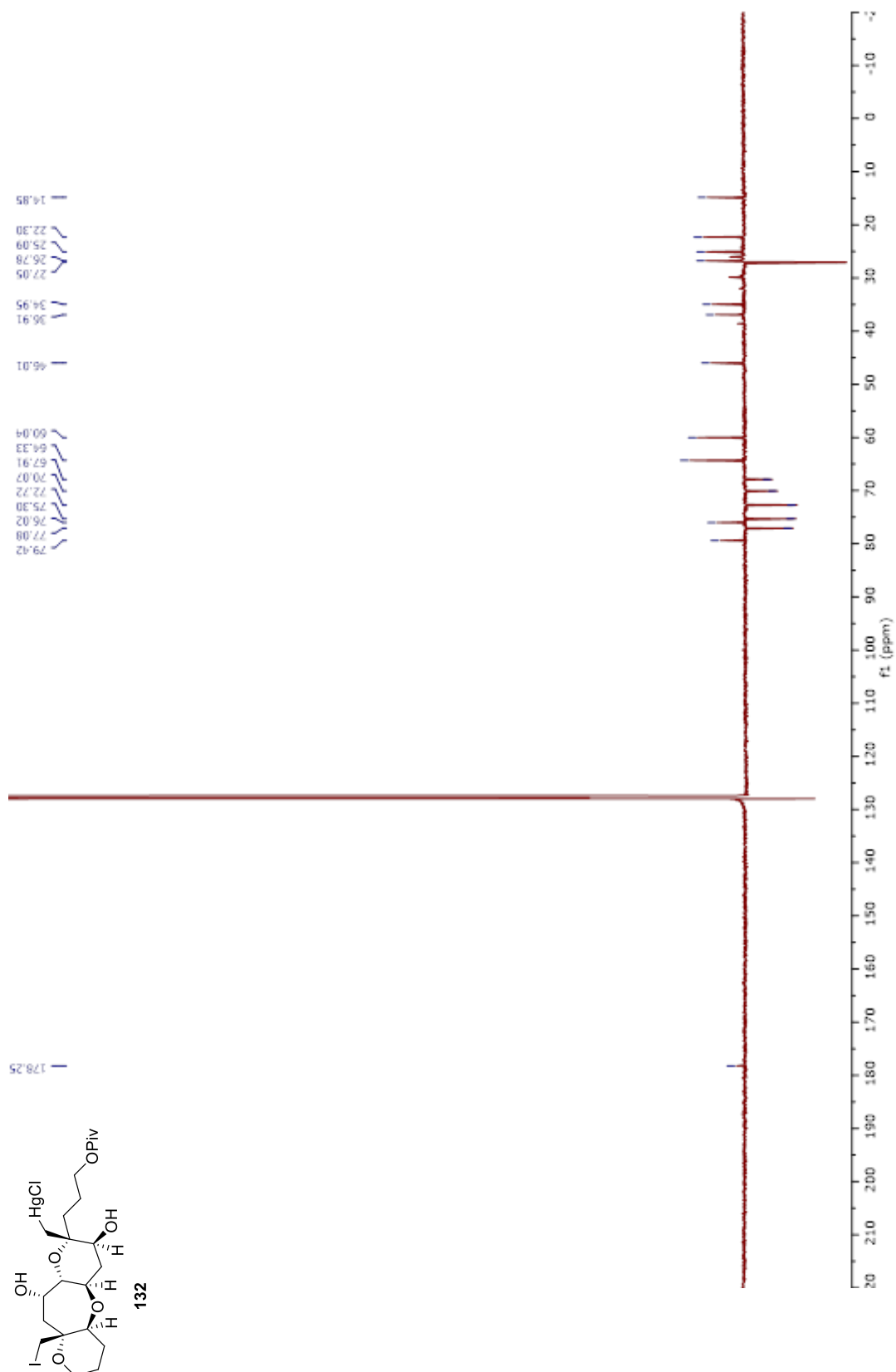
Compound **23** (126 MHz, CDCl₃) 13C JAH-12-120-A-C13



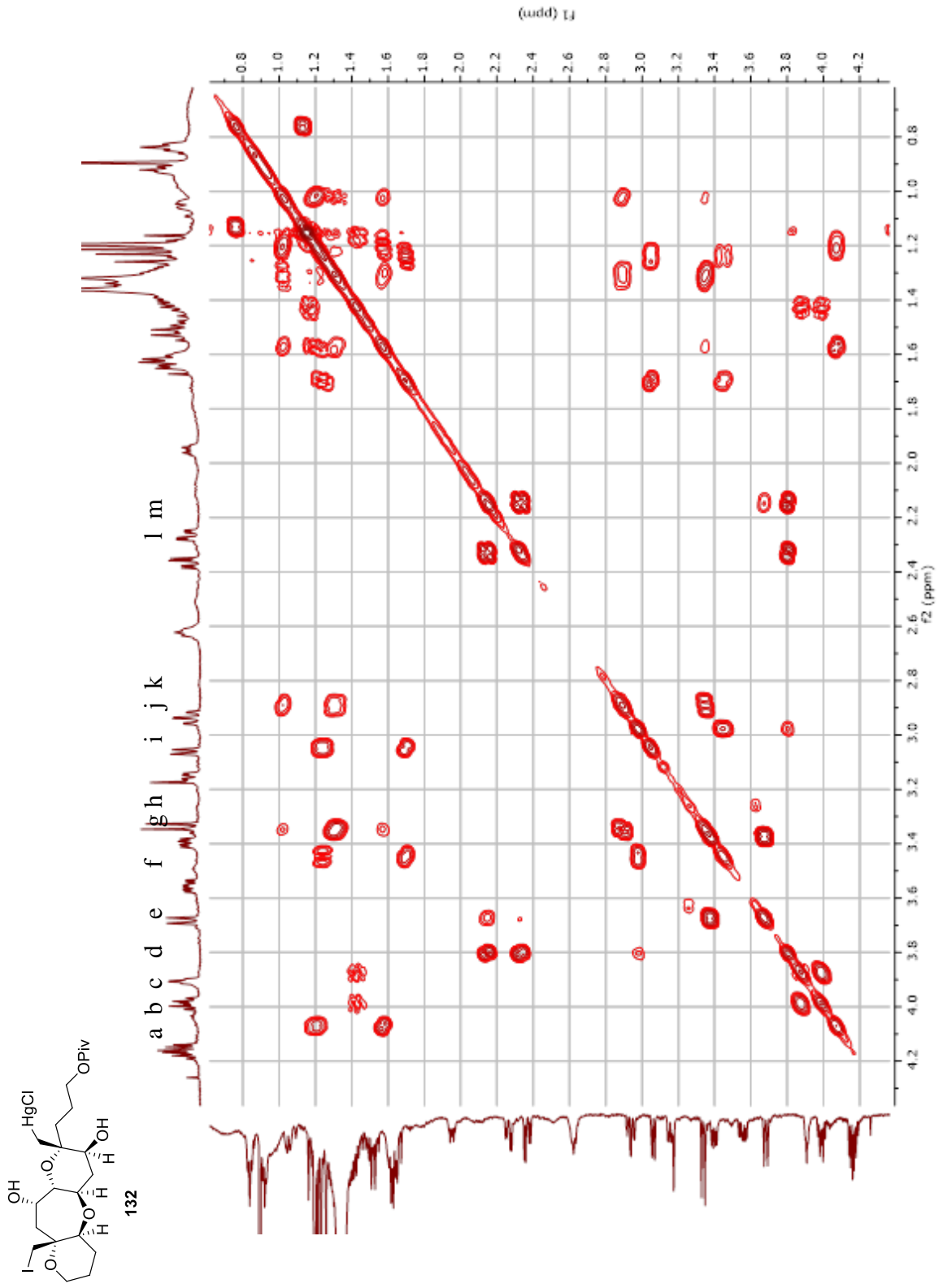
Compound **132** $^1\text{H-NMR}$ (600 MHz, C_6D_6) JAH-12-212-C6D6



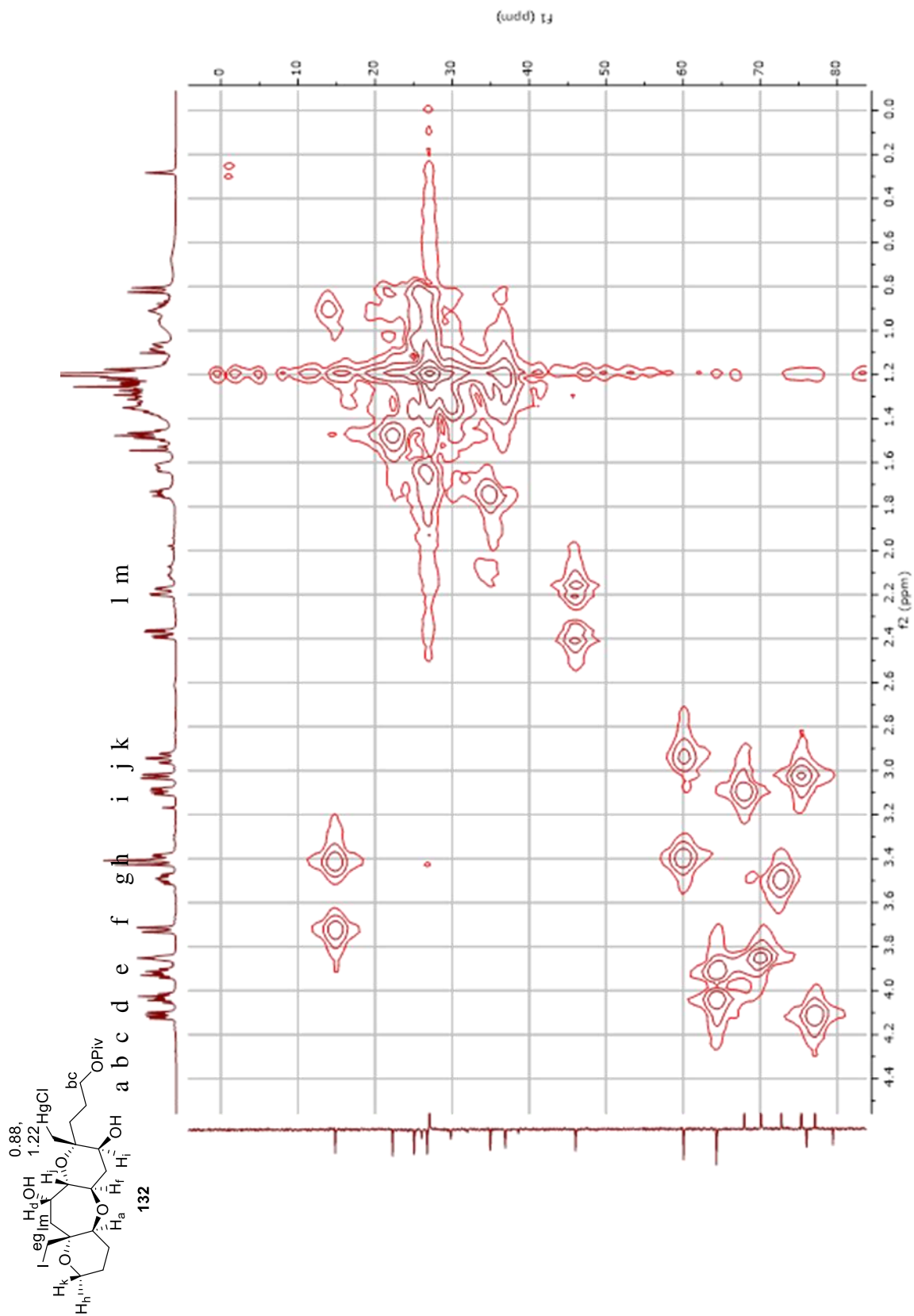
Compound **132** APT (151 MHz, C₆D₆) JAH-12-212-C6D6-APT



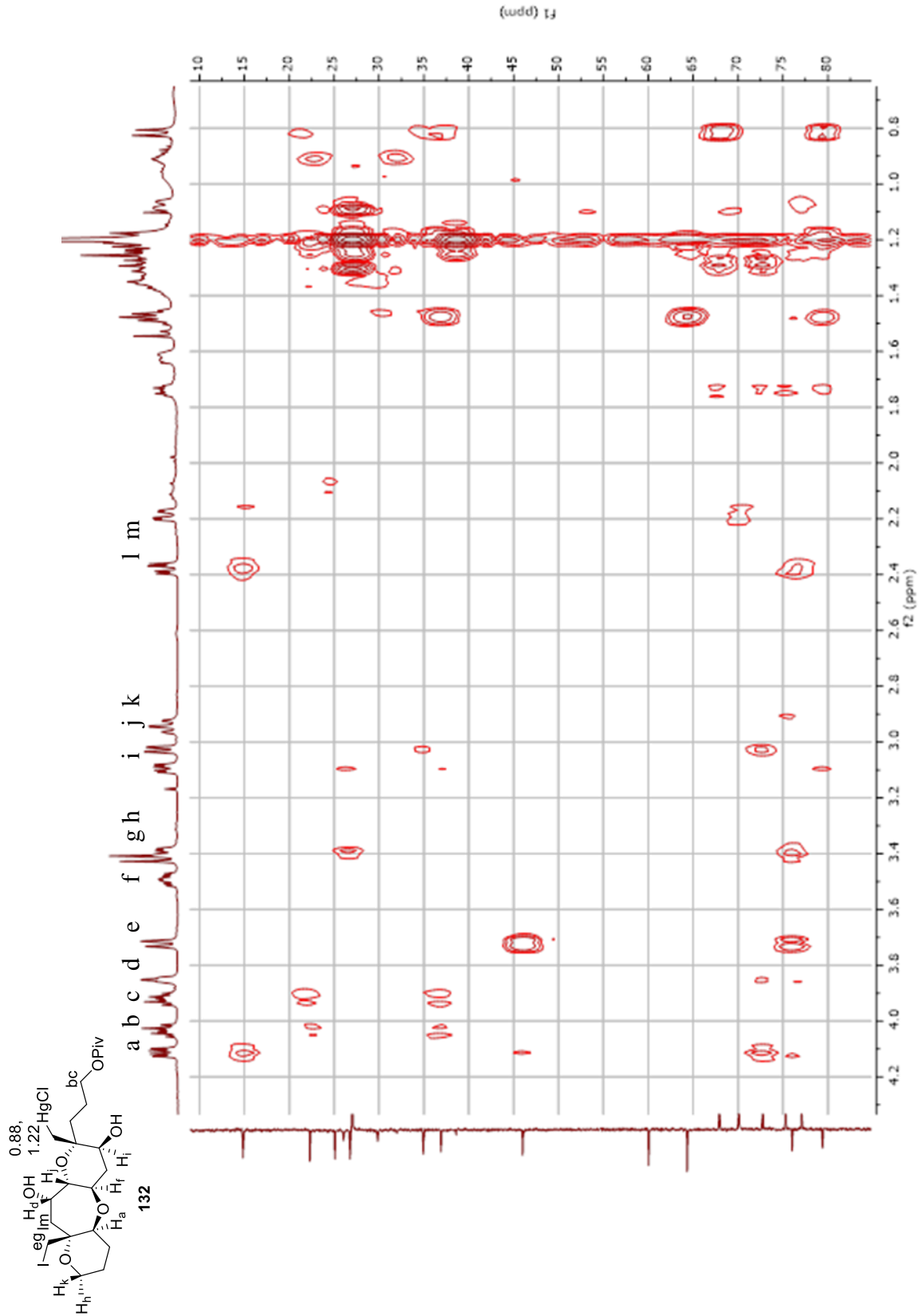
Compound **132** COSY (600 MHz, C₆D₆) JAH-12-212-C6D6-COSY



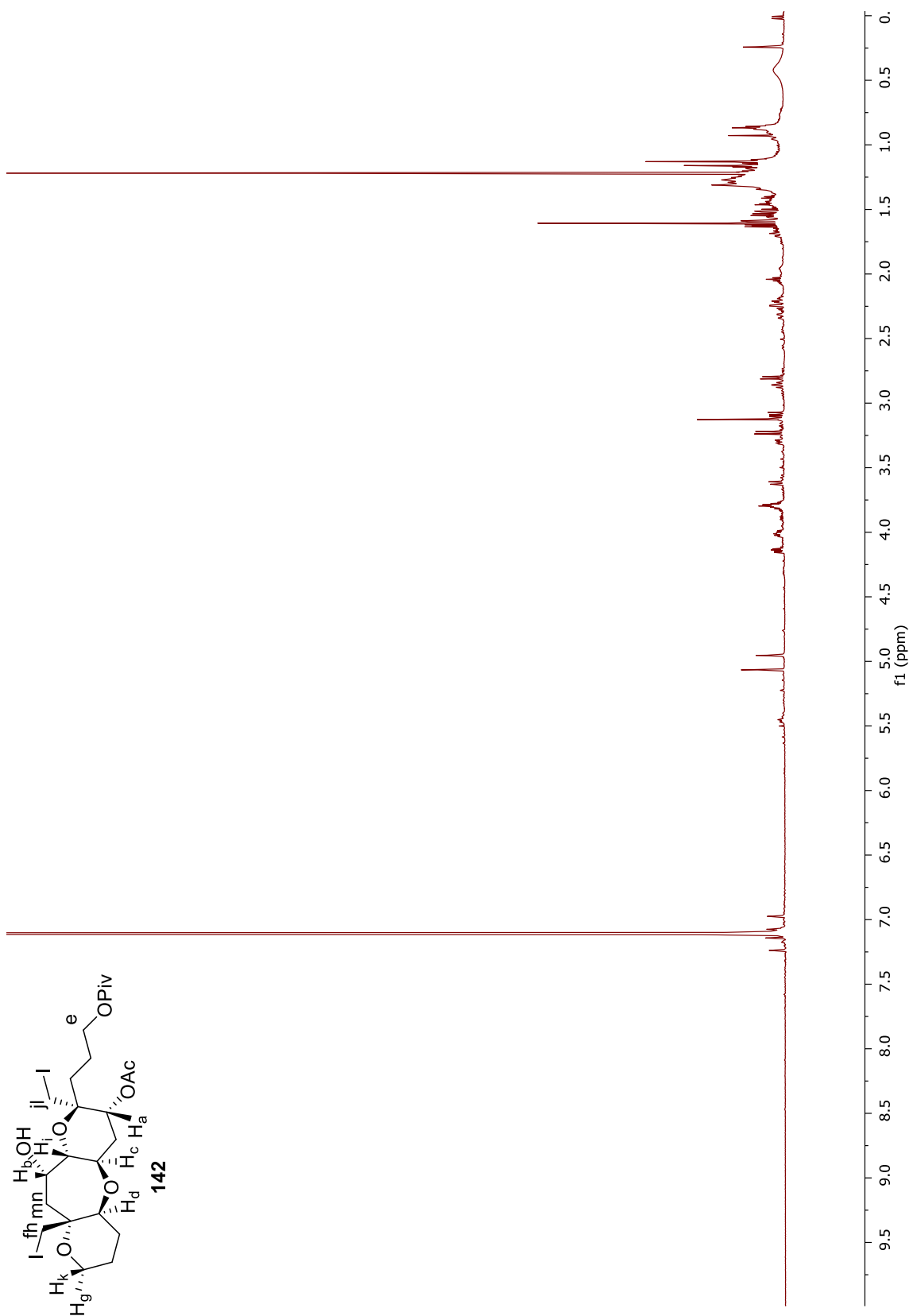
Compound **132** HMQC (600 MHz, C₆D₆) JAH-12-212-C6D6-HMQC



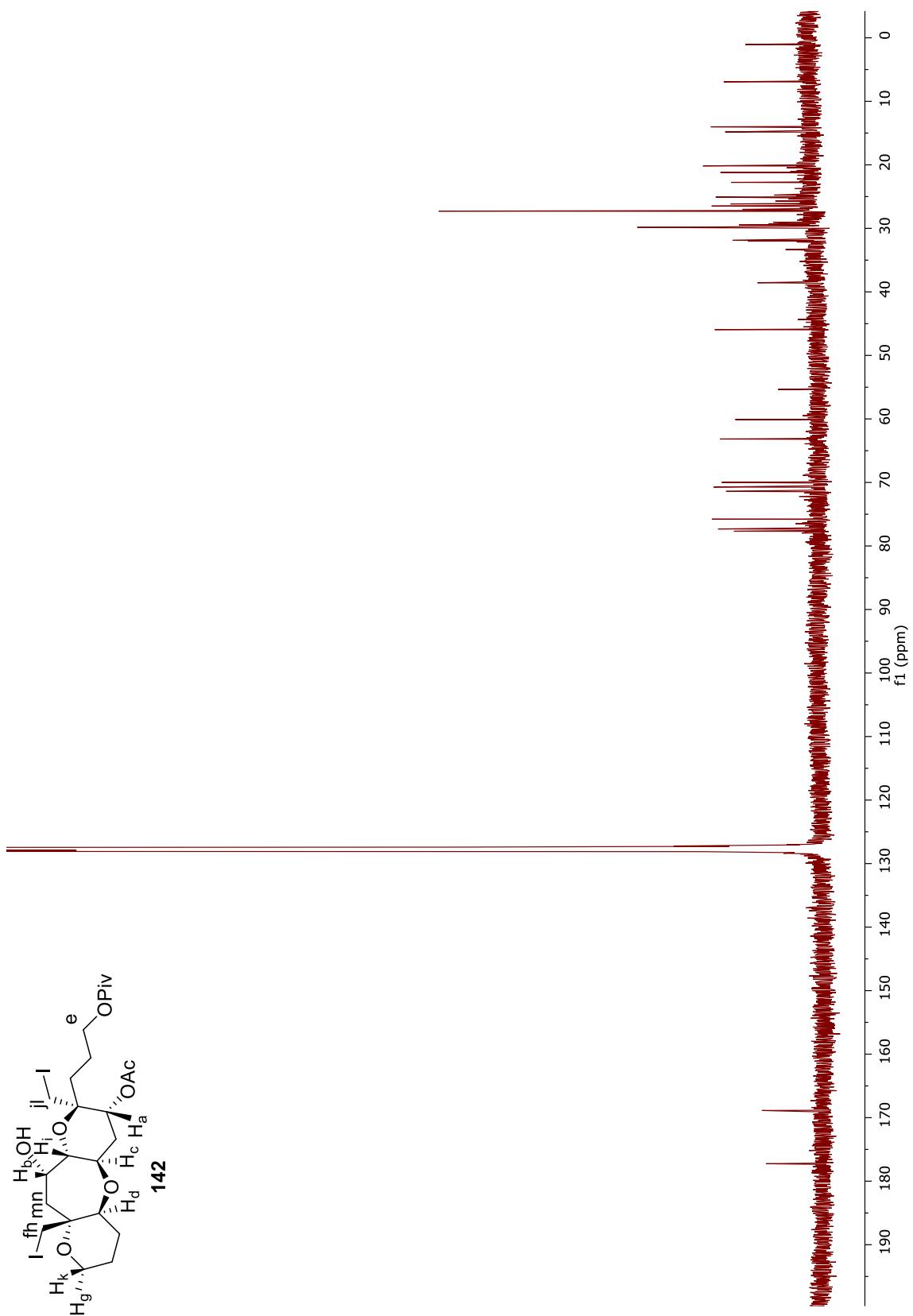
Compound **132** HMBC (600 MHz, C₆D₆) JAH-12-212-C6D6-HMBC



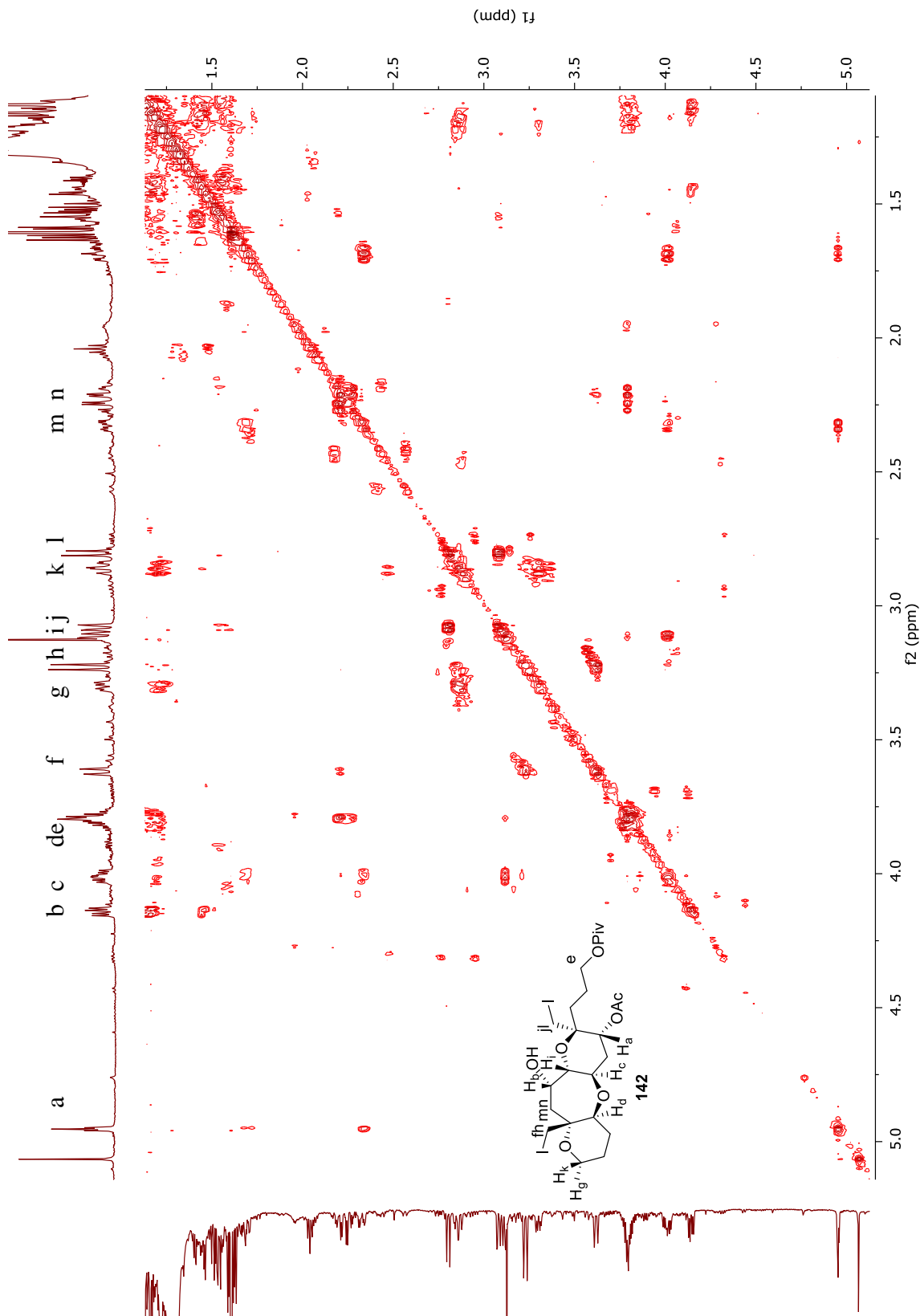
Compound **142** $^1\text{H-NMR}$ (600 MHz, C_6D_6) JAH-10-200-1-C6D6



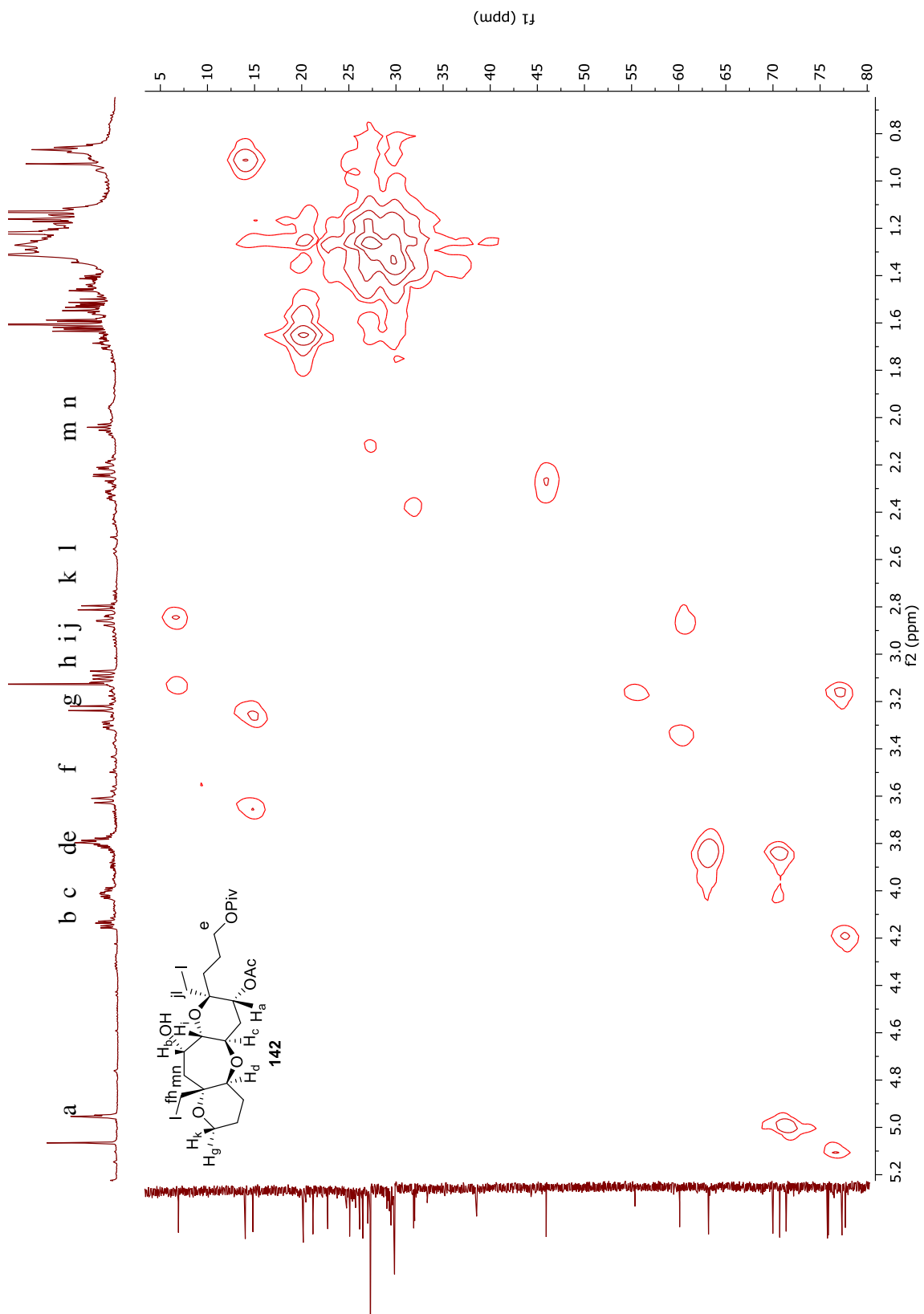
Compound **142** ^{13}C -NMR (151 MHz, C_6D_6) JAH-10-200-1-C6D6-C13



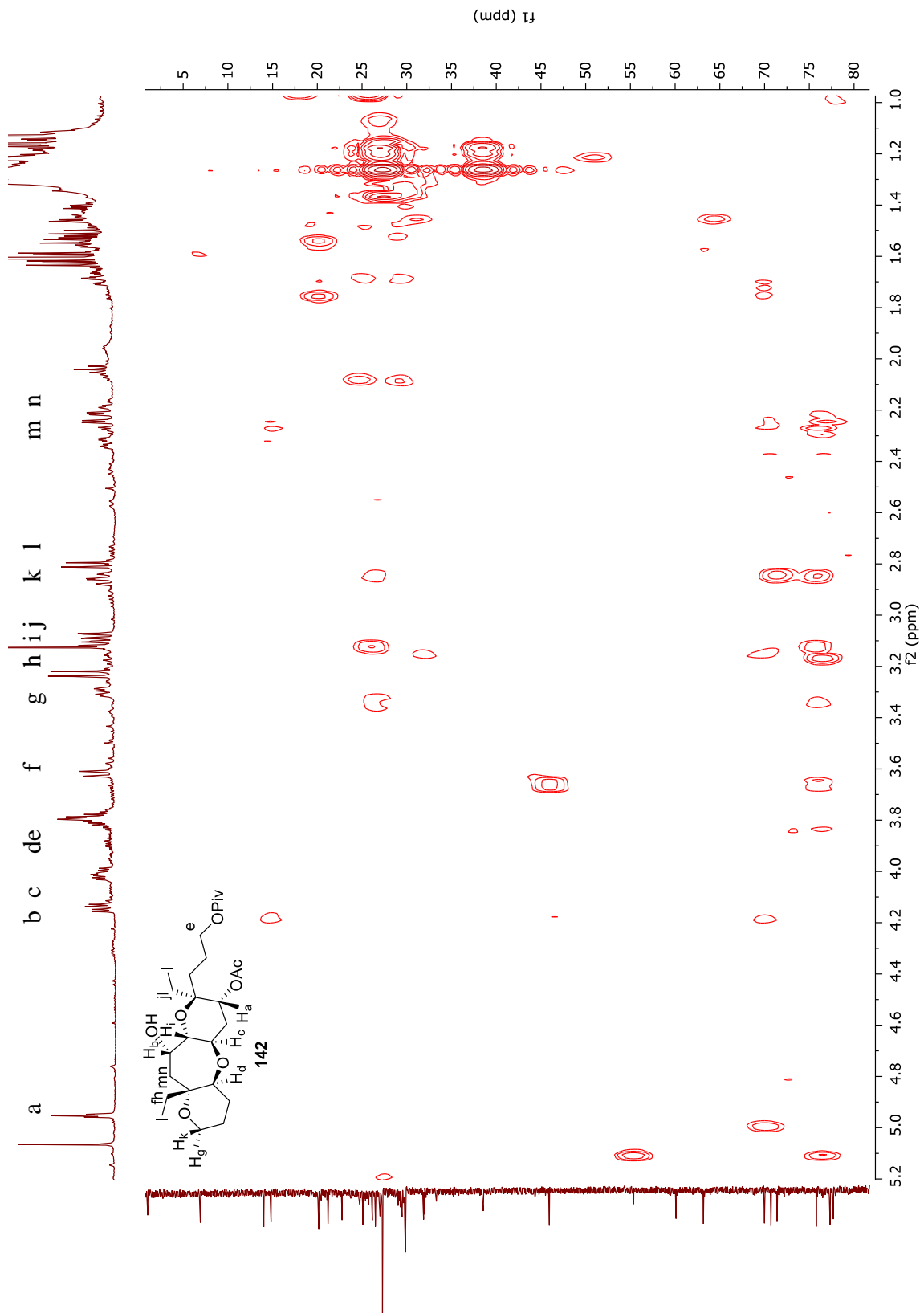
Compound **142** COSY (151 MHz, C₆D₆) JAH-10-200-1-C6D6-COSY



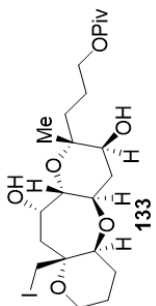
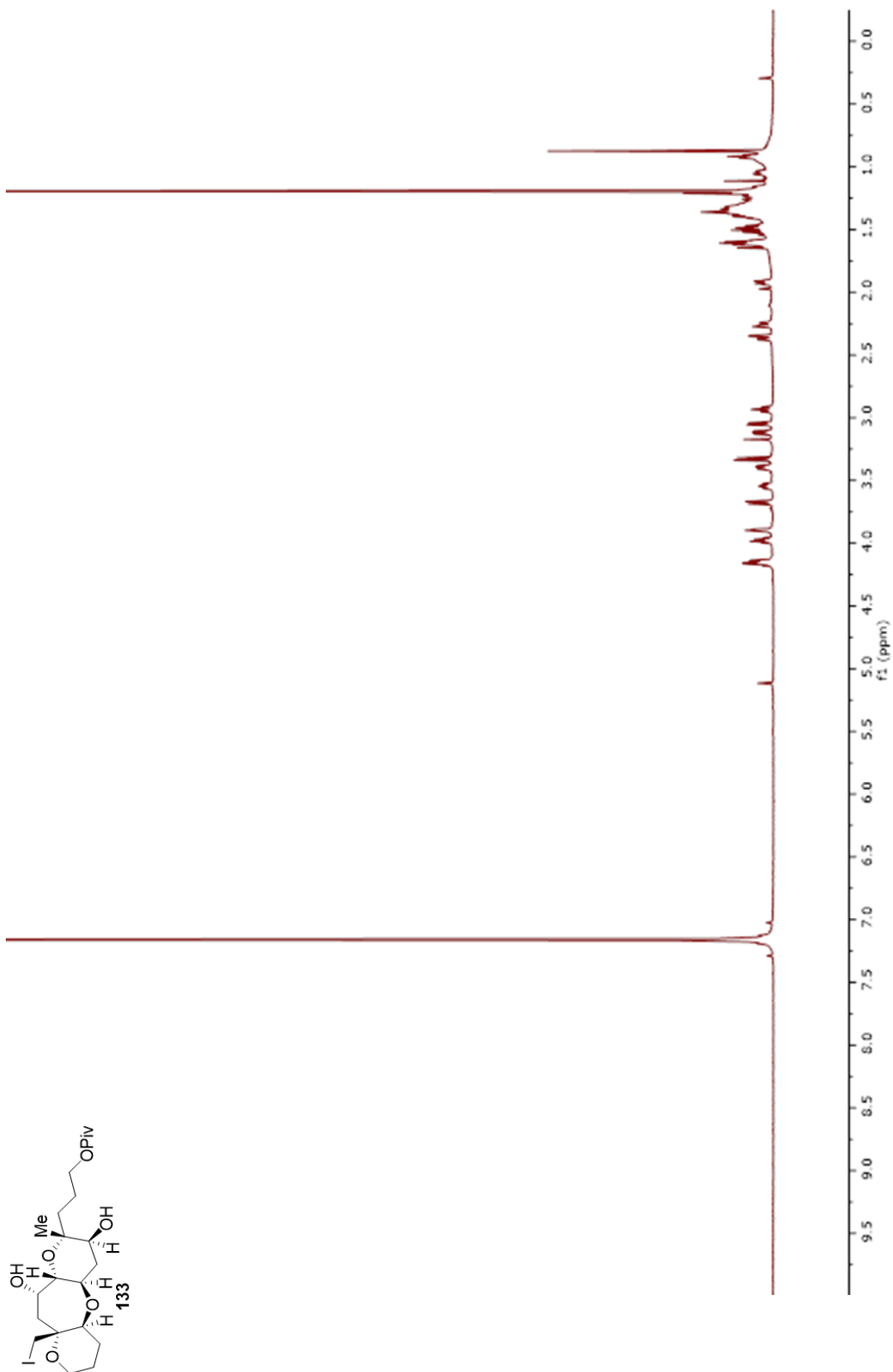
Compound **142** HMQC (151 MHz, C₆D₆) JAH-10-200-1-C6D6-HMQC



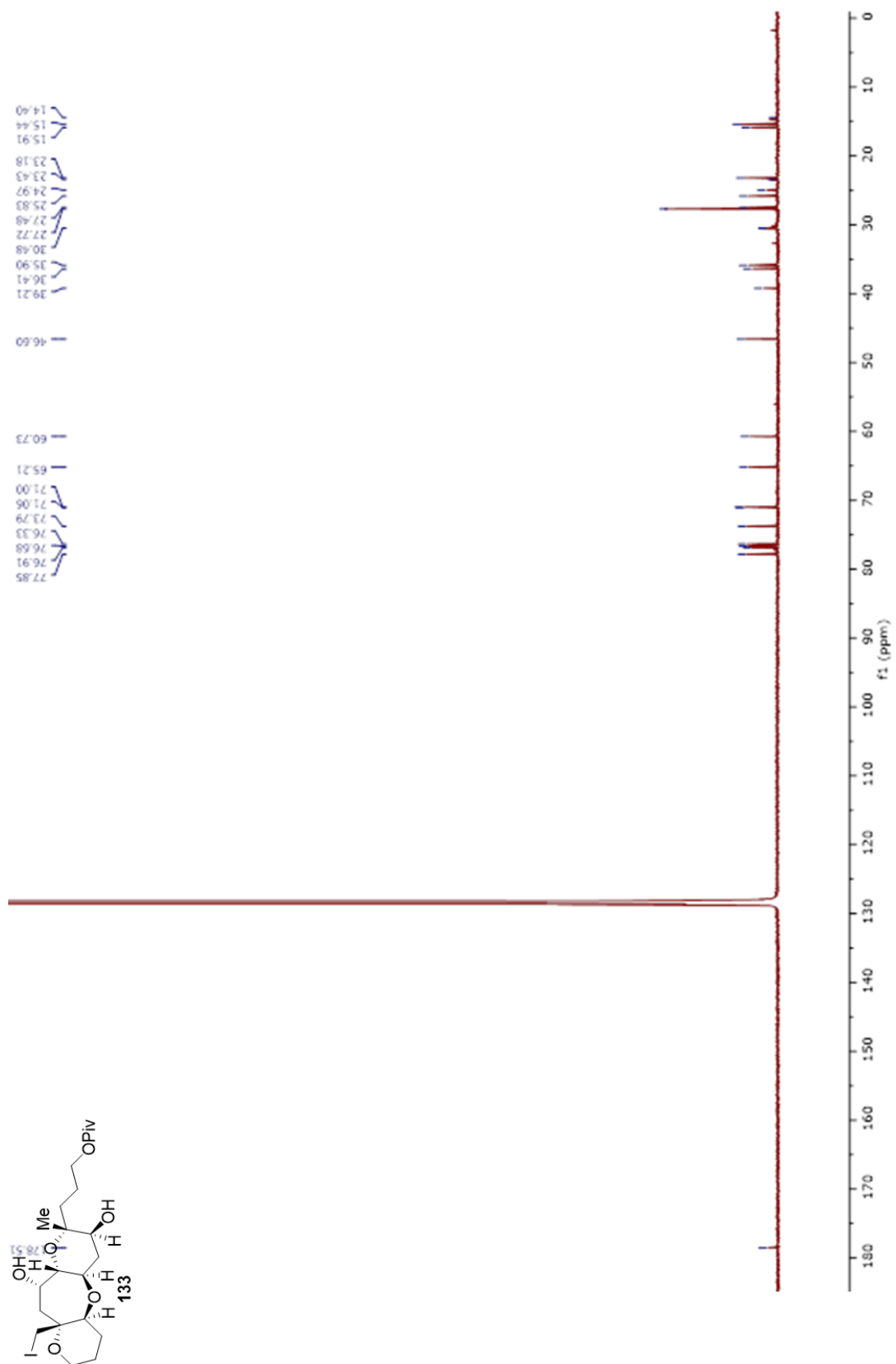
Compound **142** HMBC (151 MHz, C₆D₆) JAH-10-200-1-C6D6-HMBC



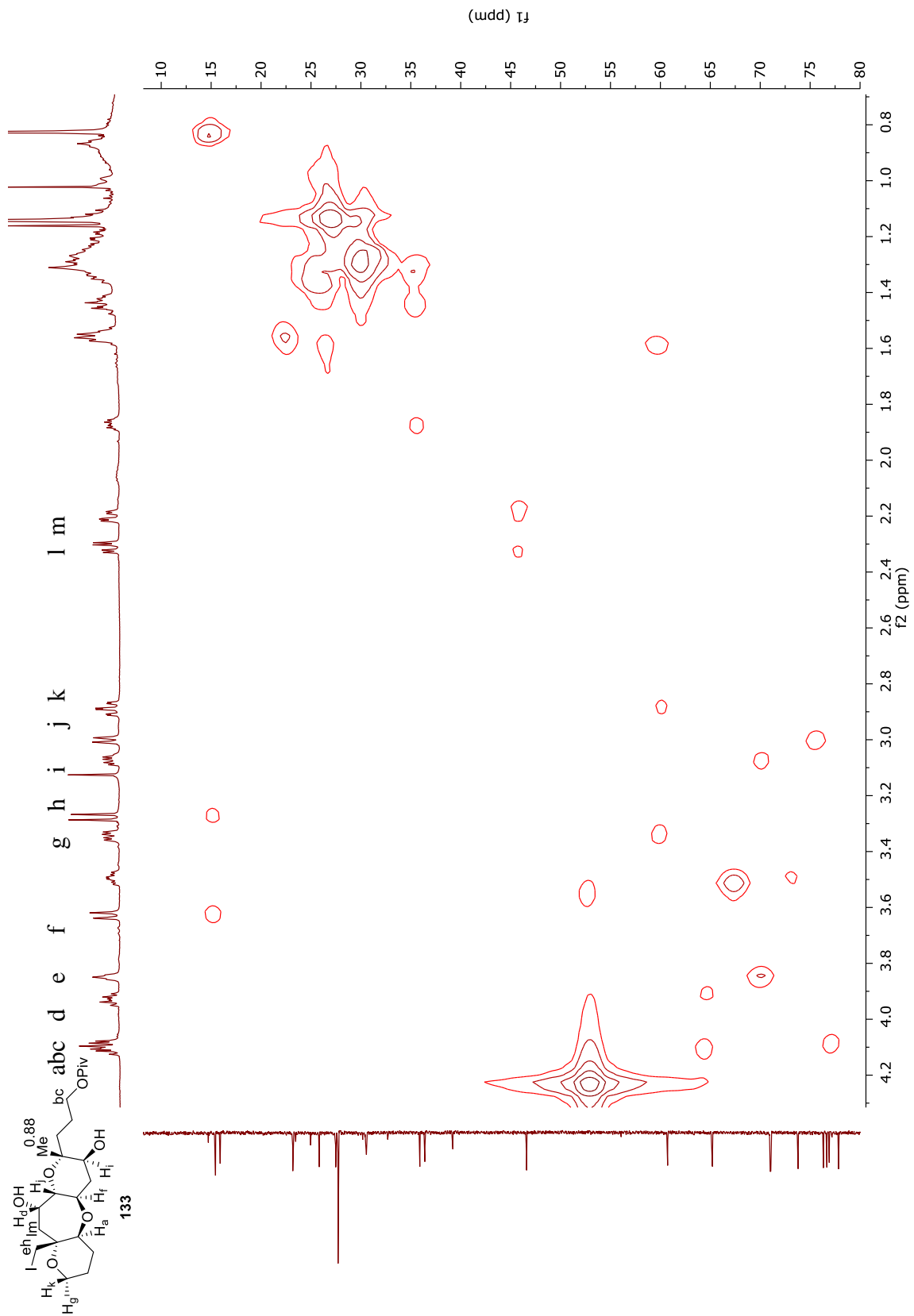
Compound **133** $^1\text{H-NMR}$ (600 MHz, C_6D_6) JAH-12-266- C_6D_6



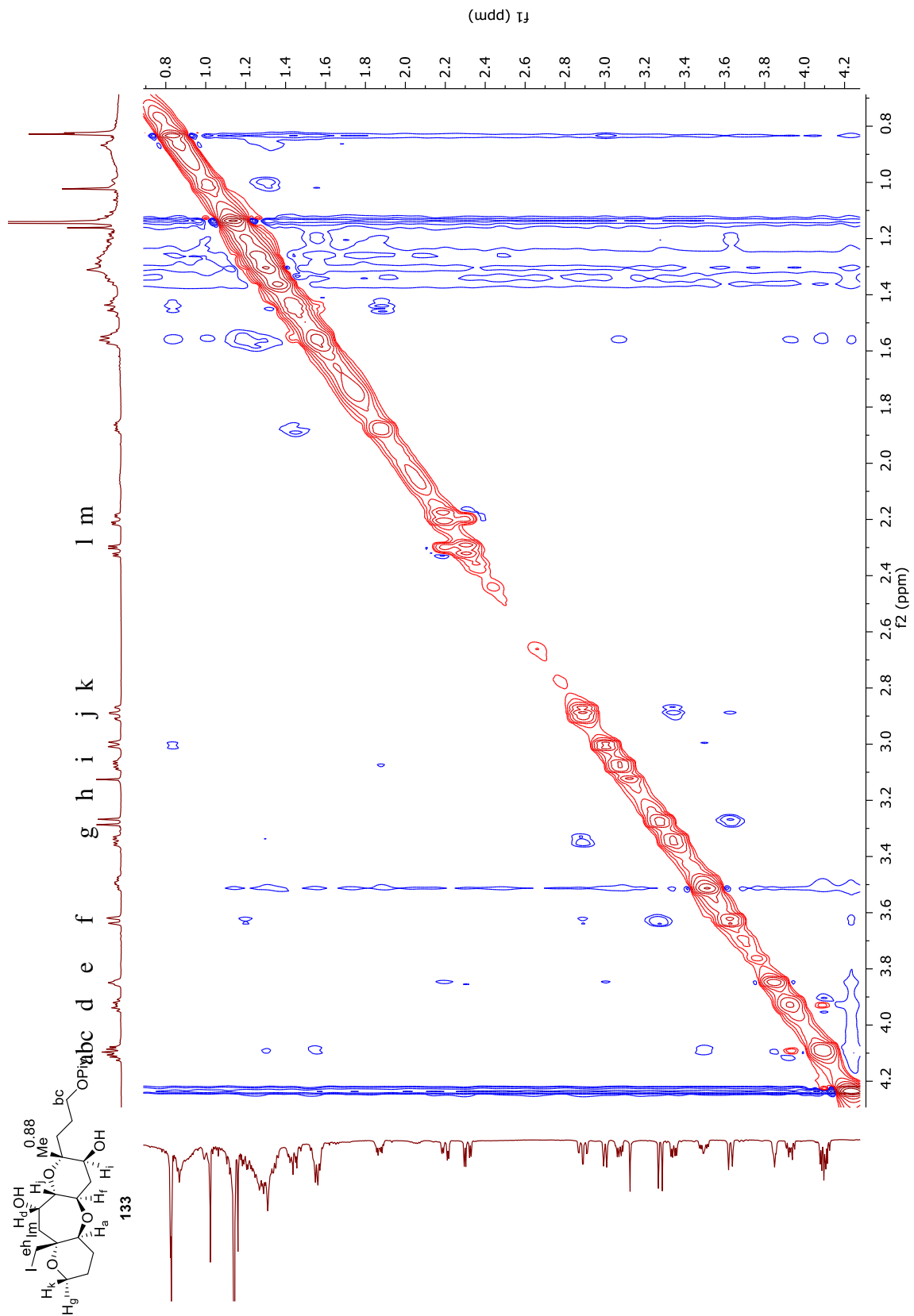
Compound **133** ^{13}C -NMR (151 MHz, C_6D_6) JAH-12-266-C6D6 -C13



Compound **133** HMQC (600 MHz, C₆D₆) JAH-12-266-C6D6 -HMQC



Compound **133** NOESY (600 MHz, C₆D₆) JAH-12-266-C6D6-NOESY



References

References

- (1) Yasumoto, T. *Chem. Rec.* **2001**, *1*, 228.
- (2) Lin, Y.-Y.; Risk, M.; Ray, S.; Van Engen, D.; Clardy, J.; Golik, J.; James, J.; Nakanishi, K. *J. Am. Chem. Soc.* **1981**, *103*, 6773.
- (3) Bourdelais, A. J.; Jacocks, H. M.; Wright, J. L. C.; Bigwarfe, P. M.; Baden, D. G. *J. Nat. Prod.* **2005**, *68*, 2.
- (4) Murata, M.; Naoki, H. *J. Am. Chem. Soc.* **1993**, *113*, 2060.
- (5) Prasad, A. V. K.; Shimizu, Y. *J. Am. Chem. Soc.* **1989**, *111*, 6476.
- (6) Pawlak, J.; Tempesta, M. S.; Golik, J.; Zagorski, M. G.; Lee, M. S.; Nakanishi, K.; Iwashita, T.; Gross, M. L.; Tomer, K. B. *J. Am. Chem. Soc.* **1987**, *109*, 1144.
- (7) Murata, M.; Legrand, A. M.; Ishibashi, Y.; Yasumoto, T. *J. Am. Chem. Soc.* **1989**, *111*, 8929.
- (8) Murata, M.; Legrand, A. M.; Ishibashi, Y.; Fukui, M.; Yasumoto, T. *J. Am. Chem. Soc.* **1990**, *112*, 4380.
- (9) Satake, M.; Morohashi, A.; Oguri, H.; Oishi, T.; HIRAMA, M.; Harada, N.; Yasumoto, T. *J. Am. Chem. Soc.* **1997**, *119*, 11325.
- (10) Nagai, H.; Torigoe, K.; Satake, M.; Murata, M.; Yasumoto, T.; Hirota, H. *J. Am. Chem. Soc.* **1992**, *114*, 1102.
- (11) Nagai, H.; Murata, M.; Torigoe, K.; Satake, M.; Yasumoto, T. *J. Org. Chem.* **1992**, *57*, 5448.
- (12) Morohashi, A.; Satake, M.; Nagai, H. *Tetrahedron* **2000**, *56*, 8995.
- (13) Ciminiello, P.; Fattorusso, E.; Forino, M.; Magno, S.; Poletti, R.; Viviani, R. *Tetrahedron Lett.* **1998**, *39*, 8897.

- (14) Satake, M.; Shoji, M.; Oshima, Y.; Naoki, H.; Fujita, T.; Yasumoto, T. *Tetrahedron Lett.* **2002**, *43*, 5829.
- (15) Yasumoto, T.; Murata, M. *Chem. Rev.* **1993**, *93*, 1897.
- (16) Poli, M. *Mol. Pharmacol.* **1986**, *30*, 129.
- (17) Trainer, V. L.; Thomsen, W. J.; Catterall, W. A.; Baden, D. G. *Mol. Pharmacol.* **1991**, *40*, 988.
- (18) Trainer, V. L.; Baden, D. G.; Catterall, W. A. *J. Biol. Chem.* **1994**, *269*, 19904.
- (19) Gawley, R. E.; Rein, K. S.; Jeglitsch, G.; Adams, D. J.; Theodorakis, E. A.; Tiebes, J.; Nicolaou, K. C.; Baden, D. G. *Chem. Biol.* **1995**, *2*, 533.
- (20) Bidard, J. N.; Vijverberg, H. P. M.; Frelin, C. *J. Biol. Chem.* **1984**, *259*, 8353.
- (21) Lombet, A.; Bidard, J. N.; Lazdunski, M. *FEBS Lett.* **1987**, *219*, 355.
- (22) Yamaoka, K.; Inoue, M.; Miyahara, H.; Miyazaki, K.; Hirama, M. *Br. J. Pharmacol.* **2004**, *142*, 879.
- (23) Cuypers, E.; Abdel-Mottaleb, Y.; Kopljar, I.; Rainier, J. D.; Raes, A. L.; Snyders, D. J.; Tytgat, J. *Toxicol.* **2008**, *51*, 974.
- (24) Inoue, M.; Hirama, M.; Satake, M.; Sugiyama, K.; Yasumoto, T. *Toxicol.* **2003**, *41*, 469.
- (25) LePage, K. T.; Rainier, J. D.; Johnson, H. W. B.; Baden, D. G.; Murray, T. F. *J. Pharmacol. Exp. Ther.* **2007**, *323*, 174.
- (26) Hirama, M.; Oishi, T.; Uehara, H.; Inoue, M.; Maruyama, M.; Oguri, H.; Satake, M. *Science* **2001**, *294*, 1904.
- (27) Chou, H. N.; Shimizu, Y. *J. Am. Chem. Soc.* **1987**, *109*, 2184.
- (28) Lee, M. S.; Repeta, D. J.; Nakanishi, K.; Zagorski, M. G. *J. Am. Chem. Soc.* **1986**,

108, 7855.

- (29) Lee, M. S.; Qin, G. W.; Nakanishi, K.; Zagorski, M. G. *J. Am. Chem. Soc.* **1989**, *111*, 6234.
- (30) Nakanishi, K. *Toxicon* **1985**, *23*, 473.
- (31) Yamazaki, M.; Izumikawa, M.; Tachibana, K.; Satake, M.; Itoh, Y.; Hashimoto, M. *J. Org. Chem.* **2012**, *77*, 4902.
- (32) Sun, P.; Leeson, C.; Zhi, X.; Leng, F.; Pierce, R. H.; Henry, M. S.; Rein, K. S. *Phytochemistry* **2016**, *122*, 11.
- (33) Nicolaou, K. C. *Angew. Chem. Int. Ed. Engl.* **1996**, *35*, 588.
- (34) Inoue, M. *Chem. Rev.* **2005**, *105*, 4379.
- (35) Morten, C. J.; Byers, J. A.; Van Dyke, A. R.; Vilotijevic, I.; Jamison, T. F. *Chem. Soc. Rev.* **2009**, *38*, 3175.
- (36) McDonald, F. E.; Tong, R.; Valentine, J. C.; Bravo, F. *Pure Appl. Chem.* **2007**, *79*, 281.
- (37) Tokiwano, T.; Fujiwara, K.; Murai, A. *Chem. Lett.* **2000**, *3*, 272.
- (38) Mori, Y.; Furuta, H.; Takase, T.; Mitsuoka, S.; Furukawa, H. *Tetrahedron Lett.* **1999**, *40*, 8019.
- (39) Fujiwara, K.; Murai, A. *Bull. Chem. Soc. Jpn.* **2004**, *77*, 2129.
- (40) Wong, O. A.; Shi, Y. *Chem. Rev.* **2008**, *108*, 3958.
- (41) McDonald, F. E.; Bravo, F.; Wang, X.; Wei, X.; Toganoh, M.; Rodriguez, J. R.; Do, B.; Neiwert, W. A.; Hardcastle, K. I. *J. Org. Chem.* **2002**, *67*, 2515.
- (42) McDonald, F. E.; Wang, X.; Do, B.; Hardcastle, K. I. *Org. Lett.* **2000**, *2*, 2917.
- (43) Clausen, D. J.; Wan, S.; Floreancig, P. E. *Angew. Chem. Int. Ed.* **2011**, *50*, 5178.

- (44) Xie, Y.; Floreancig, P. E. *Angew. Chemie - Int. Ed.* **2013**, *52*, 625.
- (45) Tokiwano, T.; Fujiwara, K.; Murai, A. *Synlett* **2000**, *3*, 335.
- (46) Baldwin, J. E. *J. Chem. Soc. Chem Comm.* **1976**, 734.
- (47) Coxson, J. M.; Hartshorn, M. O.; W. H. Swallow. *Aust. J. Chem* **1973**, *26*, 2521.
- (48) Iimori, T.; Rheingold, A. L.; Staley, D. L. *J. Am. Chem. Soc.* **1989**, *111*, 3439.
- (49) Bravo, F.; McDonald, F. E.; Neiwert, W. A.; Do, B.; Hardcastle, K. I. *Org. Lett.* **2003**, *5*, 2123.
- (50) Vilotijevic, I.; Jamison, T. F. *Science* **2007**, *317*, 1189.
- (51) Van Dyke, A. R.; Jamison, T. F. *Angew. Chemie - Int. Ed.* **2009**, *48*, 4430.
- (52) Nicolaou, K. C.; Seo, J. H.; Nakamura, T.; Aversa, R. J. *J. Am. Chem. Soc.* **2011**, *133*, 214.
- (53) Armbrust, K. W.; Beaver, M. G.; Jamison, T. F. *J. Am. Chem. Soc.* **2015**, *137*, 6941.
- (54) Bourdelais, A. J.; Campbell, S.; Jacocks, H.; Naar, J.; Wright, J. L. C.; Carsi, J.; Baden, D. G. *Cell. Mol. Neurobiol.* **2004**, *24*, 553.
- (55) Abraham, W. M.; Bourdelais, A. J.; Sabater, J. R.; Ahmed, A.; Lee, T. A.; Serebriakov, I.; Baden, D. G. *Am. J. Respir. Crit. Care Med.* **2005**, *171*, 26.
- (56) Fuwa, H.; Ebine, M.; Sasaki, M. *J. Am. Chem. Soc.* **2006**, *128*, 9648.
- (57) Fuwa, H.; Ebine, M.; Bourdelais, A. J.; Baden, D. G.; Sasaki, M. *J. Am. Chem. Soc.* **2006**, *128*, 16989.
- (58) Ebine, M.; Fuwa, H.; Sasaki, M. *Org. Lett.* **2008**, *10*, 2275.
- (59) Ebine, M.; Fuwa, H.; Sasaki, M. *Chem. A Eur. J.* **2011**, *17*, 13754.
- (60) Takamura, H.; Kikuchi, S.; Nakamura, Y.; Yamagami, Y.; Kishi, T.; Kadota, I;

- Yamamoto, Y. *Org. Lett.* **2009**, *11*, 2531.
- (61) Zhang, Y.; Rohanna, J.; Zhou, J.; Iyer, K.; Rainier, J. D. *J. Am. Chem. Soc.* **2011**, *133*, 3208.
- (62) Takamura, H.; Yamagami, Y.; Kishi, T.; Kikuchi, S.; Nakamura, Y.; Kadota, I.; Yamamoto, Y. *Tetrahedron* **2010**, *66*, 5329.
- (63) Zakarian, A.; Batch, A.; Holton, R. A. *J. Am. Chem. Soc.* **2003**, *125*, 7822.
- (64) McDonald, F. E.; Ishida, K.; Hurtak, J. A. *Tetrahedron* **2013**, *69*, 7746.
- (65) Yamamoto, Y. *J. Org. Chem.* **2007**, *72*, 7817.
- (66) Patil, N. T.; Yamamoto, Y. *Arkivoc* **2006**, *2007*, 6.
- (67) Dorel, R.; Echavarren, A. M. *Chem. Rev.* **2015**, *115*, 9028.
- (68) Hashmi, A. S. K. *Top. Organomet. Chem.* **2013**, *44*, 143.
- (69) Furstner, A.; Davies, P. W. *Angew. Chem. Int. Ed.* **2007**, *46*, 3410.
- (70) Valentine, J. C.; McDonald, F. E. *Synlett* **2006**, 1816.
- (71) Bravo, F.; McDonald, F. E.; Neiwert, W. A.; Hardcastle, K. I. *Org. Lett.* **2004**, *6*, 4487.
- (72) Molander, G. A. *Chem. Rev.* **1992**, *92*, 29.
- (73) Freeman, F. *Chem. Rev.* **1975**, *75*, 439.
- (74) Bebout, D. C. *Encyclopedia of Inorganic Chemistry*; John Wiley & Sons, Ltd, 2006.
- (75) Pougny, J. R.; Nassr, M. A. M.; Sinay, P. *J. Chem. Soc. Chem. Commun.* **1981**, 375.
- (76) De Koning, C. B.; Green, I. R.; Michael, J. P.; Oliveira, J. R. *Tetrahedron* **2001**, *57*, 9623.

- (77) Blanchette, M. A.; Malamas, M. S.; Nantz, M. H.; Roberts, J. C.; Somfai, P.; Whritenour, D. C.; Masamune, S.; Kageyama, M.; Tamura, T. *J. Org. Chem.* **1989**, *54*, 2817.
- (78) Li, D.-R.; Zhang, D.-H.; Sun, C.-Y.; Zhang, J.-W.; Yang, L.; Chen, J.; Liu, B.; Su, C.; Zhou, W.-S.; Lin, G.-Q. *Chem. - A Eur. J.* **2006**, *12*, 1185.
- (79) Boschetti, A.; Nicotra, F.; Panza, L.; Russo, G. *J. Org. Chem.* **1988**, *53*, 4181.
- (80) Bernotas, R. C.; Ganem, B. *Tetrahedron Lett.* **1985**, *26*, 1123.
- (81) Martin, O. R.; Xie, F. *Carbohydr. Res.* **1994**, *264*, 141.
- (82) Hori, K.; Hikage, N.; Inagaki, A.; Mori, S.; Nomura, K.; Yoshii, E. *J. Org. Chem.* **1992**, *57*, 2888.
- (83) R. C. Larock. *Solvomercuration/Demercuration Reactions in Organic Synthesis*; Springer: Berlin, 1986.
- (84) Larock, R. C.; Harrison, L. W. *J. Am. Chem. Soc.* **1984**, *106*, 4218.
- (85) Prieto, R.; Mueller, B.; Peters, D. *Tetrahedron Lett.* **1992**, *33*, 1679.
- (86) Nishizawa, M.; Morikuni, E.; Asho, K.; Kan, Y.; Uenoyama, K.; Imagawa, H. *Synlett* **1995**, *2*, 196.
- (87) Nishizawa, M.; Takenaka, H.; Nishide, H.; Hayashi, Y. *Tetrahedron Lett.* **1983**, *24* (25), 2581.
- (88) Nishizawa, M. *E-Eros*.
- (89) Imagawa, H.; Shigaraki, T.; Suzuki, T.; Takao, H.; Yamada, H.; Sugihara, T.; Nishizawa, M. *Chem. Pharm. Bull.* **1998**, *48*, 1341.
- (90) Riediker, M.; Schwartz, J. *J. Am. Chem. Soc.* **1982**, *104*, 5842.
- (91) Newcombe, N. J.; Ya, F.; Vijn, R. J.; Hiemstra, H.; Speckamp, W. N. *J. Chem.*

- Soc., Chem. Commun.* **1994**, 767.
- (92) Fukuyama, T.; Liu, G. *J. Am. Chem. Soc.* **1996**, *118*, 7426.
- (93) Yokoshima, S.; Tokuyama, H.; Fukuyama, T. *Angew. Chem. Int. Ed.* **2000**, *39*, 4073.
- (94) Lin, H.; Ng, W.; Danishefsky, S. J. *Tetrahedron Lett.* **2002**, *43*, 549.
- (95) Imagawa, H.; Fujikawa, Y.; Tsuchihiro, A.; Kinoshita, A.; Yoshinaga, T.; Takao, H.; Nishizawa, M. *Synlett* **2006**, *4*, 639.
- (96) Nishizawa, M.; Yadav, V. K.; Skwarczynski, M.; Takao, H.; Imagawa, H.; Sugihara, T. *Org. Lett.* **2003**, *5*, 1609.
- (97) Yamamoto, H.; Pandey, G.; Asai, Y.; Nakano, M.; Kinoshita, A.; Namba, K.; Imagawa, H.; Nishizawa, M. *Org. Lett.* **2007**, *9*, 4029.
- (98) Imagawa, H.; Kurisaki, T.; Nishizawa, M. *Org. Lett.* **2004**, *6*, 3679.
- (99) Namba, K.; Yamamoto, H.; Sasaki, I.; Mori, K.; Imagawa, H.; Nishizawa, M. *Org. Lett.* **2008**, *10*, 1767.
- (100) Namba, K.; Nakagawa, Y.; Yamamoto, H.; Imagawa, H.; Nishizawa, M. *Synlett* **2008**, *11*, 1719.
- (101) Namba, K.; Kaihara, Y.; Yamamoto, H.; Imagawa, H.; Tanino, K.; Williams, R. M.; Nishizawa, M. *Chem. - A Eur. J.* **2009**, *15*, 6560.
- (102) Tan, D. S.; Schreiber, S. L. *Tetrahedron Lett.* **2000**, *41*, 9509.
- (103) Brown, C. A.; Ahuja, V. K. *J. Org. Chem.* **1973**, *38*, 2226.
- (104) Lewis, M. D.; Cha, J. K.; Kishi, Y. *J. Am. Chem. Soc.* **1982**, *104*, 4976.
- (105) Nishizawa, M.; Skwarczynski, M.; Imagawa, H.; Sugihara, T. *Chem. Lett.* **2002**, *1*, 12.

- (106) Matsumura, K.; Hashiguchi, S.; Ikariya, T.; Noyori, R. *J. Am. Chem. Soc.* **1997**, *119*, 8738.
- (107) Hoye, T. R.; Jeffrey, C. S.; Shao, F. *Nat. Protoc.* **2007**, *2*, 2451.
- (108) Anand, N. K.; Carreira, E. M. *J. Am. Chem. Soc.* **2001**, *123*, 9687.
- (109) Grob, C. A. *Angew. Chem. Int. Ed.* **1969**, *8*, 535.
- (110) Yokoyama, H.; Matsuo, M.; Miyazawa, M.; Hirai, Y. *Synlett* **2016**, *27*, 2731.
- (111) Hopf, H.; Bohm, I.; Kleinschroth, J. *Org. Synth.* **1981**, *60*, 41.
- (112) Burgess, K.; Jennings, L. D. *J. Am. Chem. Soc.* **1991**, *113*, 6129.
- (113) Jiang, B.; Chen, Z.; Xiong, W. *Chem. Commun.* **2002**, *14*, 1524.
- (114) Helal, C. J.; Magriotis, P. A.; Corey, E. J. *J. Am. Chem. Soc.* **1996**, *118*, 10938.
- (115) Parker, K.; Ledebner, M. *J. Org. Chem.* **1996**, *61*, 3214.
- (116) Midland, M. M. *Chem. Rev.* **1989**, *89*, 1553.
- (117) Birman, V. B.; Li, X. *Org. Lett.* **2006**, *8*, 1351.
- (118) Sakamoto, Y.; Tamegai, K.; Nakata, T. *Org. Lett.* **2002**, *4*, 675.
- (119) Stoltz, K. L. PhD. Thesis Chapter 1: The development of a model system for the B-ring of brevenal and methods for the formation of seven-membered rings., Emory University, 2014.
- (120) Michaelides, I. N.; Darses, B.; Dixon, D. J. *Org. Lett.* **2011**, *13*, 664.
- (121) Miguel Pena-Lopez, M. Montserrat Martinez, M.; Sarandeses, Luis, M.; Sestelo, J. *P. Org. Lett.* **2010**, *12*, 852.
- (122) Haack, K.-J.; Shohei, H.; Fujii, A.; Ikariya, T.; Noyori, R. *Angew. Chem. Int. Ed.* **1997**, *36*, 285.
- (123) Razon, P.; N'Zoutani, M-A.; Dhulut, S.; Bezenine-Lafollée, S.; Pancrazi, A.;

- Ardisson, J. *Synthesis (Stuttg)*. **2005**, *1*, 109.
- (124) Nicolaou, K. C.; Aversa, R. J. *Isr. J. Chem.* **2011**, *51*, 359.
- (125) Chamberlin, R. A.; Mulholland, R. L. *Tetrahedron* **1984**, *40*, 2297.
- (126) Stoltz, K. L.; Alba, A.-N. R.; McDonald, F. E.; Wieliczko, M. B.; Bacsá, J. *Heterocycles* **2014**, *88*, 1519.
- (127) Nicolaou, K. C.; Hwang, C. K.; Duggan, M. E. *J. Am. Chem. Soc.* **1989**, *111*, 6682.
- (128) Aicher, T. D.; Buszek, K. R.; Fang, F. G.; Forsyth, C. J.; Jung, S. H.; Kishi, Y.; Scola, P. M. *Tetrahedron Lett.* **1992**, *33*, 1549.
- (129) Lanier, M. L.; Kasper, A. C.; Kim, H.; Hong, J. *Org. Lett.* **2014**, *16*, 2406.
- (130) Palazón, J. M.; Soler, M. A.; Ramírez, M. A.; Martín, V. S. *Tetrahedron Lett.* **1993**, *34*, 5467.
- (131) Fall, Y.; Vidal, B.; Alonso, D.; Gómez, G. *Tetrahedron Lett.* **2003**, *44*, 4467.
- (132) Pérez, M.; Canoa, P.; Gómez, G.; Terán, C.; Fall, Y. *Tetrahedron Lett.* **2004**, *45*, 5207.
- (133) Canoa, P.; Pérez, M.; Covelo, B.; Gómez, G.; Fall, Y. *Tetrahedron Lett.* **2007**, *48*, 3441.
- (134) Paddon-row, M. N.; Rondan, N. G.; Houk, K. N. *J. Am. Chem. Soc.* **1982**, *104*, 7162.
- (135) Houk, K. N.; Paddon-row, M. N.; Rondan, N. G.; Wu, Y.; Brown, F. K.; Spellmeyer, D. C.; Metz, J. T.; Li, Y.; Loncharich, R. J. *Science* **1986**, *231*, 1108.
- (136) Mootoo, D. R.; Konradsson, P.; Udodong, U.; Fraser-Reid, B. *J. Am. Chem. Soc.* **1988**, *110*, 5583.

- (137) Mootoo, D. R.; Date, V.; Fraser-Reid, B. *J. Am. Chem. Soc.* **1988**, *110*, 2662.
- (138) Zhang, H.; Wilson, P.; Shan, W.; Ruan, Z.; David, M. *Tetrahedron Lett.* **1995**, *36*, 649.
- (139) Zhang, H.; Mootoo, D. R. *J. Org. Chem.* **1995**, *60*, 8134.
- (140) Dabideen, D.; Ruan, Z.; Mootoo, D. R. *Tetrahedron* **2002**, *58*, 2077.
- (141) Lemieux, R. U.; Morgan, A. R. *Can. Journal Chem.* **1965**, *43*, 2190.
- (142) Rychnovsky, S. D.; Kim, J. *Tetrahedron Lett.* **1991**, *32*, 7219.
- (143) Okude, Y.; Hirano, S.; Hiyama, T.; Nozaki, H. *J. Am. Chem. Soc.* **1977**, *99*, 3179.
- (144) Jin, H.; Uenishi, J.; Christ, W. J.; Kishi, Y. *J. Am. Chem. Soc.* **1986**, *108*, 5644.
- (145) Takai, K.; Tagashira, M.; Kuroda, T.; Oshima, K.; Utimoto, K.; Nozaki, H. *J. Am. Chem. Soc.* **1986**, *108*, 6048.
- (146) Corey, E. J.; Helal, C. J. *Angew. Chem. Int. Ed. Engl.* **1998**, *37*, 1986.
- (147) Matsuo, G.; Kawamura, K.; Hori, N.; Matsukura, H.; Nakata, T. *J. Am. Chem. Soc.* **2004**, *126*, 14374.
- (148) Kolb, H. C.; VanNieuwenhze, M. S.; Sharpless, K. B. *Chem. Rev.* **1994**, *94*, 2483.
- (149) Dess, D. B.; Martin, J. C. *J. Org. Chem.* **1983**, *48*, 4155.
- (150) Hara, S.; Dojo, H.; Takinami, S.; Suzuki, A. *Tetrahedron Lett.* **1983**, *24*, 731.
- (151) Smith, M.; Rammler, D. H.; Goldberg, I. H.; Khorana, H. G. *J. Am. Chem. Soc.* **1962**, *84*, 430.
- (152) Takebuchi, K.; Hamada, Y.; Shioiri, T. *Tetrahedron Lett.* **1994**, *35*, 5239.
- (153) Gustafsson, T.; Schou, M.; Almqvist, F.; Kihlberg, J. *J. Org. Chem.* **2004**, *69*, 8694.
- (154) Scbes, H.; Brand, E. *J. Am. Chem. Soc.* **1954**, *76*, 3601.

- (155) Podilapu, A. R.; Kulkarni, S. S. *Org. Lett.* **2014**, *16*, 4336.
- (156) Winkler, J. W.; Uddin, J.; Serhan, C. N.; Petasis, N. A. *Org. Lett.* **2013**, *15*, 1424.
- (157) Saito, S.; Ishikawa, T.; Kuroda, A.; Koga, K.; Moriwake, T. *Tetrahedron* **1992**, *48*, 4067.
- (158) Hoover, J. M.; Stahl, S. S. *J. Am. Chem. Soc.* **2011**, *133*, 16901.
- (159) Evans, R. D.; Magee, J. W.; Schauble, J. H. *Synthesis (Stuttg)*. **1988**, 862.
- (160) Galatsis, P.; Millan, S. D. *Tetrahedron Lett.* **1991**, *32*, 7493.
- (161) Suginome, H.; Wang, J. B. *J. Chem. Soc., Chem. Commun.* **1990**, *8*, 1629.
- (162) Rawal, V. H.; Iwasa, S. *Tetrahedron Lett.* **1992**, *33*, 4687.
- (163) Yuen, T. Y.; Brimble, M. A. *Org. Lett.* **2012**, *14*, 5154.
- (164) Gao, F.; Hoveyda, A. H. *J. Am. Chem. Soc.* **2010**, *132*, 10961.
- (165) Takai, K.; Sakamoto, S.; Isshiki, T. *Org. Lett.* **2003**, *5*, 653.
- (166) Ando, K. *J. Org. Chem.* **1997**, *62*, 1934.
- (167) Griffith, W. P.; Ley, S. V.; Whitcombe, G. P.; White, A. D. *J. Chem. Soc. Chem. Commun.* **1987**, 1625.
- (168) Ebine, M.; Suga, Y.; Fuwa, H.; Sasaki, M. *Org. Biomol. Chem.* **2010**, *8*, 39.
- (169) Hansen, T. M.; Florence, G. J.; Lugo-Mas, P.; Chen, J.; Abrams, J. N.; Forsyth, C. *J. Tetrahedron Lett.* **2003**, *44*, 57.
- (170) Chatgililoglu, C. *Acc. Chem. Res.* **1992**, *25*, 188.
- (171) Ballestri, M.; Chatgililoglu, C.; Clark, B.; Giese, B.; Kopping, B. *J. Org. Chem.* **1991**, 678.
- (172) Chatterjee, A. K.; Choi, T. L.; Sanders, D. P.; Grubbs, R. H. *J. Am. Chem. Soc.* **2003**, *125*, 11360.

- (173) Danishefsky, S. J.; Armistead, D. M.; Wincott, F. E.; Selnick, H. G.; Hungate, R. *J. Am. Chem. Soc.* **1987**, *109*, 8117.
- (174) Andrus, M. B.; Lepore, S. D.; Sclafani, J. A. *Tetrahedron Lett.* **1997**, *38*, 4043.
- (175) Luche, J.-L. *J. Am. Chem. Soc.* **1978**, *100*, 2226.
- (176) Crawford, C.; Nelson, A.; Patel, I. *Org. Lett.* **2006**, *8*, 4231.
- (177) Evans, D. A.; Dart, M. J.; Duffy, J. L.; Yang, M. G. *J. Am. Chem. Soc.* **1996**, *118*, 4322.
- (178) Brown, C.; Geoghegan, J. *J. Org. Chem.* **1970**, *35*, 1844.
- (179) Kang, S. H.; Lee, J. H.; Lee, S. B. *Tetrahedron Lett.* **1998**, *39*, 59.
- (180) Benhamou, M. C.; Etemad-Moghadam, G.; Speziale, V.; Lattes, A. *Synthesis (Stuttg.)* **1979**, 891.
- (181) Nguyen, J. D.; D'Amato, E. M.; Narayanam, J. M. R.; Stephenson, C. R. *J. Nat. Chem.* **2012**, *4*, 854.
- (182) Barton, D. H. R.; Hartwig, W.; Motherwell, W. B. *J. Chem. Soc., Chem. Commun.* **1982**, 447.
- (183) Crich, D.; Beckwith, A. L. J.; Chen, C.; Yao, Q.; Davison, I. G. E.; Longmore, R. W.; Anaya de Parrodi, C.; Quintero-Cortes, L.; Sandoval-Ramirez, J. *J. Am. Chem. Soc.* **1995**, *117*, 8757.
- (184) Jenkins, I. D. *J. Chem. Soc., Chem. Commun.* **1994**, 1227.
- (185) Krosley, K. W.; Gleicher, G. J.; Clapp, G. E. *J. Org. Chem.* **1992**, *57*, 840.
- (186) Sandoval-lira, J.; Garc, J. *J. Org. Chem.* **2013**, *78*, 9127.
- (187) Deslongchamps, P. *Tetrahedron* **1975**, *31*, 2463.
- (188) Stang, E. M.; White, M. C. *J. Am. Chem. Soc.* **2011**, *133*, 14892.

- (189) Shelke, A. M.; Rawat, V.; Suryavanshi, G.; Sudalai, A. *Tetrahedron Asymmetry* **2012**, *23*, 1534.
- (190) Bauer, M.; Maier, M. E. *Org. Lett.* **2002**, *4*, 643.
- (191) Mulzer, J.; Berger, M. *J. Org. Chem.* **2004**, *69*, 891.
- (192) Durka, M.; Buffet, K.; Iehl, J.; Holler, M.; Nierengarten, J.-F.; Taganna, J.; Bouckaert, J.; Vincent, S. P. *Chem. Commun.* **2011**, *47*, 1321.
- (193) Bolte, B.; Basutto, J. A.; Bryan, C. S.; Garson, M. J.; Banwell, M. G.; Ward, J. S. *J. Org. Chem.* **2015**, *80*, 460.
- (194) Holmes, A. B.; Smith, A. L.; Williams, S. F. *J. Org. Chem.* **1991**, *56*, 1393.